NOTICE

The quality of this microform is heavily dependent upon the quality of the original thesis submitted for microfilming. Every effort has been made to ensure the highest quality of reproduction possible.

If pages are missing, contact the university which granted the degree.

Some pages may have indistinct print especially if the original pages were typed with a poor typewriter ribbon or if the university sent us an inferior photocopy.

Reproduction in full or in part of this microform is governed by the Canadian Copyright Act, R.S.C. 1970, c. C-30, and subsequent amendments.

AVIS

La qualité de cette microforme dépend grandement de la qualité de la thèse soumise au microfilmage. Nous avons tout fait pour assurer une qualité supérieure de reproduction.

S'il manque des pages, veuillez communiquer avec l'université qui a conféré le grade.

La qualité d'impression de certaines pages peut laisser à désirer, surtout si les pages originales ont été dactylographiées à l'aide d'un ruban usé ou si l'université nous a fait parvenir une photocopie de qualité inférieure.

La reproduction, même partielle, de cette microforme est soumise à la Loi canadienne sur le droit d'auteur, SRC 1970, c. C-30, et ses amendements subséquents.

Canada

Equilibrium in Aqueous Liquid-Liquid Salt Systems

by

Eric Langat Cheluget

A thesis submitted to the Faculty of Graduate
Studies and Research in partial fulfillment
of the requirements for the degree of
Doctor of Philosophy

Department of Chemical Engineering
McGill University
Montreal, Canada

ISBN 0-315-87788-X

Canada

to my parents

Abstract

Experimental equilibrium phase diagrams, tie-lines and plait points were obtained for ternary systems consisting of water, sodium chloride and: 1-propanol at 298 K; *n*-dodecylammonium chloride at 303 K; poly(ethylene glycol) 8000 at 333 K; poly (propylene glycol)-425 at 278, 298 and 333 K; poly(propylene glycol)-725 at 278 and 298 K. For the 1-propanol and polymer systems, most of the salt was in the bottom phase while the nonionic solute was concentrated in the top phase. In the *n*-dodecylammonium chloride system the salt was evenly distributed between the phases while most of the surfactant was in the top phase. For the poly(propylene glycol) systems, the size of the region of two liquid phases increases with molecular weight and temperature.

A modified form of the Flory-Huggins theory was developed for liquid-liquid equilibrium in binary aqueous systems of nonelectrolytes whose closed-loop phase diagrams contain both upper and lower consolute temperature points. The modification involved the assumption of an adjustable molecular size parameter r and new forms for the temperature dependence of the interaction parameter χ_{12}. Calculations were performed for 15 aqueous binary systems. The models correlated the liquid-liquid equilibrium data accurately.

Liquid-liquid equilibrium in aqueous biphasic salt systems was modelled using an expression for the excess Gibbs energy of the solution. The expression is based on modified forms of the Mean Spherical Approximation, the Bromley equation, and the Flory-Huggins theory. The model requires 3 and 5 adjustable parameters for ternary and quaternary systems, respectively. The model accurately correlated vapor– and liquid–liquid equilibrium data for 8 ternary and 3 quaternary aqueous biphasic salt systems.

Résumé

Les diagrammes d'équilibre de phase, compositions d'équilibre et les points critiques ont été génèrés pour les systèmes ternaires suivants: eau, chlorure de sodium avec soit du propanol-1 à 298 K ou du *n*-dodecyl chlorure d'ammonium à 303 K ou du poly(ethylène glycol) 8000 à 333 K ou du poly(propylène glycol)–425 à 278, 298 et 333 K ou du poly(propylène glycol)–725 à 278 et 298 K. Pour les systèmes polymériques et le propanol-1 la majuere partie du sel se trouvait dans la phase du bas et le soluté était concentré dans la phase du haut. Pour le système de *n*-dodecyl chlorure d'ammonium le sel était distribué uniformément entre les phases et le surfactant se trouvait dans la phase du haut. Pour les systèmes avec le poly(propylène glycol) la taille des régions liquides augmentait lorsque le poids moléculaire augmentait et lorsque la température augmentait.

L'équilibre liquide-liquide de systèmes binaires aqueux nonelectrolytes dont les diagrammes de phase contiennent les températures supérieures et inférieures de complête solubilité a été modelisé en faisant usage d'une forme modifiée de la théorie de Flory-Huggins. La modification de la théorie de Flory-Huggins consistait en la dérivation de fonctions exprimant la dépendance entre χ_{12} et la température. Les calculs ont été effectués pour 15 systèmes aqueux binaires. Les modèles étaient en accord avec les résultats expérimentaux.

L'équilibre liquide-liquide dans les systèmes salins aqueux biphasiques a été modélisé en faisant usage d'une expression pour l'excès d'énergie de la solution. Cette expression basée sur les formes modifiées de la Mean Spherical Approximation, l'équation de Bromley, et sur l'équation de la théorie de Flory-Huggins. Le modèle nécessite l'usage de 3 et 5 paramêtres ajustables pour les systèmes ternaires et quaternaires respectivement. Le modéle est en bon accord avec les données expérimentales pour les équilibres vapeur–liquide et liquide-liquide pour 8 systèmes ternaires et pour 3 systèmes quaternaires de solutions salines aqueuses biphasiques.

Acknowledgements

I am grateful to the following people and institutions for assisting me in carrying out various tasks related to the completion of this thesis:

- My supervisors, Professors Juan H. Vera and Martin E. Weber for their guidance and occasional criticism.
- Sarah Marx and Stephanie Gélinas for performing some of the experiments described in Chapter 3.
- Dr. G. Wilczek–Vera for her help in deriving some of the equations described in Chapter 4.
- Nicole Demarquette for translating the abstract.
- Gary Ng for proofreading the thesis.
- Jean Dumont, Ed Siliauskas and Bill Habib for help with experimental supplies and equipment maintenance.
- Veronica Calderhead and Henry Lim Soo for library assistance.
- The graduate students in the Workman Wing, Njuki, Adam and Mohammed who made my life at McGill tolerable.
- The Brace Research Institute and the Natural Sciences and Engineering Research Council of Canada for financial support.

Contents

Abstract i

Resume ii

Acknowledgements iii

Contents iv

List of Figures vii

List of Tables x

Nomenclature xii

1 Introduction 1

2 Liquid-Liquid Equilibrium in Binary Systems 7
- 2.1 The Flory-Huggins Theory 12
- 2.2 Molecular size: the evaluation of the "r" parameter 17
- 2.3 Modification of the $\chi_{12}(T)$ function 23
- 2.4 Results and Discussion 28

3 Liquid-Liquid Equilibrium Experiments 39
- 3.1 Experimental Materials and Methods 41
- 3.2 Equilibrium Experiments 49
- 3.3 Experimental Results and Discussion 52

4 Liquid-Liquid Equilibrium in Multicomponent Systems 84
4.1 Activities, Activity Coefficients, Reference and Standard States for Components of Liquid Solutions 87
4.1.1 Mole fraction based activity coefficients: nonelectrolyte solutions 87
4.1.2 Molality based activity coefficients: electrolytes 89
4.1.3 Multicomponent solutions containing electrolytes and nonelectrolytes 97
4.2 Calculation of Liquid-Liquid Equilibrium 103

5 An Excess Gibbs Energy Model for Multicomponent Liquid Systems 109
5.1 The Mean Spherical Approximation (MSA) model for $G^{E}_{ES\infty}$ 110
5.2 The Bromley Equation for G^{E}_{ES} 115
5.3 The Flory-Huggins Theory for G^{E}_{ESS} 123
5.4 The Bromley–Flory-Huggins model for G^{E} 126

6 Phase Equilibrium Calculations for Multicomponent Systems 128
6.1 Estimation of the values of parameters in G^{E} 128
6.2 Calculation of liquid-liquid equilibrium 141

7 Conclusions, Contributions and Recommendations 158
7.1 Conclusions 158
7.2 Original Contributions to Knowledge 160
7.3 Recommendations for Future Work 161

References 162

Appendices:

B Values of $\chi_{12}(T)$ parameters B-1
C Materials and calibration C-1
D Experimental results D-1
E Reference and standard states in multisolvent systems E-1
F The Born equation F-1
G The two-parameter Extended-Bromley equation G-1
H Integration of the Gibbs-Duhem equation to obtain γ_s from $\gamma_\pm$ . . . H-1

I Activity coefficient term from the MSA I-1
J Activity coefficient terms from the Bromley equation J-1
K Activity coefficient terms from the modified Flory-Huggins theory . K-1

List of Figures

1.1 A process involving an aqueous biphasic system for changing the salt content of brine 3

2.1 Phase diagram for poly(ethylene glycol) 2290-water (Saeki et al., 1976) 8
2.2 Phase diagram and $\chi_{12}(T)$ predicted by Flory-Huggins theory for $r = 30$ and $\Delta w = -465$ J mol^{-1} 15
2.3 Binary closed-loop phase diagram for polymer-water 18
2.4 Values of $\chi_{12}(T)$ for the n-butoxyethanol–water system with $r = 6.26$ 22
2.5 Polynomial correlation of χ_{12} with T for the n-butoxyethanol–water system 31
2.6 Experimental and calculated phase diagram for the n-butoxyethanol–water system 34
2.7 Experimental and calculated phase diagram for the poly(ethylene glycol) 2290–water system 35
2.8 Experimental and calculated phase diagram for the nicotine–water system 36
2.9 Experimental and calculated phase diagram for the C_8-lecithin–water system 37
2.10 Experimental and calculated $\chi_{12}(T)$ for the n-butoxyethanol–water system 38

3.1 Phase diagram for a typical biphasic salt–nonionic solute 2–water system 40
3.2 Refractive index calibration graph for 1-propanol–NaCl–water at 298 K 45
3.3 Incremental refractive index change versus propanol concentration . 46
3.4 Refractive index of a binary aqueous NaCl solution 47
3.5 Binodal curve for 1-propanol–NaCl–water 53
3.6 Binodal curve near the plait point 56

3.7 Phase volume ratios near the plait point 56
3.8 Complete phase diagram for 1-propanol–NaCl–water at 298 K . . . 57
3.9 Partition coefficient plot for 1-propanol–NaCl–water 59
3.10 Binodal curves for 1-propanol–NaCl–water 60
3.11 Binary phase diagram for DAC–water (Gault et al., 1988) 62
3.12 Solubility diagram for DAC–NaCl–water (Imae et al., 1988) 62
3.13 Binodal curve for DAC–NaCl–water 63
3.14 Partition coefficient plot for DAC–NaCl–water for 0.34M NaCl . . . 65
3.15 Binodal Curve for PEG 8000–NaCl–water 67
3.16 Partition coefficient plot for PEG 8000–NaCl–water 68
3.17 Cloud point curve for aqueous PPG 400 (redrawn from Malcolm and Rowlinson, 1957) 70
3.18 Binodal Curve for PPG 425–NaCl–water at 278 K 71
3.19 Binodal Curve for PPG 425–NaCl–water at 298 K 72
3.20 Binodal Curve for PPG 425–NaCl–water at 333 K 73
3.21 Binodal Curve for PPG 725–NaCl–water at 278 K 74
3.22 Binodal Curve for PPG 725–NaCl–water at 298 K 75
3.23 Complete phase diagram for PPG 425–NaCl–water at 298 K 76
3.24 Effect of temperature on the binodal curves of PPG 425–NaCl–water 78
3.25 Effect of molecular weight on the binodal curves of PPG–NaCl–water 80
3.26 Partition coefficient plot for PPG 425–NaCl–water at 298 K 81
3.27 Effect of temperature on partition coefficients for PPG 425–NaCl–water 82
3.28 Effect of molecular weight on partition coefficients of PPG–NaCl–water 83

4.1 Multicomponent liquid-liquid equilibrium 85
4.2 Hypothetical $\Delta\mu_2^{M^\theta} = 0$ surface for a water(1)-salt(2)-salt(3) system at fixed T and P. 96
4.3 Calculation of equilibrium compositions by minimizing G'. 108

5.1 Hard-sphere ion–dipolar solvent solution 112

6.1 Predictions of the MSA and Born equations for the solvation energy of Na^+ 132
6.2 Experimentally determined and calculated values of $\gamma_\pm$ for NaCl and Na_2SO_4 at 298 K. Experimental values are from Zemaitis et al. (1986) 134

6.3 Experimental and calculated values of P for the water–1-propanol binary system at 298 K (experimental values from Gmehling et al., 1977). The Flory-Huggins theory is denoted by FH. 139
6.4 Experimental and calculated values of y_2 for the water–1-propanol binary system at 298 K (experimental values from Gmehling et al., 1977). The Flory-Huggins theory is denoted by FH. 140
6.5 Experimental and calculated values of P for the water–PEG 3350 binary system at 298 K (experimental values from Haynes et al., 1989). The Flory-Huggins theory is denoted by FH. 142
6.6 Experimental and calculated binodal curves for the 1-propanol/ NaCl/water at 298 K 145
6.7 Experimental and calculated binodal curves for the 2-propanol/ NaCl/water at 298 K 146
6.8 Experimental and calculated binodal curves for the PEG 3350/ Na_2SO_4/water at 301 K 147
6.9 Experimental and calculated binodal curves for the PPG 425/NaCl/water at 298 K 148
6.10 Experimental and calculated binodal curves for the PPG 725/NaCl/water at 298 K 149
6.11 Experimental and calculated binodal curves for Dextran-70 and PEG 6000 in the presence of NaSCN at 296 K 152
6.12 Experimental (wt%E) and calculated (wt%C) binodal curves for Dextran-70 and PEG 6000 in the presence of Cs_2SO_4 at 296 K . . . 154
6.13 Experimental and calculated binodal curves for Dextran-70 and PEG 6000 in the presence of Na_2SO_4 at 296 K 156

C.1 Representative calibration plot for atomic absorption spectroscopy analysis of sodium C-4
C.2 Refractive index calibration plot for PEG 8000–NaCl–water at 298 K C-5
C.3 Refractive index calibration plot for PPG 425–NaCl–water C-7
C.4 Refractive index calibration plot for PPG 725–NaCl–water at 298 K C-9

E.1 Fugacity of salt in a binary system using the mean-ionic molality . . E-4
E.2 Fugacities of components in a binary system using mole fractions . E-5
E.3 A plot of $\ln f$ in a ternary two-solvent system (Van Ness and Abbott, 1982) E-10

List of Tables

1.1 Polymer, surfactant and salt additives forming two aqueous phases at ambient conditions* 4

2.1 Comparison of r values 29
2.2 Values of parameters for systems 33

3.1 Systems studied experimentally† 42

6.1 Systems studied 129
6.2 Marcus' ionic diameters 130
6.3 Dielectric constant values at 298 K 133
6.4 Values of the Bromley equation parameter (Zemaitis et al., 1986) . 133
6.5 Values of r determined using the ratio of molar volumes 135
6.6 Optimal values of χ_{12} and r for the Bromley-Flory-Huggins Model . 141
6.7 Optimal parameters for ternary systems 144
6.8 Experimental (wt%E) and calculated (wt%C) liquid-liquid equilibrium for the Dextran-70/PEG 6000/NaSCN/water system at 296 K 151
6.9 Experimental (wt%E) and calculated (wt%C) liquid-liquid equilibrium for the Dextran-70/PEG 6000/Cs_2SO_4/water system at 296 K 153
6.10 Experimental and calculated liquid-liquid equilibrium for the Dextran-70/PEG 6000/Na_2SO_4/water system at 296 K 155
6.11 Optimal parameters for quaternary systems 157

7.1 Systems studied experimentally 159

B.1 Temperature independent parameters for the one-bond model . . . B-2
B.2 Temperature independent parameters for the two-bond model . . . B-3
B.3 Temperature independent parameters for polynomial $\chi_{12}(T)$ B-4

B.4 Performance of different models — comparison of values of F_o as given by equation (2.54) B-5

C.1 Suppliers of materials used in experiments C-2
C.2 Refractive index data for 1-propanol–NaCl–water at 298 K C-3
C.3 Refractive index data for PEG 8000–NaCl–water at 298 K C-6
C.4 Refractive index data for PPG 425–NaCl–water at 298 K C-8
C.5 Refractive index data for PPG 725–NaCl–water at 298 K C-10

D.1 Results of turbidity titration for 1-propanol–NaCl–water at 298 K . D-3
D.2 Tie-line data for 1-propanol–NaCl–water at 298 K D-4
D.3 Results of turbidity titration for the plait point of 1-propanol–NaCl–water at 298 K D-5
D.4 Tie-line data for *n*-dodecylammonium chloride–NaCl–water at 303 K D-6
D.5 Tie-line data for poly(ethylene glycol) 8000–NaCl–water at 333 K . D-6
D.6 Tie-line data for poly(propylene glycol) 425 at 278 K D-7
D.7 Tie-line data for poly(propylene glycol) 425 at 298 K D-8
D.8 Tie-line data for poly(propylene glycol) 425 at 333 K D-9
D.9 Tie-line data for poly(propylene glycol) 725 at 278 K D-10
D.10 Tie-line data for poly(propylene glycol) 725 at 298 K D-11

Nomenclature

Upper Case Letters

A	Helmholtz energy; anion of an electrolyte; absorbance
$\mathcal{A}$	Debye-Hückel constant
B_m	Bromley equation parameter
$\mathcal{B}_m$	Bromley equation parameter
D_+, D_-	ion diameters
D_{S1}, D_{Sm}	solvent molecule size parameters
$\mathcal{E}_m$	Extended-Bromley equation parameter
F_o	objective function
G	Gibb's free energy
H	enthalpy
I	ionic strength
$\underline{\underline{J}}$	Jacobian matrix
K	dissociation factor for compounds
K_o	constant in MSA equation
M	molecular weight; electrolyte cation
N	number of points
N_C	total number of components
N_S	number of solvents
N_A	Avogadro's number
P	pressure
Q	canonical ensemble partition function
R	ideal gas constant
S	entropy
T	temperature
$\mathcal{T}$	reduced temperature
V	volume

Lower Case Letters

a	coefficients in polynomial expressions; activity
b	binary interaction parameter
c	concentration
e	electron charge
f	interchange free energy
$f(\xi)$	function of ξ
$g(\xi)$	function of ξ
k	Boltzmann's constant
m	molality
n	number of moles
r	number of segments in a molecule
v	molar volume
w	interchange energy; weight fraction
x	liquid phase mole fraction
y	vapor phase mole fraction
z	lattice coordination number; ion valence

Greek Letters

α	parameter in: $\chi_{12}(T)$ functions; activity coefficients
β	parameter in: $\chi_{12}(T)$ functions; activity coefficients
γ	parameter in: $\chi_{12}(T)$ functions; activity coefficients
ϵ	dielectric constant
ϵ_o	permittivity of free space
ζ	parameter in $\chi_{12}(T)$ functions
η	parameter in $\chi_{12}(T)$ functions
κ	constant in Bromley equation
λ	parameter in $\chi_{12}(T)$ functions
μ	chemical potential
ν	dissociation constant for electrolyte
ξ	dummy variable in excess Gibbs energy function

ρ	density
σ	parameter in $\chi_{12}(T)$ functions
ϕ	volume fraction
χ	Flory-Huggins binary interaction parameter
Δ	symbol denoting change
Φ	ionic strength constant
Ω_1, Ω_m	dummy variables in MSA expression

Superscripts

$-$	anionic
$+$	cationic
$*$	H-bonded state
$\bullet$	H-bonded state
θ	standard state
br	Bromley
E	excess property
e	experimentally determined value
ebr	Extended-Bromley
c	critical point value; calculated value
I, II	phase indices
M	mixing property
o	salt-free; non H-bonded

Subscripts

$\pm$	mean ionic property
ES	electrolyte-solvent interaction
ES$^\infty$	electrolyte-solvent interaction at infinite dilution
ESS	electrolyte-solvent-solvent interaction
i, j, k, ℓ	component indices
m	mixed-solvent
msa$^\infty$	mean spherical approximation at infinite dilution
mfi	modified Flory-Huggins theory

Chapter 1

Introduction

Conventional liquid-liquid extraction involves the contacting of two immiscible solvent phases, at least one of which is organic in nature. A variation of this technique, Aqueous Two-Phase Partitioning, is finding application in the separation of materials of biological origin. In this method, two liquid phases are created from a single homogeneous aqueous phase by the addition of one or more compounds. The additives are usually either two structurally different hydrophilic polymers, such as dextran and poly(ethylene glycol), or a polymer and a salt, such as poly(ethylene glycol) and potassium phosphate. It has been observed that many solutes of large molecular weight, including biomolecules such as proteins and enzymes, are unevenly distributed in such systems, with different components being preferentially retained in one of the phases (Albertsson, 1986; Walter et al., 1985; Greve and Kula, 1991a,b), thus providing a basis for separation.

The distinguishing feature between these and conventional liquid-liquid extraction solvent systems is that both phases are predominantly water, an environment suitable for labile biomolecules which do not survive organic solvents. The phases typically have water contents in excess of 65% by weight and low interfacial tensions, between 0.001 and 0.01 dyne/cm. By adjusting the temperature, polymer or

salt type, molecular weight and concentration of solutes, it is possible to vary the degree of partitioning of all species in the system.

It is generally accepted that the mechanism underlying the formation of aqueous two-phase systems is related to competition between hydrogen bonding and salting out processes (Gustafson et al., 1986; Ananthapadmanabhan and Goddard, 1987; Zaslavsky et al., 1989). Although the phase forming agents originally employed in aqueous two-phase systems were polymers, other solutes of lower molecular weight which hydrogen bond, such as aliphatic alcohols and both neutral and charged surfactants, will form biphasic systems with salts (Schott, 1973; De Santis et al., 1976; Firman et al., 1985; Imae et al., 1988; Greve and Kula, 1991b). These low molecular weight categories of aqueous two-phase systems have received little attention and many of the published experimental studies have involved incomplete determination of equilibrium phase diagrams.

In addition to their use as phase forming solvents for separating large molecules, biphasic salt systems also provide a method of separating components from each other. An example of a process for reducing or increasing the salt content of a stream of brine is shown in Figure 1.1. In this case, an example of which is the system poly(ethylene glycol)-Na_2SO_4-water, the addition of a polymer leads to two streams, one leaner and one richer in salt than the feed (Snyder et al., 1992). The salt-lean stream contains most of the polymer and in many cases the polymer can be recovered in a subsequent step, by changing the temperature to effect further liquid-liquid phase separation. The design, scale-up, and simulation of such a process requires phase equilibrium data and correlative thermodynamic models.

The main concern of this thesis is the experimental and modelling study of liquid-liquid equilibrium in biphasic aqueous systems which contain salt.

The experimental characterization of a given biphasic system involves the de-

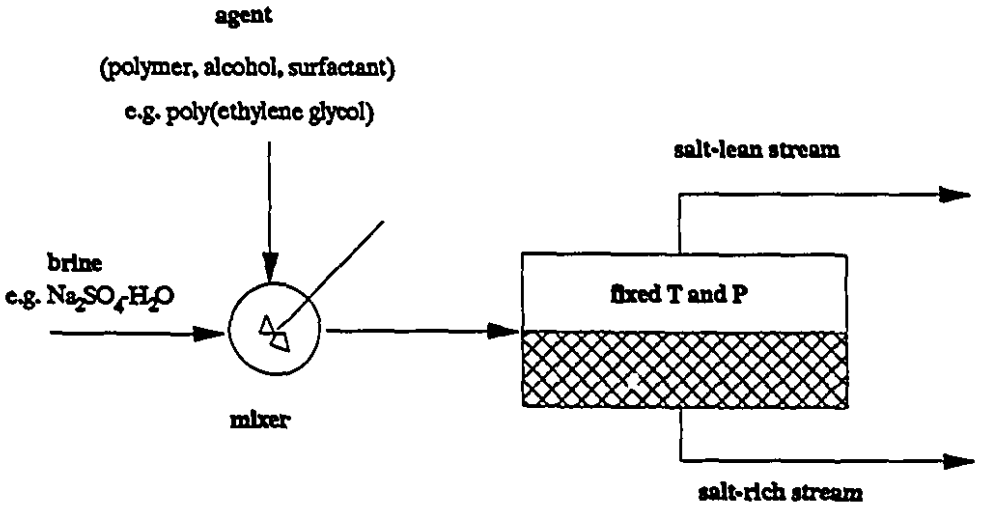

Figure 1.1: A process involving an aqueous biphasic system for changing the salt content of brine

termination of phase diagrams at a fixed temperature and pressure. At the onset of the project, a survey of the literature indicated that most published data were for polymer-polymer-water systems (Albertsson, 1986; Walter et al., 1985) and there was relatively little information for systems containing salt. A classification of the type of solutes (minimum number required) which form aqueous two-phase systems was drawn up and is displayed in Table 1. It is evident that a wide variety of compounds form two aqueous phases with water. It should be noted that in many of the biphasic systems formed by surfactants, one phase, although rich in water, is often of an anisotropic, liquid crystalline nature (Laughlin, 1978a,b; Tiddy et al., 1980).

An objective of this study is to conduct liquid-liquid equilibrium experiments for

Table 1.1: Polymer, surfactant and salt additives forming two aqueous phases at ambient conditions*

Additives	Type	Example
one polymer	nonionic	poly(propylene glycol)
	ionic	poly(acrylic acid)
two polymers	incompatible polymers	dextran–poly(ethylene glycol)
	compatible polymers	gelatin–gum arabic
polymer and salt	neutral polymer	Na_2SO_4–poly(ethylene glycol)
	charged polymer	NaCl–poly(ethylene sulfonate)
surfactant	nonionic	*n*-dodecyltetraoxyethylene glycol monoether
	zwitterionic	3-(nonyl-dimethylammonio)propyl sulfate
surfactant and salt	cationic	*n*-dodecylammonium chloride–NaCl

* both phases are primarily water (> 50 % by weight)

ternary aqueous systems containing NaCl.

Experiments carried out as part of this study, with the aim of collecting data for a process of the type illustrated in Figure 1.1 for separating aqueous solutions of NaCl, were for systems of the type alcohol-NaCl-water, surfactant-NaCl-water and polymer-NaCl-water.

The modelling component of this thesis involves the formulation of molecular thermodynamic models for multicomponent aqueous solutions containing polymers and salts. While the phase equilibria of solvent systems used in conventional liquid-liquid extraction are well understood, the same is not true of aqueous biphasic systems. Of these, the polymer-polymer-water variety, with or without biomolecules, has received the most attention, with the models proposed falling into two categories: those utilizing the osmotic virial expansion approach (Edmond and Ogston, 1968; King et al., 1988; Cabezas et al., 1990a) and those based on lattice models (Flory, 1953; Walter et al., 1985; Baksir et al., 1989; Diamond and Hsu, 1990).

When this study began, there were no comprehensive models in the literature for aqueous biphasic systems containing salt. Recently, four models have been proposed (Cabezas et al., 1990b; Gao et al., 1991a,b; Dahl and Macedo, 1992). The model of Cabezas et al. (1990b) is based on the solution theory of Hill (1957, 1960), a virial expansion approach with allowance made for the salt. It is able to predict and correlate the phase boundaries of biphasic polymer-salt systems but in its present form is limited in the number of solutes (2 polymers and one electrolyte) which it can handle. The first Gao (1991a) model is based on a combination of the UNIQUAC model for short-range intermolecular interactions and the Fowler–Guggenheim expression for long-range electrostatic interactions. It involves many adjustable parameters and several simplifying assumptions, including a dielectric constant that is independent of solvent composition. The Fowler-Guggenheim model used to ex-

press long-range interactions is inadequate for describing non-dilute solutions of the salt in the solvent, water. The second Gao (1991b) model, based on the empirical UNIFAC group contribution method and the Fowler–Guggenheim expression, has better predictive powers but suffers from the same limitations as the first model. The model of Dahl and Macedo, also based on UNIFAC through an equation of state, does not treat salts as dissociated species and thus is not realistic.

The second objective of this study is to develop thermodynamic models which will correlate phase equilibria for binary and multicomponent systems of the aqueous biphasic type.

In terms of the organization of this thesis, an introduction to liquid-liquid equilibrium and thermodynamic modelling is provided in Chapter 2, which discusses phase equilibria for binary hydrogen-bonded systems. In this chapter two original proposals for modifying the Flory-Huggins theory are made. Chapter 3 describes the methods used and results obtained in equilibrium experiments conducted as part of this study. The following chapter, 4, introduces thermodynamic concepts related to the modelling of multicomponent systems which contain salt. This leads to a presentation, in Chapter 5, of a new model for describing liquid-liquid equilibrium in these systems. Chapter 6 presents the results of phase boundary and tie-line calculations for multicomponent systems. Finally, the conclusions are summarized in Chapter 7, along with the claims to originality.

Chapter 2

Liquid-Liquid Equilibrium in Binary Systems

The phase diagrams of many aqueous binary mixtures contain regions where two liquid phases are formed. This phase behavior is sensitive to temperature and, depending on the solute, different trends are evident. For example, a dilute solution of water and poly(acrylic acid) of molecular weight 1.1 x 10^5 separates into two phases below about 5°C (Molyneux, 1975). This temperature is the *upper consolute temperature* of the system. On the other hand, an aqueous solution of poly(ethyloxazoline), homogeneous at room temperature, phase splits at temperatures above 63°C (Chen et al., 1990). This temperature is the *lower consolute temperature*, or cloud point, of the system.

Aqueous mixtures of other hydrophilic polymers, such as poly(ethylene glycol) [PEG], display both kinds of behavior; at relatively low or high temperatures and polymer concentrations the solutions are homogeneous, however at intermediate temperatures and compositions two phases are present. Figure 2.1 shows the phase behavior of an aqueous mixture of PEG of number average molecular weight 2290 as a function of temperature (Saeki et al., 1976). As illustrated in the figure, a mixture of 20 wt% PEG at 200°C separates into two phases containing 7 and 42.5 wt% PEG, respectively. This behavior, in which lower consolute temperature

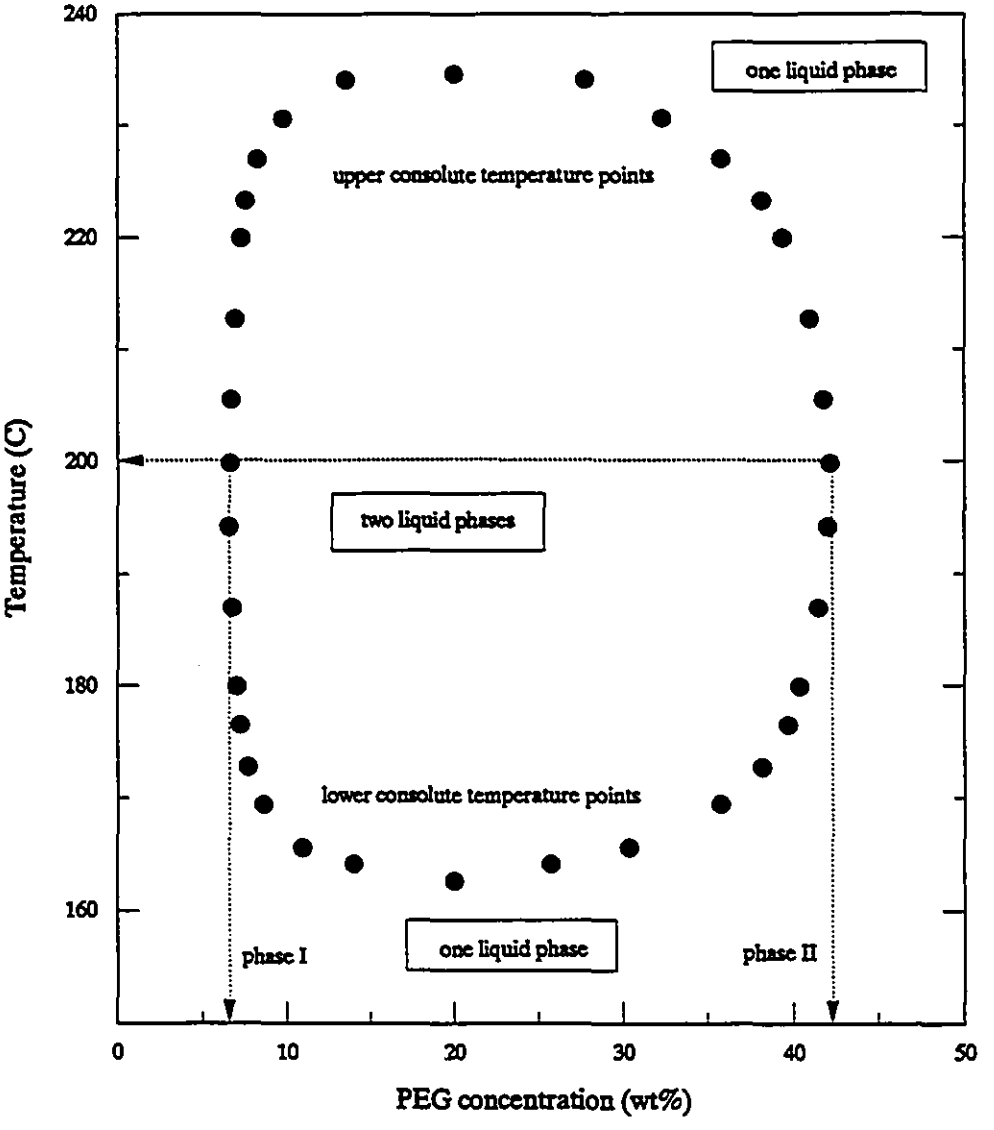

Figure 2.1: Phase diagram for poly(ethylene glycol) 2290-water (Saeki et al., 1976)

(LCT) and upper consolute temperature (UCT) points are present simultaneously, is a closed-loop solubility curve.

Closed-loop phase diagrams are not restricted to polymer solutions; the solutes may be of moderate molecular weight, such as nicotine and *n*-butoxyethanol. Many of the nonionic compounds used as phase forming materials in aqueous two-phase systems, such as poly(propylene glycol) and poly(vinyl alcohol), display similar behavior in binary solution (Malcolm and Rowlinson, 1957; Nord et al., 1951). Hence an understanding of this type of binary system may aid in modelling more complex ternary and quaternary systems.

For binary biphasic systems, the thermodynamic criterion for equilibrium is that the temperature, T, and pressure P, in both phases must be equal and the Gibbs free energy, G, should be at a minimum with respect to changes in T, P, and composition of the phases (Modell and Reid, 1974). The total free energy of a two phase system is a sum of contributions from the phases I and II:

$$G(T,P,\underline{n}) = G^I(T,P,\underline{n}^I) + G^{II}(T,P,\underline{n}^{II}) \tag{2.1}$$

where $\underline{n}$ is the vector of the number of moles of components in each phase. For a system at a fixed T and P the condition for equilibrium is that

$$dG(T,P,\underline{n}) = dG^I(T,P,\underline{n}^I) + dG^{II}(T,P,\underline{n}^{II}) = 0 \tag{2.2}$$

The minimum in the total derivative means that the partial derivatives of G with respect to the number of moles, the chemical potentials of the components, μ_i, are equal in phases I and II.

$$\mu_i^I(T,P,\underline{n}^I) = \mu_i^{II}(T,P,\underline{n}^{II}) \qquad i = 1,2 \tag{2.3}$$

where for each phase,

$$\mu_i(T,P,\underline{n}) = \left[\frac{\partial G(T,P,\underline{n})}{\partial n_i}\right]_{T,P,n_{j\neq i}} \tag{2.4}$$

and

$$G(T,P,\underline{n}) = \sum_i n_i \mu_i(T,P,\underline{n}) \tag{2.5}$$

Thermodynamic modelling involves the formulation of equations for G, the derivatives of which are then used to calculate equilibrium compositions through equation (2.3).

As early as 1937, Hirschfelder et al. suggested that the presence of closed-loop immiscibility gaps was due mainly to the presence of strong, highly directional short-range intermolecular interactions. In aqueous solutions the most common interaction of this type is hydrogen-bonding. At low temperatures, the solution is miscible over the whole composition range, with many H-bonds between unlike molecules. As the temperature is increased, bonds are broken and phase separation results. At even higher temperatures complete miscibility is restored due to entropic effects arising from enhanced thermal motion of the molecules.

There have been many attempts to model the phase behavior of such systems. One category of models uses incompressible lattice theories which take into account individual site-specific interactions (H-bonding) between the components in solution. Most of these models are based on the Ising model of ferromagnetism (Wheeler, 1975; Andersen and Wheeler, 1978; Walker and Vause, 1983; Goldstein and Walker, 1983; Kim and Kim, 1988). Although this approach has produced accurate predictions of phase boundaries for binary systems where the solute is of low molecular weight, it is difficult to apply to polymers or to generalize for

multicomponent solutions.

Simpler lattice models which utilize the mean-field approximation have been proposed. These include the Flory-Huggins theory (Flory, 1953), other mean-field Flory-based lattice models (Kjellander and Florin, 1981; Karlström, 1985) and various quasichemical models (Barker and Fock, 1953; Bodegom and Meijer, 1984; Panayiotou and Vera, 1984; Prange et al., 1989). Models which do not use the mean-field approximation, such as Freed's lattice field theory, have also been used to describe closed-loop phase diagrams (Freed, 1985; Hu et al., 1991; Hino et al., 1992). Some approaches have taken into account volumetric mixing effects using lattice-based equations of state (Sanchez and Lacombe, 1978; Sanchez and Balazs, 1989; Panayiotou and Sanchez, 1992) and free-volume theories for polymer solutions (Flory, 1965; Patterson et al., 1967; Patterson and Delmas, 1969; Saint-Victor, 1988)[1].

While many of the models cited above have succeeded in the quantitative correlation of phase boundaries, they are not amenable to direct extension to ternary and multicomponent systems containing salt. There is a need for a simple solution model which can provide accurate predictions of phase boundaries for binary systems and yet be readily generalized for ternary and more complex mixtures. The Flory-Huggins theory (Flory, 1953) is suitable for this purpose and this chapter presents modifications of this model, which permit representation of closed-loop phase diagrams.

[1]If the temperature of the system is well below the pure solvent's critical temperature, as is the case in most aqueous biphasic systems, free volume effects are not expected to be important (Robard, 1978).

2.1 The Flory-Huggins Theory

The Flory-Huggins theory describes the Gibbs free energy change in mixing a pure solvent(1) and a monodisperse polymer(2). The free energy change, ΔG_m, consists of two parts, an enthalpic (ΔH_m) and an entropic (ΔS_m) contribution.

$$\Delta G_m = \Delta H_m - T\Delta S_m \tag{2.6}$$

In solution thermodynamics, compositions are usually expressed as mole fractions, x_i. For a binary phase

$$x_1 = \frac{n_1}{n_1 + n_2} \qquad \text{and} \qquad x_2 = 1 - x_1 \tag{2.7}$$

However, for polymer solutions where there is a large difference in the molecular sizes of the components, volume fractions, ϕ_i, which better reflect size asymmetry, are used.

$$\phi_1 = \frac{n_1}{n_1 + rn_2} \qquad \text{and} \qquad \phi_2 = 1 - \phi_1 \tag{2.8}$$

The parameter r reflects the difference in size between polymer and solvent molecules. In lattice models, it is interpreted as the number of lattice sites occupied by one molecule of polymer, assuming each solvent molecule and each polymer segment occupies one site. The change in entropy due to mixing, ΔS_m, is obtained by estimating all possible configurations which molecules of the solution can adopt, along with their associated probabilities. The Flory-Huggins expression for ΔS_m is (Flory, 1953)

$$\Delta S_m = -R[n_1 \ln \phi_1 + n_2 \ln \phi_2] \tag{2.9}$$

where R is the ideal gas constant. The Flory-Huggins enthalpy change on mixing, ΔH_m, is calculated using the van Laar, or regular solution, expression:

$$\Delta H_m = RT(n_1 + rn_2)\phi_1\phi_2\chi_{12}(T) \tag{2.10}$$

The dimensionless temperature-dependent parameter $\chi_{12}(T)$ characterizes the enthalpy change in mixing a solvent molecule and a polymer segment. It is related to the coordination number of the lattice[2], z, and the interchange energy, $-\Delta w$, by the following expression

$$\chi_{12}(T) = -\frac{z\Delta w}{2RT} \tag{2.11}$$

The interchange energy $-\Delta w$ is the energy change involved in breaking a solvent-solvent molecule contact (-w_{11}) and a polymer-polymer segment contact (-w_{22}) to form two solvent-polymer segment contacts (w_{12}).

$$\Delta w = w_{11} + w_{22} - 2w_{12} \tag{2.12}$$

The chemical potentials of the polymer and solvent, relative to their standard states, can be obtained from ΔG_m by differentiation

$$\mu_i = \mu_i^\circ + \left[\frac{\partial \Delta G_m}{\partial n_i}\right]_{T,P,n_{j\neq i}} \tag{2.13}$$

The chemical potential of the solvent is given by

$$\mu_1 = \mu_1^\circ + RT\left[\ln\phi_1 + (1 - \frac{1}{r})\phi_2 + \chi_{12}(T)\phi_2^2\right] \tag{2.14}$$

[2]Number of molecules or polymer segments directly neighboring a given solvent molecule.

where μ_1° is the standard state chemical potential. The corresponding expression for the polymer is

$$\mu_2 = \mu_2^\circ + RT\left[\ln \phi_2 - (r-1)\phi_1 + r\chi_{12}(T)\phi_1^2\right] \tag{2.15}$$

For a given temperature, once a value for Δw is chosen, $\chi_{12}(T)$ can be calculated using equation (2.11). This value of $\chi_{12}(T)$ can be used in the expressions for the chemical potentials, equations (2.14) and (2.15). The chemical potentials are substituted into equations (2.3), and these two equations solved simultaneously for ϕ_2^I and ϕ_2^{II}, the polymer volume fractions in the co-existing phases. If this is done for different temperatures, it is observed that the theory predicts phase separation only when $\chi_{12}(T)$ has a magnitude greater than that corresponding to the value at the upper *critical consolute temperature*, which is the maximum temperature in the two-phase region. The thermodynamic stability criteria defining this temperature are (Hill, 1960)

$$\frac{\partial \mu_1}{\partial \phi_2} = 0 \tag{2.16}$$

and

$$\frac{\partial^2 \mu_1}{\partial \phi_2^2} = 0 \tag{2.17}$$

In the Flory-Huggins theory Δw is considered to be independent of composition and temperature and hence, as shown by equation (2.11), the $\chi_{12}(T)$ parameter is inversely proportional to temperature and the theory predicts two-phase co-existence only at low temperatures, i.e. only UCT behavior. Figure 2.2 shows typical predictions of the Flory-Huggins model for a polymer solution. In this sample calculation $r = 30$ and $\Delta w = -465$ J mol^{-1}. The failure to predict an immiscibility loop is

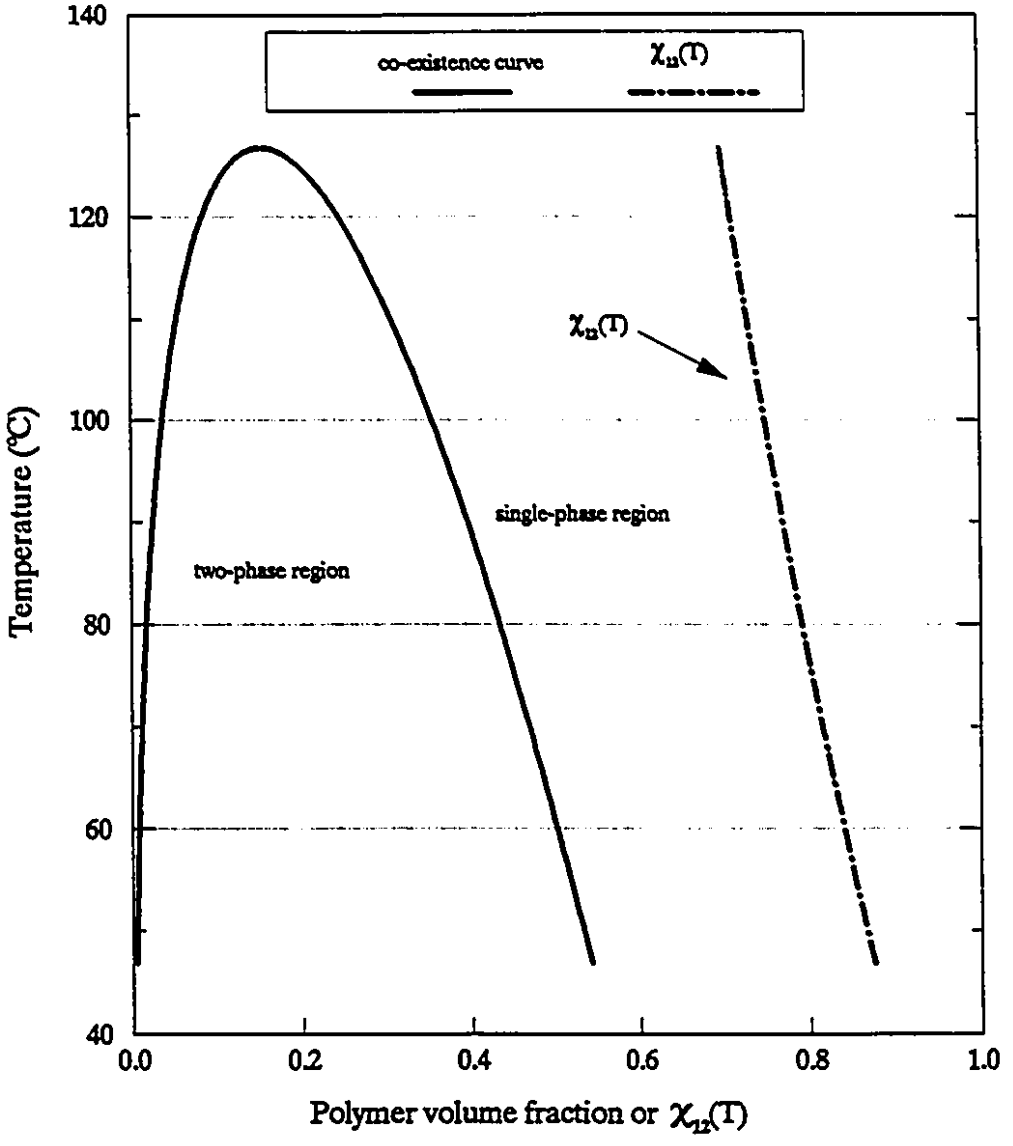

Figure 2.2: Phase diagram and $\chi_{12}(T)$ predicted by Flory-Huggins theory for $r = 30$ and $\Delta w = -465$ J mol^{-1}

inherent in the formulation of the theory, which does not explicitly take into account any directional interactions or volumetric changes on mixing. Experimental determinations of $\chi_{12}(T)$ from vapor pressure and heat of mixing measurements are inconsistent (Flory, 1953), prompting the phenomenological interpretation of $-\Delta w$ as an interchange free energy with enthalpic (Δw_H) and entropic (Δw_S) contributions

$$\Delta w_G = \Delta w_H - T\Delta w_S \tag{2.18}$$

and thus

$$\chi_{12}(T) = \chi_H + \chi_S = -\frac{z\Delta w_H}{RT} + \frac{z\Delta w_S}{R} \tag{2.19}$$

In order to predict LCT behavior, the temperature dependence of this parameter requires modification. One such modification is that proposed by Patterson et al. (1967). In this case the free volume of the solution, determined from an equation of state, is taken into account in the expression for $\chi_{12}(T)$. However, this model does not permit the representation of closed-loop phase diagrams[3] (Saeki et al., 1976).

In this chapter the relationship between χ_{12} and temperature for binary systems is examined. In Chapter 5 the dependence of χ_{12} on composition for ternary and more complex mixtures containing salts is discussed. The next section describes two new methods for evaluating the size parameter r, which is used in calculating volume fractions.

[3]For many binary systems $\chi_{12}(T)$ is found experimentally to be a function not only of temperature but also of composition (Orwoll, 1977). As a result, several expressions relating $\chi_{12}(T)$ to composition have been developed (Orofino and Flory, 1957; Panayiotou and Vera, 1984; Qian et al., 1991a,b).

2.2 Molecular size: the evaluation of the "r" parameter

Binary phase diagrams of the closed-loop type are plots of temperature versus the composition of one of the components. Since commercial polymers and surfactants are polydisperse, experimental compositions are usually expressed as mass fractions. For a binary system, the mole fraction x_i is related to the molecular weights M_i, and mass fractions w_i as follows:

$$x_2 = \frac{w_2/M_2}{w_1/M_1 + w_2/M_2} \tag{2.20}$$

Lattice models of polymer solutions normally express composition in terms of volume fractions ϕ_i. For compound 2 in a binary system,

$$\phi_2 = \frac{rx_2}{x_1 + rx_2} = \frac{1}{1 + (1/r)(x_1/x_2)} \tag{2.21}$$

where r is related to the relative size of polymer and solvent molecules. The value of r is often calculated as the ratio of the molar volume of the pure polymer to that of the pure solvent (Flory, 1953):

$$r = \frac{v_2}{v_1} \tag{2.22}$$

For phase diagrams which are not symmetric about a mole fraction of 0.5, which is the majority of experimentally determined cases, agreement between theory and experiment is improved through the use of an empirically determined parameter similar to r (Johnston et al., 1983). Most commercial water soluble polymers are polydisperse and do not have a unique value of r. Many aqueous solutes displaying closed-loop profile phase diagrams have relatively low molecular weights (n-butoxyethanol, nicotine, lutidine, etc) and are not consistent with the repeating

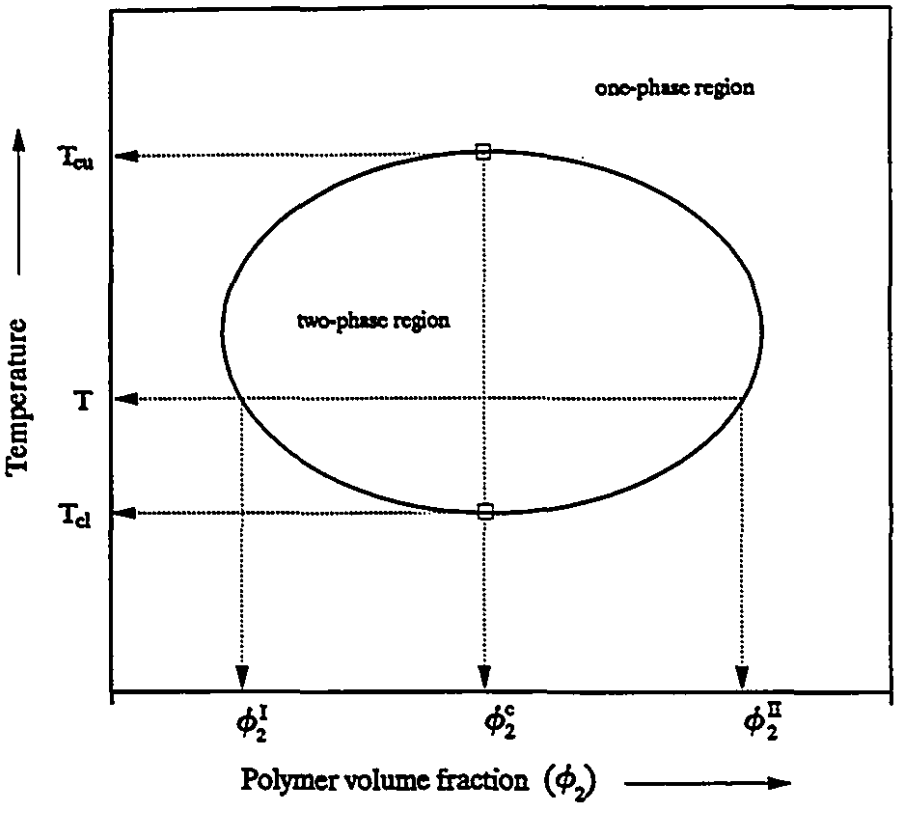

Figure 2.3: Binary closed-loop phase diagram for polymer-water

unit point of view. Since calculations with the Flory-Huggins model with values of r determined from pre-mixing volume ratios gave poor results, two methods of obtaining r were devised.

In the first method the volume fraction at the critical consolute temperature, ϕ_2^c in Figure 2.3, is matched to the critical weight fraction[4] determined experimentally, w_2^c. This is possible since the solutions of the two equations (2.16-17), which apply

[4]The weight fraction at the lower or upper critical consolute temperature

at the critical point, yield expressions for the critical volume fraction and the critical value of $\chi_{12}(T)$ in terms of r. For the Flory-Huggins theory, the expression relating the critical volume fraction to r is:

$$\phi_2^c = \frac{1}{1+\sqrt{r}} \tag{2.23}$$

At the critical point, equation (2.21) gives

$$\phi_2^c = \frac{1}{1+(1/r)(x_1^c/x_2^c)} \tag{2.24}$$

Comparison of equations (2.23) and (2.24) yields

$$r^{3/2} = \frac{x_1^c}{x_2^c} = \frac{(w_1^c/w_2^c)}{(M_1/M_2)} \tag{2.25}$$

This method, although rigorous, has the disadvantage that in practice the critical weight fraction is known only approximately. The temperature versus composition curve is quite flat in the critical region and the exact maximum is difficult to locate (see Figure 2.1). For polymer solutions, the situation is aggravated by the uncertainty in the knowledge of the molecular weight of the polymer.

The second method is useful if two experimental points on the co-existence curve are available (for a fixed temperature, such as T in Figure 2.3). Using the Flory-Huggins theory, two values of $\chi_{12}(T)$ are calculated by equating the chemical potentials for each component, as given by equations (2.14) and (2.15), in the different phases. For the solvent, using equation (2.14), the following expression is obtained, where ϕ_i^I and ϕ_i^{II} are the volume fractions of compound i in each of the

equilibrium phases:

$$\chi_{12}^1(T) = \frac{1}{(\phi_2^I)^2 - (\phi_2^{II})^2}\left\{\ln\frac{\phi_1^{II}}{\phi_1^I} + \left(1 - \frac{1}{r}\right)(\phi_2^{II} - \phi_2^I)\right\} \tag{2.26}$$

A similar expression for the polymer, obtained from equation (2.15), is

$$\chi_{12}^2(T) = \frac{1}{r\,[(\phi_1^I)^2 - (\phi_1^{II})^2]}\left\{\ln\frac{\phi_2^{II}}{\phi_2^I} - (1-r)(\phi_2^I - \phi_2^{II})\right\} \tag{2.27}$$

According to the Flory-Huggins theory there is one value of $\chi_{12}(T)$ at a given temperature, Hence the following relation should hold independent of the temperature variation of χ_{12}:

$$\chi_{12}^1(T) = \chi_{12}^2(T) = \chi_{12}(T) \tag{2.28}$$

In general, however, if a value of r, obtained either from a match of critical points or from a ratio of molar volumes, is used to calculate ϕ_i^I and ϕ_i^{II} with experimentally determined mole fractions, using equation (2.21), and these values are substituted into equations (2.26) and (2.27), the result is that $\chi_{12}^1(T) \neq \chi_{12}^2(T)$. Combination of equations (2.26) and (2.27), and elimination of $\chi_{12}(T)$ yields a single equation in which the only parameter is r.

$$\frac{1}{(\phi_2^I)^2 - (\phi_2^{II})^2}\left\{\ln\frac{\phi_1^{II}}{\phi_1^I} + \left(1 - \frac{1}{r}\right)(\phi_2^{II} - \phi_2^I)\right\} -$$

$$\frac{1}{r\,[(\phi_1^I)^2 - (\phi_1^{II})^2]}\left\{\ln\frac{\phi_2^{II}}{\phi_2^I} - (1-r)(\phi_2^I - \phi_2^{II})\right\} \;=\; 0 \tag{2.29}$$

For data which are perfectly represented by the Flory-Huggins theory, the effective value of r satisfying equation (2.29), and hence the equality of the chemical po-

tential of each compound in both phases is the *same* for *all* data points (for different temperatures and compositions). However for most data this is only approximately true. If r is evaluated from a single experimental point at a temperature between the upper and lower critical consolute temperatures, and this value is used to calculate equilibrium compositions at different temperatures, calculated compositions deviate from the experimental data.

If experimental data for several temperatures are available, it is preferable to choose the value of r that best satisfies equation (2.29) for all temperatures for which experimental data are available. Hence the optimal effective r is the value of r that minimizes the objective function F_o, given by

$$F_o = \frac{1}{N_E} \sum_{i=1}^{N_E} \mid \chi_{12}^1(T) - \chi_{12}^2(T) \mid \tag{2.30}$$

where N_E is the number of experimental points[5].

For most aqueous biphasic systems with immiscibility gaps, the effective value of r, minimizing equation (2.29), yields only small differences in $\chi_{12}^1(T)$ and $\chi_{12}^2(T)$ indicating that the Flory-Huggins method is suitable for correlating equilibrium data. As an example, the effective value of r for the system n-butoxyethanol—water is 6.26, and Figure 2.4 shows values of $\chi_{12}^1(T)$ and $\chi_{12}^2(T)$, calculated according to equations (2.25) and (2.26) using experimental data for temperatures lying between the lower and upper critical consolute points.

[5]Although other objective functions, such as a sum of the squares of differences may be used, the absolute difference was chosen in order to favor the middle range of temperature between the upper and lower critical consolute temperatures.

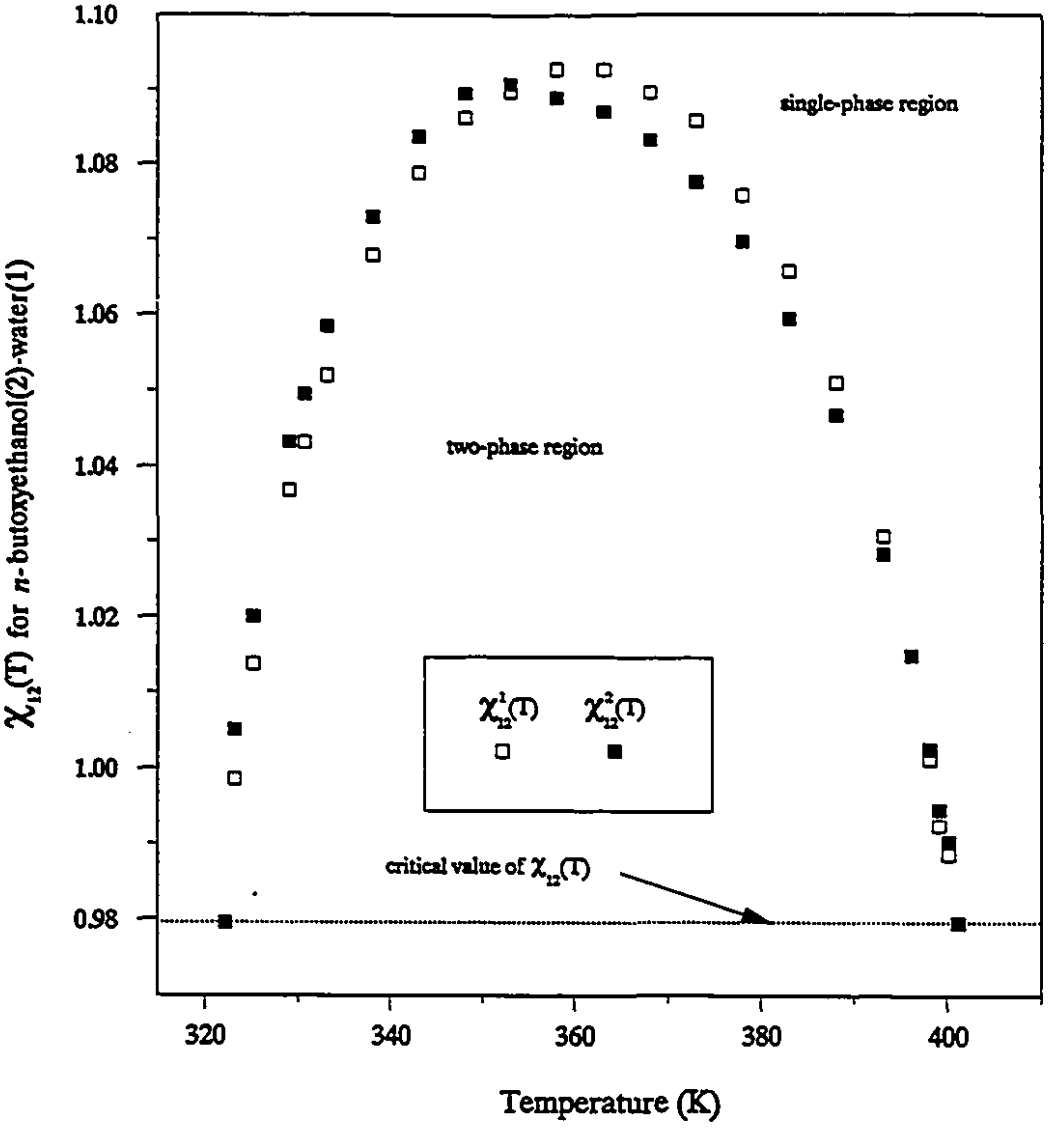

Figure 2.4: Values of $\chi_{12}(T)$ for the n-butoxyethanol–water system with $r = 6.26$

2.3 Modification of the $\chi_{12}(T)$ function

As shown in Figure 2.2, the Flory-Huggins theory in its original form cannot represent closed-loop phase diagrams. This section describes two proposals for representing the variation of χ_{12} with temperature. The first approach is based on the partition function method of statistical mechanics while the second uses a polynomial function.

The first approach is a generalization of a model proposed by Goldstein (1984, 1985). His ideas are extended by assuming two energetically different states of hydrogen-bonding in the solution. As discussed in Section 2.1, experiments indicate that χ_{12} contains both enthalpic and entropic contributions, and the Flory-Huggins interchange energy $-\Delta w$ is an interchange free energy. Hence equation (2.11) can be expressed as

$$\chi_{12}(T) = -\frac{z\Delta f}{2RT} \tag{2.31}$$

where $-\Delta f$ is a temperature-dependent free energy change involved in the breakup of a solvent–solvent molecule contact (of free energy f_{11}°) and a polymer–polymer segment contact (of free energy f_{22}°), both contacts of which are not H-bonded, to form two H-bonded solvent molecule–polymer segment contacts (of free energy $f_{12}^{\circ *\bullet}$). In this study it is further assumed that the solvent molecule and polymer segments form H-bonds with two energetic levels, one level being denoted by an asterisk ($*$) and another by a bullet ($\bullet$). Following equation (2.12), the interchange free energy is

$$\Delta f = f_{11}^{\circ} + f_{22}^{\circ} - 2f_{12}^{\circ *\bullet} \tag{2.32}$$

The solvent molecule-solvent molecule and polymer segment-polymer segment free energies can be expanded in enthalpic (H°_{ii}) and entropic (S°_{ii}) contributions as

$$f^{\circ}_{11} = H^{\circ}_{11} - TS^{\circ}_{11} \tag{2.33}$$

and

$$f^{\circ}_{22} = H^{\circ}_{22} - TS^{\circ}_{22} \tag{2.34}$$

For the H-bonded states, if volumetric effects are ignored, the Gibbs free energy is assumed to equal the Helmholtz energy, A_{12}. The Helmholtz free energy can be evaluated from a partition function, Q_{12}, valid for the canonical ensemble, using the following relation (Hill, 1960).

$$f^{\circ *\bullet}_{12} \quad = \quad G_{12} \quad \simeq A_{12} \quad = \quad -RT \ln Q_{12} \tag{2.35}$$

The partition function is a sum over all energy states of the system, which depend on all possible microscopic configurations of all molecules, weighted by their probabilities (Hill, 1960). Here, following Goldstein, it is assumed that bulk averaging of these states leads to three favored states: two with and one without H-bonding. Hence the following form is adopted for the Q_{12}.

$$f^{\circ *\bullet}_{12} = \exp(-\frac{f^{\circ}_{12}}{RT}) + \exp(-\frac{f^{*}_{12}}{RT}) + \exp(-\frac{f^{\bullet}_{12}}{RT})$$

$$= \exp(-\frac{f^{\circ}_{12}}{RT}) \left[1 + \exp(\frac{f^{\circ}_{12} - f^{*}_{12}}{RT}) + \exp(\frac{f^{\circ}_{12} - f^{\bullet}_{12}}{RT})\right] \tag{2.36}$$

where f°_{12} is the free energy in a non H-bonded state, f^{*}_{12} is the free energy of an H-bonded state ($*$) and $f^{\bullet}_{12}$ is the free energy of an H-bonded state ($\bullet$). Each of

these free energies can be expanded in enthalpic and entropic contributions:

$$f_{ii}^{\theta} = H_{ii}^{\theta} - TS_{ii}^{\theta} \tag{2.37}$$

Substitution of equations (2.32–36) in (2.31) yields the expression

$$\frac{\chi_{12}(T)}{z} = \alpha + \frac{\beta}{T} - \ln\left[1 + \exp(\frac{\gamma}{T} + \sigma) + \exp(\frac{\zeta}{T} + \lambda)\right] \tag{2.38}$$

where the parameter α is related to the non H-bonding interchange entropy difference by

$$\alpha = \frac{1}{2R}(S_{11}^{\circ} + S_{22}^{\circ} - 2S_{12}^{\circ}) \tag{2.39}$$

and σ and λ express the scaled entropy change on forming H-bonds:

$$\lambda = -\frac{1}{R}(S_{12}^{\circ} - S_{12}^{\bullet}) \tag{2.40}$$

and

$$\sigma = -\frac{1}{R}(S_{12}^{\circ} - S_{12}^{=}) \tag{2.41}$$

The parameter β is the related to the interchange enthalpy difference by

$$\beta = -\frac{1}{2R}(H_{11}^{\circ} + H_{22}^{\circ} - 2H_{12}^{\circ}) \tag{2.42}$$

while the parameters γ and ζ are scaled enthalpy changes in the formation of H-bonds

$$\gamma = \frac{1}{R}(H_{12}^{\circ} - H_{12}^{\bullet}) \tag{2.43}$$

and

$$\zeta = \frac{1}{R}(H_{12}^{\circ} - H_{12}^{*}) \tag{2.44}$$

Equation (2.38), which expresses the relation between χ_{12} and T for a system which has two levels of H-bonding, is referred to as the "two-bond" model. If only one level of H-bonding(*) is present, the third term in Q_{12} is zero and the following "one-bond" model for $\chi_{12}(T)$ results

$$\frac{\chi_{12}(T)}{z} = \alpha + \frac{\beta}{T} - \ln\left[1 + \exp(\frac{\gamma}{T} + \sigma)\right] \tag{2.45}$$

By neglecting the α parameter, which is the scaled (non H-bonding) interchange entropy, Goldstein's (1984) model is recovered:

$$\frac{\chi_{12}(T)}{z} = \frac{\beta}{T} - \ln\left[1 + \exp(\frac{\gamma}{T} + \sigma)\right] \tag{2.46}$$

Saint-Victor (1988) has combined equation (2.46) with a free volume contribution using an equation of state in order to model the closed-loop phase behavior of H-bonded systems.

In the second approach a polynomial is used to represent $\chi_{12}(T)$. This empirical function has the form

$$\chi_{12}(T) = \sum_{i=0}^{5} a_i \mathcal{T}^i \tag{2.47}$$

where $\mathcal{T}$ is a reduced temperature, $\mathcal{T} = T/1000$.

In this study four expressions are used to model $\chi_{12}(T)$: the "two-bond" model, equation (2.38); the "one-bond" model, equation (2.45); Goldstein's model, equation (2.46); and the "polynomial" function, equation (2.47). Each of these models

is capable of representing closed-loop phase diagrams as well as phase diagrams which contain only UCT or LCT points. The numerical values of the parameters in each of the models are determined using experimental data. The upper and lower critical consolute temperatures are used to determine two of the parameters in each model. A detailed discussion of these procedures is presented in Appendix A.

For a given temperature, the calculation of points (ϕ_2^I and ϕ_2^{II}) on the coexistence curve requires the simultaneous solution of expressions equating the chemical potentials in the two equilibrium phases. Applying equations (2.14) and (2.15) to phase I and phase II and rearranging yields

$$F_1(\phi_2^I, \phi_2^{II}) = \frac{\mu_1^I - \mu_1^{II}}{RT} = 0 \tag{2.48}$$

$$F_2(\phi_2^I, \phi_2^{II}) = \frac{\mu_2^I - \mu_2^{II}}{RT} = 0 \tag{2.49}$$

which can be expressed in vector form as

$$\underline{F}(\underline{\phi_2}) = 0 \tag{2.50}$$

These equations were solved using the Newton-Raphson method (Carnahan et al., 1969) where successive estimates of the polymer volume fractions were calculated with the aid of a Jacobian matrix ($\underline{\underline{J}}$) of partial derivatives

$$\Delta\underline{\phi_2} = \underline{\underline{J}}^{-1}\underline{F} \tag{2.51}$$

where in going from the i-th to the i+1-th iteration

$$\Delta\underline{\phi_2} = \underline{\phi_2}^{i+1} - \underline{\phi_2}^{i} \tag{2.52}$$

and the elements of $\underline{\underline{J}}$ are

$$J_{iI} = \frac{\partial F_i}{\partial \phi_2^I} \quad ; \quad J_{iII} = \frac{\partial F_i}{\partial \phi_2^{II}} \quad i = 1,2 \tag{2.53}$$

Initial estimates of ϕ_2^I and ϕ_2^{II} were supplied by experimentally determined compositions. Near both critical temperatures the results often converged to the trivial solution in which both phases have the same composition. This problem arose because the elements of the Jacobian matrix became zero, as evident from equations (2.16) and (2.17) which define the critical point. Use of initial estimates with large differences in the composition of the two phases helped to overcome this problem.

2.4 Results and Discussion

Liquid-liquid equilibrium compositions were calculated for fifteen aqueous systems using the four models described in the previous section. Three involve a high molecular weight polymer, poly(ethylene glycol), while the other systems involve solutes of lower molecular weight. All of the systems except one, C_8-lecithin[6]–water, exhibit closed-loop phase diagrams. The solute in the latter system is a nonionic surfactant and the system has an UCT solubility curve. It is included as an example of the application of the models to a nonionic surfactant system, and to illustrate that the model can handle systems with only UCT or LCT behavior.

A comparison of the values of r calculated using three different methods is presented in Table 2.1 The first column displays values of r calculated as the ratio of the molar volume of the solute to the solvent while the other two are obtained using the methods of Section 2.2. The selection of the optimal value of r required the minimization of the objective function (2.29). Minimizations were performed

[6] C_8-lecithin is 1,2-dioctanonyl-*sn*-glycerol-3-phosphocholine

Table 2.1: Comparison of r values

System	r-value				Data reference
	Molar volume† eq. (2.22)	Critical match eq. (2.25)	Optimal eq. (2.30)	Average Deviation‡ for optimal r	
PEG 2 290	117.0*	68.0	60.8	0.001	a
PEG 2 270	116.0*	63.4	57.2	0.001	a
PEG 2 180	111.3*	50.9	54.5	0.000	a
1-Aza Cycloheptane	6.38	5.10	5.16	0.036	b
i-Butoxyethanol	7.28	7.12	5.52	0.006	b
n-Butoxyethanol	7.38	7.35	6.26	0.004	b
2,6-Dimethyl pyridine	6.39	5.61	5.00	0.012	b
2-Methylpiperidine	6.53	8.04	4.53	0.038	b
3-Methylpiperidine	6.52	6.66	4.82	0.053	b
4-Methylpiperidine	6.35	5.61	5.90	0.023	b
Nicotine	8.93	6.26	5.34	0.021	b
1-Propoxy-2-propanol	7.39	6.17	4.46	0.007	b
2-Propoxy-1-propanol	7.47	5.61	4.78	0.006	b
Tetrahydrofuran	4.51	2.52	2.44	0.006	b
C_8-Lecithin	—	99.93	114.3	0.005	◇

† using density data from CRC (1986), unless specified otherwise.

‡ average deviation $= \frac{1}{N_E} \sum_{i=1}^{N_E} \mid \chi_{12}^1(T) - \chi_{12}^2(T) \mid$

* using polymer density data from the Aldrich Chemical Company, Inc.
b) Sørensen and Arlt (1980a)
a) Saeki et al. (1976)
◇ UCT system, using data from Blankschtein et al. (1985).

using a routine based on Powell's multidimensional method, without derivatives, as implemented by Press et al. (1989). In general, the values of r determined by the three techniques reflect molecular size. The values obtained for the polymers using molar volume ratios are higher than those obtained using the other two methods. The fourth column shows that the average deviation of the two values of $\chi_{12}(T)$ is small when the optimal value of r is utilized, thus indicating that the Flory-Huggins theory represents the data well.

The results of the three H-bonding models are compared with the predictions of the polynomial function for $\chi_{12}(T)$. As described in Appendix A, the coefficients of this polynomial were found using experimental information in the form of T and $\chi_{12}(T)$ values which are, for a given temperature, the mean of $\chi^1_{12}(T)$ and $\chi^2_{12}(T)$. Figure 2.5 shows polynomial fits of the mean $\chi_{12}(T)$ for n-butoxyethanol—water, using coefficients determined with the method described in Appendix A. For this system, which has co-existence loop of a typical shape, a fifth order polynomial is required for accurate representation of $\chi(T)$.

Figures 2.6, 2.7, 2.8, and 2.9 present phase diagrams for the n-butoxyethanol–, poly(ethylene glycol)–, nicotine–, and C_8-lecithin-water systems. The predictions involve values of the parameters which minimize, over N_E experimental points, the following objective function

$$F_o = \sum_{j=1}^{N_E} \{ \mid \phi_2^{c^I} - \phi_2^{e^I} \mid + \mid \phi_2^{c^{II}} - \phi_2^{e^{II}} \mid \} \tag{2.54}$$

where ϕ_2^c and ϕ_2^e are calculated and experimental volume fractions, respectively.The critical consolute temperatures and volume fractions used in the calculations are given in Table 2.2. The optimal values for parameters for closed-loop systems for all the models except Goldstein's are tabulated in Tables B.1–B.3 in Appendix B.

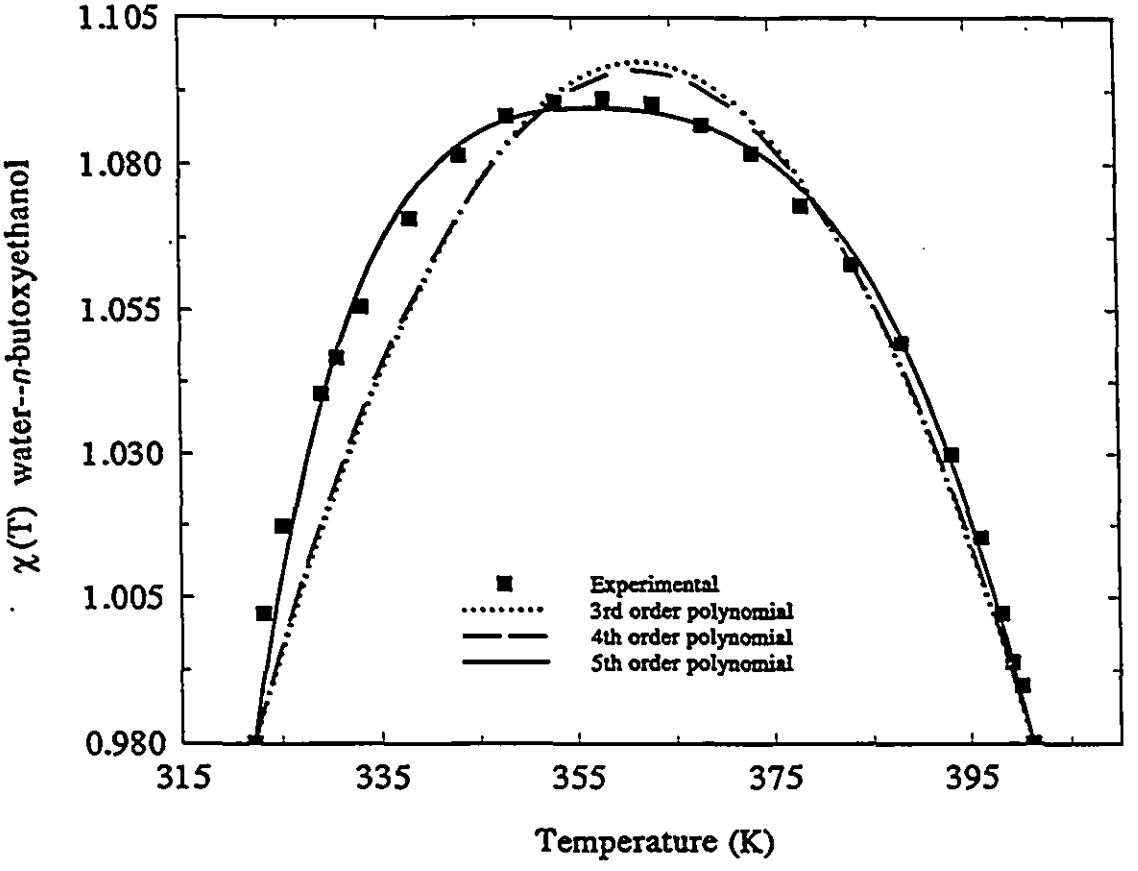

Figure 2.5: Polynomial correlation of χ_{12} with T for the n-butoxyethanol–water system

In terms of the magnitude of the parameters, experimentally determined H-bond energies are in the range 12 to 25 kJ mol^{-1} (Joesten and Schaad, 1974). Using the one-bond model, it is possible to calculate an interchange enthalpy from the optimal values of the parameters. This enthalpy change is equivalent to the H-bonding energy. A calculation for the system *n*-butoxyethanol–water gives 20 kJ mol^{-1}, which is within the range of experimentally determined values. It should be noted, however, that different combinations of the parameters α and β yield the same value of the objective function, rendering the assignment of entropic and enthalpic contributions arbitrary.

Goldstein's expression for $\chi_{12}(T)$, which contains no entropic parameter, does not fit the data. The loops obtained are too narrow, due to use of χ_{12} values which are smaller than those measured in experiments, see Figure 2.10. However, since the entropy of mixing decreases with increasing solute molecular size, the accuracy of Goldstein's model improves with molecular weight. The calculations show that the entropic parameter has a large effect on the calculated $\chi_{12}(T)$ and equilibrium compositions, since the results of the one-bond model are significantly better than those of the Goldstein model.

The two-bond model offers a small improvement in accuracy over the one bond model, and may not justify the use of two additional parameters. The use of a fifth order polynomial function yields only small improvement over the two-bond model. These and previous observations are confirmed in the numerical comparison of the performance of the models, which is presented in Table B.4 in Appendix B. Based on the observations made above, it is evident that in this study the one bond model, equation (2.45), is the best model for representing $\chi_{12}(T)$ since it gives good accuracy and requires few adjustable parameters.

Table 2.2: Values of parameters for systems

System	N_E^*	T_{cu}(K)	T_{cl}(K)	ϕ_2^c	χ_c
PEG 2 290	16	507.7	435.7	0.114	0.636
PEG 2 270	14	505.2	437.2	0.117	0.641
PEG 2 180	7	489.7	448.7	0.119	0.644
1-Aza cycloheptane	13	501.2	340.1	0.306	1.037
i-Butoxyethanol	21	423.4	297.7	0.298	1.016
n-Butoxyethanol	20	401.2	322.2	0.286	0.980
2,6-Dimethyl pyridine	10	438.1	318.5	0.309	1.047
2-Methylpiperidine	10	501.2	352.5	0.320	1.080
3-Methylpiperidine	9	508.2	330.1	0.313	1.059
4-Methylpiperidine	12	462.7	358.1	0.292	0.996
Nicotine	12	506.2	334.7	0.302	1.027
1-Propoxy-2-propanol	15	444.9	307.7	0.321	1.086
2-Propoxy-1-propanol	11	435.2	316.0	0.314	1.062
Tetrahydrofuran	16	410.3	345.0	0.390	1.346
C_8-Lecithin	8	317.7	—	0.086	0.598

$*$ number of experimental data points

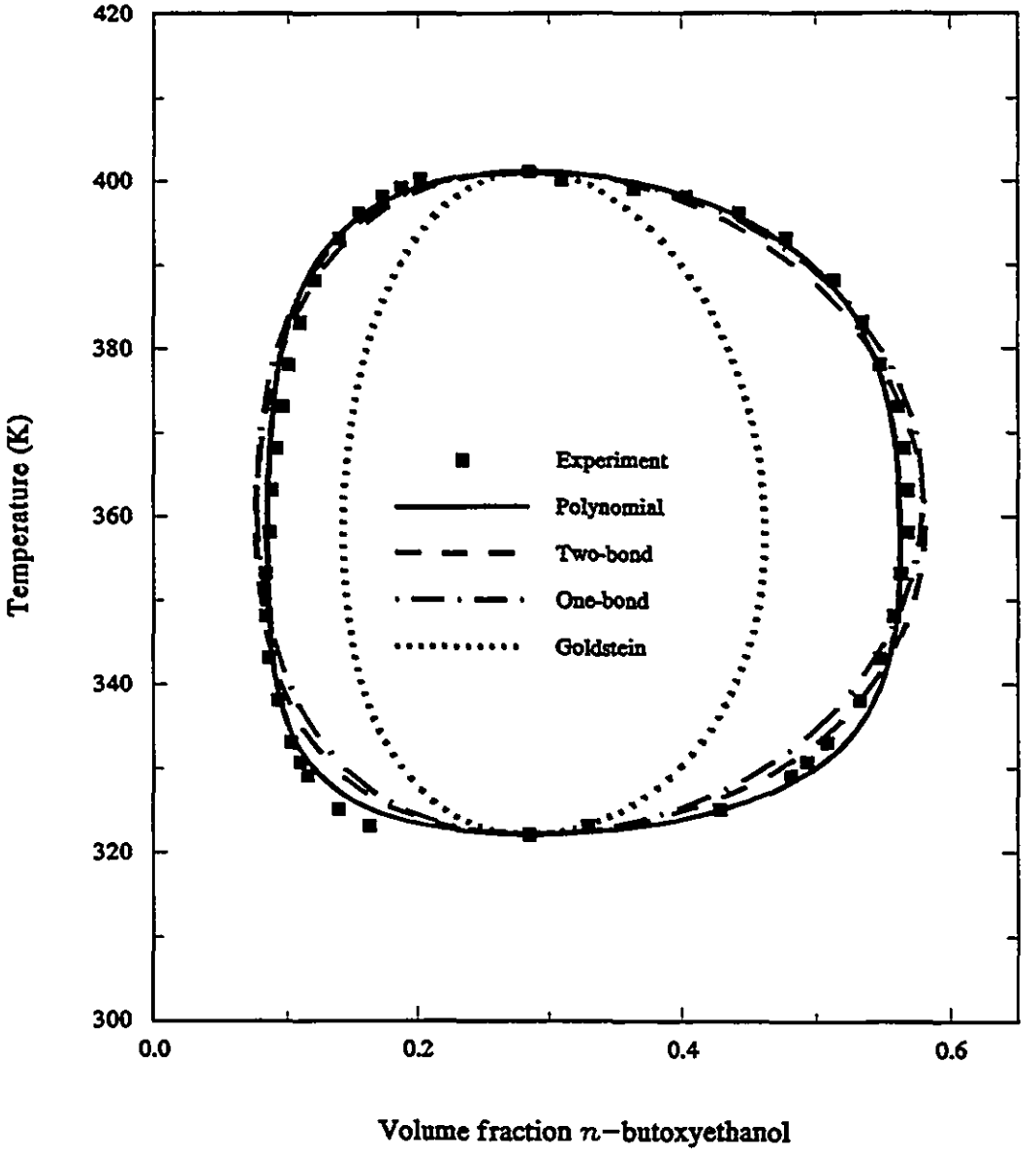

Figure 2.6: Experimental and calculated phase diagram for the n-butoxyethanol–water system

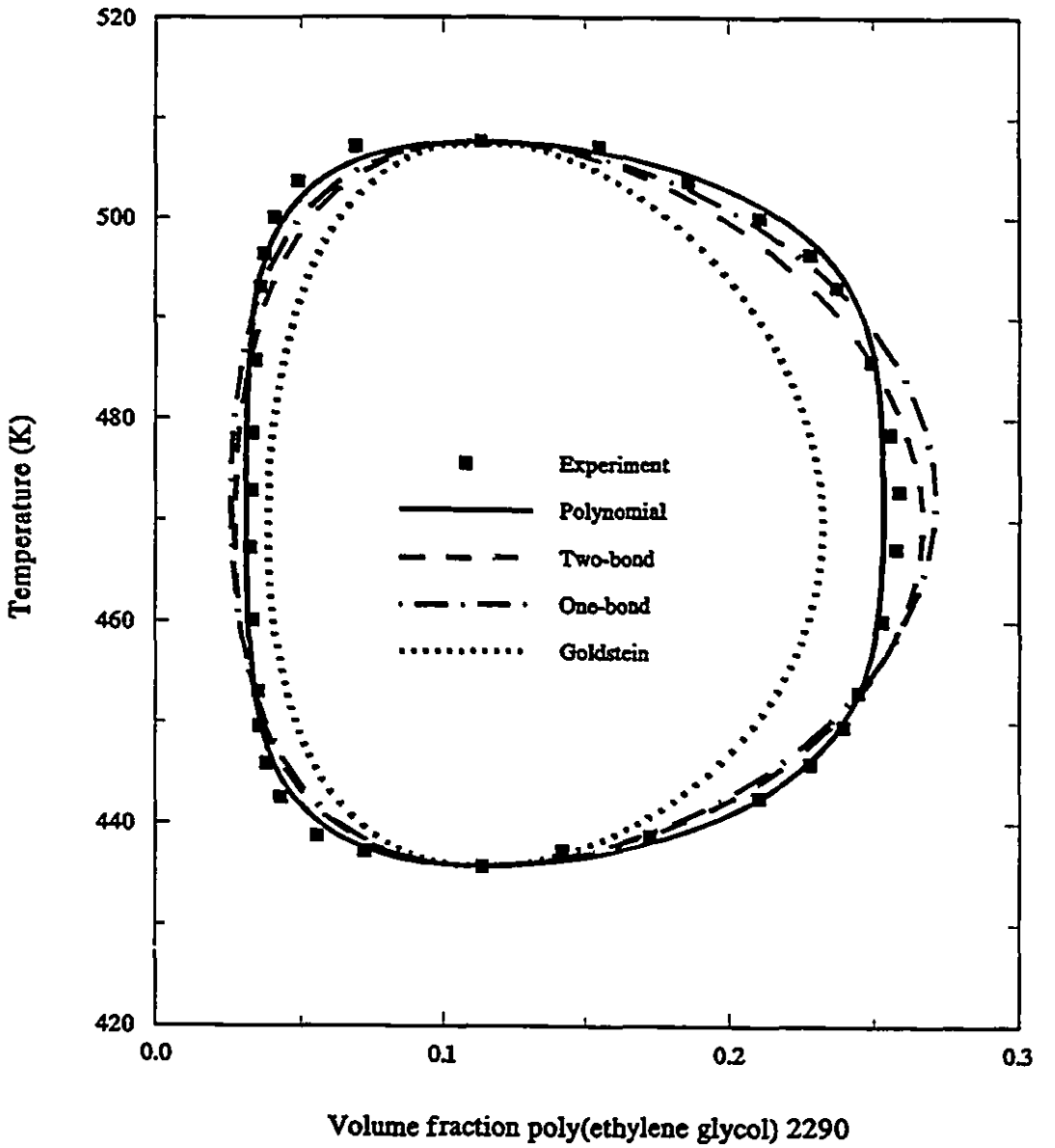

Figure 2.7: Experimental and calculated phase diagram for the poly(ethylene glycol) 2290–water system

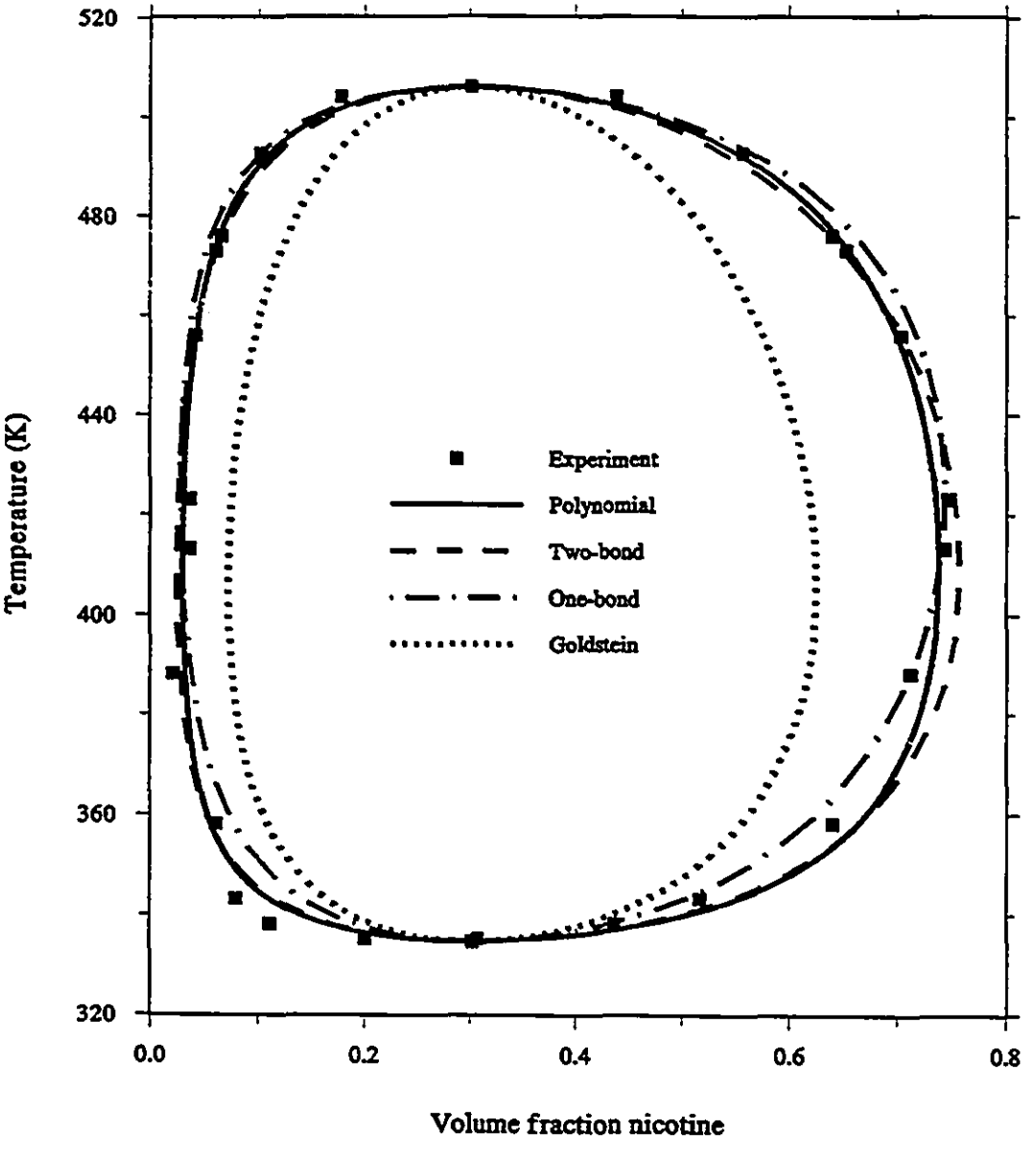

Figure 2.8: Experimental and calculated phase diagram for the nicotine–water system

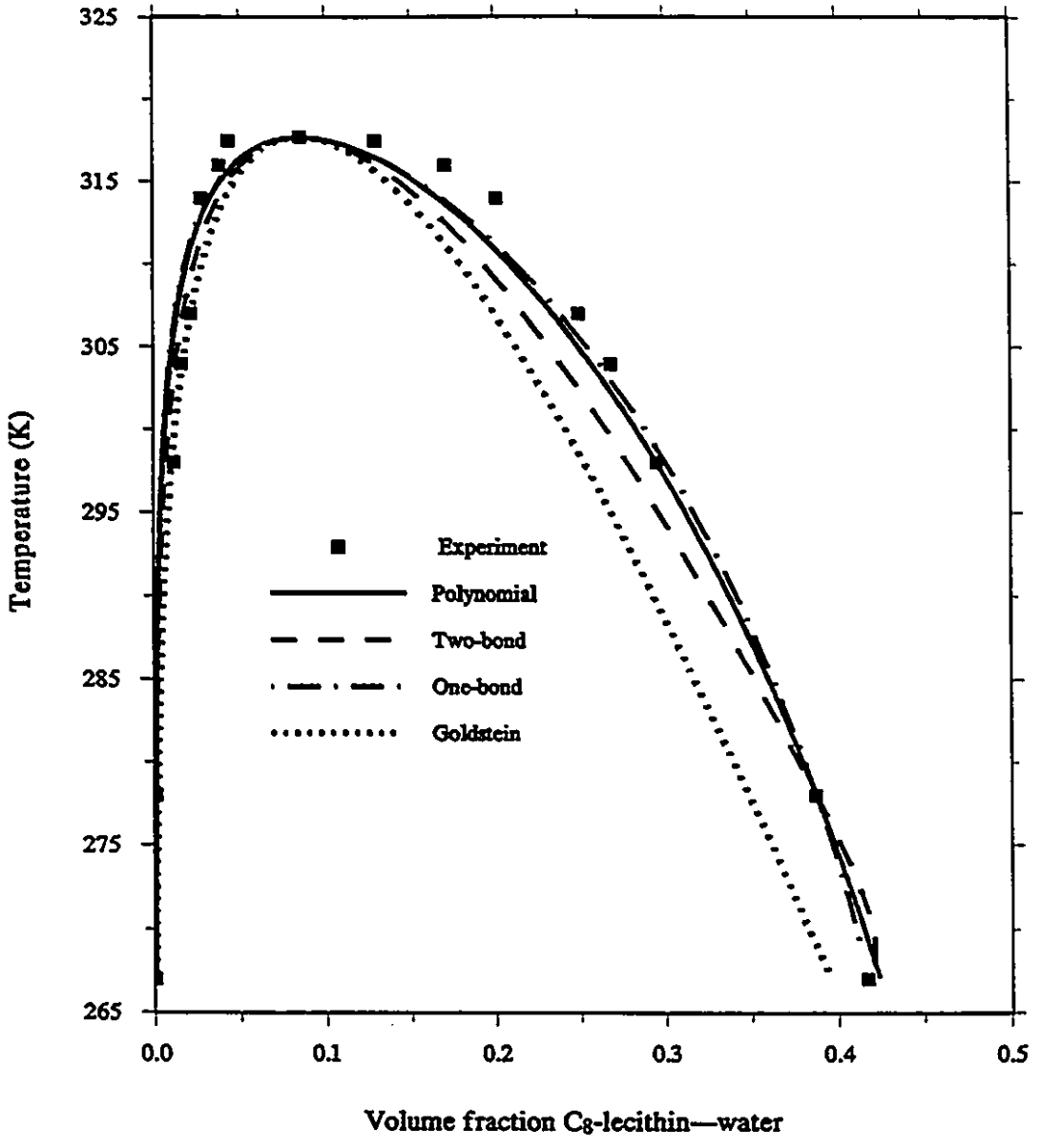

Figure 2.9: Experimental and calculated phase diagram for the C_8-lecithin–water system

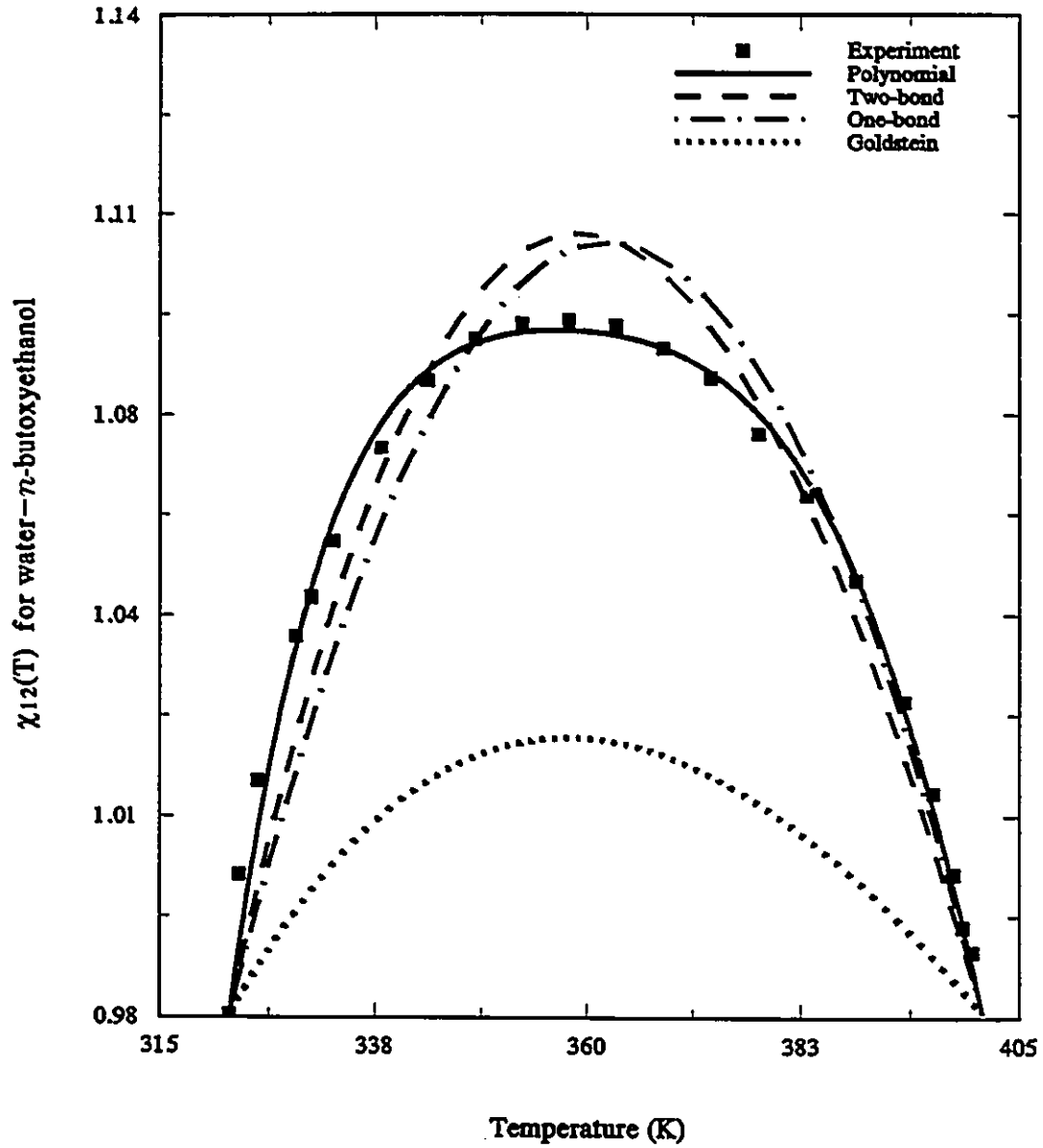

Figure 2.10: Experimental and calculated $\chi_{12}(T)$ for the n-butoxyethanol–water system

Chapter 3

Liquid-Liquid Equilibrium Experiments

This chapter describes liquid-liquid equilibrium experiments for ternary systems consisting of water, NaCl and a third component. At a fixed temperature and pressure, full experimental characterization of biphasic behavior for such equilibrated mixtures requires the determination of the compositions of equilibrium phases and the amounts of solutes necessary to form two phases.

Figure 3.1 presents a schematic representation of the phase diagram of a typical ternary aqueous two-phase system containing salt. The line separating the single phase region from the two-phase region is the *binodal curve*. In the biphasic region, a sample with feed composition (C_s^F, C_p^F) splits to yield a bottom phase (C_s^B, C_p^B) and a top phase (C_s^T, C_p^T) whose compositions are connected by a *tie-line*. Differing feed compositions along a particular tie-line produce differing relative amounts of equilibrium phase compositions. Smaller amounts of both solutes in the two-phase region yield shorter tie-lines and more similar equilibrium phases. The two phases are identical at the *plait point*. In this study three kinds of experiments were conducted: those measuring the location of tie-lines; those determining the binodal curve; and those locating the plait point.

As described in Chapter 1, a literature survey was used to identify compounds

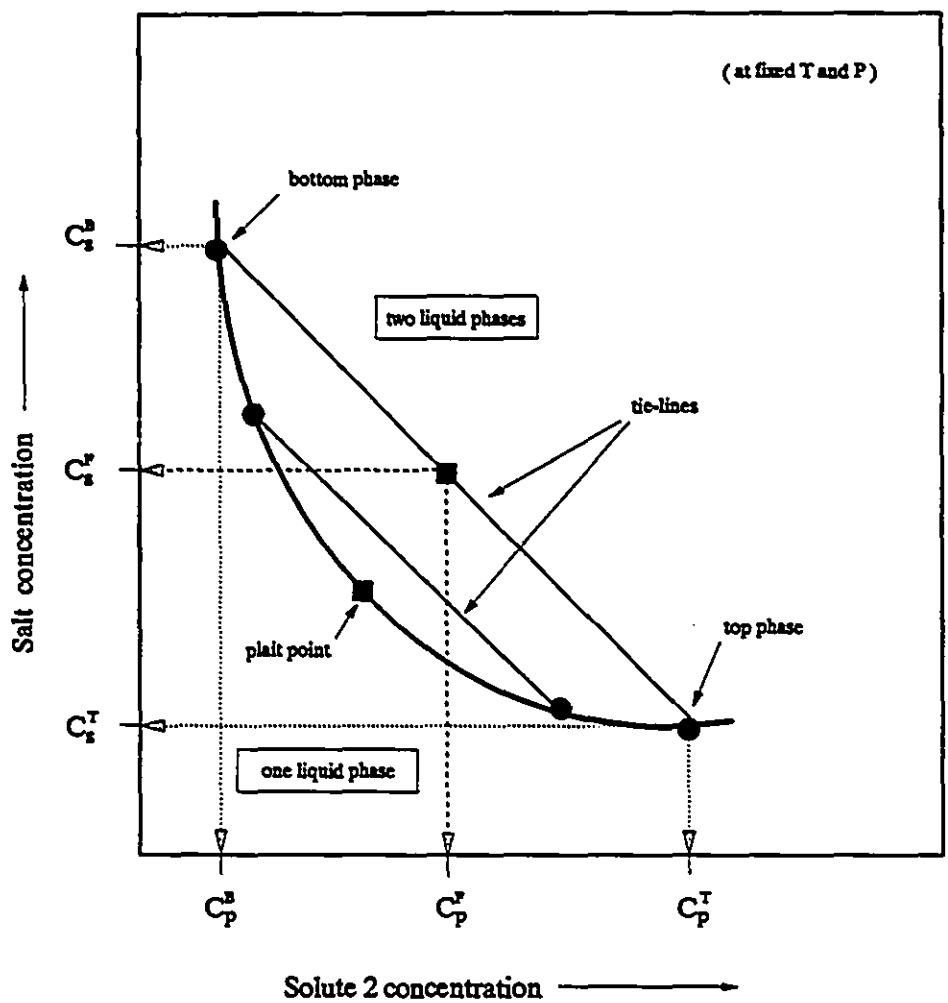

Figure 3.1: Phase diagram for a typical biphasic salt–nonionic solute 2–water system

which form two aqueous phases at ambient or near ambient conditions. For some systems, preliminary screening experiments were conducted to ascertain if they formed two-phases at the temperature of interest. The systems studied here are listed in Table 3.1. The data supplement the existing data base of aqueous two-phase systems containing NaCl.

One system contains a cationic surfactant, *n*-dodecylammonium chloride which Imae et al. (1988) found to form two phases near room temperature for low concentrations of salt and surfactant. Here liquid-liquid equilibrium experiments for this system were carried out at 30°C. As shown in Figure 2.1, poly(ethylene glycol) is a hydrophilic polymer which is completely miscible with water at room temperature. While it forms two aqueous phases with some salts at room temperature (Florin et al., 1984; Ananthapadmanabhan and Goddard, 1987), it forms two phases with NaCl only at higher temperatures. Experiments for this system were conducted at 60°C. The greatest experimental effort was devoted to the poly(propylene glycol)–NaCl–water system. This polymer is similar structurally to poly(ethylene glycol), but is more hydrophobic. In aqueous solution it behaves like PEG, with material of weight average molecular weight 400 showing a LCT curve at about 40°C (Malcolm and Rowlinson, 1957). Addition of NaCl to an aqueous solution of poly(propylene glycol) [PPG] at room temperature yields two phases. For this system, the effects of molecular weight and temperature on the phase diagram were investigated.

3.1 Experimental Materials and Methods

The specifications and suppliers of materials used in the experiments are listed in Table C.1 in Appendix C. Unless otherwise indicated, all materials were reagent grade and were used without further purification. Sodium chloride was dried in an

Table 3.1: Systems studied experimentally†

System	Temperature (K)
1-Propanol—NaCl—H_2O	298
n-Dodecylammonium chloride—NaCl—H_2O	303
Poly(ethylene glycol) 8000—NaCl—H_2O	333
Poly(propylene glycol) 425—NaCl—H_2O	278, 298, 333
Poly(propylene glycol) 725—NaCl—H_2O	278, 298

† The numbers beside the polymer names are approximate weight-average molecular weights. The sample polydispersities are discussed in Section 3.1.

oven at 110°C for 60 hours and stored in a desiccator. Distilled water of resistivity greater than 0.3 MΩ.cm was used in all experiments. The ratio of weight average to number average molecular weight, of the PEG and PPG samples reported by the manufacturers was 1.05. Oven drying tests at 60°C confirmed that the PEG contained less than 0.5wt% water.

Atomic absorption spectroscopy measurements for sodium were performed using a Thermo Jarell Ash Corporation Model Smith-Hieftje II instrument at a wavelength of 330.2 nm. Refractive index measurements were performed at 25°C using a Carl Zeiss Model 41433 refractometer. Temperatures were maintained within ± 1°C of their set points using water baths supplied by Neslab Instruments[1].

Stock solutions of sodium chloride [5M], *n*-dodecylammonium chloride [20 wt%] and poly(ethylene glycol) [60 wt%] were used in making phase samples. They were prepared by dissolving appropriate amounts of solid in distilled water. For the propanol and poly(propylene glycol), which are liquids at room temperature, the pure compounds were used directly to make phase samples.

1-Propanol–NaCl–Water

The sodium, and hence sodium chloride, concentration was determined using atomic absorption spectroscopy (AAS). Before each analysis of unknown (diluted) samples, a calibration plot of absorbance (A) versus concentration was prepared. Generally, these were nonlinear for the range 0-120 NaCl ppm by weight, and a sample is presented in Figure C.1 in Appendix C. For each run, the concentrations of samples, C_{Na}, in ppm, were calculated using a quadratic equation

$$C_{Na} = a_0 + a_1 A + a_2 A^2 \tag{3.1}$$

[1]The 60°C baths used ethylene glycol.

where a_i are linear regression coefficients obtained from calibration data. Here the regressions were performed using the LOTUS 123 spreadsheet program. This method was used to analyze for sodium chloride for all systems studied here.

The concentration of propanol was determined using refractive index measurements. Since the refractive index of phase samples depends on the propanol and NaCl concentration, plots of refractive index versus propanol concentration were prepared for different concentrations of NaCl. The results are displayed in Figure 3.2. By subtracting the value of the refractive index at the intercept (NaCl-water binary) from each of the values, it is possible to superimpose the data of Figure 3.2 as shown in Figure 3.3. The incremental refractive index change due to propanol (ΔRI) was related to the concentration of propanol (C_p, in weight fraction) by a second order polynomial. Linear regression gave

$$\Delta \mathrm{RI} = 0.0929 C_p - 0.0505 C_p^2 \tag{3.2}$$

The values of the refractive index at the intercepts of the curves in Figure 3.2 are the refractive indices of binary NaCl-water solutions. These values are plotted as a function of salt concentration in Figure 3.4. The following relation between the refractive index at the intercept and salt concentration (C_{NaCl}, in weight fraction) was obtained by linear regression.

$$\mathrm{RI}_o = 1.3325 + 0.177 C_{\mathrm{NaCl}} \tag{3.3}$$

By combining equations (3.2) and (3.3), the refractive index of the solution can be related to the concentration of salt and alcohol

$$\mathrm{RI} = 1.3325 + 0.177 C_{\mathrm{NaCl}} + 0.0929 C_p - 0.050 C_p^2 \tag{3.4}$$

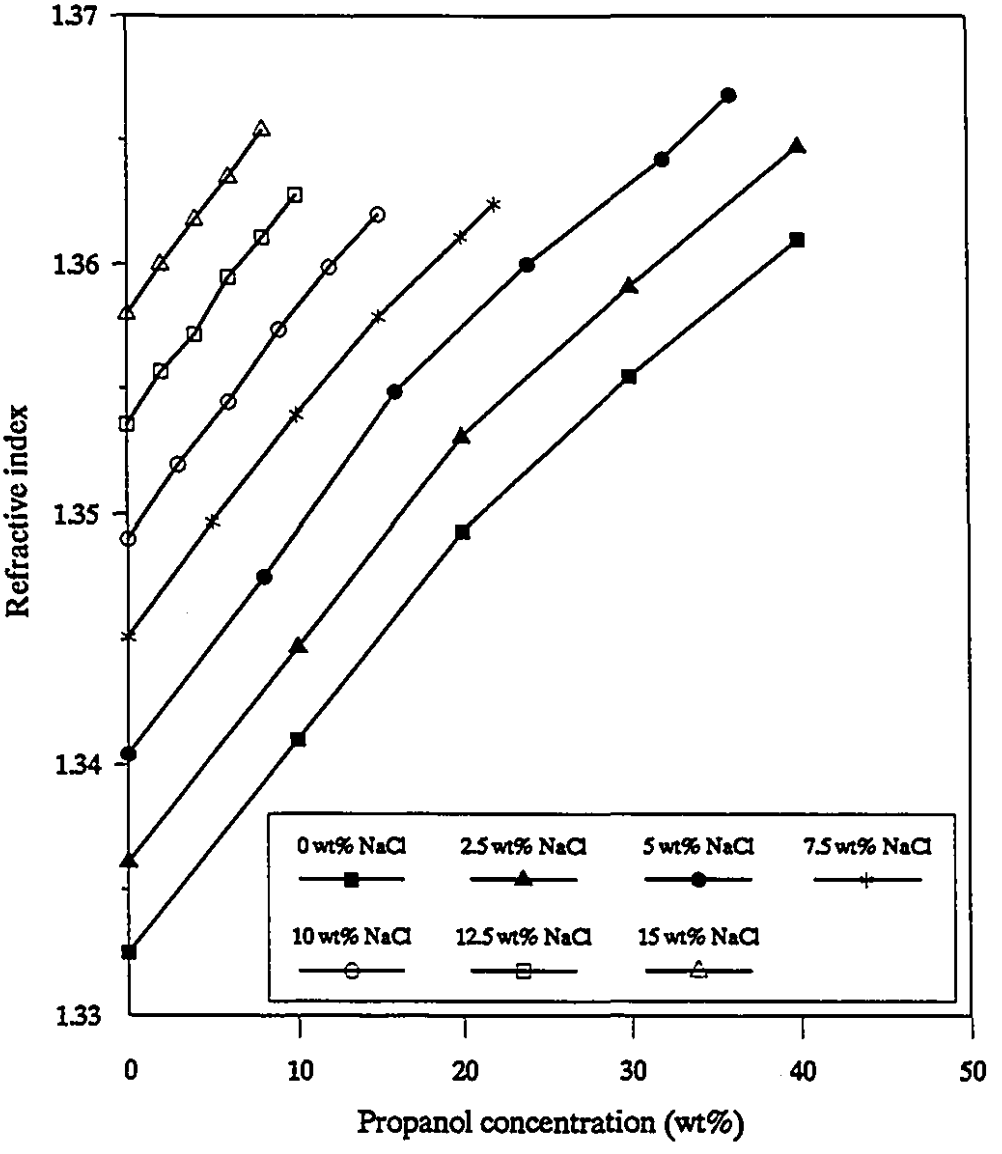

Figure 3.2: Refractive index calibration graph for 1-propanol–NaCl–water at 298 K

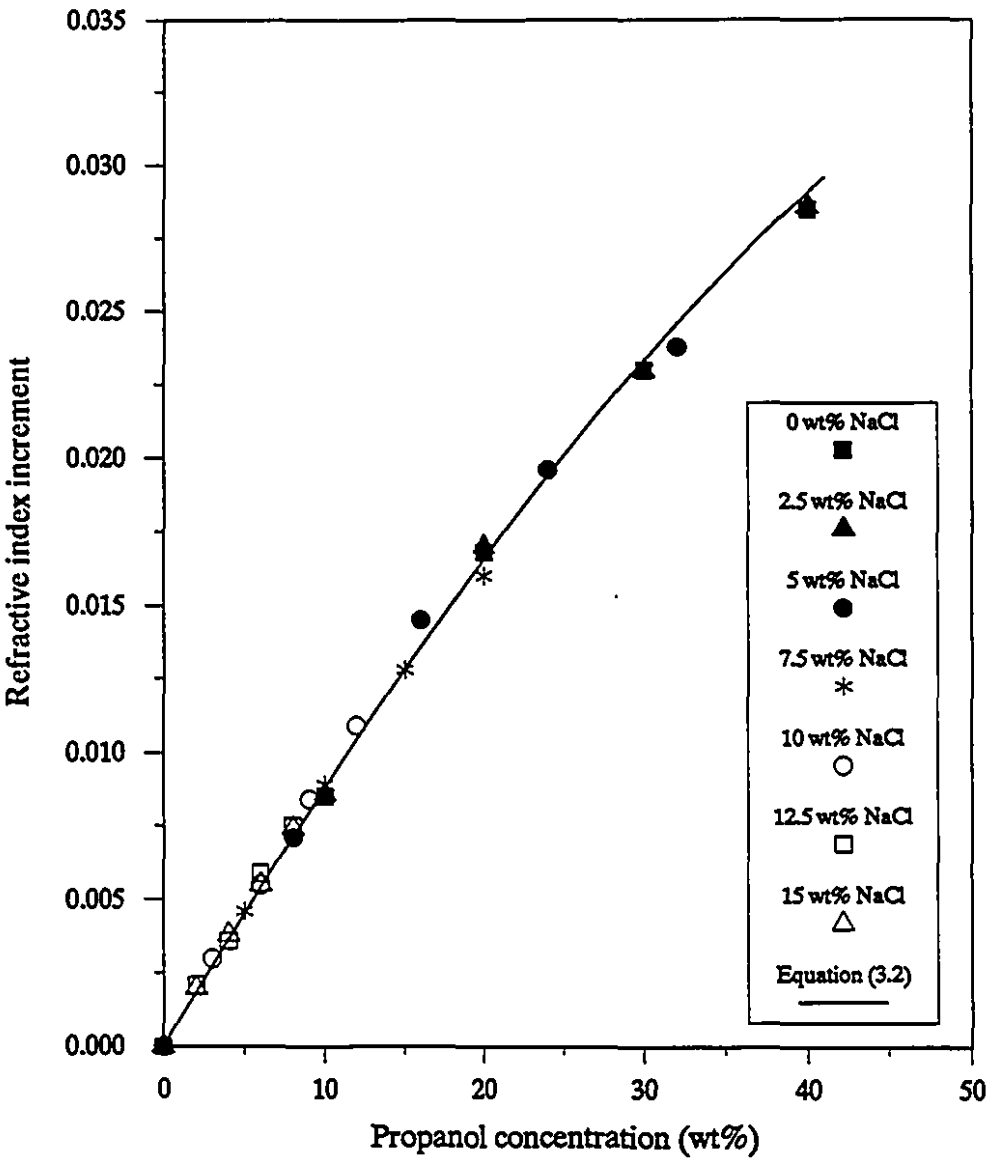

Figure 3.3: Incremental refractive index change versus propanol concentration

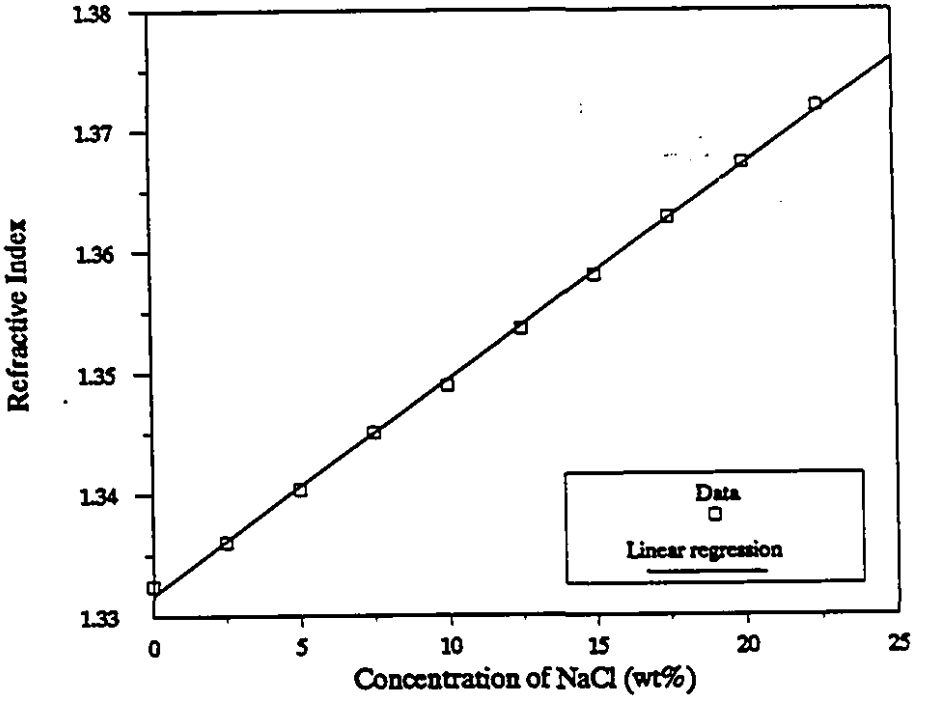

Figure 3.4: Refractive index of a binary aqueous NaCl solution

Once the salt concentration was determined using AAS, and the refractive index of the solution was measured, the concentration of propanol in a phase was calculated from

$$C_p = \frac{0.0929 - \sqrt{(0.0929)^2 + 4(0.0505)(1.3325 + 0.177C_{\mathrm{NaCl}} - \mathrm{RI})}}{2(0.0505)} \tag{3.5}$$

n-Dodecylammonium Chloride–NaCl–Water

Initial attempts to determine the concentration of *n*-dodecylammonium chloride using refractive index measurements were unsuccessful since the presence of two phases at low surfactant concentrations made it impossible to prepare a calibration

graph. Attempts to measure the chloride concentration using a specific ion electrode were also unsuccessful because the electrode signal drifted over time, possibly due to the adsorption of the surfactant amphiphile [H_3C-$(CH_2)_{11}$-$\overset{\oplus}{N}H_3$] on the membrane.

The Mohr method (Brown and Sallee, 1963) of titrating chloride ions was unsuitable since interference from the surfactant eliminated the sharp color change at the end point. Attempts to measure the surfactant concentration by forming a complex with β-cyclodextrin (Sasaki et al., 1989, 1990) were also unsuccessful due to erratic drift in the spectrophotometric reading, perhaps due to slow rates of complex formation.

The method finally used to determine the surfactant concentration was gravimetric analysis. Samples of known weight were removed and dried at low pressure (for 2 days, under water aspiration) and then in an oven at 55°C for one week. Knowledge of the salt concentration allowed the determination of the concentration of *n*-dodecylammonium chloride.

Poly(ethylene glycol) 8000–NaCl–Water

The concentration of polymer was determined using refractive index measurements. The calibration plot is presented as Figure C.2 in Appendix C. For PEG 8000 the refractive index versus composition curves for all salt concentrations were linear and had the same slope. The following relation describes the data

$$\mathrm{RI} = \mathrm{RI}_o + 0.1202 C_{PEG} \tag{3.6}$$

where RI_o is given by equation (3.3) and C_{PEG} is the weight fraction of polymer. Rearrangement of the equation above permits the calculation of C_{PEG} if C_{NaCl} is known.

Poly(propylene glycol)–NaCl–Water

The concentrations of the two fractions of poly(propylene glycol), of molecular weight 425 and 725, were determined using refractive index measurements. The calibration plots are presented as Figures C.3 and C.4 in Appendix C. For both polymers the refractive index versus composition curves for all salt concentrations investigated were linear with similar slopes and the following relations describe the data:

$$\mathrm{RI} = \mathrm{RI}_o + 0.136 C_{PPG} \tag{3.7}$$

for PPG of molecular weight 425 and

$$\mathrm{RI} = \mathrm{RI}_o + 0.131 C_{PPG} \tag{3.8}$$

for PPG of molecular weight 725. The polymer concentrations were obtained in a manner similar to that used for PEG.

3.2 Equilibrium Experiments

This section describes the three kinds of experiments conducted in this project: those measuring the compositions of phases in equilibrium, or tie-lines; the turbidity titration method of determining the binodal curve; and a method for determining the plait point. The latter two experiments were conducted only on the propanol system.

Tie-line Determination

The location of the binodal curve was determined roughly by mixing known amounts of the components arbitrarily until two phases were observed. Once this was completed, feed compositions yielding roughly equal volumes of top and bottom phases were calculated. Thereafter, 60–95 ml feed samples were prepared by mixing appropriate amounts of stock solutions of NaCl, second solute and water in 100 ml graduated pyrex cylinders. These cylinders were capped using either paraffin wax film, or in the case of experiments conducted at 60°C, rubber balloons anchored using rubber bands. The balloons were used because the high temperature softened the wax film and allowed escape of water vapor.

The cylinders were placed in a water bath at the desired temperature for 24 hours. Since equilibrium compositions depend on the temperature, it was necessary to ensure that phase separation did not occur before the sample attained the temperature of the bath. Hence the samples were withdrawn and shaken thoroughly at least twice within an hour of being immersed in the bath.

After equilibrium was achieved, the cylinders were withdrawn and phase volumes recorded. Aliquots of 15 ml were withdrawn using syringes. The top phase was sampled first, with care being taken to leave a layer of material at least 0.5 cm thick above the interface. The bottom phase was withdrawn using a syringe with a long needle. A tiny bubble of air was retained in the needle tip and expelled once in the bottom phase to prevent contamination from upper phase material. In cases where precipitated solid salt was present, care was taken to ensure that the sample was withdrawn gently, with the needle tip well away from salt crystals. For samples at 60°C, the above operations were performed rapidly, as the temperature of the cylinders fell quickly after removal from the bath. This was particularly important for the measurement of density which was carried out immediately after sample

withdrawal.

Once the samples were withdrawn, the density of both phases was determined using a 10 ml pycnometer. Following this, a 5 ml sample of each phase was pipetted and diluted by a volumetric factor of 2000 for sodium analysis. Another 5 ml pipette sample was withdrawn for refractive index or gravimetric analysis. The refractive index samples were equilibrated in a second water bath, maintained at 25°C. For refractive index measurement, the samples were diluted by a factor of 2 to 4.

Turbidity Titration

For the propanol system, the location of the binodal curve was determined using turbidity titration (Albertsson, 1986). Samples with varying NaCl concentrations were prepared in 25 ml test tubes and equilibrated at 25°C. Small amounts of propanol were added dropwise to the tubes. After each addition the tubes were capped, shaken vigorously, and allowed to settle under observation. This was continued until a sample became turbid, indicating the presence of two phases. Once this happened, the sample was back titrated by adding water dropwise with shaking until the turbidity vanished. The composition before the addition of the last drop before clearing was a point on the binodal curve. More propanol was added and the process repeated to obtain another point on the binodal curve.

Plait-Point Determination

For the propanol system the precise location of the plait point was found using turbidity titration with volumetric analysis. The method involved the preparation of 80 ml of an aqueous solution of 50 wt% propanol in a 250 ml graduated cylinder. To this was titrated, dropwise with shaking, a 5 M sodium chloride solution until turbidity was observed. Upon this occurrence, the composition was recorded and

the mixture left to settle for at least one hour. Settling gave two clear phases whose volumes were recorded. Following this the system, was back titrated to the single phase region using water, and the procedure repeated until an inversion in the ratio of phase volumes was observed.

3.3 Experimental Results and Discussion

The experimental results are presented in the form of binodal curves illustrating the location of phase boundaries and the compositions of equilibrium phases. For systems for which the complete phase diagram was determined, the information is presented in the form of a triangular plot. The partitioning of non-aqueous components of the mixtures is illustrated using partition coefficient plots.

1-Propanol–NaCl–Water

The experiments for this system were carried out at 298 K. Phase separation was achieved within one hour of shaking. The equilibrium phases were transparent and separated by a sharp interface. The top phases were rich in alcohol and low in salt while the converse was true for the bottom phases. The top phases were more viscous and less dense (0.95–0.98 g/ml) than the bottom phases (1.04–1.07 g/ml). Density differences increased with tie-line length, decreasing the phase separation time. For turbidity titrations, shaking in the two-phase region made the mixture milky-white in color. For compositions around the plait point this light scattering was very strong, and persisted even after the solutions (in the single and two-phase region) were allowed to settle for several hours — this was due to the phenomenon of critical opalescence.

Results of the turbidity titrations and tie-line analysis are given in Figure 3.5.

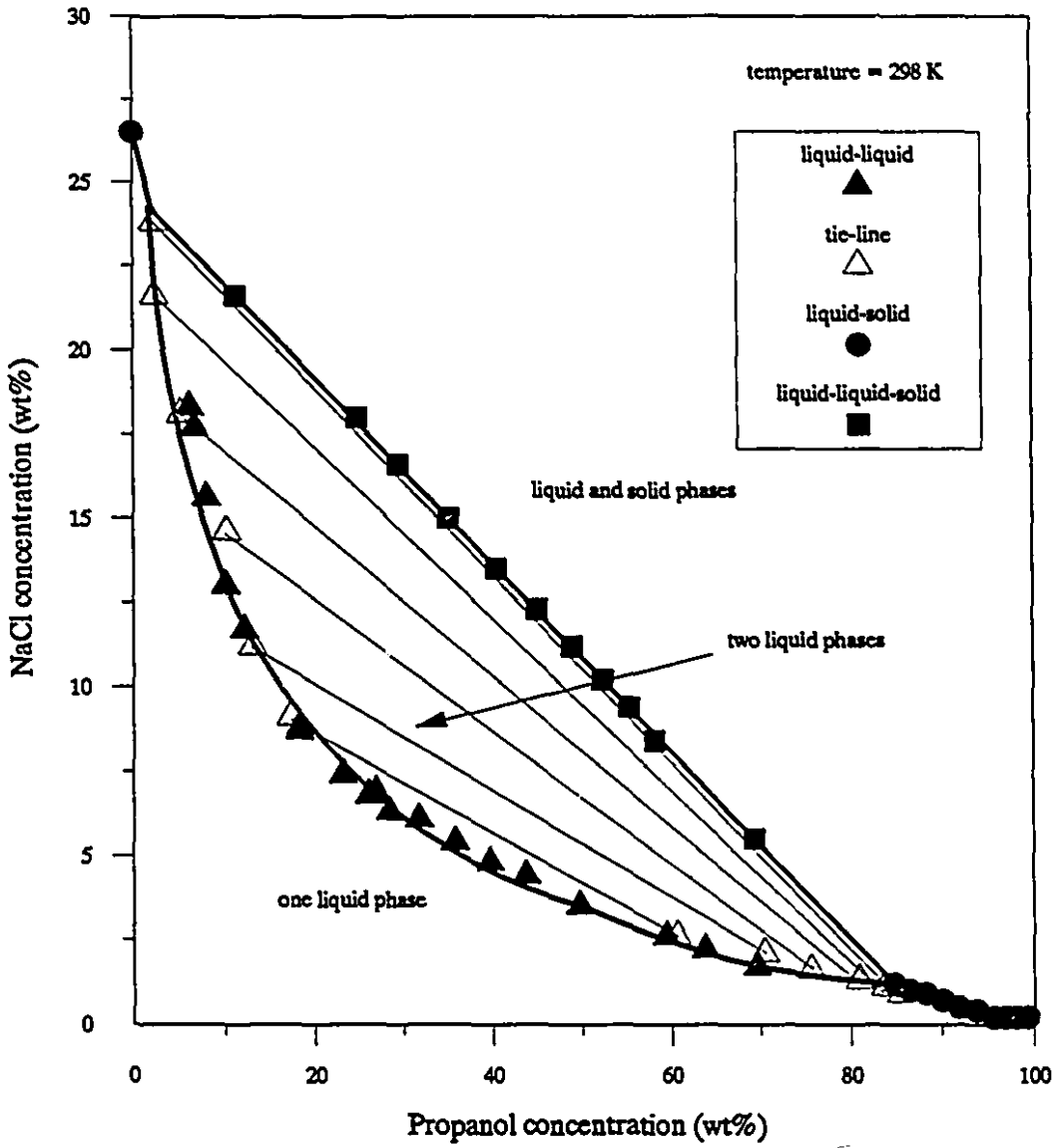

Figure 3.5: Binodal curve for 1-propanol–NaCl–water

The data points indicated by filled triangles were determined using turbidity titrations. The solid circles were obtained by titrating NaCl solution into propanol solution until solid salt precipitated. Results of tie-line experiments are indicated by open triangles. The data in this figure are tabulated in Tables D.1 and D.2, Appendix D. The tie-line compositions, obtained by AAS and refractive index analysis were verified by performing mass balances to determine if the amounts of NaCl and propanol used to create the feed phase corresponded to the amounts in the top and bottom phases, based on equilibrium compositions. The mass balances for all tie-lines closed to within 6%. Three replicates of one tie-line indicated that the compositions have a standard deviation of 0.25 wt% corresponding to a 95% confidence interval of ± 0.29wt%.

Figure 3.5 shows that concentrations of propanol as low as 3% can yield two phases provided the mixture is rich in NaCl. Conversely, two phases exist for low concentrations of salt provided the mixture has a high propanol concentration. One of the two equilibrium phases, in general, is rich in water and NaCl, while the other is rich in propanol. This type of phase diagram is typical of aqueous two-phase systems except for the fact that one phase is very rich in propanol and contains relatively little water. At 298 K propanol is completely soluble in water (Schneider and Russo, 1966) and the addition of NaCl decreases its solubility in the process of "salting out" (Ananthapadmanabhan and Goddard, 1987). Relative to other salts, the effect of sodium chloride is smaller than that of other salts containing polyvalent ions (e.g. Na_2SO_4 and $CaCO_3$ – see Do and Park, 1974; Firman et al., 1985) in accord with the position of NaCl in the lyotropic series (Voet, 1937).

The plait point for this system was located using turbidity titration as described in the previous section. The results of these experiments are illustrated in Figures 3.6 and 3.7, with the corresponding data listed in Table D.3, Appendix D. The

first figure shows the binodal curve around the plait point region. Filled and open symbols bracket the phase boundary. For each two-phase datum, the volumes of co-existing equilibrium phases were measured. The percentage of the total volume in the bottom phase is plotted against the propanol concentration in Figure 3.7. The plait point, which corresponds to the concentration of propanol yielding equal volumes, is 35.7 wt% propanol and 5.25 wt% NaCl.

The phase diagram for the system is presented in the form of a triangular diagram in Figure 3.8 where the compositions are in wt%. This figure indicates that a large portion in the middle of the phase diagram consists of mixtures of two liquid phases, (I) and (II), in equilibrium with solid salt. The two-liquid region occupies a small portion of the total phase diagram, although the co-existing phases are generally quite different in composition. There are two single liquid–solid regions, one rich in water and one rich in propanol.

In order to examine partitioning behavior in the system, it is convenient to define, for each component, a partition coefficient (K) as follows

$$K = \frac{C_{bot}}{C_{top}} \tag{3.9}$$

where C_{top} and C_{bot} are the concentrations in the top and bottom phases, respectively. If a value of the salt concentration on the ordinate of the binodal curve is selected and propanol concentrations at the intersection of this salt concentration value with tie-lines are read off, is possible to generate a semilogarithmic plot of partition coefficients versus propanol concentration as shown in Figure 3.9. For the selected salt concentration, the propanol concentration read off a particular tie-line is plotted against the partition coefficients calculated using the concentrations of salt and alcohol for that tie-line. Four values of the NaCl concentration, 5, 10, 13

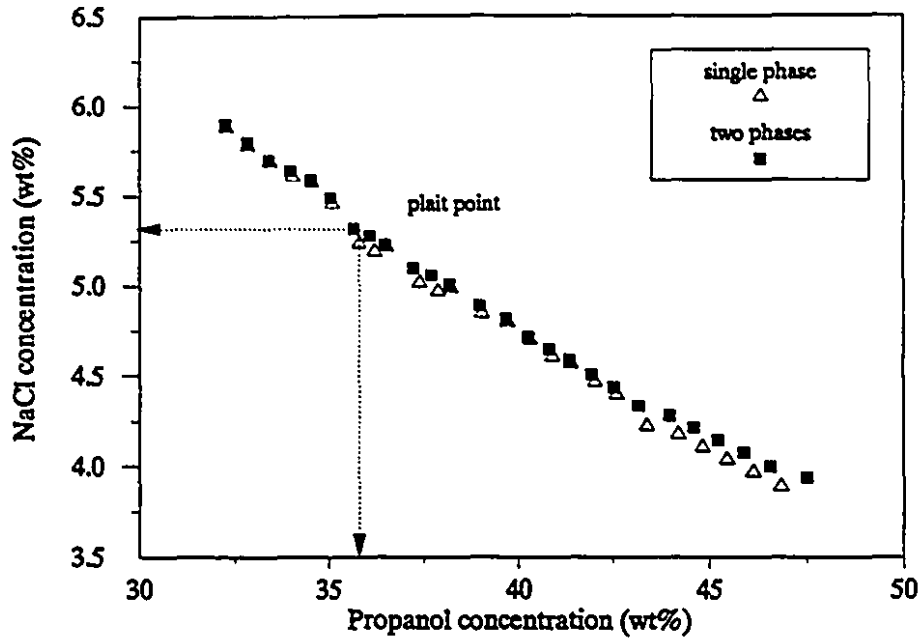

Figure 3.6: Binodal curve near the plait point

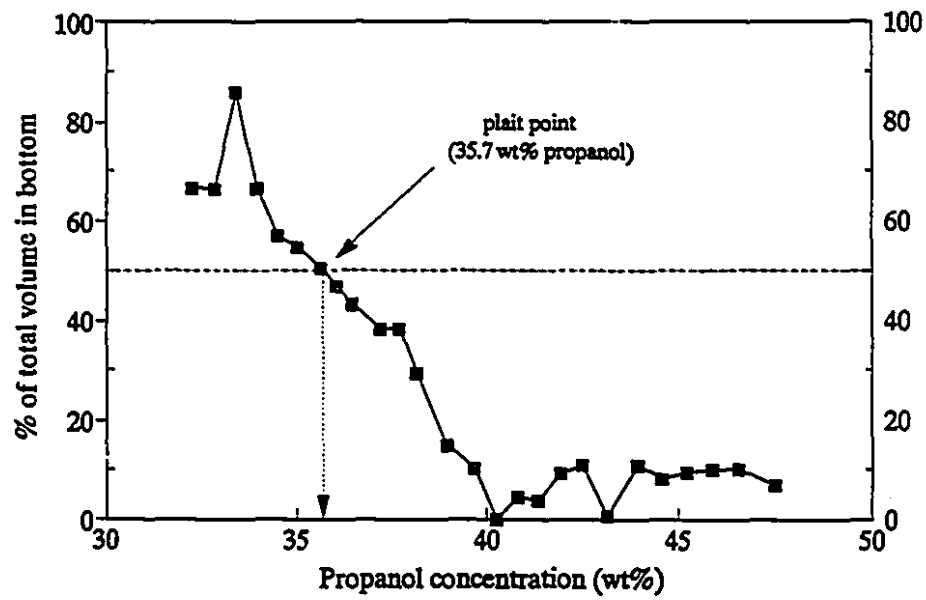

Figure 3.7: Phase volume ratios near the plait point

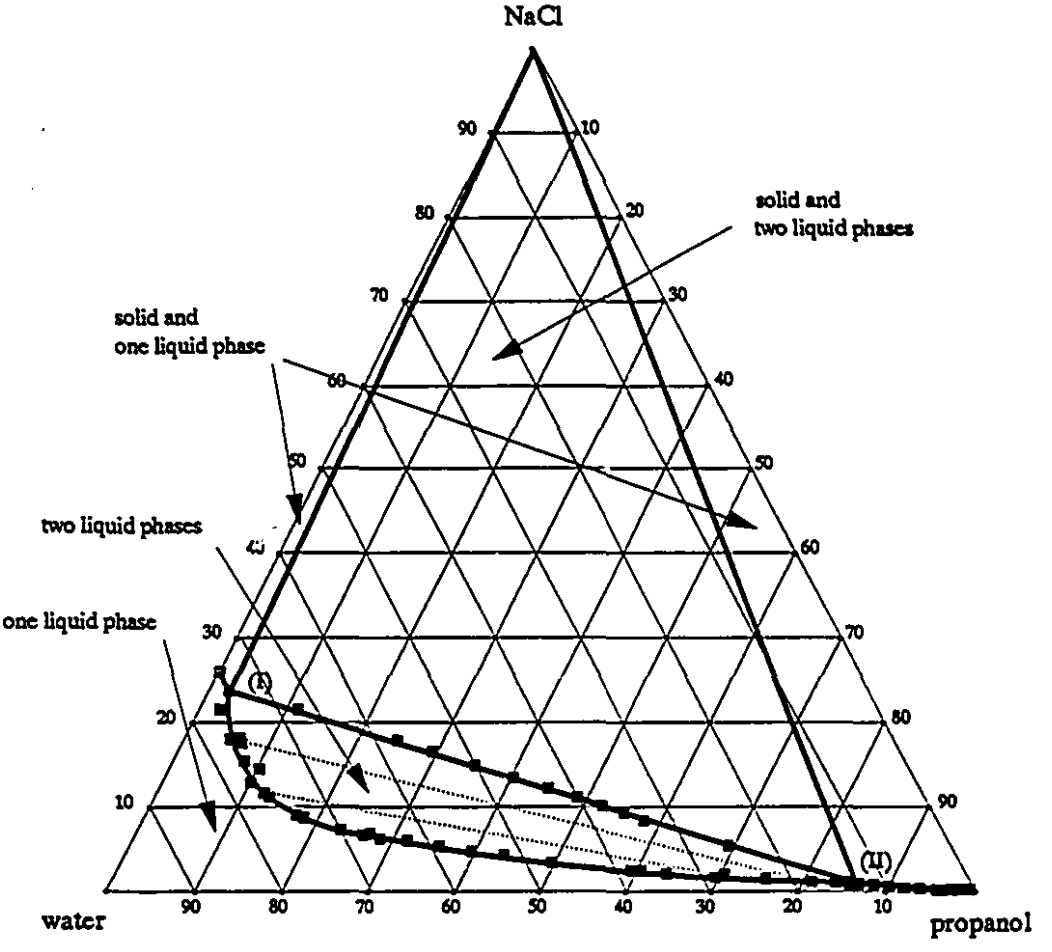

Figure 3.8: Complete phase diagram for 1-propanol–NaCl–water at 298 K

and 15wt% were selected. Solid lines connect values of the partition coefficients. The end points of these lines correspond to the boundaries of the binodal curve. From this figure the separation obtained by adding various amounts of propanol to a given brine solution can be determined. For example, the partition coefficient of NaCl in a solution containing 10wt% NaCl and 30wt% propanol is about 7.5. This figure shows that partition coefficients for NaCl range from 3–30 while those for propanol range from 0.3–0.025.

Experimental studies of this system have also been completed by Do and Park (1974), at 303 K, and by De Santis et al. (1976), at 298 K. The present data are compared to the literature data in Figure 3.10. The results of the three studies are similar and the effect of a 5°C change in temperature is negligible. The results of De Santis et al. (1976) are identical to those obtained here with the exception that they recorded a slightly higher NaCl concentration in the salt-rich phase for their three-phase tie-line.

n-Dodecylammonium Chloride–NaCl–Water

Experiments for this cationic surfactant system were carried out at 303 K. Initial experiments at 298 K determined that the surfactant tends to precipitate out of solution at this temperature since the Krafft point is approximately 297 K (Imae et al., 1988). At temperatures below the Krafft temperature the surfactant, which has a critical micelle concentration [CMC] of 0.013 M or 0.29 wt%, (Corrin and Harkins, 1947), cannot form micelles and is essentially insoluble. The phase behavior of an aqueous solution of *n*-dodecylammonium chloride (DAC) is shown in Figure 3.11 (Gault et al., 1988). This cationic surfactant solution exhibits complex phase behavior including several anisotropic liquid-crystal mesophases [hexagonal, nematic, lamellar and coagel (Tiddy, 1980)] most of which involve regular arrangements of

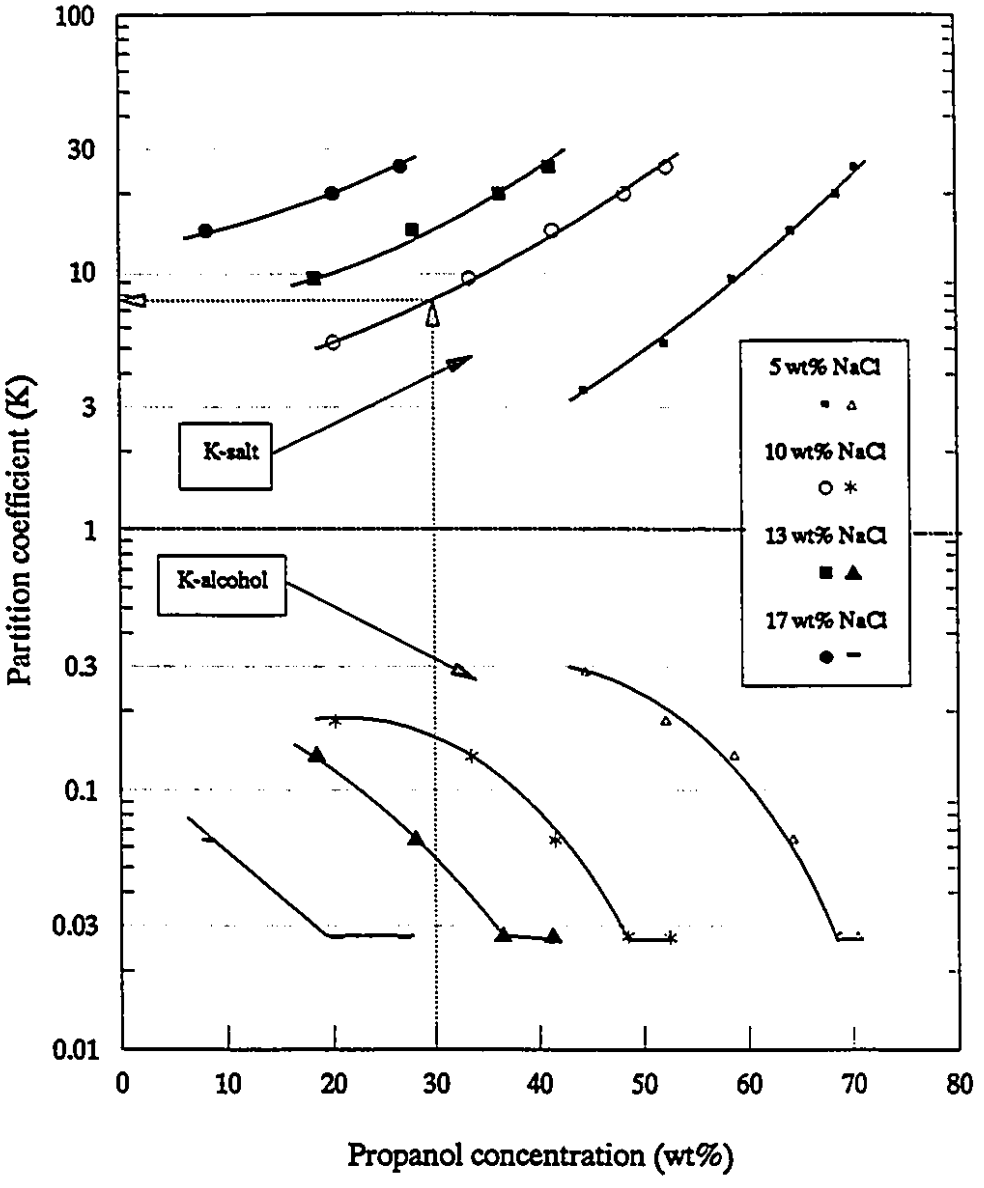

Figure 3.9: Partition coefficient plot for 1-propanol–NaCl–water

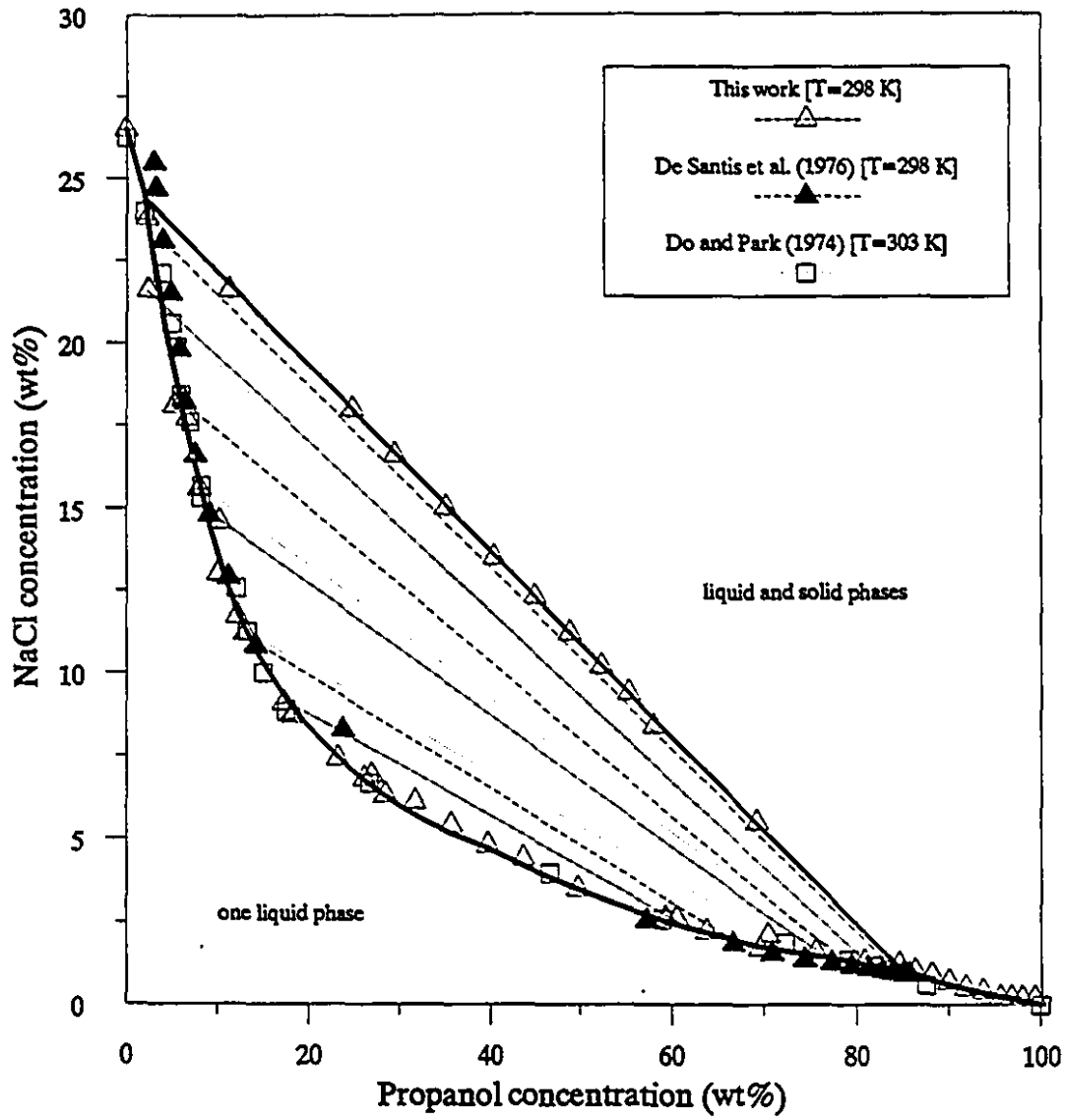

Figure 3.10: Binodal curves for 1-propanol–NaCl–water

cylindrical and sheet-like micelle structures. These anisotropic phases are present at concentrations above 25 wt%, corresponding to a molality of 1.5. Studies by Ralston et al. (1941), Broome et al. (1950) and Gault et al. (1988) determined that at temperatures above the Krafft point and concentrations below 25wt%, only isotropic phases are present.

The addition of small amounts of NaCl to dilute binary solutions of DAC results in liquid-liquid phase separation. Figure 3.12 shows the variation of solubility with temperature for an aqueous solution of DAC containing 0.5 M NaCl (Imae et al., 1988). With this amount of salt, the system forms two phases at very low surfactant concentrations, provided the temperature is above the Krafft temperature.

The addition of small amounts of NaCl at 303 K yielded two phases. The time required to obtain clear phases after shaking ranged from 1 to 2 hours. The top phases, although clear, had a faint blue tinge. Examination under a polarizing microscope showed them to be isotropic. The densities ranged from 1.013–1.016 g/ml and the viscosity was not much different from that of water. The bottom phases were denser (1.018–1.022 g/ml) and completely clear.

The binodal curve for this system is presented as Figure 3.13. It was not possible to map a greater portion of the phase diagram because mixing more concentrated solutions of NaCl and surfactant produced a heterogeneous coagel-like phase consisting of solid white hydrate interspersed with clear liquid. This mixture could not be resolved into two clear phases even after centrifugation for 2 hours at 12000 rpm.

As described previously, concentrations were determined using AAS and oven drying. The results of the analyses were validated by checking mass balances, which agreed to within 7%. The standard deviation of the concentrations of surfactant in three tie-line replicates was 0.006 M corresponding to a 95% confidence interval of

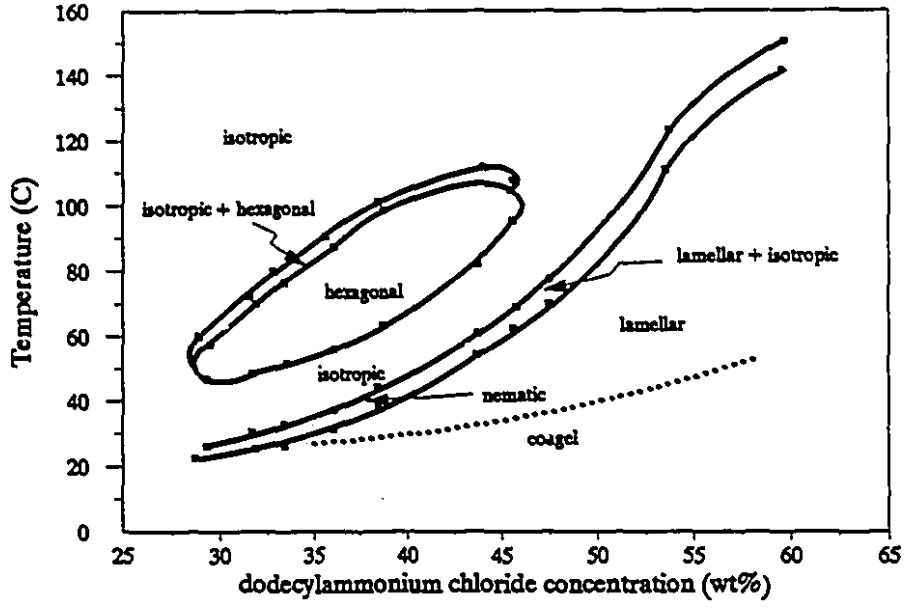

Figure 3.11: Binary phase diagram for DAC–water (Gault et al., 1988)

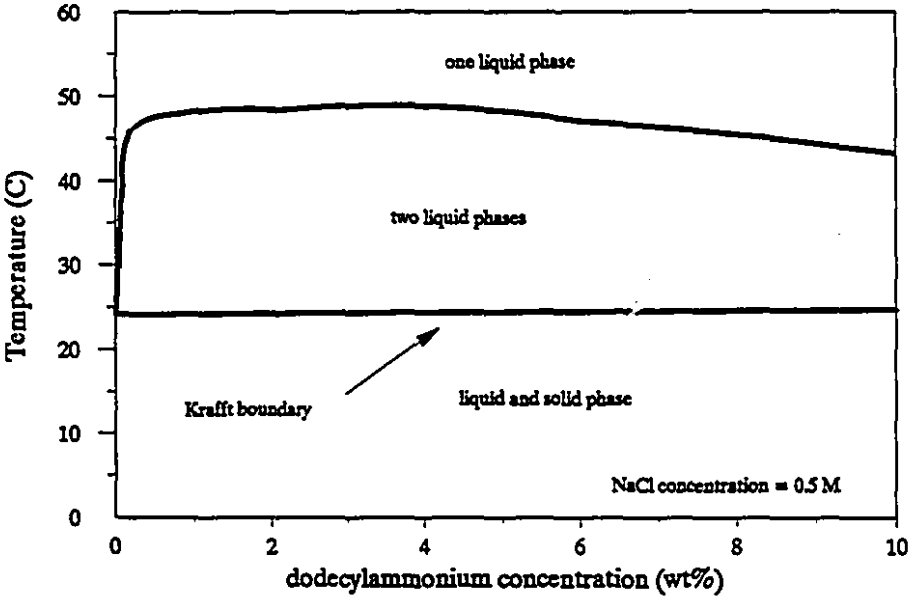

Figure 3.12: Solubility diagram for DAC–NaCl–water (Imae et al., 1988)

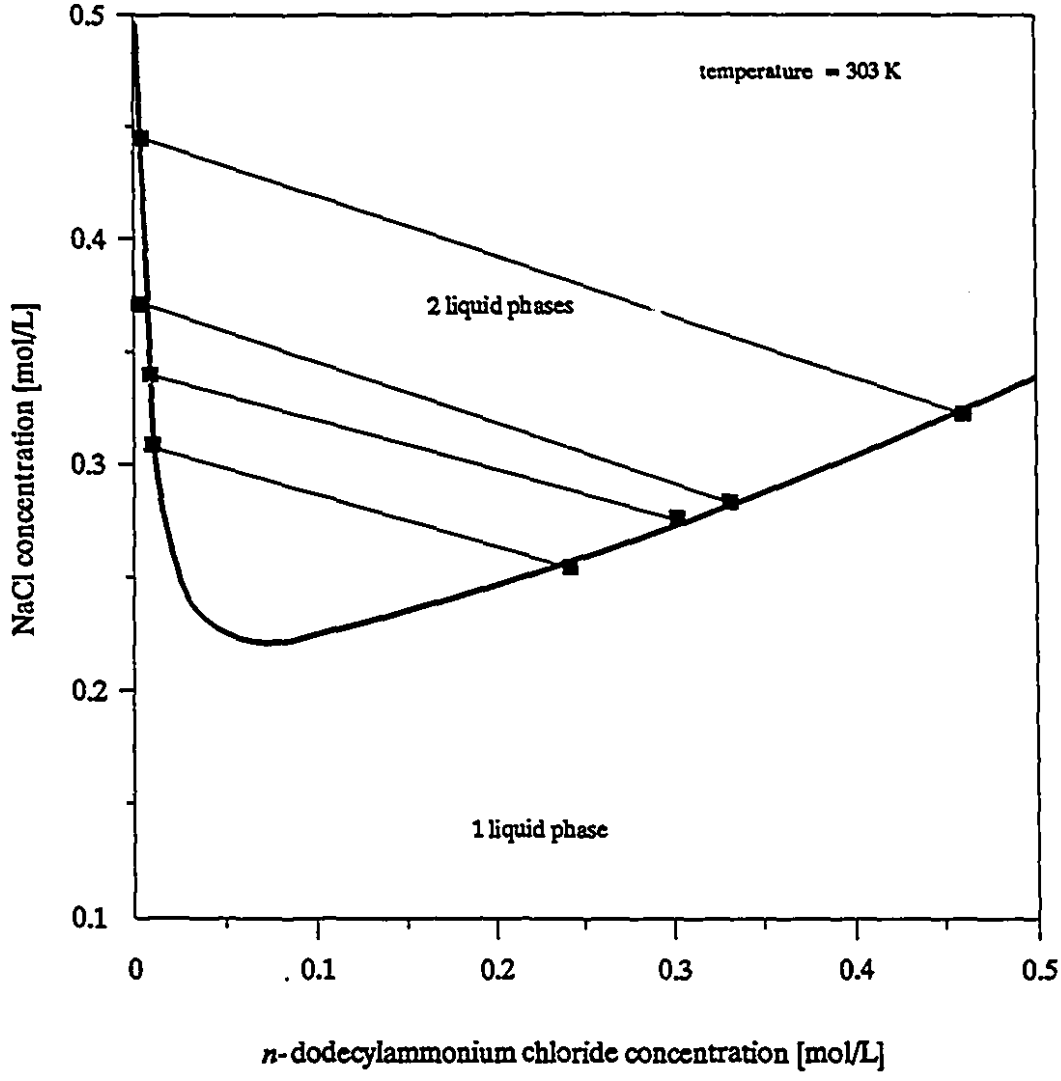

Figure 3.13: Binodal curve for DAC–NaCl–water

± 0.011 M. The location of the plait point was estimated using the intersection of the binodal curve and a line joining the middle points of tie-lines as described by Albertsson (1986). The value obtained is 0.22 M NaCl and 0.06 M DAC.

The location of the binodal curve indicates that both equilibrium phases are predominantly water. The shape of the binodal curve is similar to that displayed by other aqueous cationic surfactant–salt systems (Imae et al., 1988; Rizzatti and Gault, 1986), aqueous zwitterionic surfactant–salt systems (Herrmann, 1964; Imae and Ikeda, 1986, Imae et al., 1986; Abe et al., 1988) and aqueous polyelectrolyte-salt systems (Eisenberg and Mohan, 1959; Thalberg et al., 1990, 1991a,b).

The driving force for phase separation in this and similar systems is not clearly understood. While the positively charged amphiphilic components of alkylammonium halide surfactants may hydrogen bond with water (Imae, 1988), in binary solution at concentrations above the CMC they form spherical micelles. The addition of NaCl leads to the formation of rod-like micelles at a critical salt concentration, equal to 0.06 M at 30°C for *n*-dodecylammonium chloride (Tanford, 1973). Considering the above factors, it is likely that the phase separation is driven by competition between hydrogen bonding, salting out, hydrophobic effects (Huot and Jolicoeur, 1985) and electrostatic interactions.

The tie-lines in Figure 3.13 are close to horizontal indicating weak partitioning of the salt and strong partitioning of the surfactant. This is confirmed in Figure 3.14, which is a semilogarithmic plot of the partition coefficients. The partition coefficients for NaCl range from 1.1 to 1.4 while those for the surfactant are in the range 0.04 to 0.009.

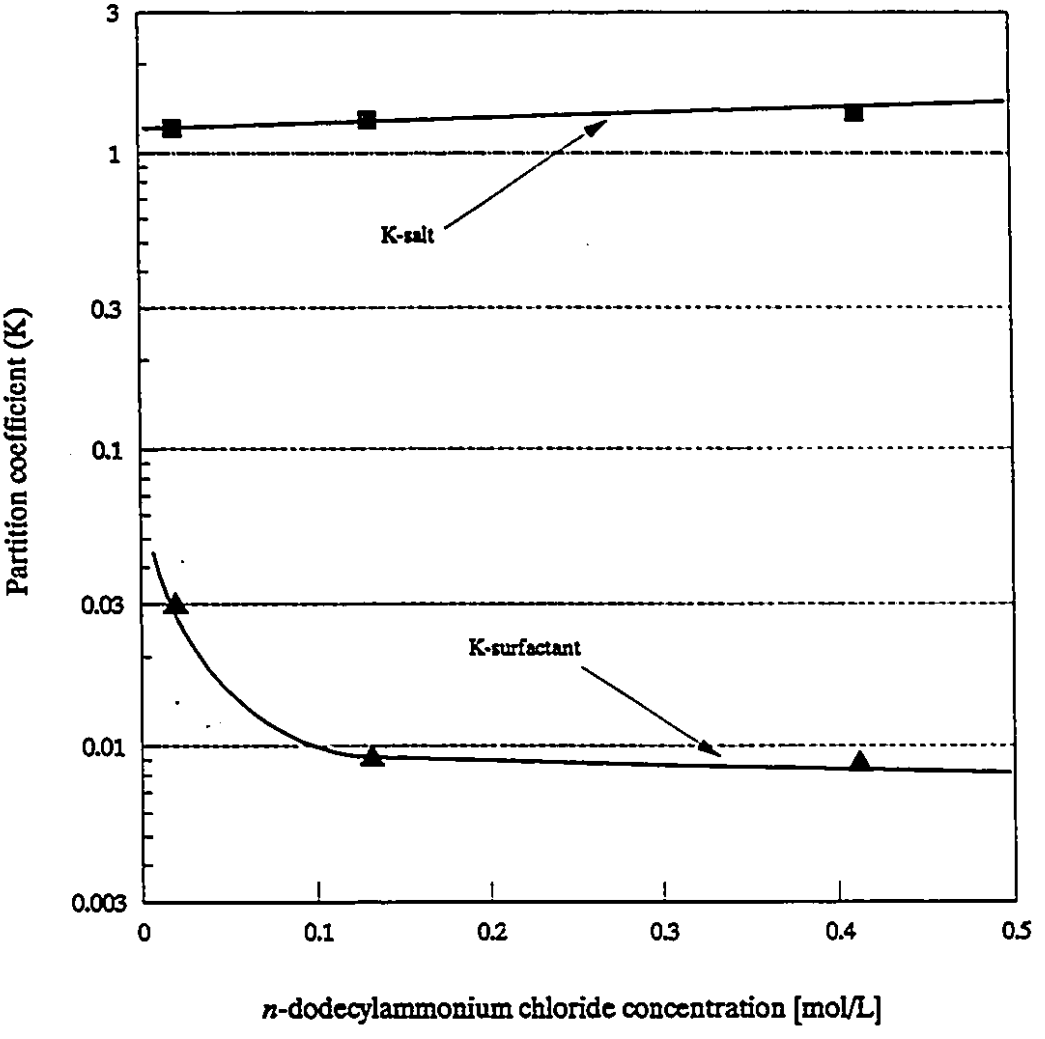

Figure 3.14: Partition coefficient plot for DAC–NaCl–water for 0.34M NaCl

Poly(ethylene glycol) 8000–NaCl–Water

Since the addition of NaCl to an aqueous solution of PEG 8000 did not yield two-liquid phases under ambient conditions, experiments were conducted at 333 K . Phase separation was slow, requiring at least 24 hours. The equilibrated top phases were transparent when in the bath but slowly turned cloudy upon removal from the bath as the temperature dropped. Hence sampling of the phases was completed rapidly. The top phases were rich in PEG, low in salt, quite viscous, and had densities at 333 K ranging from 1.133 to 1.161 g/ml. The bottom phases were rich in NaCl and transparent even upon removal from the bath. For phase systems saturated in salt, cooling of the bottom phase samples resulted in the precipitation of salt. The densities of the bottom phases ranged from 1.134 to 1.197 g/ml.

The binodal curve for this system is presented as Figure 3.15. Two liquid phases are obtained only for low concentrations of the polymer, less than 45 wt%, Hence both phases are rich in water and the concentration of salt is high in both phases. The plait point was estimated to be 15 wt% NaCl and 9 wt% PEG. As discussed by Florin et al. (1984), the phase separation in this system is likely the result of water structure effects, in particular the competition for water of hydration between ethylene oxide units of the polymer and Na^+ and Cl^- ions. This is the process underlying the typical salting out process (Molyneux, 1975; Ananthapadmanabhan and Goddard, 1987). For PEG–salt systems, the size of the two-phase region increases with the size and charge of the electrolyte anion in accord with the lyotropic series (Albertsson, 1986; Eiteman and Gainer, 1989; Zaslavsky et al., 1989; Vernau and Kula, 1990; Pathak et al., 1991; Gao et al., 1991a; Snyder et al., 1992).

The partitioning behavior of nonaqueous components of the solution is illustrated in Figure 3.16. In this figure the solid lines connecting the partition coeffi-

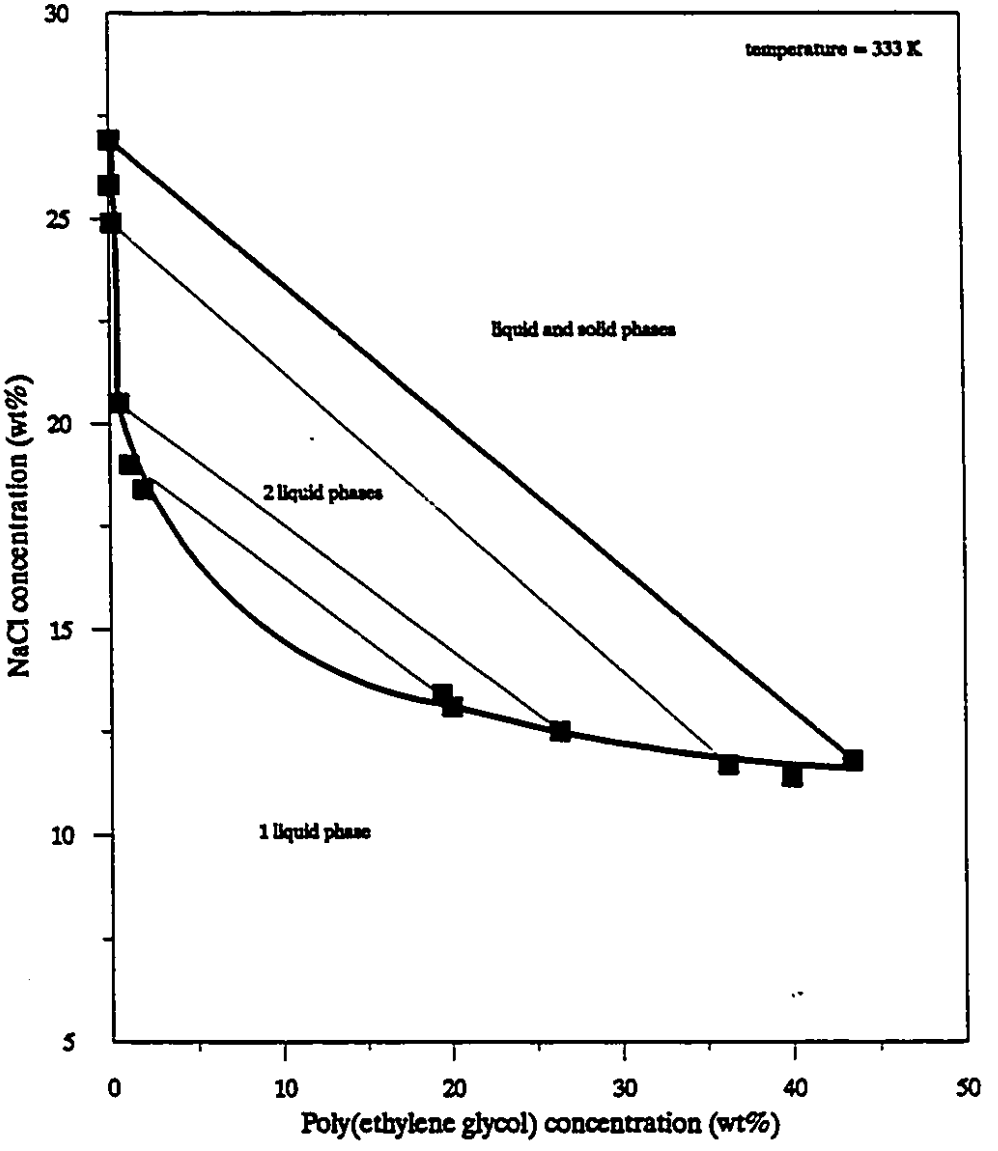

Figure 3.15: Binodal Curve for PEG 8000–NaCl–water

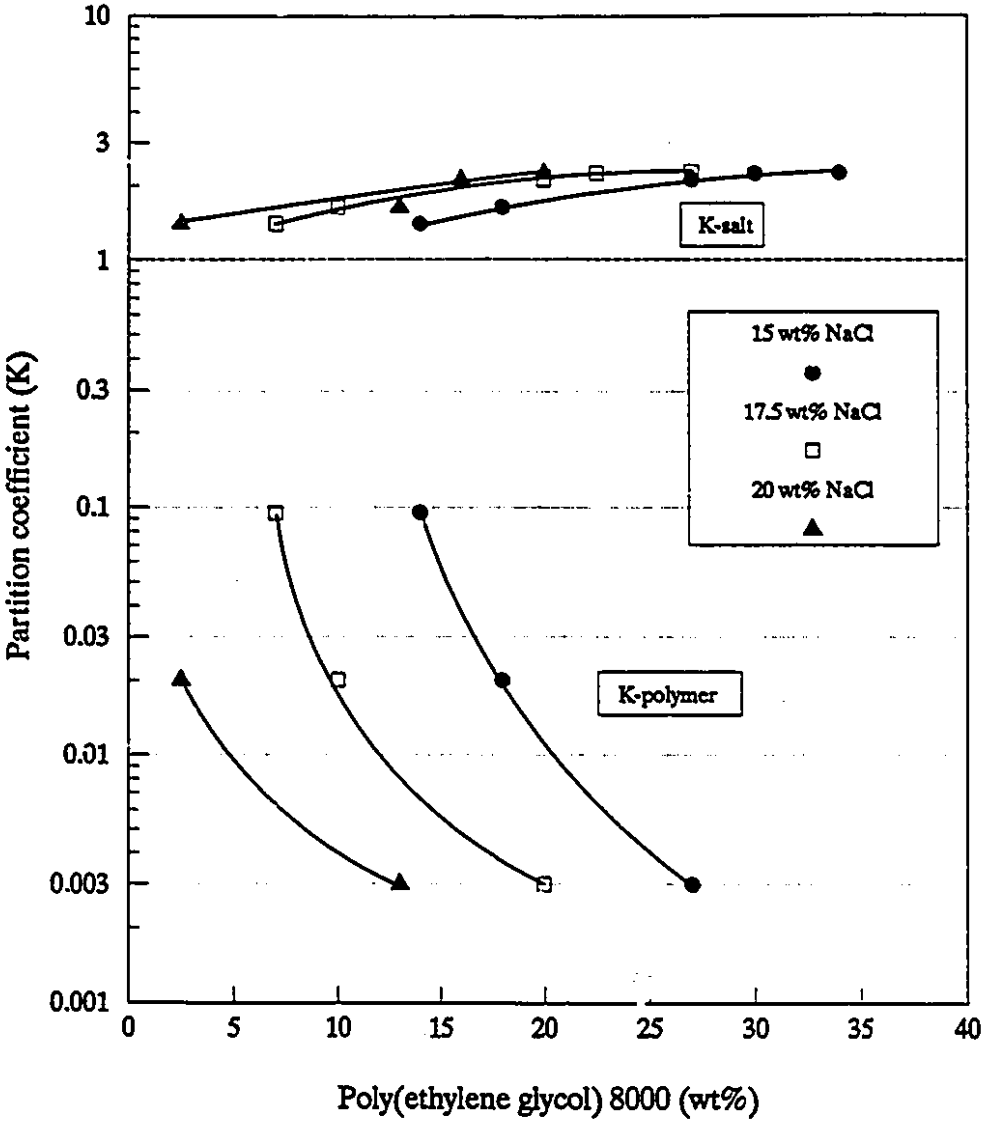

Figure 3.16: Partition coefficient plot for PEG 8000–NaCl–water

cients cover the range from the left-most to the right-most tie-line in Figure 3.15. For the polymer partition coefficients, only the three left-most tie-lines are represented. The salt is not strongly partitioned, with partition coefficients ranging from 1.5 to about 2. The polymer, however, is strongly partitioned to the top phase, with partition coefficients around 0.1 at low PEG concentrations to near zero at high PEG concentrations. These results are in qualitative agreement with the single tie-line determined at 83.4°C by Florin et al. (1984) for an aqueous system of NaCl and PEG of average molecular weight $4x10^6$.

Poly(propylene glycol)–NaCl–Water

For this polymer, experiments were carried out at three temperatures and for two molecular weight fractions. The first fraction had a weight average molecular weight of 425 and was studied at 278, 298, and 333 K. The second fraction had a higher molecular weight, 725, and for this system experiments were performed at 278 and 298 K.

The phase behavior of a binary aqueous solution of PPG 400 is displayed in the form of a cloud point curve in Figure 3.17 (Malcolm and Rowlinson, 1957). For this fraction of polymer, two phases are obtained for temperatures above 325 K. Addition of NaCl lowers the cloud point resulting in the presence of two phases at lower temperatures.

Phase separation was quick, with clear phases visible within 2 hours of shaking. Both equilibrium phases were clear although at 278 and 333 K faint cloudiness was observed in the top phases when samples were withdrawn from the temperature controlled baths. As with PEG, this was due to the change in temperature. The top phases were viscous and contained most of the polymer, and the densities, at 298 K, were in the range 1.030-1.036 g/ml for PPG 425 and 1.022-1.031 g/ml for

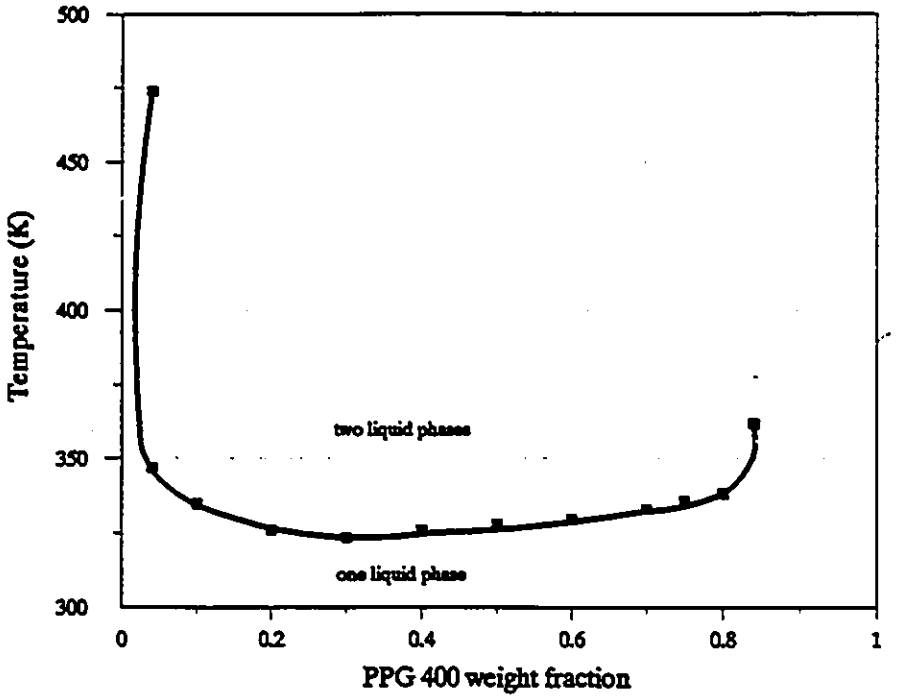

Figure 3.17: Cloud point curve for aqueous PPG 400 (redrawn from Malcolm and Rowlinson, 1957)

PPG 725. The bottom phases were less viscous and had corresponding densities in the ranges of 1.069–1.100 g/ml and 1.062–1.131 g/ml.

The binodal curves of PPG 425, at 278, 298, and 333 K are presented in Figures 3.18–3.20. The plait points were estimated to be (4 wt%NaCl, 43 wt%PPG), (2 wt%NaCl, 56 wt%PPG) and (0.5 wt%NaCl, 50 wt%PPG), respectively. The corresponding binodal curves for PPG 725 at 278 and 298 K are shown in Figures 3.21 and 3.22. The plait points for this system were estimated to be (1 wt%NaCl, 52 wt%PPG) and (0.4 wt%NaCl, 56 wt%PPG), respectively. The complete phase diagram for PPG 425 at 298 K, in triangular coordinates, is shown in Figure 3.23.

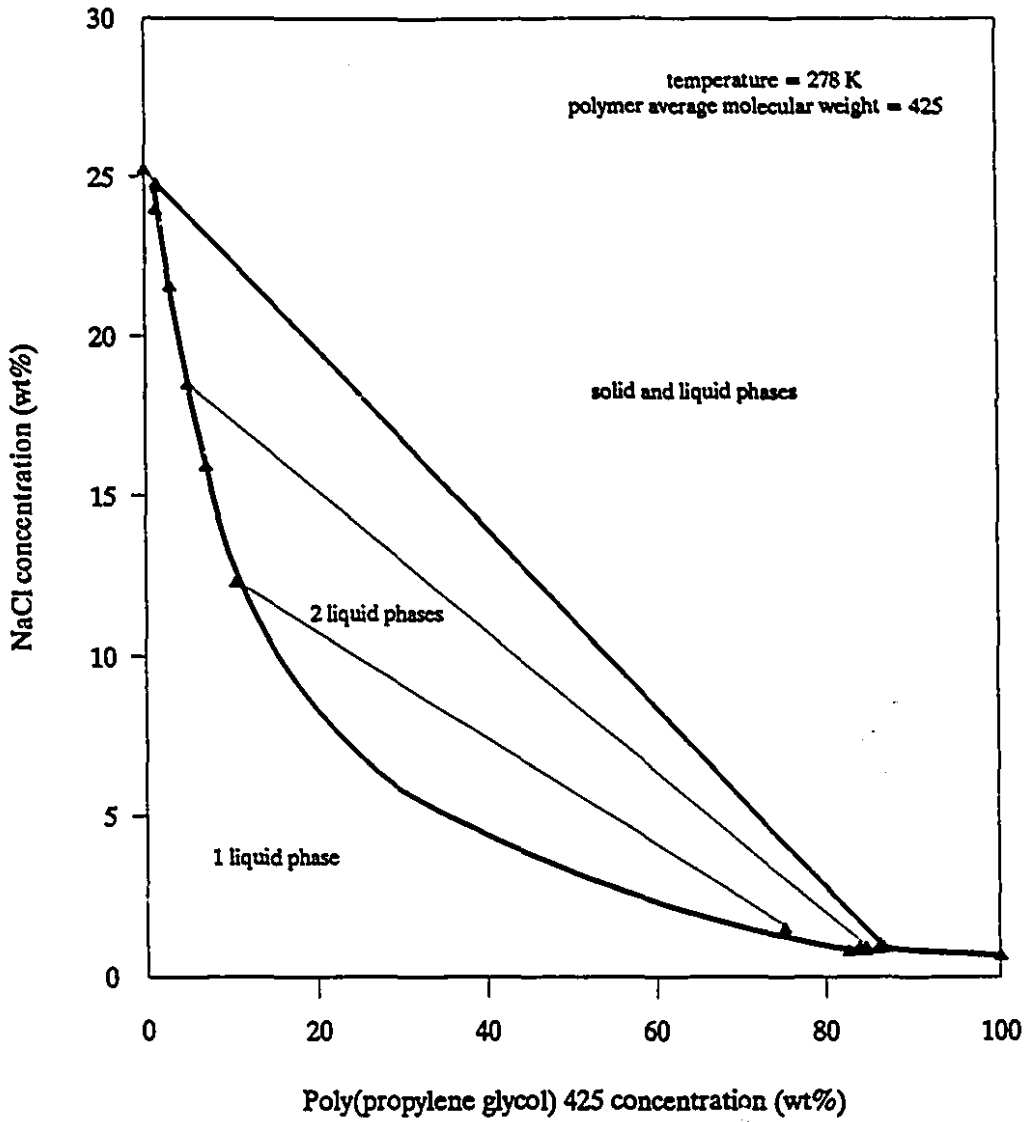

Figure 3.18: Binodal Curve for PPG 425–NaCl–water at 278 K

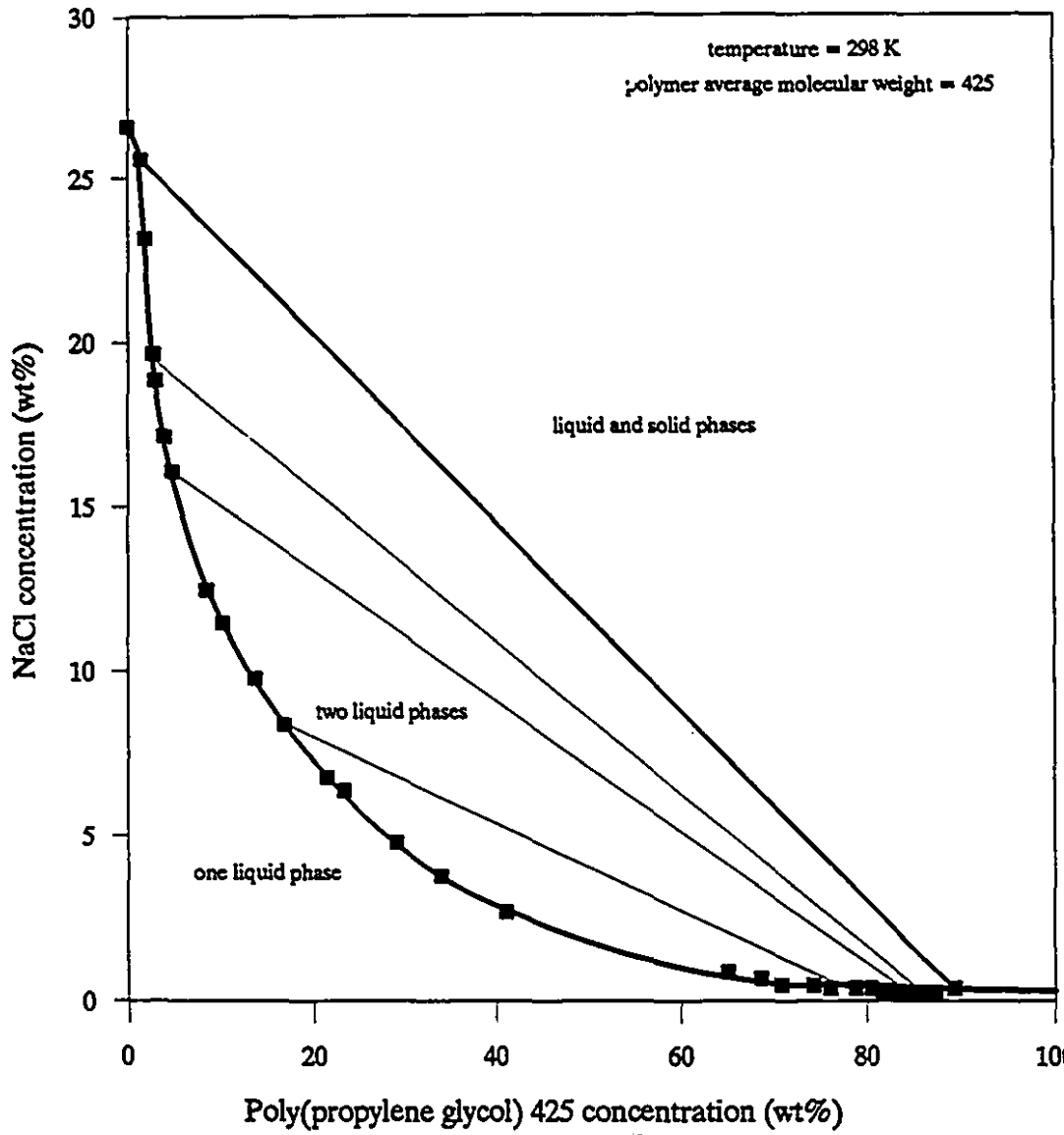

Figure 3.19: Binodal Curve for PPG 425–NaCl–water at 298 K

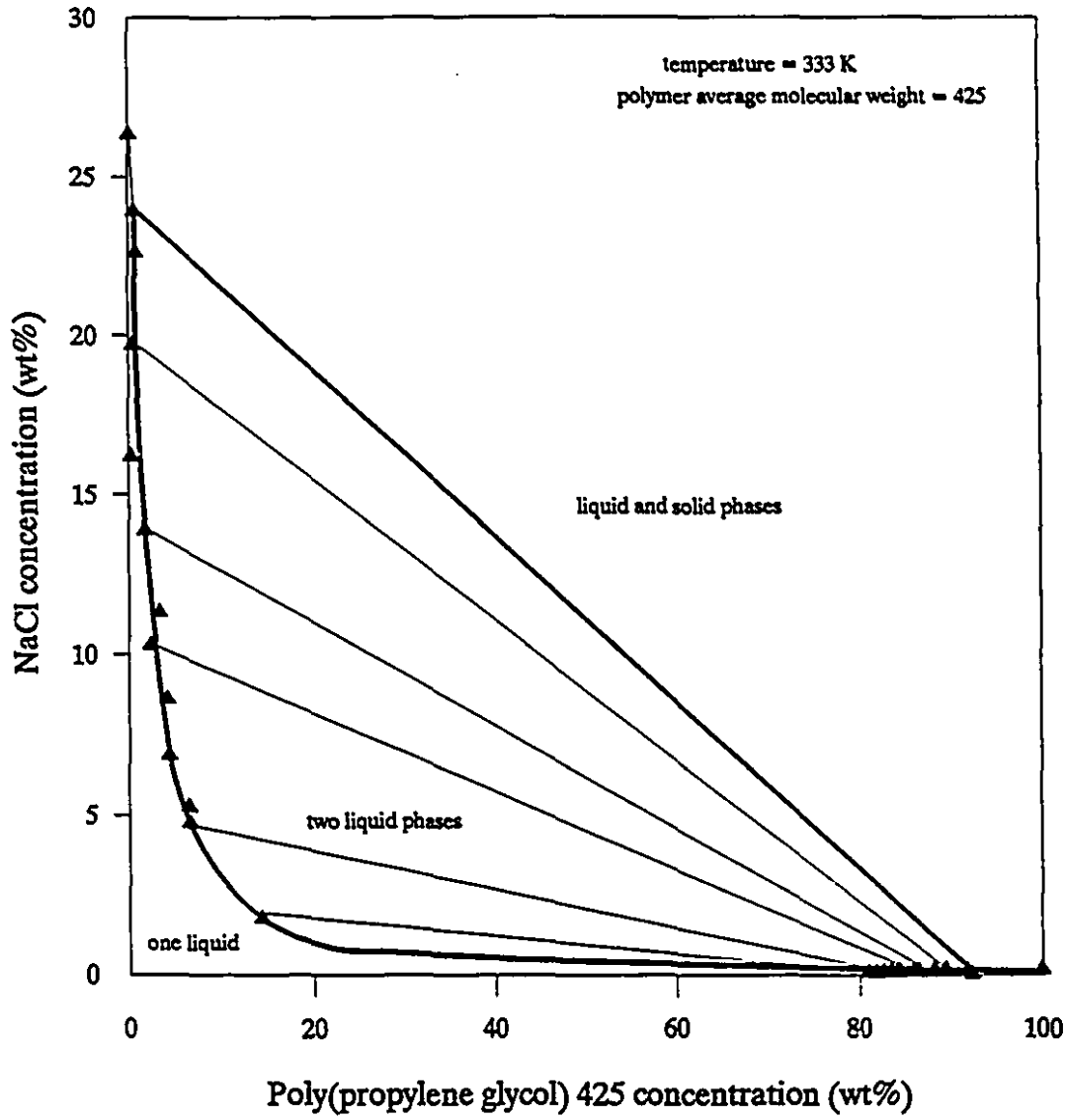

Figure 3.20: Binodal Curve for PPG 425–NaCl–water at 333 K

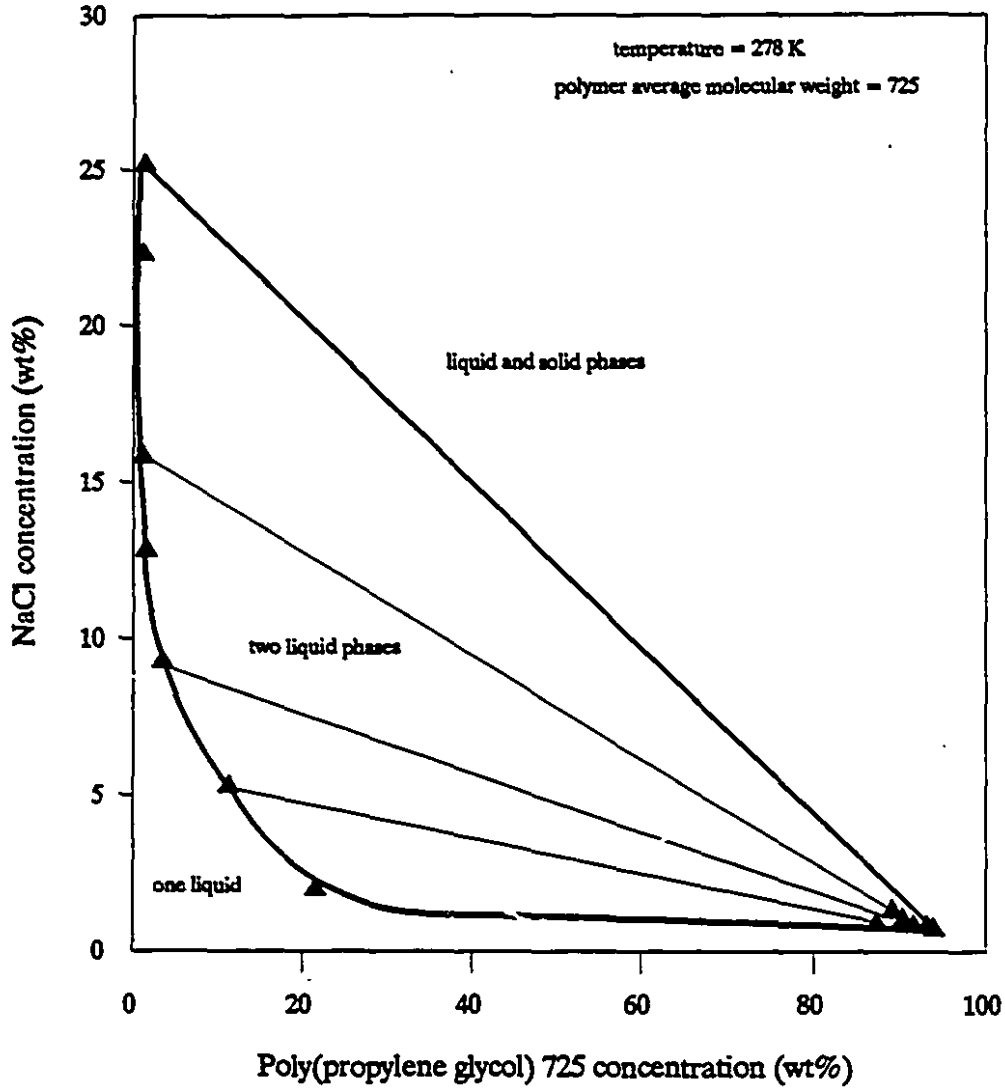

Figure 3.21: Binodal Curve for PPG 725–NaCl–water at 278 K

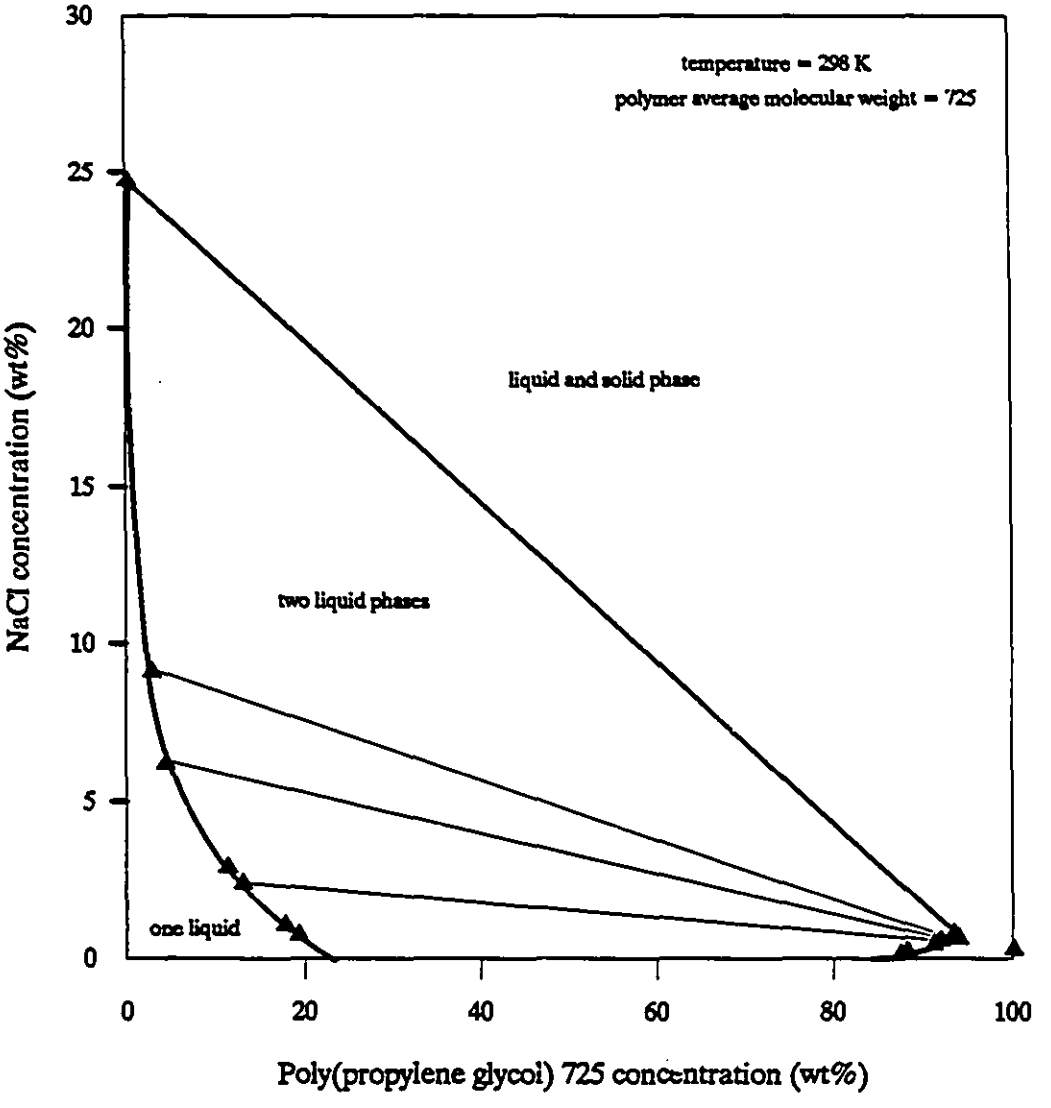

Figure 3.22: Binodal Curve for PPG 725–NaCl–water at 298 K

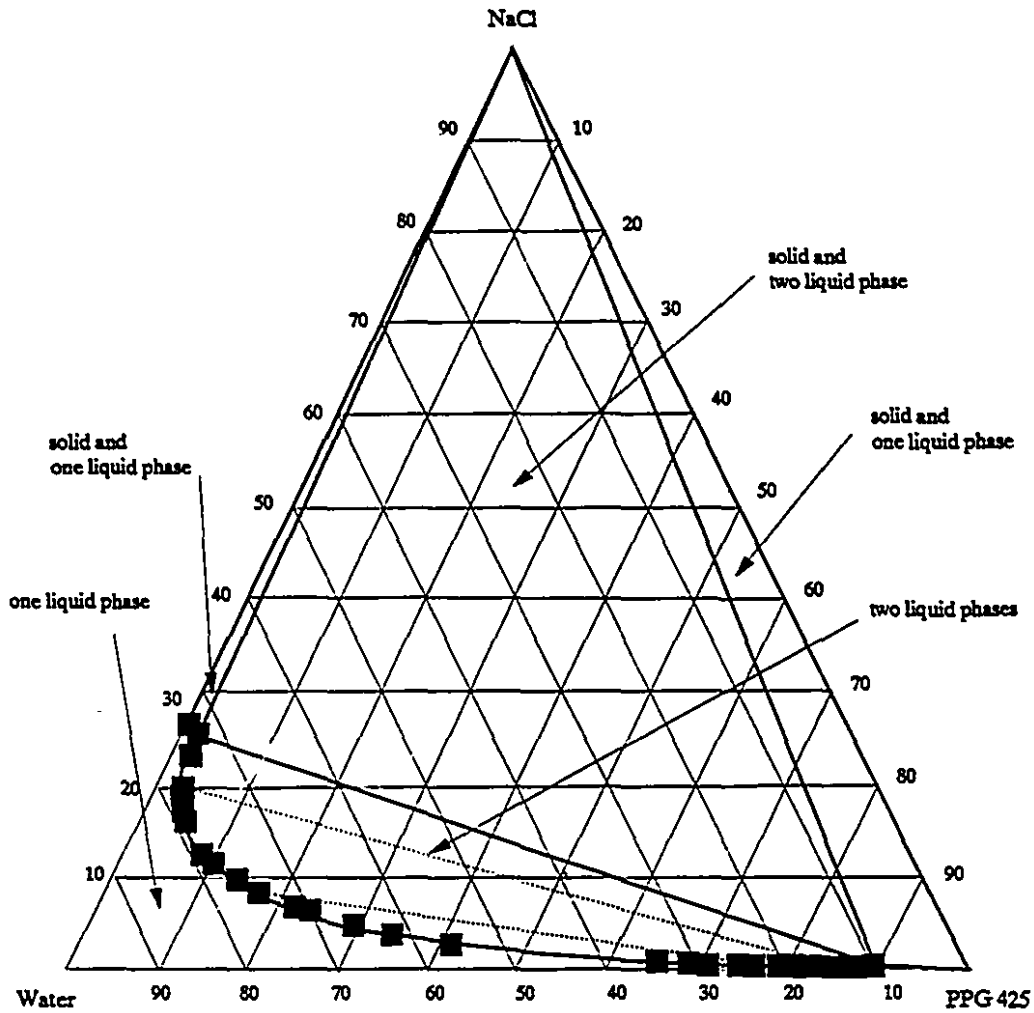

Figure 3.23: Complete phase diagram for PPG 425–NaCl–water at 298 K

This type of phase diagram is typical of two-phase systems in which the cause for phase separation is the salting out of a hydrogen bonded solute (Kjellander and Florin, 1980; Florin et al., 1984). Poly(propylene glycol) is a hydrogen bonding polymer, as is evident for the LCT curve of Figure 3.17. The monomer of PPG is structurally similar to PEG

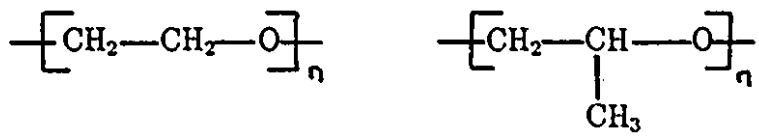

PEG PPG

except that the methyl group gives the unit a more hydrophobic character. This is reflected in the comparison of Figures 2.1 and 3.17, which shows that the polymer-rich equilibrium phase is more concentrated in the case of PPG. In addition, aqueous solutions of PPG separate at lower temperatures. Similarly, the region of the binodal curve corresponding to two liquid phases is larger for PPG than it is for PEG, and the polymer-rich phase is more concentrated with PPG. The triangular phase diagram for PPG 425 at 298 K, Figure 3.23, is similar to that for the propanol system (Figure 3.8) and contains identical regions.

The effect of temperature on the phase diagram is illustrated in Figure 3.24. The effect of increasing the temperature is to make the polymer and salt more incompatible, increasing the size of the two phase region. This is similar to the widening of the loop with temperature in a binary LCT curve. For a given feed composition, as the temperature is increased, the top phases contain less salt and the bottom phases less polymer. This effect is similar to that observed with other polymer–salt and polymer–polymer aqueous two-phase systems (Albertsson, 1986; Sjöberg and Karlström (1989); Pathak et al., 1991; Ho Gutiérrez, 1992). Studies

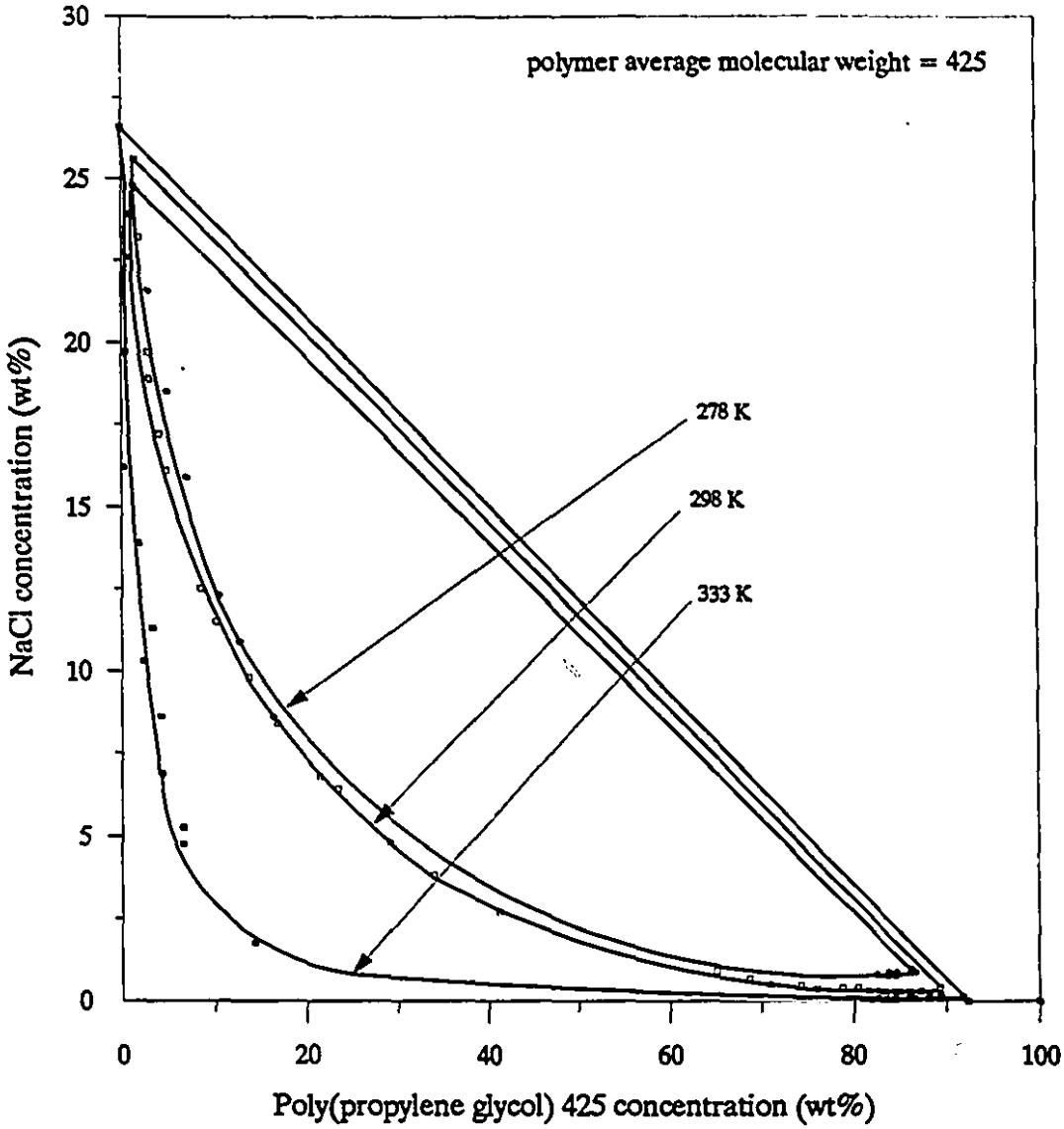

Figure 3.24: Effect of temperature on the binodal curves of PPG 425–NaCl–water

on the effects of salts on the cloud points of polymers (Bailey and Callard, 1959; Florin et al., 1984; Firman et al., 1985) and nonionic surfactants (Schott, 1973; Tokiwa and Matsumoto, 1975; Schott et al., 1984) show that inorganic salts may raise or lower the cloud point. Those salts raising the cloud point are "salting in" the polymer while those lowering the cloud point are "salting out" the organic solute. Figure 3.24 is consistent with the interpretation of NaCl as a salting out electrolyte.

Similarly, the effect of increasing the average polymer molecular weight is to increase the size of the two-phase region, as shown in Figure 3.25. Hence the 725 molecular weight fraction is less compatible with NaCl. A similar trend has been observed with aqueous two-phase salt systems containing PEG and other polymers (Albertsson, 1986; Snyder et al., 1992). This result is consistent with the observation that the solubility of PPG in water decreases with increasing molecular weight (Molyneux, 1983).

As for the separation of the polymer and salt, Figure 3.26 shows the partition coefficients for the PPG 425 system at 298 K. Both the polymer and salt are strongly partitioned to opposite phases. For this system the partition coefficient for the salt ranges from 6 to 85. The corresponding values for the polymer are 0.5 to 0.015. The effect of changing the temperature is illustrated in Figure 3.27, which shows partition coefficients for the PPG 425 system at three temperatures. An increase in the temperature results in more complete partitioning of the components as the values of the partition coefficients for the salt increase while those for the polymer decrease. Molecular weight effects on separation are presented in Figure 3.28 which indicates that with an increase in polymer molecular weight the separation of the polymer becomes more complete while that of the salt becomes less complete.

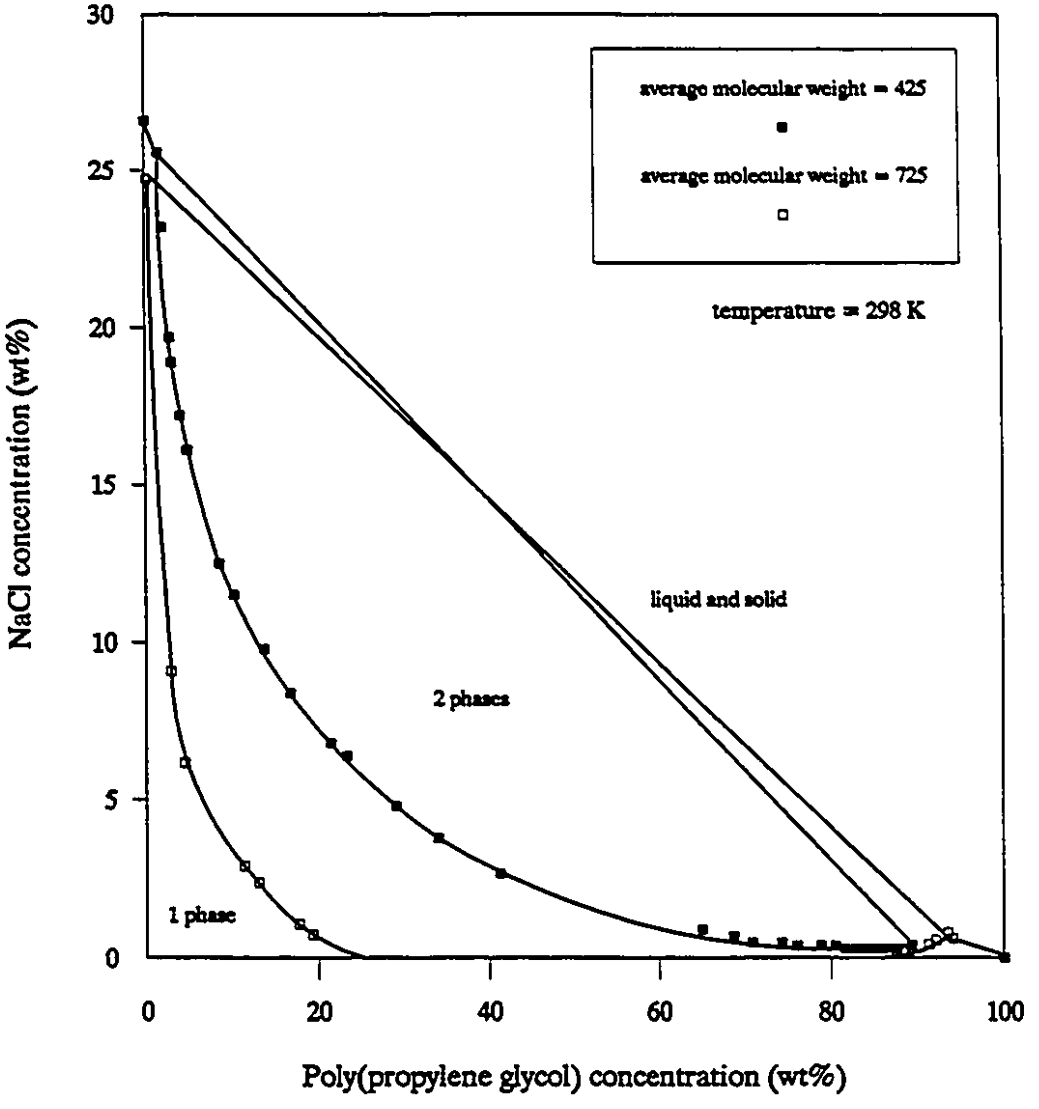

Figure 3.25: Effect of molecular weight on the binodal curves of PPG–NaCl–water

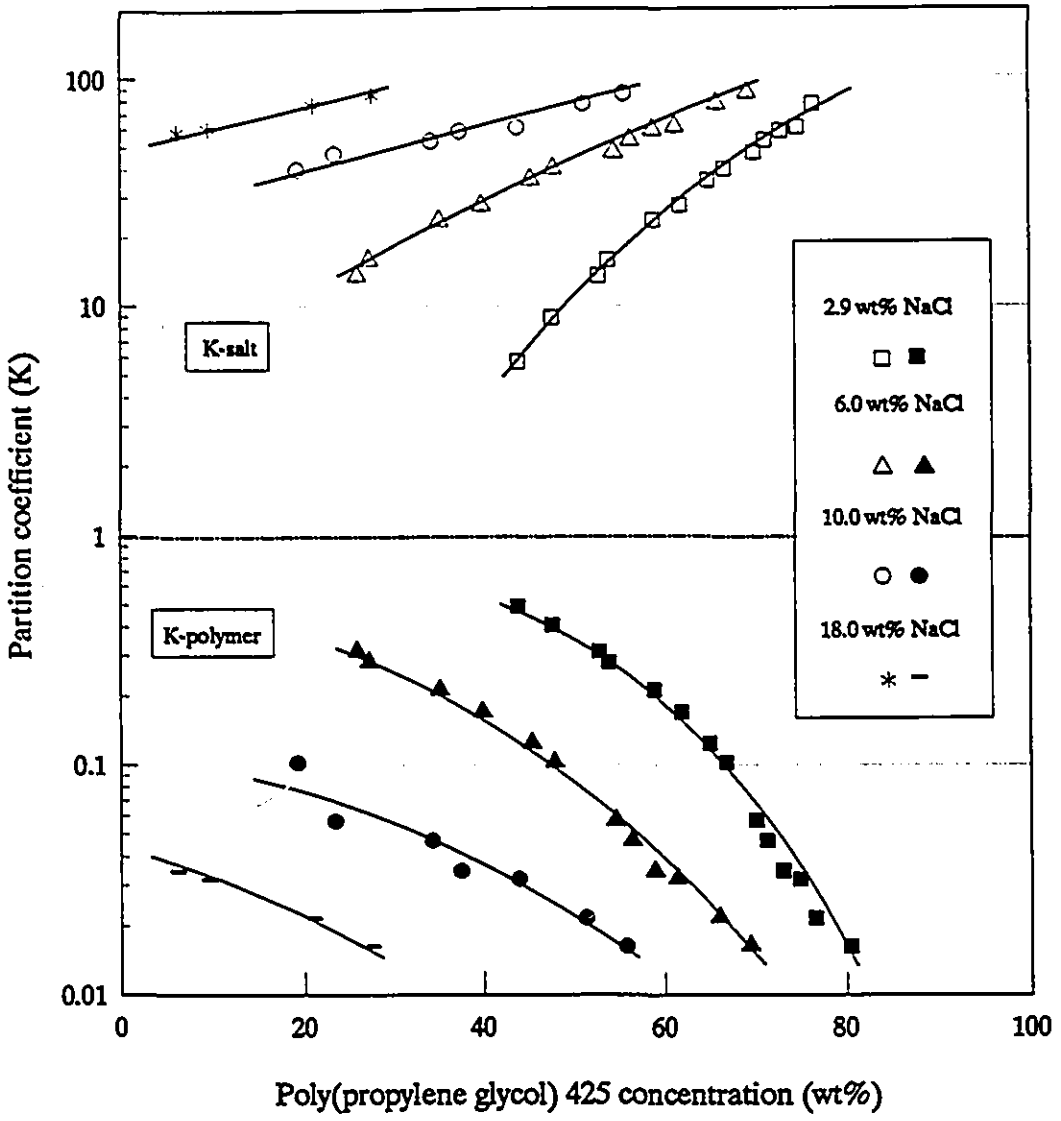

Figure 3.26: Partition coefficient plot for PPG 425–NaCl–water at 298 K

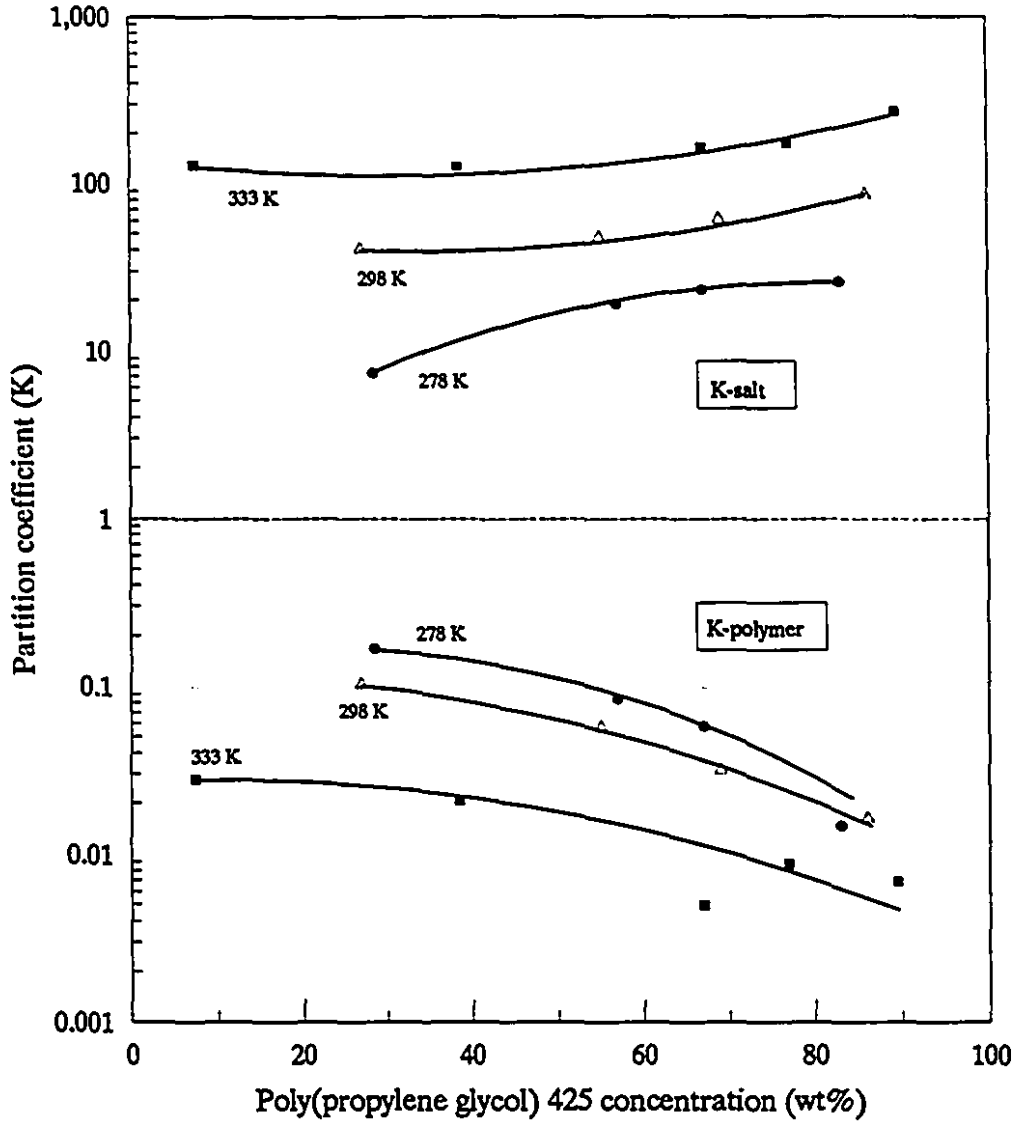

Figure 3.27: Effect of temperature on partition coefficients for PPG 425–NaCl–water

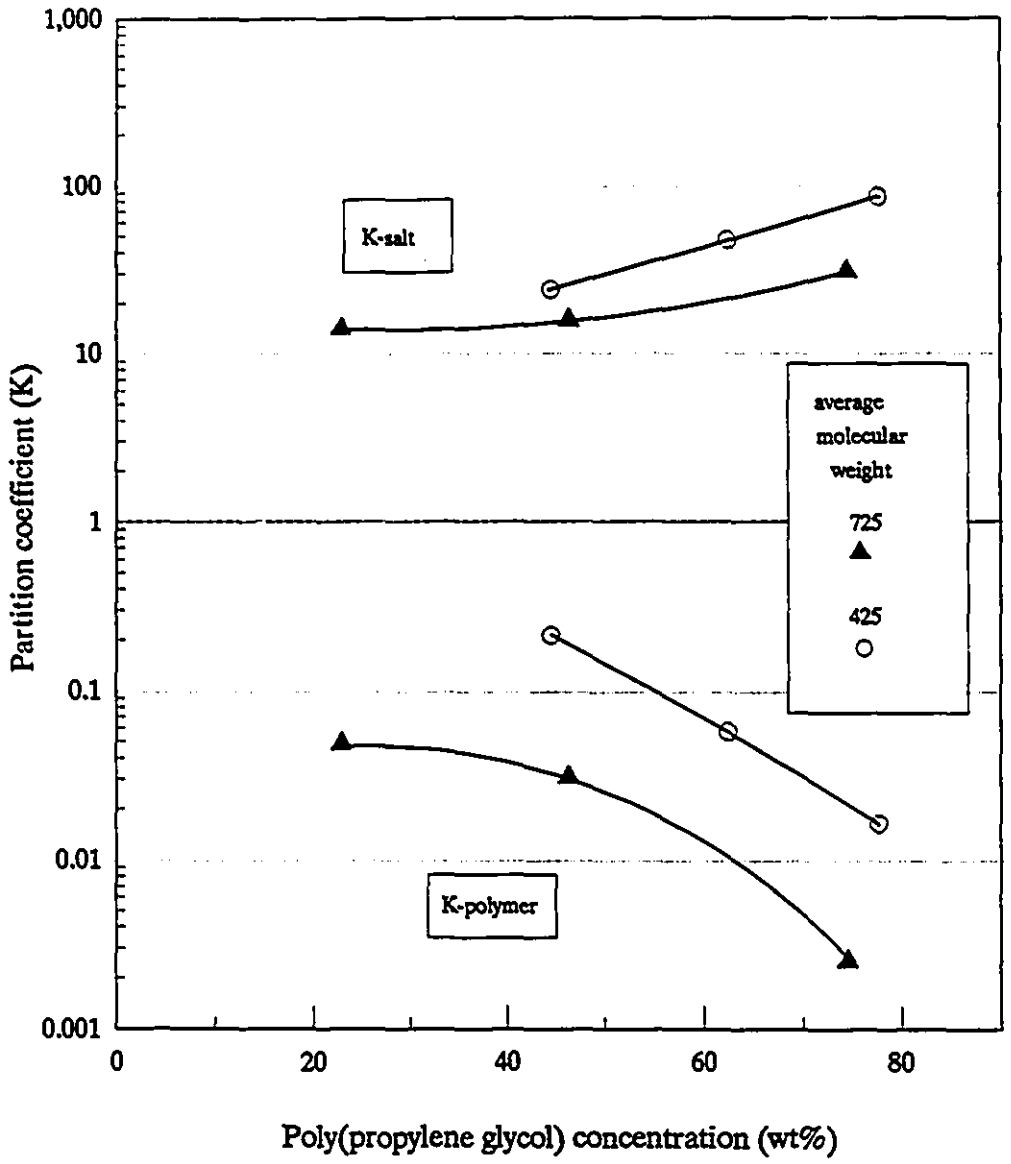

Figure 3.28: Effect of molecular weight on partition coefficients of PPG–NaCl–water

Chapter 4

Liquid-Liquid Equilibrium in Multicomponent Systems

The treatment of liquid-liquid equilibrium in multicomponent systems containing salts is an extension of the treatment for binary systems described in Chapter 2. Here the system consists of N_C components, of which N_S are nonelectrolytes and N_C-N_S are strong electrolytes. The biphasic system, illustrated in Figure 4.1, is at equilibrium when temperature, T, and pressure, P are equal in the phases and the Gibbs free energy is at a minimum with respect to changes in T, P, and the N_C-1 independent mole fractions or molalities in each of the phases.

When the composition of each phase, $\underline{c}$, is expressed using mole fractions, x_i, and molalities, m_i, with T and P fixed, the total free energy of the system is the sum of contributions from the two phases

$$G(T,P,\underline{c}) = G^I(T,P,\underline{c}^I) + G^{II}(T,P,\underline{c}^{II}) \tag{4.1}$$

For each phase the Gibbs free energy is calculated relative to its value (G^θ) when all the components are in their standard states which depend on the temperature

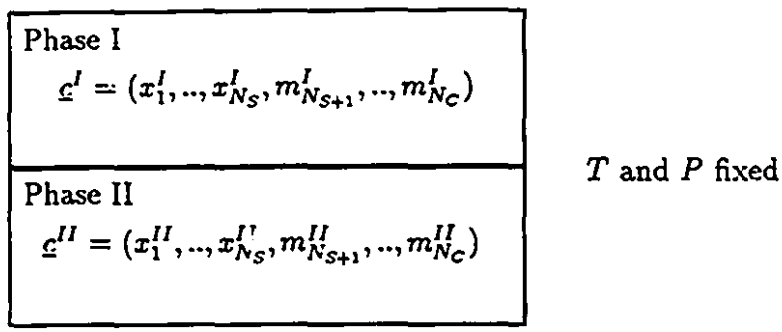

Figure 4.1: Multicomponent liquid-liquid equilibrium

and, possibly, the pressure and composition of the system in that phase.

$$G(T, P, \underline{c}) = G^{\theta}(T, P, \underline{c}) + \Delta G^{M^{\theta}}(T, P, \underline{c}) \tag{4.2}$$

where $\Delta G^{M^{\theta}}$ is the change in free energy on mixing the components from their standard states to their conditions in the solution. The equilibrium criterion

$$dG(T, P, \underline{c}) = dG^I(T, P, \underline{c}^I) + dG^{II}(T, P, \underline{c}^{II}) = 0 \tag{4.3}$$

requires that the chemical potentials of the components, μ_i, be equal in phase I and phase II

$$\mu_i^I(T, P, \underline{c}^I) = \mu_i^{II}(T, P, \underline{c}^{II}) \qquad i = 1, \ldots, N_C \tag{4.4}$$

where, for each phase,

$$\mu_i(T,P,\underline{c}) = \left[\frac{\partial G(T,P,\underline{c})}{\partial n_i}\right]_{T,P,n_{j\neq i}} \qquad i = 1,\ldots,N_C \tag{4.5}$$

and

$$G(T,P,\underline{c}) = \sum_{i=1}^{N_C} n_i \mu_i(T,P,\underline{c}) \tag{4.6}$$

Differentiation of equation (4.2) yields

$$\mu_i(T,P,\underline{c}) = \mu_i^{\theta}(T,P,\underline{c}) + \sum_{k=1}^{N_C} n_k \left[\frac{\partial \mu_k^{\theta}(T,P,\underline{c})}{\partial n_i}\right]_{T,P,n_{j\neq i}} + \left[\frac{\partial \Delta G^{M^{\theta}}(T,P,\underline{c})}{\partial n_i}\right]_{T,P,n_{j\neq i}} \tag{4.7}$$

where the two derivative terms on the right hand side of the equation above represent the difference in the value of the chemical potential of component i in going from its standard state to its state in the solution. This value is the change in chemical potential of i on mixing from the standard state ($\Delta\mu_i^{M^{\theta}}$).

$$\begin{aligned}\Delta\mu_i^{M^{\theta}}(T,P,\underline{c}) &= \mu_i(T,P,\underline{c}) - \mu_i^{\theta}(T,P,\underline{c}) \\ &= \sum_{k=1}^{N_C} n_k \left[\frac{\partial \mu_k^{\theta}(T,P,\underline{c})}{\partial n_i}\right]_{T,P,n_{j\neq i}} + \left[\frac{\partial \Delta G^{M^{\theta}}(T,P,\underline{c})}{\partial n_i}\right]_{T,P,n_{j\neq i}}\end{aligned} \tag{4.8}$$

The *activity* of the component, a_i, is defined through $\Delta\mu_i^{M^{\theta}}$

$$\Delta\mu_i^{M^{\theta}}(T,P,\underline{c}) \equiv RT \ln a_i^{\theta}(T,P,\underline{c}) \tag{4.9}$$

If a model of the activities of the components of a solution as functions of temperature, and pressure and composition is available, then equations (4.4), (4.8) and (4.9) can be used to calculate the value of compositions at equilibrium for a fixed

T and P.

4.1 Activities, Activity Coefficients, Reference and Standard States for Components of Liquid Solutions

The following three sections describe thermodynamic relations between chemical potentials, activities, activity coefficients and their associated reference and standard states. The first section describes the relations for a solution in which the concentrations of all components are expressed by mole fractions and in which the standard states of all components are independent of the composition of the system. The second deals with the activities of solutes in an electrolyte solution where the concentrations of the salts are measured in molalities and the standard states of all components are independent of composition. Finally, multicomponent solutions in which the concentrations are expressed by both mole fractions and molalities, and in which the standard states of the components may be dependent on composition, are examined.

4.1.1 Mole fraction based activity coefficients: nonelectrolyte solutions

This section describes the activities and activity coefficients in a system where the *concentrations of all components are expressed by mole fractions*, $\underline{x}$, such as mixtures of alcohols and water. For this case the chemical potential of a component i of an *ideal solution* whose standard state is at the T and P of the system and at a particular fixed composition of the system that does not change with T or P is (Wood and Battino, 1990)

$$\mu_i^{id}(T, P, \underline{x}) = \mu_i^{\theta}(T, P) + RT \ln x_i \tag{4.10}$$

which corresponds to equation (4.9) with the activity equal to the mole fraction. The chemical potential of a component i in a real solution differs from the above by an additional term, μ_i^E,

$$\mu_i(T, P, \underline{x}) = \mu_i^{id}(T, P, \underline{x}) + \mu_i^E(T, P, \underline{x}) \tag{4.11}$$

which is the *excess chemical potential*, and represents the difference between $\mu_i - \mu_i^\theta$ and $RT \ln x_i$. This quantity is similar to the change in chemical potential on mixing from the standard state, $\Delta\mu_i^{M^\theta}$, of equation (4.8):

$$\Delta\mu_i^{M^\theta}(T, P, \underline{x}) = \mu_i(T, P, \underline{x}) - \mu_i^\theta(T, P) \tag{4.12}$$

Equations (4.10), (4.11), and (4.12) are combined to yield

$$\Delta\mu_i^{M^\theta}(T, P, \underline{x}) = RT \ln x_i + \mu_i^E(T, P, \underline{x}) \tag{4.13}$$

In a manner similar to the definition of the activity, equation (4.9), a mole fraction based activity coefficient γ_i is defined as

$$\mu_i^E(T, P, \underline{x}) \equiv RT \ln \gamma_i(T, P, \underline{x}) \tag{4.14}$$

Substitution of the above expression in equation (4.13) shows that for components whose concentration is expressed in mole fraction the activity is equal to the product of the mole fraction and activity coefficient

$$a_i = x_i \gamma_i \tag{4.15}$$

Both $\Delta\mu_i^{M^\theta}$ and μ_i^E are functions of T, P, and composition, although the states of the system in which their values are equal to zero are not defined. The *reference*

state of component i is a particular state of the system for which μ_i^E is defined to be zero. At the T and P of the solution and the composition of the system in the reference state, $\mu_i^E \equiv 0$ and hence, from equation (4.14), $\gamma_i = 1$. Usually the same composition of the system is used for the reference state at every T and P.

For a component i, it is possible to define $\Delta\mu_i^{M^\theta} \equiv 0$ for a particular state of the system, valid at all T and P. This is the *standard state* for the component i. Equation (4.9) shows that in its standard state the activity of i is equal to 1. Values of μ_i^E and $\Delta\mu_i^{M^\theta}$ are not independent since assignment of zero to one of the quantities fixes the value of the other as shown by equation (4.13).

For most liquid systems composed of nonelectrolyte liquids the reference state for all components at every T and P is chosen as the pure component in the liquid phase at the T and P of the solution. This is known as the *symmetric convention* for the normalization of activity coefficients. This choice of reference state ensures, through equation (4.13), that $\mu_i^E = \Delta\mu_i^{M^\theta} = 0$ for the pure state and, through equations (4.10), (4.11) and (4.12), that the values of chemical potential of i in the reference and standard states are the same. Other choices of reference states for mole-fraction based systems are possible as discussed by Wood and Battino (1990).

4.1.2 Molality based activity coefficients: electrolytes

This section describes the relations between activities, activity coefficients, reference and standard states for *salts whose concentrations are expressed by molalities* in a system composed of *one or more strong electrolytes dissolved in a single solvent.* Each strong electrolyte $M_{\nu_+}A_{\nu_-}$ consisting of cation M of charge z_+ and anion A of charge z_- will dissociate in aqueous solution in the following manner

$$M_{\nu_+}A_{\nu_-} \rightleftharpoons \nu_+ M^{z+} + \nu_- A^{z-} \tag{4.16}$$

where ν_+ and ν_- are stoichiometric coefficients representing the number of positive and negative ions, respectively, formed from one molecule of electrolyte, i.e. for Na_2SO_4, $z_+ = 1$, $\nu_+ = 2$, $z_- = -2$, and $\nu_- = 1$.

Since most electrolytes have limited solubility in solvents, the concentration range is often amplified to facilitate better the tabulation of data by using molalities ($\underline{m}$) to express composition. While it is not usually possible to determine the chemical potential of a single ion because the concentration of a single ion cannot be varied independently of its counterion due to the requirement for electroneutrality (Denbigh, 1955), it is possible to write down expressions relating the chemical potentials of ions to their concentrations in solution. For a single salt which is strongly ionized the chemical potentials of the cations and anions, relative to a standard state which is independent of system composition, forming an *ideal solution* are given by

$$\mu_+^{id}(T, P, \underline{m}) = \mu_+^{\theta}(T, P) + RT \ln m_+ \tag{4.17}$$

and

$$\mu_-^{id}(T, P, \underline{m}) = \mu_-^{\theta}(T, P) + RT \ln m_- \tag{4.18}$$

where μ_+^{θ} and μ_-^{θ} are standard state values of the chemical potentials, undefined for now, and m_+ and m_- are the molalities of the ions. The expressions for chemical potentials in nonideal solutions, following equation (4.11), are

$$\mu_+(T, P, \underline{m}) = \mu_+^{id}(T, P, \underline{m}) + \mu_+^{E}(T, P, \underline{m}) \tag{4.19}$$

and

$$\mu_-(T,P,\underline{m}) = \mu_-^{id}(T,P,\underline{m}) + \mu_-^E(T,P,\underline{m}) \tag{4.20}$$

where μ_j^E is the excess chemical potential for ion j. Molality based "ionic activity coefficients," γ_j, are defined through μ_j^E by analogy to equation (4.14)

$$\mu_+^E(T,P,\underline{m}) \equiv RT \ln \gamma_+(T,P,\underline{m}) \tag{4.21}$$

and

$$\mu_-^E(T,P,\underline{m}) \equiv RT \ln \gamma_-(T,P,\underline{m}) \tag{4.22}$$

Substitution of the relations above in equations (4.19–20) and comparison to equation (4.9) indicates that the activities of the ions are

$$a_+ = m_+\gamma_+ \tag{4.23}$$

and

$$a_- = m_-\gamma_- \tag{4.24}$$

and hence the chemical potentials are

$$\mu_+(T,P,\underline{m}) = \mu_+^\theta(T,P) + RT \ln m_+\gamma_+(T,P,\underline{m}) \tag{4.25}$$

and

$$\mu_-(T,P,\underline{m}) = \mu_-^\theta(T,P) + RT \ln m_-\gamma_-(T,P,\underline{m}) \tag{4.26}$$

For a binary solution of water(1) and electrolyte(2) the Gibbs free energy in terms of the nonionized components, according to equation (4.6), is

$$G = n_1\mu_1 + n_2\mu_2 \tag{4.27}$$

which can be expressed in terms of the solvent and the ionic species as

$$G = n_1\mu_1 + n_+\mu_+ + n_-\mu_- \tag{4.28}$$

where $n_+ = \nu_+ n_2$ is the number of moles of cations and $n_- = \nu_- n_2$ is the number of moles of anions and μ_+ and μ_- are the corresponding chemical potentials. The result of substituting these relations into equation (4.28) and equating (4.27) and (4.28) is

$$\mu_2 = \nu_+\mu_+ + \nu_-\mu_- \tag{4.29}$$

which relates the chemical potential of the electrolyte, treated as a compound, to that of species derived from it.

The chemical potential of the neutral electrolyte is obtained by substituting equations (4.25–26) into (4.29) yielding

$$\mu_2(T,P,\underline{m}) = \nu_+\mu_+^\theta(T,P) + \nu_-\mu_-^\theta(T,P) + RT\ln m_+^{\nu_+} m_-^{\nu_-} \gamma_+^{\nu_+}\gamma_-^{\nu_-}(T,P,\underline{m}) \tag{4.30}$$

Defining the *mean ionic activity coefficient*, $\gamma_\pm$, as

$$\gamma_\pm^\nu = \gamma_+^{\nu_+}\gamma_-^{\nu_-} \tag{4.31}$$

and the *mean ionic molality*, $m_{\pm}$, as

$$m_{\pm}^{\nu} = m_{+}^{\nu_+} m_{-}^{\nu_-} = m_2^{\nu} (\nu_{+}^{\nu_+} \nu_{-}^{\nu_-}) \tag{4.32}$$

with $\nu = \nu_+ + \nu_-$ and substituting equations (4.31) and (4.32) into equation (4.30) yields

$$\mu_2(T, P, \underline{c}) = \nu_+ \mu_+^{\theta}(T, P) + \nu_- \mu_-^{\theta}(T, P) + RT \ln m_{\pm}^{\nu} \gamma_{\pm}^{\nu}(T, P, \underline{m}) \tag{4.33}$$

where on the right hand side of equation (4.32) the molalities of ions of strong electrolytes have been expressed in terms of the molality of the salt as $m_+ = \nu_+ m_2$ and $m_- = \nu_- m_2$. The standard state for the neutral electrolyte is:

$$\mu_2^{\theta}(T, P) = \nu_+ \mu_+^{\theta}(T, P) + \nu_- \mu_-^{\theta}(T, P) \tag{4.34}$$

substitution of the equation above in equation (4.30) and comparison with equation (4.9) yields

$$\begin{aligned} \mu_2(T, P, \underline{m}) - \mu_2^{\theta}(T, P) &= RT \ln [\nu_{+}^{\nu_+} \nu_{-}^{\nu_-}] m_2^{\nu} \gamma_{\pm}^{\nu}(T, P, \underline{m}) \\ &= \Delta\mu_2^{M^{\theta}}(T, P, \underline{m}) \end{aligned} \tag{4.35}$$

and from equation (4.9)

$$a_2 = [\nu_{+}^{\nu_+} \nu_{-}^{\nu_-}] m_2^{\nu} \gamma_{\pm}^{\nu}(T, P, \underline{m}) \tag{4.36}$$

which is the expression for the activity of a neutral electrolyte in a solvent.

While the derivation above is for a binary solution, identical relations apply for each neutral electrolyte in a multicomponent solution (Wood and Battino, 1990).

For solutions of one or more electrolytes in a single solvent, the concentration of the solvent cannot be expressed in molality. However changes in the activity of the solvent and the solutes are interrelated through the Gibbs-Duhem equation.

Comparison of equations (4.35), (4.17–18), and (4.25–26) indicates that for any neutral electrolyte j in an ideal solution the chemical potential is given by the following expression

$$\mu_j^{id}(T,P,\underline{m}) = \mu_j^{\theta}(T,P) + RT\ln[\nu_+^{\nu_+}\nu_-^{\nu_-}] + \nu RT\ln m_j \tag{4.37}$$

while that for an electrolyte in a real solution is

$$\mu_j(T,P,\underline{m}) = \mu_j^{id}(T,P,\underline{m}) + \mu_j^{E}(T,P,\underline{m}) \tag{4.38}$$

where the ν's are dissociation constants for electrolyte j and the excess chemical potential μ_j^E is related to the mean ionic activity coefficient $\gamma_{j,\pm}$

$$\mu_j^{E}(T,P,\underline{m}) = \nu RT\ln\gamma_{j,\pm}(T,P,\underline{m}) \tag{4.39}$$

Combination of equations (4.35), (4.37), and (4.38) yields

$$\Delta\mu_j^{M^{\theta}}(T,P,\underline{m}) = RT\ln[\nu_+^{\nu_+}\nu_-^{\nu_-}] + \nu RT\ln m_j + \mu_j^{E}(T,P,\underline{m}) \tag{4.40}$$

Most electrolyte solutions of practical interest consist of one or more electrolytes dissolved in a single solvent (water). The chemical potential is then a function of T, P and N_C-1 molalities. The reference state for a particular electrolyte j, where $\mu_j^E \equiv 0$, is usually taken to be its state when infinitely dilute in the solvent; a binary solution where $\gamma_{j,\pm} \rightarrow 1$ as $m_j \rightarrow 0$. However the more general case involves the reference state of each salt being defined as a solution which is infinitely dilute in *all*

salts, for all T and P. Thus $\gamma_{j,\pm} \to 1$ as $\underline{m} \to 0$, and the definition of the reference state fixes the standard state. With this choice of reference state the standard state value of the chemical potential for electrolyte j, from equation (4.37) and (4.38) is

$$\mu_j^\theta(T,P) = \mu_j^\infty(T,P,\underline{m}^\infty) - RT\ln K_j - \nu RT\ln m_j^\infty \tag{4.41}$$

where $K_j = [\nu_+^{\nu_+}\nu_-^{\nu_-}]$ and the superscript ∞ refers to infinite dilution properties. At the standard state $\Delta\mu_j^{M^\theta} \equiv 0$ and, from equation (4.40), the compositions of the standard states for the j-th electrolyte can only be determined by the solution of

$$RT\ln K_j + \nu RT\ln m_j = -\mu_j^{E^\infty}(T,P,\underline{m}) \tag{4.42}$$

where $\mu_j^{E^\infty}$ is the excess chemical potential defined to be zero at the reference state (∞). For the common case where the reference state is infinite dilution of the single salt j in the solvent, the right hand side of equation (4.42) would be equal to $-\mu_j^{E^\infty}(T,P,m_j)$. If $\Delta\mu_i^{M^\theta} = 0$ at a fixed T and P is visualized as an N_C-1 dimensional surface then all points satisfying equation (4.43) on this surface represent different standard states for component i. Figure 4.2 shows a schematic depiction of the $\Delta\mu_2^{M^\theta} = 0$ surface for a hypothetical water(1)–salt(2)–salt(3) electrolyte solution in which there are two standard states for component 2 satisfying $\Delta\mu_2^{M^\theta} = 0$, each corresponding to a different composition of the system.

Thus, for both electrolytes and nonelectrolytes, once a reference state is defined it fixes the standard state. However, in general, the compositions of the system in standard states for the components are unknown except for the case where all components have the pure-compound standard state. For electrolytes, this deficiency is overcome by assigning hypothetical standard states to the components in order

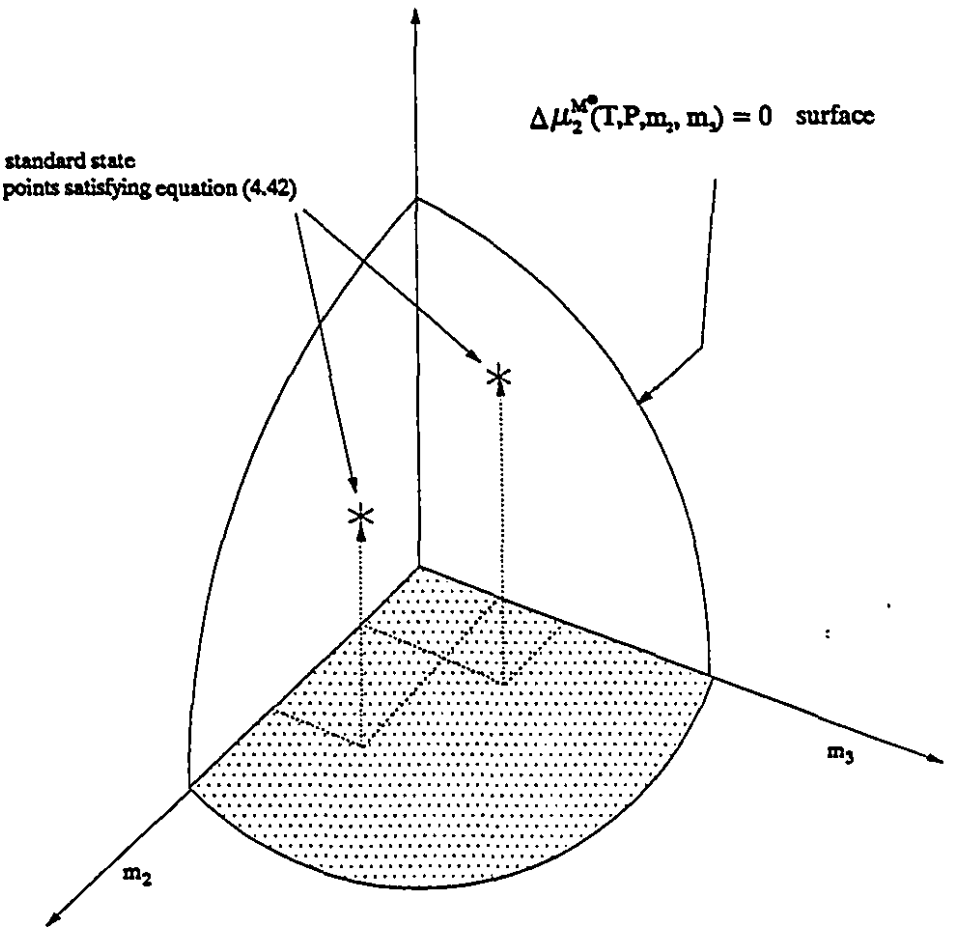

Figure 4.2: Hypothetical $\Delta\mu_2^{M^\theta} = 0$ surface for a water(1)-salt(2)-salt(3) system at fixed T and P.

to facilitate the calculation of numerical values of the thermodynamic properties (Robinson and Stokes, 1959). The usual practice is to take the standard state for strong electrolytes to be that of a *hypothetical solution at a mean ionic molality of one, i.e* $m_{\pm} = 1$. *In addition, the mean ionic activity coefficient of this hypothetical solution is defined to be equal to one for all* T *and* P, i.e. $\gamma_{\pm} = 1$. Substitution of the conditions above in equation (4.35) indicates that if $\gamma_{\pm} = 1$ and $m_{\pm} = 1$, then $\mu_j = \mu_j^{\theta}$.

4.1.3 Multicomponent solutions containing electrolytes and nonelectrolytes

This section deals with activity coefficients in solutions containing a mixture of electrolytes and nonelectrolytes such as the system illustrated in Figure 4.1 in which there are N_C *components, of which* N_S *are nonelectrolytes whose concentrations are expressed by mole fractions and* N_C-N_S *are electrolytes whose concentrations are measured using molality.* The discussion takes into account the situation where the standard state chemical potentials of some or all of the components depend on the composition of the system.

The activity of any compound i in a multicomponent solution can be written in the following general form

$$a_i^{\theta} = K_i c_i^{\nu_i} \gamma_i^{\nu_i} \tag{4.43}$$

where c_i is the concentration of i, γ_i is the activity coefficient with respect to the standard state θ used to define a_i^{θ}, ν_i is a stoichiometric coefficient for i, and K_i is a constant. Usually, for nonelectrolytes $c_i = x_i$ and ν_i and K_i are equal to 1, as in equation (4.15). For strongly dissociating electrolytes, $c_i = m_i$, $\nu_i = \nu_+ + \nu_-$,

$K_i = [\nu_+^{\nu_+}\nu_-^{\nu_-}]$, and $\gamma_i = \gamma_{i,\pm}$ as discussed in the previous section. In general, any standard state can be used to define the activities, including one that is a function of the composition of the system.

$$\mu_i(T, P, \underline{c}) = \mu_i^{\theta}(T, P, \underline{c}) + RT \ln a_i^{\theta}(T, P, \underline{c}) \tag{4.44}$$

A component mixing to form an ideal solution has an activity coefficient equal to 1 and, from equation (4.43),

$$a_i^{id} = K_i c_i^{\nu_i} \tag{4.45}$$

The *excess Gibbs energy* is the difference between the Gibbs energy of a solution and that of an ideal solution having the same composition

$$G^E = G - G^{id} \tag{4.46}$$

The free energies can be expressed in terms of chemical potentials

$$G^E = \sum_i n_i \mu_i - \sum_i n_i \mu_i^{id} \tag{4.47}$$

where the summations run from 1 to N_C. Substituting for μ_i and μ_i^{id} in terms of the activities a_i and a_i^{id} through equations (4.43), (4.44), and (4.45) and (4.47) yields

$$\frac{G^E}{RT} = \sum_i n_i \ln \gamma_i^{\nu_i} \tag{4.48}$$

The Gibbs-Duhem equation expresses the fact that for a thermodynamic system such as that of Figure 4.1 which has $N_C + 2$ state variables (T, P and N_C chemical

potentials), only $N_C + 1$ of the variables are independent.

$$SdT - VdP + \sum_i n_i d\mu_i = 0 \tag{4.49}$$

For a fixed T and P the equation is

$$\sum_i n_i d\mu_i = 0 \tag{4.50}$$

Substituting the expressions for the chemical potentials of the components from equation (4.44) yields

$$\sum_i n_i d\mu_i^\theta(T, P, \underline{c}) = -RT \sum_i n_i d \ln a_i^\theta(T, P, \underline{c}) \tag{4.51}$$

The standard states of the components of a system are, in general, functions of the system's composition as discussed in the previous section. Recognizing that at a fixed T and P the total derivatives in equation (4.51), dY, can be expanded in partial derivatives taken with respect to the number of moles of the components as,

$$dY = \sum_\ell \left(\frac{\partial Y}{\partial n_\ell}\right)_{T,P,n_{j\neq\ell}} dn_\ell \tag{4.52}$$

it is possible to express equation (4.51) as

$$\sum_i n_i \left[\frac{\partial \mu_i^\theta}{\partial n_k}\right]_{T,P,n_{\ell\neq k}} - RT \sum_i n_i \left[\frac{\partial \ln a_i^\theta}{\partial n_k}\right]_{T,P,n_{\ell\neq k}} = 0 \tag{4.53}$$

Expansion of the activity according to equation (4.43) yields

$$\sum_i \nu_i n_i \left[\frac{\partial \ln \gamma_i}{\partial n_k}\right]_{T,P,n_{c\neq k}} = -\sum_i n_i \left[\frac{\partial \mu_i^\theta / RT}{\partial n_k}\right]_{T,P,n_{c\neq k}} - \sum_i \nu_i n_i \left[\frac{\partial \ln c_i}{\partial n_k}\right]_{n_{c\neq k}} \quad (4.54)$$

In addition, for each k, differentiation of G^E/RT, equation (4.48), with respect to n_k and rearrangement, gives

$$\nu_k \ln \gamma_k = \left[\frac{\partial G^E/RT}{\partial n_k}\right]_{T,P,n_{c\neq k}} - \sum_i \nu_i n_i \left[\frac{\partial \ln \gamma_i}{\partial n_k}\right]_{T,P,n_{c\neq k}} \quad (4.55)$$

Finally, combination of equations (4.54) and (4.55) gives the expression for the activity coefficient in terms of the Gibbs free energy of the solution

$$\ln \gamma_k = \frac{1}{\nu_k}\left[\frac{\partial G^E/RT}{\partial n_k}\right]_{T,P,n_{c\neq k}} + \sum_i \frac{n_i}{\nu_k}\left[\frac{\partial \mu_i^\theta/RT}{\partial n_k}\right]_{T,P,n_{c\neq k}} + \sum_i \frac{\nu_i}{\nu_k} n_i \left[\frac{\partial \ln c_i}{\partial n_k}\right]_{n_{c\neq k}} \quad (4.56)$$

The expression above is the general form for the activity coefficient of a compound k in a multicomponent system. The first term on the right hand side is obtained from a model of the excess Gibbs energy of the solution. The middle term is present only if the standard state of one or more components is a function of composition. If there are no salts in the system, and all compositions are expressed using mole fractions with all $\nu_i = 1$, as in Section 4.1.1, then the last term is zero for all components.

From equation (4.44) and (4.45), the chemical potential of a component forming an ideal solution in a system of the type of Figure 4.1 is given by

$$\mu_k^{id}(T,P,\underline{c}) = \mu_k^\theta(T,P,\underline{c}) + RT \ln K_i c_i^{\nu_i} \quad (4.57)$$

while that for a component of a real solution is

$$\mu_k(T,P,\underline{c}) = \mu_k^{id}(T,P,\underline{c}) + \mu_k^E(T,P,\underline{c}) \tag{4.58}$$

with

$$\mu_k^E(T,P,\underline{c}) = \nu_k RT \ln \gamma_k(T,P,\underline{c}) \tag{4.59}$$

Comparison of equations (4.56) and (4.59) indicates that

$$\mu_k^E = \left[\frac{\partial G^E}{\partial n_k}\right]_{T,P,n_{\ell\neq k}} + \sum_i n_i \left[\frac{\partial \mu_i^\theta}{\partial n_k}\right]_{T,P,n_{\ell\neq k}} + RT \sum_i \nu_i n_i \left[\frac{\partial \ln c_i}{\partial n_k}\right]_{n_{\ell\neq k}} \tag{4.60}$$

and at the reference state for component k, $\mu_k^E = 0$, from equation (4.59) $\gamma_k = 1$, and the sum of the terms on the right hand side of equation (4.60) equal zero. As with equation (4.56), the only time when

$$\mu_k^E = \left[\frac{\partial G^E}{\partial n_k}\right]_{T,P,n_{\ell\neq k}} \tag{4.61}$$

is if the standard states of all components are independent of composition, all concentrations are expressed in mole fractions and all $\nu_i = 1$.

The system of Figure 4.1 has N_S nonelectrolytes, which in this study are treated as solvents whose concentrations are expressed in mole fractions, x_i,

$$x_i = \frac{n_i}{\sum_{\ell=1}^{N_C} n_\ell} \qquad i = 1,\ldots,N_S \tag{4.62}$$

and N_C-N_S electrolytes, whose concentrations are expressed in molalities m_i based

on all solvents, each of molecular weight M_ℓ

$$m_i = \frac{n_i 1000}{\sum_{\ell=1}^{N_S} n_\ell M_\ell} \qquad i = N_{S+1}, \ldots, N_C \tag{4.63}$$

For this system, if the standard states of all components are independent of composition, i.e.

$$\left[\frac{\partial \mu_i^\theta}{\partial n_k}\right]_{T,P,n_{\ell \neq k}} = 0 \qquad i = 1, \ldots, N_C \tag{4.64}$$

then the activity coefficient for a component k is given by

$$\ln \gamma_k = \frac{1}{\nu_k}\left[\frac{\partial G^E/RT}{\partial n_k}\right]_{T,P,n_{\ell k}} + \sum_{i=1}^{N_C} \frac{\nu_i}{\nu_k} n_i \left[\frac{\partial \ln c_i}{\partial n_k}\right]_{n_{\ell \neq k}}$$
$$k = 1, \ldots, N_C \tag{4.65}$$

In this study the standard states of all the components are independent of composition and hence equation (4.65) is used in evaluating activity coefficients. Using this equation, the activity coefficient of a solvent is

$$\ln \gamma_k = \left[\frac{\partial G^E/RT}{\partial n_k}\right]_{T,P,n_{\ell \neq k}} + 1 - \sum_{\ell=1}^{N_S} x_\ell - M_k \frac{\sum_{j=N_S+1}^{N_C} \nu_j m_j}{1000}$$
$$k = 1, \ldots, N_S \tag{4.66}$$

while that for an electrolyte is

$$\ln \gamma_{k,\pm} = \frac{1}{\nu_k}\left[\frac{\partial G^E/RT}{\partial n_k}\right]_{T,P,n_{\ell \neq k}} + 1 - \frac{1}{\nu_k} \sum_{\ell=1}^{N_S} x_\ell$$
$$k = N_{S+1}, \ldots, N_C \tag{4.67}$$

Equations (4.66) and (4.67) are used to calculate activity coefficients from excess Gibbs energy models in this study. For multicomponent systems containing one or more salts, it is convenient to build the excess Gibbs energy of the solution so that the reference state for the solvents is the pure compound while that for each salt is the state of infinite dilution of the salt in *one* of the solvents. This ensures that the standard states of the salts are independent of composition, as described in Appendix E. Hence

$$\gamma_i \to 1 \text{ as } x_i \to 1 \quad \text{for solvents (nonelectrolytes)} \qquad i = 1, \ldots, N_S \tag{4.68}$$

$$\gamma_{i,\pm} \to 1 \text{ as } m_i \to 0 \quad \text{for salts in solvent 1} \qquad i = N_{S+1}, \ldots, N_C \tag{4.69}$$

This is the *unsymmetric convention* for the normalization of activity coefficients. In equation (4.69) solvent 1 is chosen for all electrolytes, and while this is usually the case in practice, it is possible to choose different solvents for different salts[1].

4.2 Calculation of Liquid-Liquid Equilibrium

A multicomponent liquid mixture can separate into two or more phases depending on the temperature, pressure, number of components and composition of the system. At a fixed temperature and pressure Gibbs phase rule determines the maximum number of phases which can be present at equilibrium as a function of the number of components in the system. A given ternary system will separate into two liquid phases if its composition lies in the region enclosed by the binodal curve

[1]For systems consisting of salts and two or more nonelectrolytes there are several ways of normalizing the activity coefficients. Cabezas et al. (1990b) and Gao et al. (1991a,b) used the pure compound reference state for water and the infinitely dilute state in water for all of the solutes, including polymers.

(see Figure 3.1). In the general case for a multicomponent system, at a given temperature, pressure, and composition, the number of phases which are present at equilibrium corresponds to the number which are thermodynamically stable under the given conditions.

If a model for the Gibbs free energy of a multicomponent system is available, for a fixed temperature and pressure, it is possible to obtain relations between the chemical potentials of the components and between their derivatives, which determine whether a system of a given composition is prone to separating into two phases (Modell and Reid, 1974). Although these stability relations permit the calculation of the stability boundary, the *spinodal curve*, and the critical (plait) point, they cannot be used to calculate phase boundaries such as the binodal curve. For a system at a given temperature, pressure and overall composition, the tangent-plane stability criterion (Michelsen, 1982; Heidemann, 1983; Cairns and Furzer, 1990) is used to calculate the number of stable equilibrium phases. In order for a given phase F of mole fractions $\underline{z}$ to be stable, the free energy of the system cannot be lowered by a split into two or more phases. If the chemical potentials of components in this phase are denoted by $\mu_i^F(\underline{z})$, this phase is stable provided the following is true for *all* possible sets of mole fractions $\underline{x}$

$$\sum_{i=1}^{N_c} x_i \left[\mu_i(\underline{x}) - \mu_i^F(\underline{z})\right] \geq 0 \tag{4.70}$$

The equation above must be satisfied for any set of trial mole fractions $\underline{x}$ which represent the composition of a new phase.

If it is assumed that only two phases are present, the condition for liquid-liquid equilibrium in a multicomponent solution is that the total Gibbs free energy of the two-phase system, G, given by equation (4.1), is at a minimum with respect to

changes in the compositions of the phases. While it is possible to calculate equilibrium compositions by equating the activities of components in different phases (Prausnitz et al., 1980), the approach followed here is to minimize the total free energy directly. Using equations (4.6), (4.8), and (4.9), equation (4.1) can be expressed as

$$G = \sum_{i=1}^{N_C} \left[n_i^I \left(\mu_i^{\theta I} + RT \ln a_i^I \right) + n_i^{II} \left(\mu_i^{\theta II} + RT \ln a_i^{II} \right) \right] \tag{4.71}$$

If the standard state chemical potentials are independent of composition and equal in both phases, $\mu_i^{\theta I} = \mu_i^{\theta II} = \mu_i^{\theta}$, and if the activities of the components are given by equation (4.43), the total free energy is

$$G = \sum_{i=1}^{N_C} \left(n_i^I + n_i^{II} \right) \mu_i^{\theta} + RT \sum_{i=1}^{N_C} \left[n_i^I \ln K_i (c_i^I \gamma_i^I)^{\nu_i} + n_i^{II} \ln K_i (c_i^{II} \gamma_i^{II})^{\nu_i} \right] \tag{4.72}$$

The equation above can be rearranged to give G', the dimensionless composition-dependent part of the total free energy

$$G' = \frac{G - G^{\theta}}{RT} = \sum_{i=1}^{N_C} \left[n_i^I \ln K_i (c_i^I \gamma_i^I)^{\nu_i} + n_i^{II} \ln K_i (c_i^{II} \gamma_i^{II})^{\nu_i} \right] \tag{4.73}$$

where

$$G^{\theta} = \sum_{i=1}^{N_C} \left(n_i^I + n_i^{II} \right) \mu_i^{\theta} = \sum_{i=1}^{N_C} n_i^F \mu_i^{\theta} \tag{4.74}$$

and the superscript F indicates the total amount in both phases. When equation (4.74) is applied to the multicomponent system of Figure 4.1, the activities can be

separated into terms for solvents and terms for salts

$$G' = \sum_{i=1}^{N_S} \left[n_i^I \ln x_i^I \gamma_i^I + n_i^{II} \ln x_i^{II} \gamma_i^{II} \right]$$

$$+ \sum_{i=N_{S+1}}^{N_C} \left[n_i^I \ln K_i (m_i^I \gamma_{i,\pm}^I)^{\nu_i} + n_i^{II} \ln K_i (m_i^{II} \gamma_{i,\pm}^{II})^{\nu_i} \right] \tag{4.75}$$

where the mole fractions and molalities are given by equations (4.62) and (4.63), respectively, and the activity coefficients are given by equations (4.66) and (4.67). Since the activity coefficients are functions of composition, trial and error is used to select the equilibrium compositions of the phases, which minimize G'.

In minimizing the free energy it is convenient to consider a two-phase system in which the total number of moles in the feed phase is equal to 1. For this system, the amount of material in the feed must equal that in the equilibrium phases and hence each component obeys a mass balance:

$$x_i^F = x_i^I n^I + x_i^{II} n^{II} \qquad i = 1, \ldots, N_C \tag{4.76}$$

where the superscript F represents the feed phase, n is the total number of moles in a phase,

$$x_i^F = n_i^F \qquad i = 1, \ldots, N_C \tag{4.77}$$

and, for each component,

$$n_i^F = n_i^I + n_i^{II} \qquad i = 1, \ldots, N_C \tag{4.78}$$

Here Powell's multidimensional method (Press et al., 1989) is used to provide

iterative estimates of the compositions of the phases. Since this method does not provide bounds on the range of the values of estimates of the phase compositions, it is necessary to use dummy variables e_i, which represent scaled mole numbers of the components in phase I, in order to avoid nonphysical values of the composition, such as negative numbers. These variables are related to the mole numbers as

$$n_i^I = \frac{n_i^F}{1+\mid e_i \mid} \qquad i = 1,\ldots,N_C \tag{4.79}$$

and since the absolute value of e_i is always a positive number, $0 < n_i^I < n_i^F$ as required. Equations (4.78) are used to calculate the number of moles in phase II while equations (4.62) and (4.63) are used to calculate the compositions of the phases.

A flow chart describing the method of calculating equilibrium compositions in two-phase systems is shown in Figure 4.3. Although not shown explicitly, once the mole fractions of components in the loop are calculated, equation (4.63) is used to calculate the molalities of the salts.

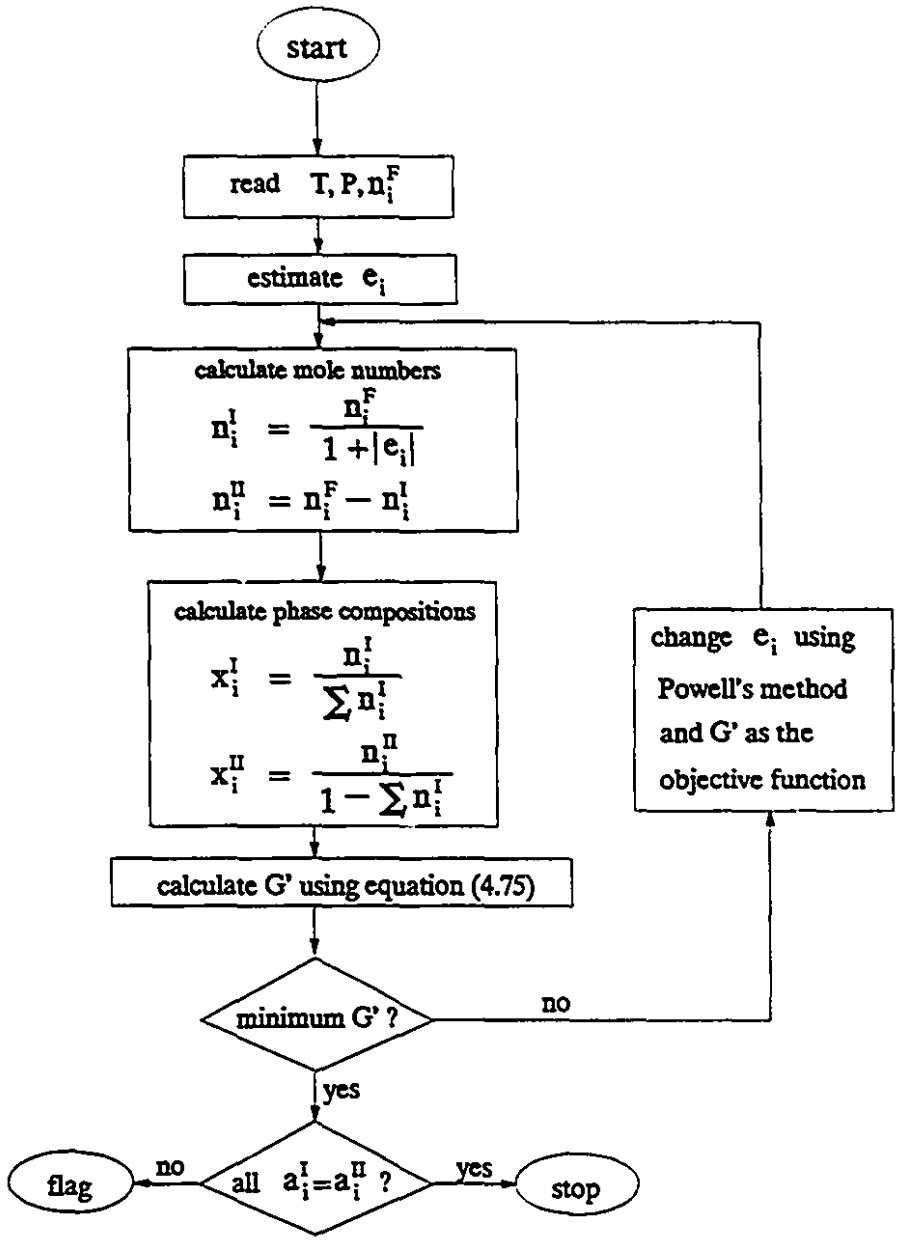

Figure 4.3: Calculation of equilibrium compositions by minimizing G'.

Chapter 5

An Excess Gibbs Energy Model for Multicomponent Liquid Systems

As discussed in Chapter 4, the activity coefficient of a compound in a multicomponent system containing salt is obtained from a model of the excess Gibbs energy. The systems studied here contain water, salt and either an alcohol or a polymer. This chapter describes a model for the G^E of solutions containing *one salt and one or more solvents.* The excess Gibbs energy function models the interaction between components of the solution. In this study the function is constructed to reflect the interactions between solvents and between solvents and salt, both at finite salt concentrations and at infinite dilution of salt, hence permitting the use of a composition-independent standard state chemical potential for the salt.

The excess Gibbs energy model reflects the following physical processes: dissolution of an electrolyte in water in the state of infinite dilution and transfer of the electrolyte, at infinite dilution, from water to a mixed-solvent ($G^E_{ES\infty}$); mixing of pure solvents to form a mixed-solvent and correcting the solvent-solvent interaction for the effect of salt (G^E_{ESS}); mixing of salt and mixed-solvent to form the final

solution(G^{E}_{ES}). The excess Gibbs energy function takes the form

$$G^{E} = G^{E}_{ES\infty} + G^{E}_{ES} + G^{E}_{ESS} \tag{5.1}$$

where the subscript ES^{∞} indicates electrolyte–solvent interaction at infinite dilution, ES indicates electrolyte–solvent interaction at finite salt concentrations, and ESS indicates solvent–solvent interaction in the presence of salt.

A model for G^{E}, denoted the Bromley–Flory-Huggins model, is presented. This model uses the Mean Spherical Approximation (MSA) theory for $G^{E}_{ES\infty}$. The G^{E}_{ES} term is modelled using the Bromley equation for electrolyte solutions, while a modified form of the Flory-Huggins theory for polymer solutions is used to evaluate G^{E}_{ESS}.

5.1 The Mean Spherical Approximation (MSA) model for $G^{E}_{ES\infty}$

The pure compound reference state is used for all nonelectrolytes (water, alcohols and polymers), treated as solvents, while the infinite dilution reference state is used for the salt. To avoid the dependence of the standard state chemical potential of the salt on composition (see Appendix E), the reference state for the salt is taken as its state *at infinite dilution in water*. The $G^{E}_{ES\infty}$ term models the change in free energy in transferring ions, at infinite dilution, from pure water to a solution of water and alcohol or water and polymer.

The *solvation* or Born energy of an ion is the energy which an ion that is not interacting with other ions possesses because of being immersed in a solvent. If the ion is in a vacuum, this energy is the ion's *self energy*. If the solvent is treated as a continuum of dielectric constant ε, it is possible to estimate the change in free energy in transferring the ion from a vacuum to its state in the solvent.

In the *primitive* model of electrolyte solutions (Hill, 1960; Kusalik and Patey, 1988) ions are modelled as hard-spheres. The solvent is treated as a continuum of fixed dielectric constant, ϵ, and its effect on the free energy of the system is expressed through this parameter. Using this simple model of the solution, the solvation energy of the ions can be calculated in several ways, one of which uses classical electrostatics and is described in Appendix F. The result is equation (F.8), which is the Born equation.

The assumption that the solvent is a continuum is unrealistic, hence the free energy predicted by the Born equation does not agree with experimentally determined values (Harned and Robinson, 1968). The *nonprimitive* approach to modelling electrolyte solutions treats both the ions and solvents as molecules. One such approach models the electrolyte solution as a mixture of *ions of equal size, treated as hard-spheres with centrally embedded point charges, immersed in a solvent consisting of hard-spheres of a diameter different from the ions and with embedded point dipoles.* The components of the solution are illustrated in Figure 5.1. Analytic equations for approximate thermodynamic properties for this system are derived using the MSA approach as described below.

From a molecular point of view, the thermodynamic properties of a solution can be determined from a knowledge of the pair distribution function which expresses the probability of finding two particles at given locations in a solution. The pair distribution function depends on the direct correlation function through the Ornstein-Zernike integral equation (Hansen and McDonald, 1986). The direct correlation function depends on intermolecular interaction potentials in the system. For the hard-sphere ion–dipolar solvent system, there are three types of interactions; ion–ion, ion–dipole, and dipole–dipole. The MSA involves simplifying assumptions about the form of the pair distribution and direct correlation func-

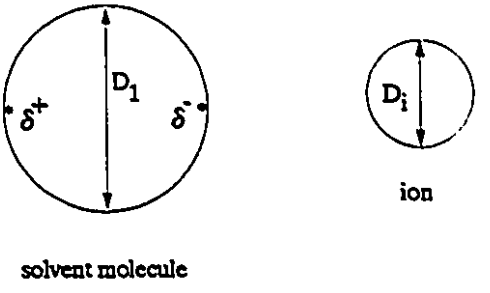

Figure 5.1: Hard-sphere ion–dipolar solvent solution

tions which permit the analytic solution of the Ornstein-Zernike integral equation, to yield the thermodynamic properties of the system (Chan et al., 1979; Blum and Wei, 1987; Wei and Blum, 1987; Zhou et al., 1988; Blum and Fawcett, 1992). The results give an expression for the free energy of interaction between ions and dipoles at infinite dilution of the ions; the solvation energy. Using the MSA the expression corresponding to the Born equation for the interaction between an ion i of charge z_i and a dipolar solvent 1 of dielectric constant ε_1 is (Chan et al., 1979)

$$\mu^{E}_{msa^{\infty},i} = -\frac{z_i^2 e^2}{4\pi\varepsilon_o(D_i + 2D_{S1})}\left(1 - \frac{1}{\varepsilon_1}\right) \tag{5.2}$$

where e is the electron charge and ε_o is the permittivity of free[1] space, equal to $8.854\text{x}10^{-12}$ C^2 J^{-1} m^{-1}. The diameter of the ionic hard-spheres is equal to D_i and

[1]The factor $4\pi\varepsilon_o$ is introduced in order to express the equation above in the same units as the Born equation in Appendix F.

the parameter D_{S1} is given by the following equation:

$$D_{S1} = \left(\frac{1}{2} - \frac{3\xi_1}{1+4\xi_1}\right) D_1 \tag{5.3}$$

where D_1 is the diameter of the dipolar solvent hard-spheres and the parameter ξ_1, which is in the range $0 < \xi_1 < \frac{1}{2}$, is related to the solvent's dielectric constant ε_1 as follows:

$$\varepsilon_1 = \frac{(1+4\xi_1)^2(1+\xi_1)^4}{(1-2\xi_1)^6} \tag{5.4}$$

Using the diameter of the solvent hard spheres as an adjustable parameter, equation (5.2) accurately correlates the solvation energies of monovalent, monoatomic ions in many solvents (Blum and Fawcett[2], 1992). In the limit where the molecular nature of the solvent is ignored and the diameter of the solvent hard-spheres is vanishingly small, $D_1 \rightarrow 0$, the MSA and the Born equations are identical.

Using equation (5.2), the change in free energy accompanying the transfer of n_e moles of electrolyte e, at infinite dilution, from solvent 1, of dielectric constant ε_1, to solvent m, of dielectric constant ε_m, is

$$\frac{G^{E}_{mix,\infty}}{RT} = \frac{K_o}{RT} n_e \left[\Omega_1 \left(1 - \frac{1}{\varepsilon_1}\right) - \Omega_m \left(1 - \frac{1}{\varepsilon_m}\right)\right] \tag{5.5}$$

where the constant K_o is equal to

$$K_o \equiv \frac{e^2 N_A}{4\pi\varepsilon_o} = 6.95\text{x}10^{-5} \frac{\text{J.m}}{\text{mol}} \tag{5.6}$$

[2]The parameter λ_1 of Blum and Fawcett (1992) is equal to $\lambda_1 = \frac{1+4\xi_1}{1-2\xi_1}$. Although the symbols are different, equation (5.2) is identical to Blum and Fawcett's equation (55).

and N_A is Avogadro's number. The Ω's have the following form:

$$\Omega_1 = \frac{\nu_+ z_+^2}{D_+ + 2D_{S1}} + \frac{\nu_- z_-^2}{D_- + 2D_{S1}} \tag{5.7}$$

and

$$\Omega_m = \frac{\nu_+ z_+^2}{D_+ + 2D_{Sm}} + \frac{\nu_- z_-^2}{D_- + 2D_{Sm}} \tag{5.8}$$

The parameter D_{Sm} is related to the diameter of the solvent hard-spheres D_m in a manner similar to equation (5.3):

$$D_{Sm} = \left(\frac{1}{2} - \frac{3\xi_m}{1 + 4\xi_m}\right) D_m \tag{5.9}$$

with

$$\varepsilon_m = \frac{(1 + 4\xi_m)^2 (1 + \xi_m)^4}{(1 - 2\xi_m)^6} \tag{5.10}$$

The parameters D_{S1} and D_{Sm} are related to the diameters of the solvent hard-spheres through the parameters ξ_1 and ξ_m which, in turn, are functions of the dielectric constants ε_1 and ε_m. In order to calculate values of D_{S1} and D_{Sm}, ξ_1 and ξ_m must be determined from equations (5.4) and (5.10). Values of ξ_1 and ξ_m satisfying equations (5.4) and (5.10) were determined using the Newton-Raphson method. For example, to determine ξ_1, equation (5.4) was rearranged to

$$f(\xi_1) = \varepsilon_1 - \frac{(1 + 4\xi_1)^2 (1 + \xi_1)^4}{(1 - 2\xi_1)^6} = 0 \tag{5.11}$$

and the solution was found by iterating ξ_1 in the manner

$$\xi_1^{(i+1)} = \xi_1^{(i)} - \frac{f(\xi_1^{(i)})}{f'(\xi_1^{(i)})} \tag{5.12}$$

where i is the iteration number and $f'(\xi_1)$ is the derivative of $f(\xi_1)$:

$$f'(\xi_1) = \frac{12(1+4\xi_1)(2+5\xi_1)(1+\xi_1)^3}{(2\xi_1-1)^7} \tag{5.13}$$

The MSA expression for the solvation energy is used to calculate the change in free energy in transferring electrolyte ions, at infinite dilution, from water to a mixed-solvent. The mixed-solvent consists of water and one or more compounds which are either polymers or alcohols. In order to calculate the change in free energy the dielectric constant ε_m and diameter of the mixed-solvent "hard spheres" must be known. For a mixed-solvent there is no "correct" hard-sphere diameter since the mixture contains several molecular species. As discussed in Chapter 6, the hard-sphere diameter of the mixed-solvent is assumed to be independent of composition and equal to the diameter of a molecule of water[3]. The calculation of the mixed-solvent dielectric constant is discussed in the next section.

5.2 The Bromley Equation for G^E_{ES}

There are many models for describing the thermodynamic behavior of electrolyte solutions. One of the oldest and most widely known of these models is that proposed by Debye and Hückel (1923). This model assumes that ions are spheres of material

[3]In the work of Blum and Fawcett (1992), the diameter of the solvent hard spheres was adjusted to match the predictions of the model with experimental data for the solvation energies of several ions in 17 pure solvents. Since cations were considered separately from anions, two "effective" diameters were calculated for the same solvent.

of the same dielectric constant as the solvent with point charges embedded in their cores. The solvent is treated as a continuum of fixed dielectric constant. The Boltzmann distribution function is used to express the distribution of ions around a central one and the electrical potential due to these ions is calculated using a linearized form of the Poisson–Boltzmann equation in which only the first two terms of an infinite series are retained (Zemaitis et al., 1986). The calculation of the free energy takes into account only long-range electrostatic forces. The mean ionic activity coefficient of salt(2), in a binary solution with solvent(1), is

$$\ln \gamma_{\pm} = -\mathcal{A} \mid z_+ z_- \mid \sqrt{I} \tag{5.14}$$

where z_i is the valence of ion i and I is the ionic strength of the solution, given by

$$I = m\Phi \tag{5.15}$$

and m is the molality of the salt:

$$m = \frac{1000 n_2}{n_1 M_1} \tag{5.16}$$

in which M_1 is the molecular weight of the solvent. The value of the constant Φ depends on the electrolyte through:

$$\Phi = \frac{1}{2}\left[\nu_+ z_+^2 + \nu_- z_-^2\right] \tag{5.17}$$

The Debye–Hückel parameter, $\mathcal{A}$, is a function of the solvent density, ρ_1, dielectric constant, ε_1, and the temperature

$$\mathcal{A} = \left(\frac{e}{\sqrt{\varepsilon_1 kT}}\right)^3 \sqrt{\frac{2\pi N_A \rho_1}{1000}} \tag{5.18}$$

In this equation, e is the electron charge, k is Boltzmann's constant and N_A is Avogadro's number.

Since the Debye–Hückel theory is based on a crude model of the electrolyte solution, and since the model is solved only approximately, equation (5.14) is valid only for dilute solutions of ionic strength 0.001 or less. This relation is called the Debye–Hückel Limiting Law.

There have been numerous modifications of the Debye–Hückel Limiting Law, designed to extend the range of validity of the model to higher concentrations (Horvath, 1985). One empirical extension of this model is that of Bromley (1973) which represents the thermodynamic properties of a wide variety of aqueous solutions of strong electrolytes. This model which requires only one adjustable parameter, determined from data for each binary, is used to model the long-range electrostatic interactions of G^{E}_{ES}.

The Bromley (1973) expression for the mean ionic activity coefficient of a salt in a binary solution is

$$\log \gamma_{\pm}^{\mathrm{br}} = -\frac{\mathcal{A} \mid z_+ z_- \mid \sqrt{I}}{\ln(10)(1+\varrho\sqrt{I})} + \frac{(0.06+0.6\mathcal{B}) \mid z_+ z_- \mid I}{\left(1+\frac{1.5}{\mid z_+ z_- \mid} I\right)^2} + \mathcal{B} I \tag{5.19}$$

where $\mathcal{A}$ is the Debye–Hückel parameter. The parameter ϱ is set to 1 for most salts. Each electrolyte–solvent pair has a characteristic value of the Bromley constant $\mathcal{B}$, which is obtained by matching the predictions of the model to experimental data. This expression represents the mean ionic activity coefficient of electrolytes at concentrations up to a molality of about 6 (Zemaitis et al., 1986). For more concentrated solutions, the model can be extended by the addition of a second term containing a second adjustable parameter, $\mathcal{E}$. This two-parameter model, the

Extended-Bromley equation, is described in Appendix G[4] .

The ionic strength of a solution with a mixed-solvent is calculated using equation (5.15) where Φ is given by equation (5.17) and m is the molality of the salt based on the mixed-solvent:

$$m = \frac{n_e 1000}{\sum_{\ell=1}^{N_S} n_\ell M_\ell} \tag{5.20}$$

The Bromley parameter $\mathcal{B}$ characterizes the interaction between electrolyte–solvent pairs. The value characterizing the interaction between the electrolyte and mixed-solvent, $\mathcal{B}_m$, is obtained from those characterizing the constituent binaries through a mixing rule based on salt-free solvent mole fractions:

$$\mathcal{B}_m = \sum_{\ell=1}^{N_S} (x_\ell^\circ)^2 \mathcal{B}_\ell + \sum_{\ell=1}^{N_S-1} \sum_{k=\ell+1}^{N_S} x_\ell^\circ x_k^\circ b_{\ell k}^b \tag{5.21}$$

where $\mathcal{B}_\ell$ is the value of $\mathcal{B}$ characterizing the interaction between solvent ℓ and the electrolyte and $b_{\ell k}^b$ is a binary interaction parameter which is obtained from fitting the model to binary experimental data. This mixing rule is similar to the commonly used quadratic mixing rule but has the advantage that values of $\mathcal{B}_\ell$ can be negative. If

$$b_{\ell k}^b = \mathcal{B}_\ell + \mathcal{B}_k \tag{5.22}$$

[4]Preliminary calculations involved the use of an excess Gibbs energy model in which the electrolyte–solvent interactions of G_{ES}^E were expressed using a modified form of the Pitzer (1973) equation. The model, which contains 3 adjustable parameters per binary electrolyte–solvent pair, was able to correlate liquid-liquid equilibrium data for aqueous biphasic salt systems. Comparison of the results of preliminary calculations using the Bromley–Flory-Huggins model and the Pitzer–Flory-Huggins expression indicated that only a small improvement in accuracy was obtained by using the Pitzer equation.

equation (5.21) reduces to the following linear form in composition:

$$\mathcal{B}_m = \sum_{\ell=1}^{N_S} x_\ell^\circ \mathcal{B}_\ell \tag{5.23}$$

The properties of the mixed-solvent are estimated from the properties of the pure solvents making up the mixed-solvent. The properties of the solvent appear in $\mathcal{A}_m$, the Debye–Hückel parameter for the mixed solvent:

$$\mathcal{A}_m = \left(\frac{e}{\sqrt{\varepsilon_m kT}}\right)^3 \sqrt{\frac{2\pi N_A \rho_m}{1000}} = A(T)\,\frac{\rho_m^{1/2}}{\varepsilon_m^{3/2}} \tag{5.24}$$

where ρ_m and ε_m are the density and dielectric constant of the mixed-solvent, respectively. The temperature dependent parameter $A(T)$ is equal to $4.2017\text{x}10^6/T^{3/2}$ $\text{kg}^{1/2}$ $\text{cm}^{3/2}$ $\text{mol}^{-1/2}$ $\text{g}^{-1/2}$.

The next two subsections describe the methods used to evaluate the density and dielectric constant of the mixed-solvent.

Mixed-solvent density

Most methods for estimating the density of a liquid solution of nonelectrolytes require pure-compound critical properties or expressions for partial molar volumes (Reid et al., 1977). Studies involving mixed-solvents and electrolytes (Rastogi and Tassios, 1987; Jansson and Furzer, 1989; Macedo et al., 1990; Kikic et al., 1991) have typically dealt with mixtures of water and aliphatic alcohols, for which accurate volumetric data are available. However, the mixed-solvents in this study involve polymers which are not well characterized in terms of molecular weight, solution volumetric properties or critical properties. Preliminary calculations involving two and three parameter Redlich-Kister polynomial expressions (Prausnitz, 1969) for

the density of the mixed-solvent in terms of those of the pure solvents indicated that use of complicated expressions for the density had little effect on the calculated phase equilibria. Thus, in order to reduce the complexity of the G^E function, the density of the mixed-solvent is calculated from the pure compound densities of its constituents and the salt-free weight fractions of the solvents using the following relation:

$$\rho_m = \sum_{i=1}^{N_S} w_i^o \rho_i \tag{5.25}$$

The salt-free weight fraction of solvent i is

$$w_i^o = \frac{n_i M_i}{\sum_{\ell=1}^{N_S} n_\ell M_\ell} \tag{5.26}$$

Mixed-solvent dielectric constant

The dielectric constants of mixtures have been estimated using different mixing rules. For mixtures of nonelectrolytes, Oster (1946) proposed a volumetrically based mixing rule that requires expressions for the partial molar volumes of the components. Modified forms of this mixing rule were used by Harvey and Prausnitz (1987), Raastchen et al. (1987), Gering et al. (1989), and Kikic et al. (1991). Other studies (Harned and Owen, 1958; Rastogi and Tassios, 1987) involved the use of mixing rules based on mole fractions. For electrolyte solutions, the dielectric constant of the solvent is a function of the salt concentration (Akhadov, 1981) and some electrolyte models have incorporated this dependence (Beutier and Renon, 1978; Ball et al., 1985).

Preliminary calculations involving the use of cubic polynomial expressions to represent the changes in dielectric constant with solvent composition and salt con-

centration yielded poor results for the prediction of phase equilibrium for the H_2O-NaCl-propanol system. The problem was similar to that reported by Rastogi and Tassios (1987), where the derivative of the dielectric constant with respect to the number of moles of a component gave a contribution to the activity coefficient which was of the wrong sign. Since there are no accurate volumetric and dielectric data for the polymer solutions in this study, the dielectric constant of the mixed-solvent is calculated using a linear mixing rule based on salt-free mole fractions of the solvents:

$$\epsilon_m = \sum_{i=1}^{N_S} x_i^o \epsilon_i \tag{5.27}$$

where the salt-free mole fraction of solvent i is

$$x_i^o = \frac{n_i}{\sum_{\ell=1}^{N_S} n_\ell} \tag{5.28}$$

Substituting the parameters for the electrolyte–mixed-solvent in the expression for the mean ionic activity coefficient, equation (5.19), and lumping constants,

$$\ln \gamma_{\pm}^{\mathrm{br}} = \frac{\alpha_m \sqrt{I}}{1 + \varrho\sqrt{I}} + \frac{\beta_m I}{(1 + \kappa I)^2} + B_m I \tag{5.29}$$

where

$$\alpha_m = - \mid z_+ z_- \mid \mathcal{A}_m \tag{5.30}$$

$$\beta_m = \ln(10) \mid z_+ z_- \mid (0.06 + 0.6\mathcal{B}_m) \tag{5.31}$$

$$B_m = \ln(10)\mathcal{B}_m \tag{5.32}$$

and

$$\kappa = \frac{1.5}{|\, z_+ z_- \,|} \tag{5.33}$$

Using equation (5.29) an expression for the mole fraction-based activity coefficient γ_s^{br} of the mixed-solvent is obtained by integrating equation (4.49), the Gibbs-Duhem equation, as described in Appendix H. The excess Gibbs energy is calculated using equation (4.48) as

$$\frac{G^E_{br}}{RT} = \nu n_e \ln \gamma_{\pm}^{br} + n_s \ln \gamma_s^{br} \tag{5.34}$$

where n_s is the number of moles of mixed-solvent in the system

$$n_s = \sum_{i=1}^{N_S} n_i \tag{5.35}$$

The activity coefficient of the salt, $\gamma_{\pm}^{br}$, is given by equation (5.29) while γ_s^{br} is given by:

$$\ln \gamma_s^{br} = -\frac{\nu n_e}{n_s}\left[1 + \frac{\alpha\sqrt{I}}{3} f(\varrho\sqrt{I}) + \frac{\beta I g(\kappa I)}{2} + \frac{BI}{2}\right] - \ln x_s \tag{5.36}$$

where

$$f(\xi) = \frac{3}{\xi^3}\left[1 + \xi - \frac{1}{1+\xi} - 2\ln(1+\xi)\right] \tag{5.37}$$

and

$$g(\xi) = \frac{2}{\xi}\left[\frac{1+2\xi}{(1+\xi)^2} - \frac{\ln(1+\xi)}{\xi}\right] \tag{5.38}$$

Equation (5.34) gives the expression for G^E_{ES}/RT for the Bromley model. The equivalent expression for the two-parameter Extended-Bromley equation is given in Appendix G.

5.3 The Flory-Huggins Theory for G^E_{ESS}

The Flory-Huggins theory of polymer solutions is the extension of the regular solution theory to mixtures containing large molecules. This model requires one adjustable parameter for each pair of dissimilar components in the solution (see Chapter 2) and has been widely used to describe liquid-liquid equilibrium in polymer solutions (Scott, 1949; Flory, 1953; Tompa, 1956; Koningsveld and Staverman, 1968; Robard, 1978). It has been applied to aqueous two-phase systems containing polymers by Walter et al. (1985), Gustafsson et al. (1986) and Zaslavsky et al. (1989). The Walter et al. (1985) study used the Flory-Huggins theory to model the partitioning of a protein in a two-phase system consisting of two polymers in water. Gustafsson et al. (1986) examined the usefulness of the theory in modelling the binodal curve of the dextran/PEG/water two-phase system. Zaslavsky et al. (1989) used the model to analyze trends in experimental data for ternary aqueous two-phase polymer systems. They calculated values of the interaction parameters for quaternary systems containing salts, by treating the systems as pseudoternaries.

Here, the Flory–Huggins theory is used to describe solvent-solvent interactions in the presence of salt because of its simplicity and accuracy[5]. The model describes the thermodynamic properties of aqueous solutions of solutes of low molecular weight,

[5]Preliminary liquid-liquid equilibrium calculations were performed with an excess Gibbs energy model based on a modified form of the Local-Composition Guggenheim model (Vera et al., 1977) for G^E_{ESS}. The results of these calculations showed that the accuracy of correlations using this model, which requires two more adjustable parameters per binary solvent pair than the modified Flory-Huggins theory, was not significantly better than that of the Flory-Huggins theory.

since the theory reduces to the regular solution theory (Hildebrand et al., 1970) for low molecular weights. The effect of the salt is expressed through the interaction parameters, which are functions of the system composition.

The Flory-Huggins expression for the change in Gibbs energy on mixing for a polymer solution containing N_S components is (Tompa, 1956)

$$\frac{\Delta G_m}{RT} = \left(\sum_{\ell=1}^{N_S} r_\ell n_\ell\right)\left[\sum_{\ell=1}^{N_S} \frac{\phi_\ell}{r_\ell} \ln \phi_\ell + \sum_{\ell=1}^{N_S-1} \sum_{k=\ell+1}^{N_S} \chi_{\ell k} \phi_\ell \phi_k\right] \tag{5.39}$$

where r_ℓ and ϕ_ℓ are the number of molecular segments and volume fraction of component ℓ, respectively. The $\chi_{\ell k}$ are binary interaction coefficients, similar to χ_{12} in Chapter 2, and there are $(N_S - 1)N_S/2$ different parameters for a solution containing N_S components. The $\chi_{\ell k}$'s are independent of composition and dependent on temperature and molecular interaction energy in the manner of equation (2.11). The excess Gibbs energy can be obtained from ΔG_m using the relation

$$\frac{G^E}{RT} = \frac{\Delta G_m}{RT} - \sum_{\ell=1}^{N_S} n_\ell \ln x_\ell \tag{5.40}$$

where x_ℓ is the mole fraction of component ℓ.

A modified form of the Flory-Huggins theory is used to describe the solvent–solvent interactions in the presence of electrolyte for a system consisting of water, one or more polymers or alcohols, and a single salt. The model is applied to the solvents (water, polymers, alcohols) and is generalized to include parameters which are dependent on salt concentration. For this system, consisting of N_S solvents and one salt ($N_C = N_S + 1$), the expression for the excess Gibbs energy is

$$\frac{G^E_{\text{mfl}}}{RT} = \left(\sum_{\ell=1}^{N_S} r_\ell n_\ell\right)\left[\sum_{\ell=1}^{N_S} \frac{\phi^o_\ell}{r_\ell} \ln \frac{\phi^o_\ell}{x^o_\ell} + \sum_{\ell=1}^{N_S-1} \sum_{k=\ell+1}^{N_S} \tilde{\chi}_{\ell k} \phi^o_\ell \phi^o_k\right] \tag{5.41}$$

where x_ℓ° is the salt-free mole fraction of solvent ℓ as defined in equation (5.28) and ϕ_i° is the corresponding salt-free volume fraction

$$\phi_i^\circ = \frac{r_i n_i}{\sum_{\ell=1}^{N_S} r_\ell n_\ell} \tag{5.42}$$

Zaslavsky et al. (1988) found that a quaternary mixture of water, two polymers and an electrolyte could be treated as a pseudoternary system of two polymers dissolved in a water–salt pseudo–solvent. Binodal curve calculations revealed that the presence of salt modified the value of polymer-solvent interaction parameters. King et al. (1988) made similar observations using the virial expansion model of Edmond and Ogston (1968). Here the binary solvent–solvent interaction parameters $\bar{\chi}_{\ell k}$ are assumed to depend on the concentration of salt in the system in a linear manner[6]. With the subscript e denoting the electrolyte (salt),

$$\bar{\chi}_{\ell k} = \chi_{\ell k}^\circ + x_e \chi_{\ell k}^1 \tag{5.43}$$

where x_e is the mole fraction of the electrolyte in the system

$$x_e = \frac{n_e}{\sum_{i=1}^{N_C} n_i} \tag{5.44}$$

and $\chi_{\ell k}^1$ is a parameter which characterizes the effect of salt on the molecular interaction energy between solvent ℓ and k. In the absence of salt, the model reduces to the standard Flory-Huggins theory.

[6]Preliminary calculations using other, more complicated multiparametric functions, including a second order polynomial, indicated that only a small improvement in the accuracy of correlations is obtained over the linear model

5.4 The Bromley–Flory-Huggins model for G^E

The Bromley–Flory-Huggins expression combines the MSA, the Bromley equation and the modified Flory-Huggins theory. In the absence of polymer or alcohol, the model reduces to the one adjustable parameter Bromley electrolyte–solvent model. With no electrolyte present the model reduces to the one parameter per solvent pair binary Flory-Huggins model.

This section presents the expressions for the activity coefficients of the solvents and the electrolyte. As described in Chapter 4, these activity coefficients obey the unsymmetric normalization. The reference state for the solvents (water and polymer/alcohol) is the pure state while that for the salt is its state at infinite dilution in water, solvent 1. From Chapter 4, the activity coefficient of a solvent i is

$$\ln \gamma_i = \left[\frac{\partial G^E/RT}{\partial n_i}\right]_{T,P,n_{k\neq i}} + \qquad \ln \gamma_i^{gds} \qquad i = 1,\ldots,N_S \tag{5.45}$$

where

$$\ln \gamma_i^{gds} = 1 - \sum_{\ell=1}^{N_S} x_\ell - \frac{\nu m M_i}{1000} \qquad i = 1,\ldots,N_S \tag{5.46}$$

M_i is the molecular weight of solvent i and m is the molality of the salt. The corresponding expression for the mean ionic activity coefficient of the salt is

$$\ln \gamma_\pm = \frac{1}{\nu}\left[\frac{\partial G^E/RT}{\partial n_c}\right]_{T,P,n_{\ell\neq c}} + \qquad \ln \gamma_\pm^{gds} \tag{5.47}$$

where

$$\ln \gamma_\pm^{gds} = 1 - \frac{1}{\nu}\sum_{\ell=1}^{N_S} x_\ell \tag{5.48}$$

The excess Gibbs energy is the sum of three terms:

$$G^{E} = G^{E}_{msa^{\infty}} + G^{E}_{br} + G^{E}_{mfl} \tag{5.49}$$

The activity coefficients are obtained by differentiating the excess Gibbs energy function as described in appendices I, J and K. Using equation (5.45) the activity coefficient for component i, which is a solvent, has the form:

$$\ln \gamma_i^{bfh} = \ln \gamma_i^{msa^{\infty}} + \ln \gamma_i^{br} + \ln \gamma_i^{mfl} + \ln \gamma_i^{gds} \qquad i = 1, \ldots, N_S \tag{5.50}$$

where $\gamma_i^{msa^{\infty}}$ is given by equation (I.3) in Appendix I, γ_i^{br} is given by equation (J.7) in Appendix J, and γ_i^{mfl} is given by equation (K.5) in Appendix K. The corresponding expression for the salt is obtained from equation (5.47) and is equal to

$$\ln \gamma_{\pm}^{bfh} = \ln \gamma_{\pm}^{msa^{\infty}} + \ln \gamma_{\pm}^{br} + \ln \gamma_{\pm}^{mfl} + \ln \gamma_{\pm}^{gds} \tag{5.51}$$

where $\gamma_{\pm}^{msa^{\infty}}$ is given by equation (I.4) in Appendix I, $\gamma_{\pm}^{br}$ is given by equation (J.8) in Appendix J, and $\gamma_{\pm}^{mfl}$ is given by equation (K.6) in Appendix K.

Chapter 6

Phase Equilibrium Calculations for Multicomponent Systems

This chapter describes the results of phase equilibrium calculations using the Bromley–Flory–Huggins model for ternary and quaternary aqueous two-phase systems containing salt. The 11 systems studied here are listed in Table 6.1. Due to the nature of the model, only systems with strong electrolytes were chosen. The quaternary systems consisted of aqueous mixtures of Dextran-70, PEG 6000 and a strong electrolyte. The first section of this chapter describes the estimation of parameters used in the excess Gibbs energy model while the second discusses the results of binodal curve calculations for ternary and quaternary systems.

6.1 Estimation of the values of parameters in G^E

This section describes the estimation of the values of parameters used in the model for the excess Gibbs energy. The first part discusses the choice of values for the ion and solvent sizes used in $G^E_{\text{msa}\infty}$. This is followed by a listing of the values of the binary electrolyte–solvent parameter, $\mathcal{B}_1$, used in the G^E_{br}. The third part describes the estimation of the size and the molecular interaction energy parameters, r and

Table 6.1: Systems studied

Ternary systems	**T(K)**	**References**
1-Propanol-NaCl-H_2O	298	this study
2-Propanol-NaCl-H_2O	298	De Santis et al. (1976)
Acetonitrile-KBr-H_2O	298	Renard and Oberg (1965)
PEG 3350-Na_2SO_4-H_2O	301	Ho Gutiérrez (1992)
PEG 8000-NaCl-H_2O	298	this study
PEG 8000-Na_2SO_4-H_2O	301	Ho Gutiérrez (1992)
PPG 425-NaCl-H_2O	298	this study
PPG 725-NaCl-H_2O	298	this study
Quaternary systems	**T(K)**	**References**
Dextran-70†/PEG 6000/NaSCN/H_2O	296	Zaslavsky et al. (1988)
Dextran-70/PEG 6000/Cs_2SO_4/H_2O	296	Zaslavsky et al. (1988)
Dextran-70/PEG 6000/Na_2SO_4/H_2O	296	Zaslavsky et al. (1988)

† of number average molecular weight 28 700.

Table 6.2: Marcus' ionic diameters

anion	D_- (nm)	cation	D_+ (nm)
Cl^-	0.366	K^+	0.268
Br^-	0.388	Na^+	0.196
SO_4^{2-}	0.480	Cs^+	0.338
SCN^-	0.447*		

* value is obtained from Marcus et al. (1988)

χ_{ik}, of G^E_{mR} for binary alcohol- and polymer-water mixtures using experimental vapor-liquid equilibrium (VLE) data.

MSA diameters for $G^E_{mse\infty}$

The values of the diameters of ions determined by Marcus (1983) are used for D_+ and D_-. These diameters are listed in Table 6.2. As discussed in Chapter 5, the diameters of mixed-solvent molecules are assumed to equal that of a water molecule. From the Bjerrum quadrupolar model of the water molecule (Franks, 1984), the diameter of solvent molecules is 0.282 nm.

The predictions of molar solvation energies for the Na^+ ion in solvents of differing dielectric constants, using the MSA and Born equations, are presented in Figure 6.1. The absolute value of the solvation energy predicted by the MSA equation is smaller than that predicted by the Born equation. Values for the MSA solvation energy are based on a solvent diameter equal to that of a water molecule. The effect of reducing

the diameter of the solvent is to increase the magnitude of the solvation energy predicted by the MSA and in the limit of a vanishingly small solvent diameter, the predictions of the two models are equal.

The MSA and Bromley equations require values of the dielectric constants of pure solvents. Table 6.3 lists the dielectric constants used in this study. The values for the polymers are estimated form those of polymers with a similar molecular structure (Van Krevelen and Hoftyzer, 1976). The dielectric constant values correspond to 298 K although for the PEG systems the values are used in equilibrium calculations at 301 K and 333 K.

The electrolyte–water parameter for G^E_{br}

In the absence of alcohol or polymer the Bromley–Flory–Huggins model reduces to the Bromley equation for the mean ionic activity coefficient of an electrolyte in a binary aqueous solution, equation (5.19). For each binary solution, the Bromley equation has one adjustable parameter B_1. The value of this parameter was determined for many binary aqueous electrolyte solutions by matching the predictions of the model with experimental data.

The values of the parameters are presented in Table 6.4. As examples, the predictions of the model using optimal values of the parameter for aqueous solutions of NaCl and Na_2SO_4, at 298 K, are presented in Figure 6.2. The predictions of the Bromley model deviate from experimental data at high salt concentration. For weak electrolytes such as K_3PO_4, and other electrolytes of the 2:2 type, such as $MgSO_4$, the model does not predict $\gamma_\pm$ as accurately (Zemaitis et al., 1986).

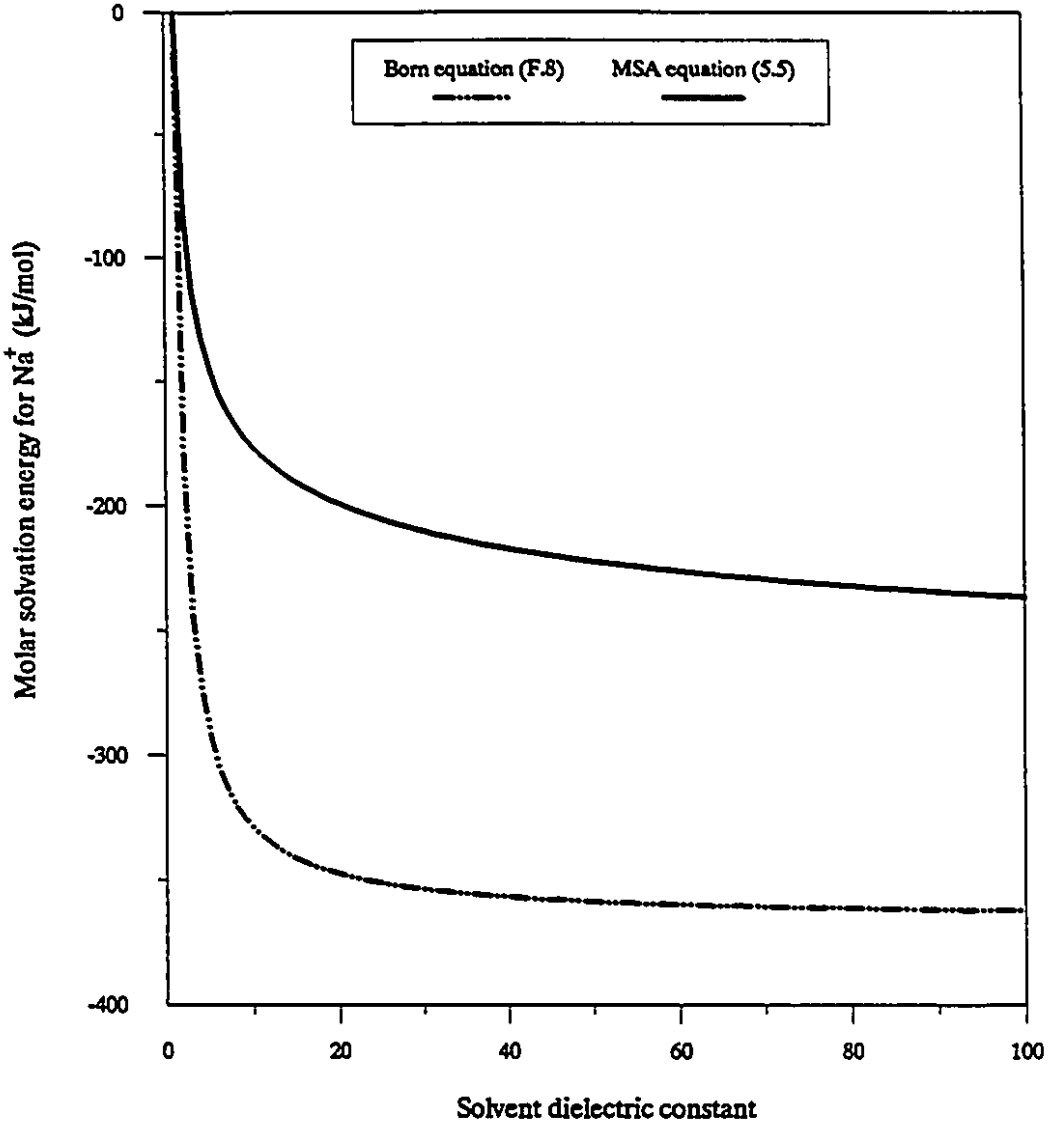

Figure 6.1: Predictions of the MSA and Born equations for the solvation energy of Na^+

Table 6.3: Dielectric constant values at 298 K

Compound	Dielectric constant	Reference
water	78.5	CRC (1986)
1-propanol	20.3	CRC (1986)
2-propanol	18.3	CRC (1986)
Acetonitrile	34.3	Akhadov (1981)
PEG 3350	5	estimated
PEG 4000	5	estimated
PEG 6000	5	estimated
PEG 8000	5	estimated
PPG 425	5	estimated
PPG 725	5	estimated
Dextran-70	3	estimated

Table 6.4: Values of the Bromley equation parameter (Zemaitis et al., 1986)

binary aqueous solutions of	B_1
KCl	0.0240
KBr	0.0296
NaCl	0.0574
NaSCN	0.0758
Cs_2SO_4	-0.0012
Na_2SO_4	-0.0204
K_2SO_4	-0.0320

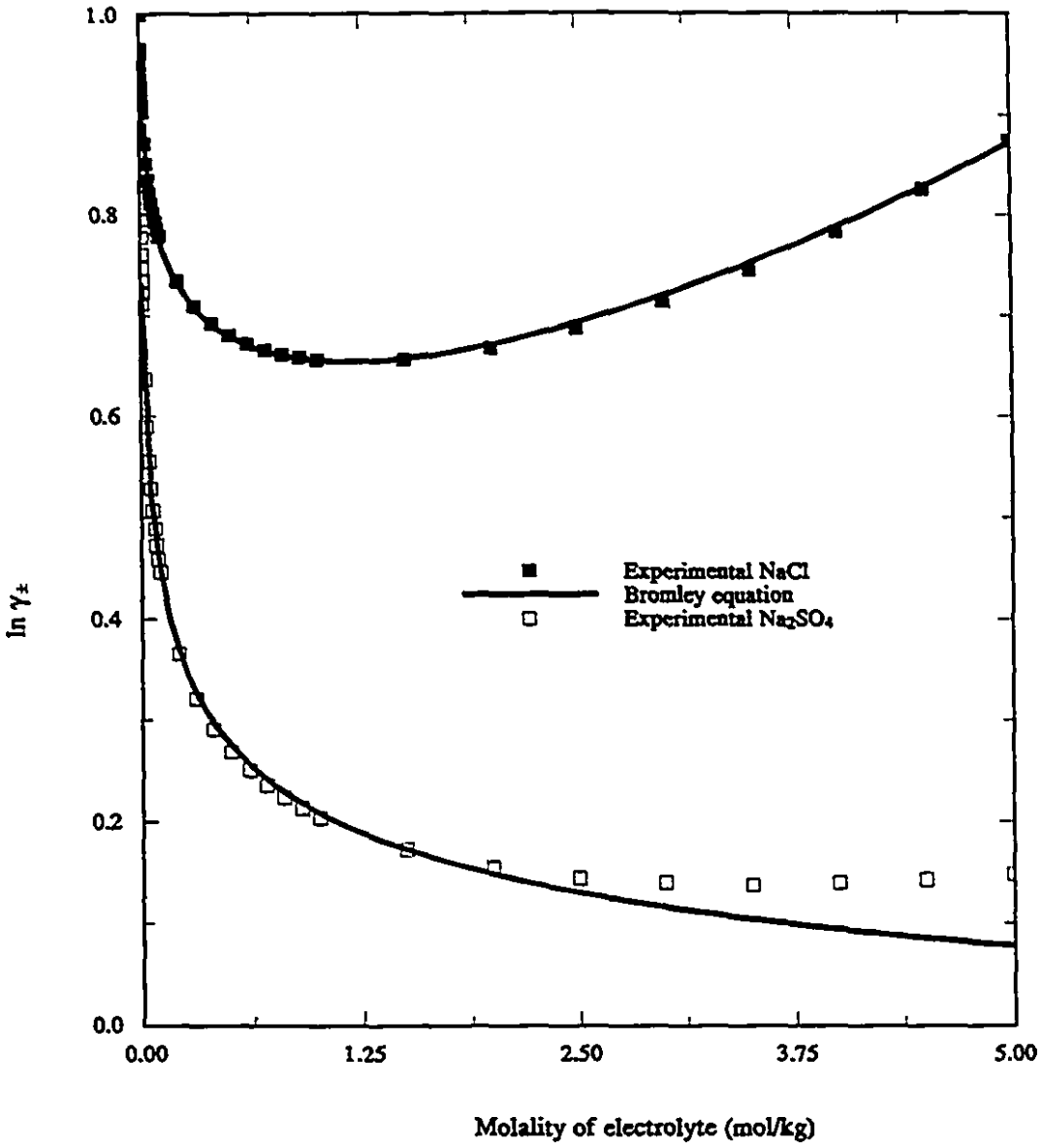

Figure 6.2: Experimentally determined and calculated values of $\gamma_\pm$ for NaCl and Na_2SO_4 at 298 K. Experimental values are from Zemaitis et al. (1986)

Table 6.5: Values of r determined using the ratio of molar volumes

Compound	Density (g/ml)	Reference	Molecular weight*	Reference	r_i
1-propanol	0.8035	CRC (1986)	60.1	CRC (1986)	4.16
2-propanol	0.7855	CRC (1986)	60.1	CRC (1986)	4.25
Acetonitrile	0.7857	CRC (1986)	41.1	CRC (1986)	2.91
PEG 3350	1.2	Albertsson (1986)	3 400	Ho Gutiërrez (1992)	155.1
PEG 6000	1.2	Zaslavsky et al. (1989)	6 000	Zaslavsky et al. (1989)	277.8
PEG 8000	1.2	Albertsson (1986)	8 000	Aldrich Chemical Co.	370.4
PPG 425	1.05	Aldrich Chemical Co.	425	Aldrich Chemical Co.	22.5
PPG 725	1.05	Aldrich Chemical Co.	725	Aldrich Chemical Co.	38.4
Dextran-70	1.6	Zaslavsky et al. (1989)	28 700	Zaslavsky et al. (1989)	974.6

* number average molecular weight

Values of the solvent molecular size parameter r

Two methods of determining the value of r were examined. Initial calculations used a value of r determined using the ratio of molar volumes, equation (2.22). For polymers the molar volumes were estimated using density data. The values of r obtained using ratios of molar volumes are shown in Table 6.5. The results of VLE calculations, described in the next section, indicated that for the alcohols, acetonitrile and PPG, use of molar volume based r's resulted in poor correlation of VLE data (see Figures 6.3 and 6.4). Hence calculations for these systems were done with values of r determined by matching the predictions of the Flory-Huggins model with experimental VLE data.

Determination of solvent–solvent interaction parameters from VLE

For the ternary systems studied here, the binary alcohol- or polymer–water mixtures formed in the absence of salt are not biphasic liquids at the temperatures at which binodal curves were determined. If VLE data at the temperature of interest are available, it is possible to obtain values for binary alcohol- and polymer–water interaction parameters χ°_{ik}.

The criterion for equilibrium between vapor and liquid phases is that for each component the values of its fugacity in both phases are equal. For a binary alcohol- or polymer–water system, this is expressed as

$$f_i^V = f_i^L \qquad i = 1,2 \tag{6.1}$$

where f_i is the fugacity of component i and the superscripts V and L denote the vapor and liquid phases. For an ideal vapor phase with mole fractions $\underline{y}$ and a nonideal liquid phase with mole fractions $\underline{x}$, equation (6.1) is (Smith and Van Ness, 1987)

$$y_i P = x_i \gamma_i P_i^s \qquad i = 1,2 \tag{6.2}$$

where γ_i is the activity coefficient of component i, P is the system pressure and P_i^s is the vapor pressure of component i. For the alcohols and acetonitirile, VLE data is available in the compilation by Gmehling et al. (1977). These data are measurements of equilibrium pressures and vapor phase compositions corresponding to liquid compositions at a fixed temperature. For a given system at a fixed T and x_2, the Flory-Huggins model can be used to calculate γ_i and P and y_2 using the

following relations:

$$P = x_1\gamma_1 P_1^s + x_2\gamma_2 P_2^s \tag{6.3}$$

and

$$y_2 = \frac{x_2\gamma_2 P_2^s}{P} \tag{6.4}$$

In order to determine the values of binary alcohol– and polymer–water interaction parameters the calculated P and y_2 were compared to experimentally determined values. For the alcohols and acetonitrile, for each binary system of water(1) and alcohol(2), the value of χ_{12}^o was determined by matching the predicted P and y_2 to values measured experimentally. The optimal value of χ_{12}^o minimized the following maximum likelihood objective function over N_E experimental points (Prausnitz et al., 1980)

$$F_o = \sum_{k=1}^{N_E} \frac{(P_k - P_k^c)^2}{\sigma_{P_k}^2} + \frac{(y_k - y_k^c)^2}{\sigma_{y_k}^2} \tag{6.5}$$

where P_k and P_k^c are the measured and estimated pressures for experimental point k, respectively. The measured and calculated vapor mole fractions are y_k and y_k^c, respectively, while σ_{P_k} and σ_{y_k} are the standard deviations in experimental measurements of P_k and y_k. For the aqueous alcohol and acetonitrile binary systems the solution pressures reported by Gmehling et al. (1977) are in the range 23–120 mmHg and the uncertainty in the measurements is estimated to be ±0.05 mmHg. Similarly the uncertainty in the vapor phase compositions is estimated to be ±0.0005. It is assumed that the uncertainty in the experimental data is the same for all data points. Assuming that the uncertainty in the data corresponds to

a 95% confidence interval, then $\sigma_P = 0.05/3$ mmHg and $\sigma_y = 0.0005/3$. For high molecular weight polymer systems of PEG and Dextran, the estimated uncertainty is ± 0.003 mmHg and for these systems, $\sigma_P = 0.003/3$ mmHg.

For the Bromley–Flory-Huggins model with r determined using the ratio of molar volumes, values of χ_{12}^{o} were calculated by minimizing F_o, given by equation (6.7), using Powell's multidimensional method (Press et al., 1989). The results of predictions of P and y_2 using optimal parameters were poor, as shown in Figures 6.3 and 6.4, which compare calculated and experimentally determined values for the water(1) and 1-propanol(2) system. In order to improve the VLE correlations of this model, both r and χ_{12} were varied to minimize F_o. The result was a significant improvement in the predictions of P and y_2. Vapor-liquid equilibrium data are available for some of the water-polymer binary systems of this study. Since polymers are nearly nonvolatile, the experimental data consists of liquid compositions with corresponding solution pressures P at a fixed T. Assuming that the vapor phase is water vapor in the ideal gas state, the equality of the chemical potential of water in both phases yields (Tompa, 1956):

$$\frac{P}{P_1^s} = x_1\gamma_1 \tag{6.6}$$

where P_1^s is the vapor pressure of water. Using the Flory-Huggins model for the activity coefficient of the water in the liquid phase, P can be calculated as

$$P = x_1\gamma_1 P_1^s \tag{6.7}$$

Optimal values of the parameters for the model can be obtained by minimizing F_o, with the mole fraction term on the right hand side set to zero. Calculations for the PEG 3350–water system, shown in Figure 6.5, indicate that the Flory-Huggins

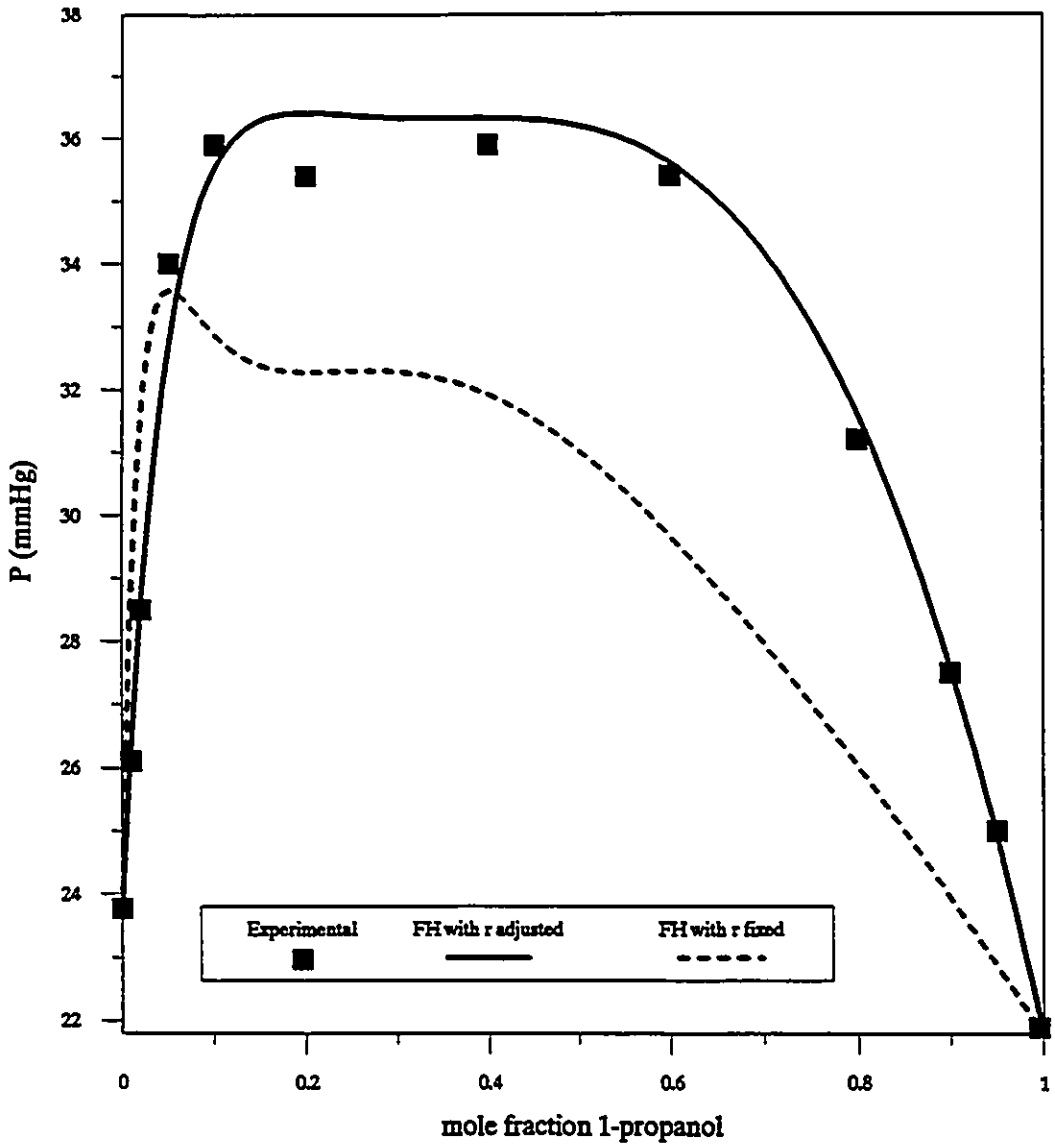

Figure 6.3: Experimental and calculated values of P for the water–i-propanol binary system at 298 K (experimental values from Gmehling et al., 1977). The Flory-Huggins theory is denoted by FH.

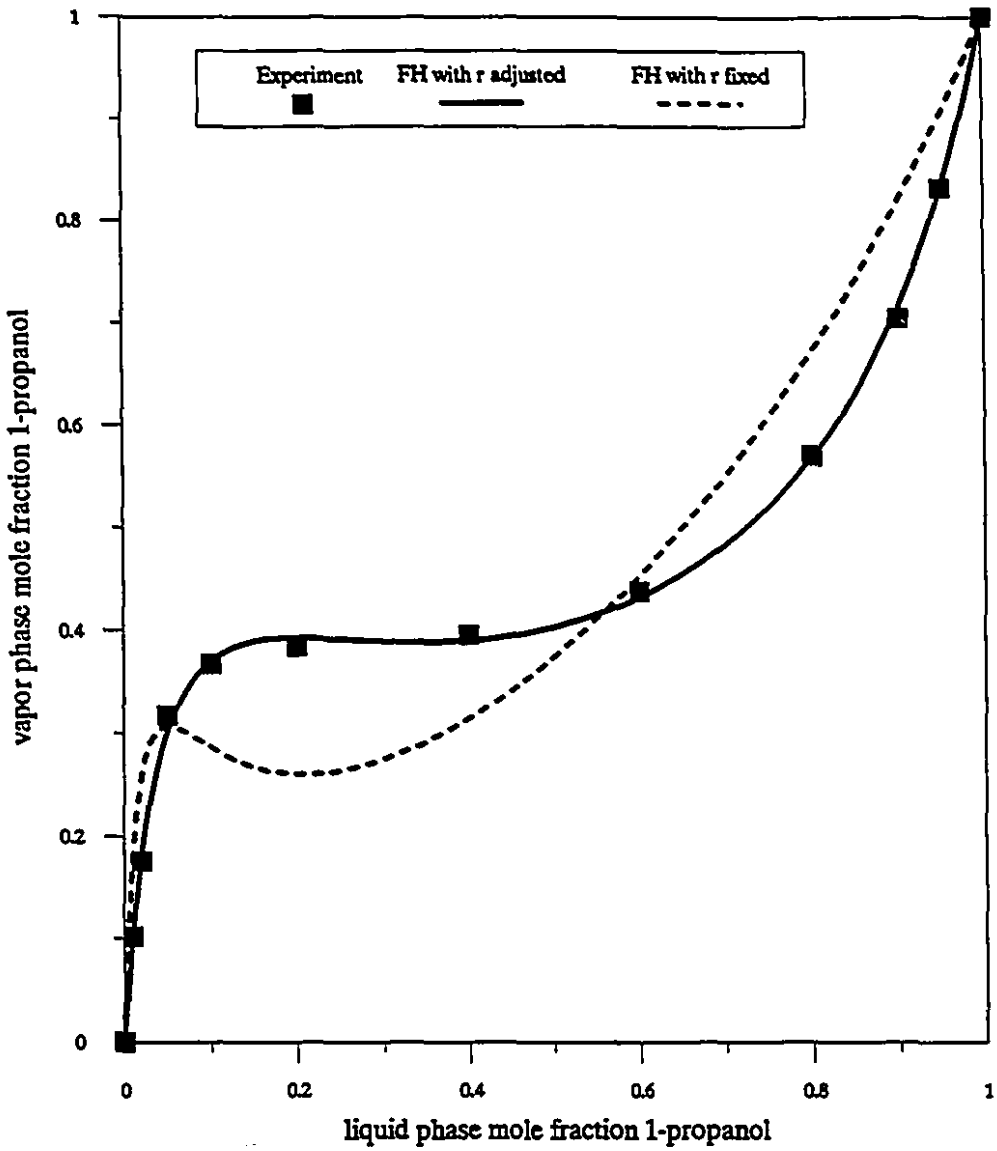

Figure 6.4: Experimental and calculated values of y_2 for the water–1-propanol binary system at 298 K (experimental values from Gmehling et al., 1977). The Flory-Huggins theory is denoted by FH.

Table 6.6: Optimal values of χ_{12} and r for the Bromley-Flory-Huggins Model

compound	one parameter*			two parameter				T(K)	data reference
	χ_{12}	$\Delta P^{\dagger}$	$\Delta y^{\ddagger}$	r_i	χ_{12}	ΔP	Δy		
1-propanol	1.272	3.61	0.085	1.98	1.513	0.57	0.0079	298	Gmehling et al. (1977)
2-propanol	1.218	6.28	0.084	1.63	1.369	0.58	0.0038	298	Gmehling et al. (1977)
Acetonitrile	1.515	16.83	0.071	1.47	1.976	6.48	0.0390	303	Gmehling et al. (1977)
PPG 400	1.318	4.54	—	6.07	0.9482	0.25	—	303	Malcolm and Rowlinson (1957)
PEG 3350	0.426	0.0135	—	—	—	—	—	298	Haynes et al. (1989)
PEG 8000	0.464	0.0149	—	—	—	—	—	298	Haynes et al. (1989)
Dextran-70	0.511	0.0141	—	—	—	—	—	298	Haynes et al. (1989)

* r from ratio of molar volumes from Table 6.5

$$\dagger \qquad \Delta P = \sqrt{\frac{\sum_{k=1}^{N_E}(P_k - P_k^c)^2}{N_E}}$$

$$\ddagger \qquad \Delta y = \sqrt{\frac{\sum_{k=1}^{N_E}(y_k - y_k^c)^2}{N_E}}$$

model with a molar volume ratio based r accurately correlates the vapor pressure data. The results of the VLE correlation are presented in Table 6.6.

6.2 Calculation of liquid-liquid equilibrium

Ternary systems

Liquid-liquid equilibrium calculations were performed for 8 systems. For each ternary system, the Bromley–Flory-Huggins model contains five adjustable param-

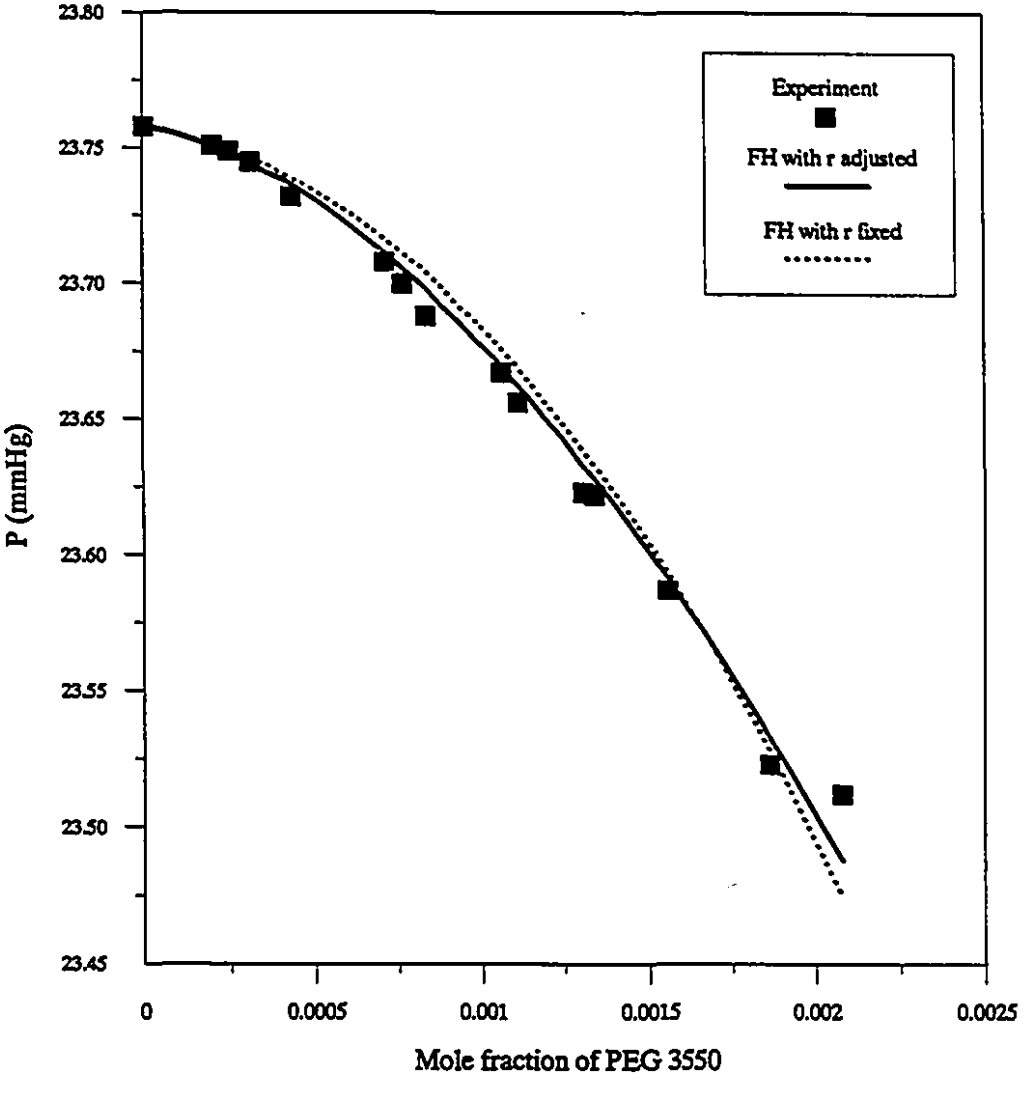

Figure 6.5: Experimental and calculated values of P for the water–PEG 3350 binary system at 298 K (experimental values from Haynes et al., 1989). The Flory-Huggins theory is denoted by FH.

eters: $\mathcal{B}_1$, $\mathcal{B}_2$, b_{12}^b, χ_{12}^o and χ_{12}^1. As described in the previous section, values of $\mathcal{B}_1$ and χ_{12}^o were obtained using binary data. The values of the remaining three parameters were determined using liquid-liquid equilibrium data for the ternary system. For a given ternary system, the optimal set of values of $\mathcal{B}_2$, b_{12}^b and χ_{12}^1 minimized the following objective function[1]

$$F_o = \frac{1}{N_E}\sum_{i=1}^{N_E}\left\{\sqrt{\sum_{j=2}^{N_C}\left(w_{ij}^{Ie}-w_{ij}^{Ic}\right)^2}+\sqrt{\sum_{j=2}^{N_C}\left(w_{ij}^{IIe}-w_{ij}^{IIc}\right)^2}\right\} \tag{6.8}$$

where w_{ij}^{Ie} is the experimentally determined weight fraction of component j in phase I for tie-line i. The corresponding calculated weight fraction of component i in phase I is w_{ij}^{Ic} and the objective function is calculated over N_E tie-lines. The minimization[2] of the objective function was accomplished using a routine based on Powell's multidimensional method (Press et al., 1989).

The results of binodal curve calculations using optimal values of the parameters are presented in Figures 6.6 to 6.10 and Table 6.6. The binodal curves of the 1-propanol and 2-propanol systems, Figures 6.6 and 6.7, are well represented by the model. The predictions of the model for the 1-propanol system are compared to those obtained by Dahl and Macedo (1992) using a MHV2 group contribution equation of state method. The results of the Bromley-Flory-Huggins method are more

[1]It should be noted that the summation of weight fraction differences runs over $N_C - 1$ components only; if all the components are included in the summation, as is often done (Sørensen and Arlt, 1980b), the fit is biased since $\sum_i w_i = 1$.

[2]For the 1-propanol system, VLE data for the ternary salt system at 1 atm pressure (Johnson and Furter, 1960) were used to obtain initial estimates of the values of the parameters. Liquid-liquid equilibrium calculations using these parameters yielded a binodal curve that was close to the experimentally determined one. For the other systems no systematic method for obtaining initial estimates of parameters was available. For many sets of initial estimates the results converged to the trivial solution in which both phases have the same composition.

Table 6.7: Optimal parameters for ternary systems

systems	T(K)	$\mathcal{B}_2$	b_{12}^b	χ_{12}^l
1-Propanol–NaCl–H_2O	298	10.53	2.80	-3.81
2-Propanol–NaCl–H_2O	298	8.54	1.94	-1.97
Acetonitrile–KBr–H_2O	298	9.55	-3.43	-11.11
PEG 8000–NaCl–H_2O	298	1.1	15.6	8.9
PEG 3350–Na_2SO_4–H_2O	301	0.0	5.5	9.64
PEG 8000–Na_2SO_4–H_2O	301	5.5	8.31	10.5
PPG 425–NaCl–H_2O	298	132.1	4.32	7.64
PPG 725–NaCl–H_2O	298	165.5	-3.13	35.75

accurate. However, the compositions of the salt-rich bottom phases are more accurately represented than the alcohol-rich phases. The range of predicted propanol concentrations in the top phases is smaller than that determined experimentally. The calculations for the Na_2SO_4–PEG 3350 system, Figure 6.8, are less accurate, with the model predicting less polymer in the bottom phases than is observed experimentally. Comparison of the results of the Bromley–Flory-Huggins model with that proposed by Cabezas et al. (1990b)[3] confirm this observation. For the PPG systems the predictions are accurate although the errors are similar to those for alcohol and PEG systems.

[3]The results of calculations using this model were provided by Kabiri-Badr (1990) and correspond to a temperature of 298 K

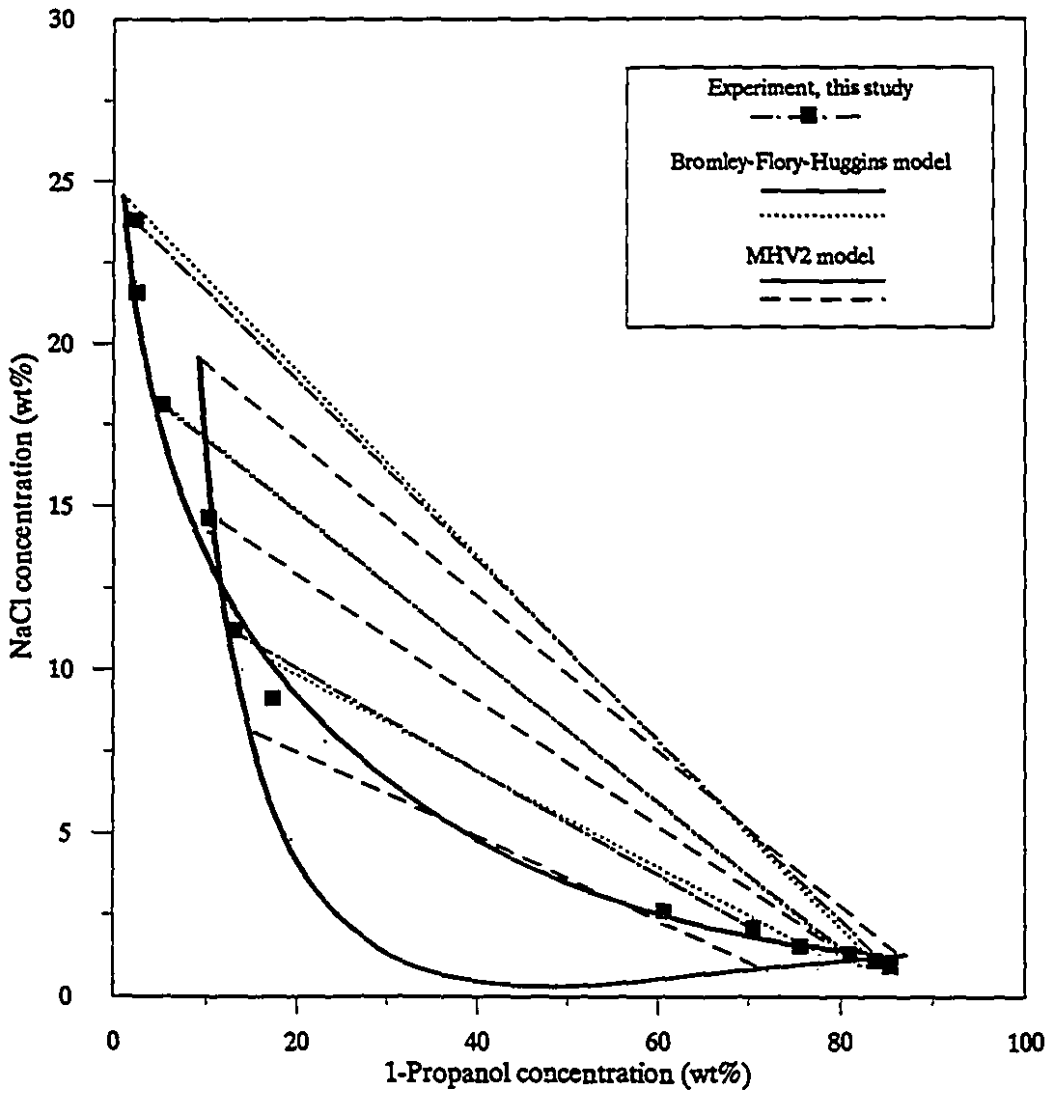

Figure 6.6: Experimental and calculated binodal curves for the 1-propanol/ NaCl/water at 298 K

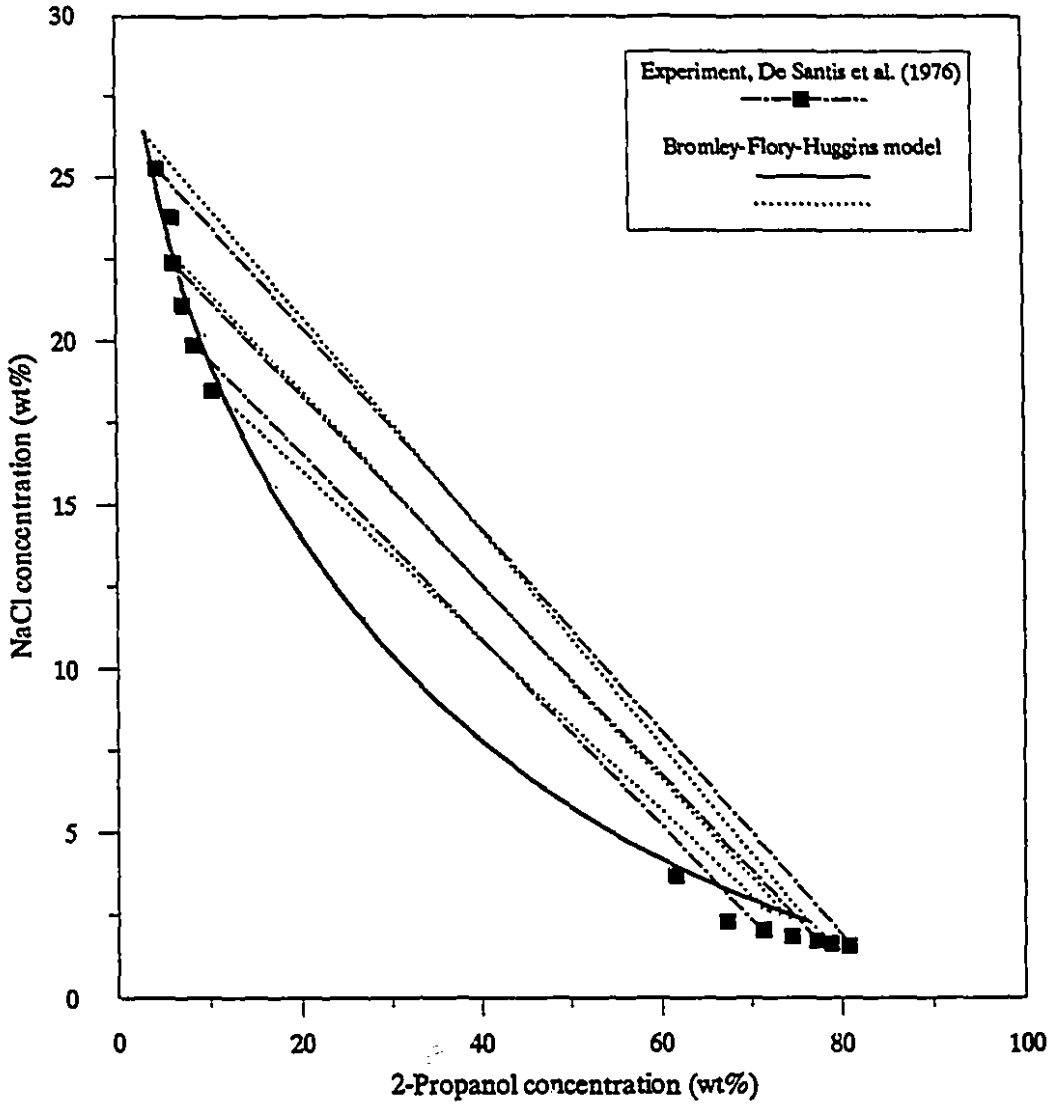

Figure 6.7: Experimental and calculated binodal curves for the 2-propanol/ NaCl/water at 298 K

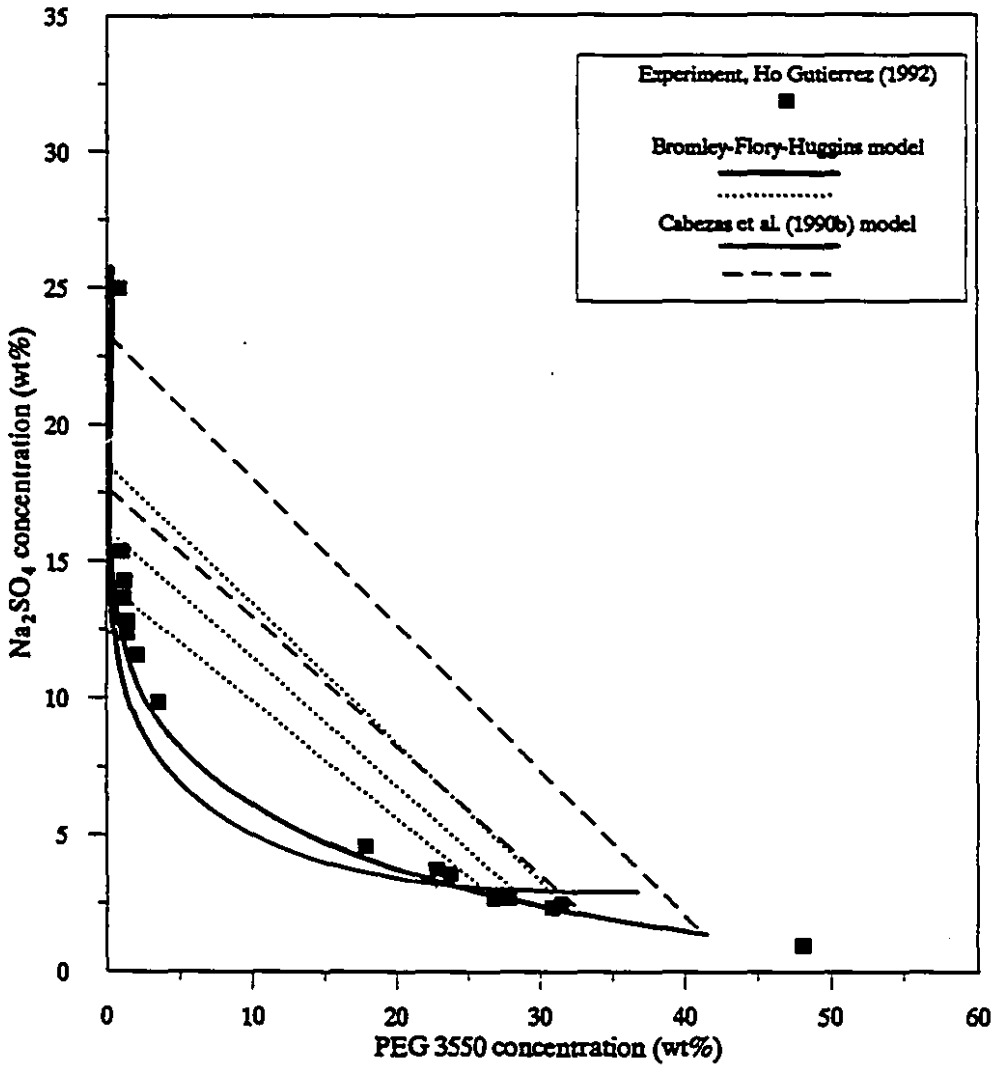

Figure 6.8: Experimental and calculated binodal curves for the PEG 3350/ Na_2SO_4/water at 301 K

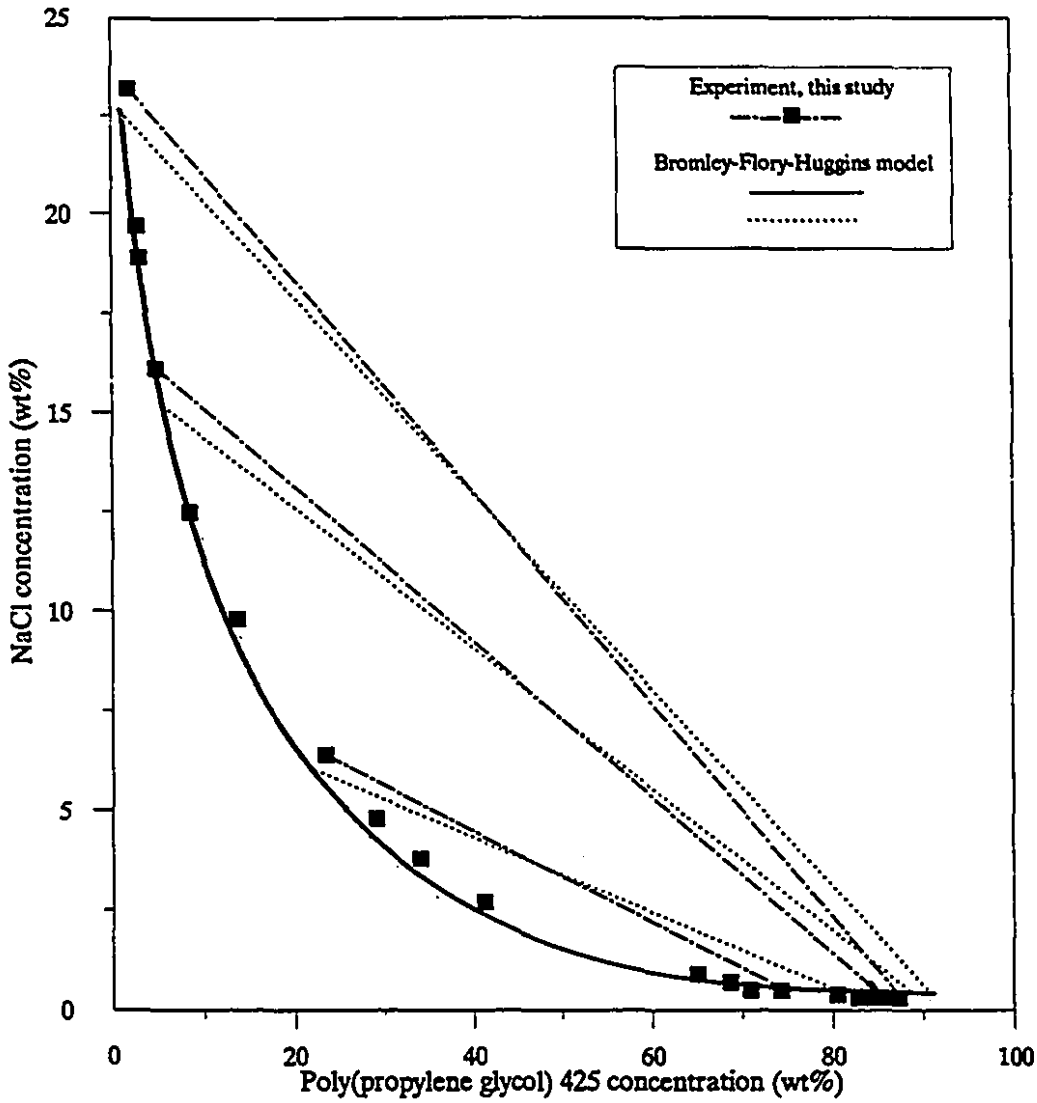

Figure 6.9: Experimental and calculated binodal curves for the PPG 425/NaCl/water at 298 K

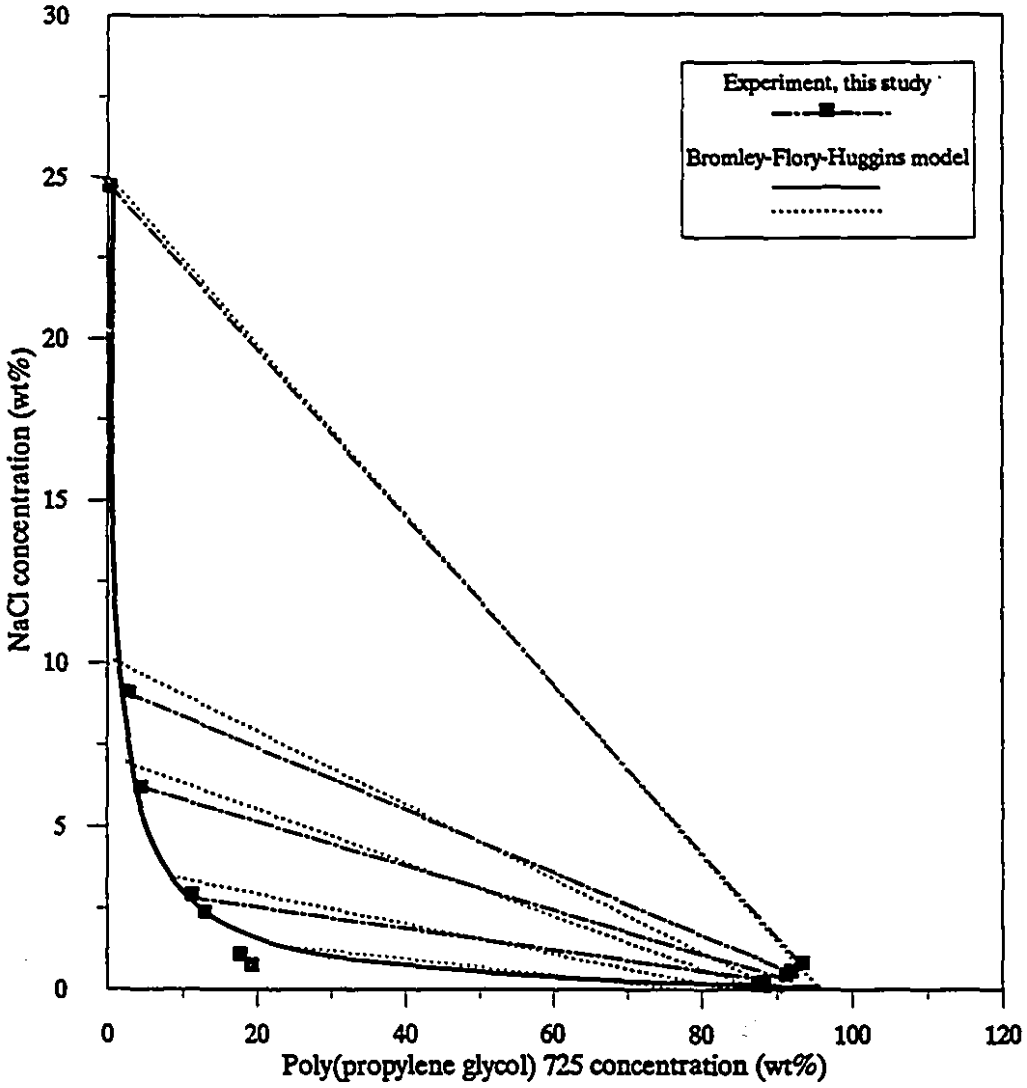

Figure 6.10: Experimental and calculated binodal curves for the PPG 725/NaCl/water at 298 K

Quaternary systems

Calculations were performed for three quaternary systems containing Dextran-70, PEG 6000 and either NaSCN, Cs_2SO_4 or Na_2SO_4. All three systems contain salt at an overall concentration of 0.10 mol/kg. The values of the polymer–water and polymer–polymer interaction parameters χ_{ik} were determined using liquid-liquid equilibrium data in the form of the binodal curve for the two polymers at 296 K (Zaslavsky et al., 1989). These parameters are $\chi_{12} = 0.5$, $\chi_{13} = 0.456$, and $\chi_{23} = 0.038$ where water is component 1, Dextran is component 2, and PEG is component 3. Preliminary calculations with these systems indicated that the parameters $\mathcal{B}_2$ and $\mathcal{B}_3$ do not have a significant effect on the phase equilibrium, hence they were set to zero. The resulting quaternary model has 5 adjustable parameters χ^1_{12}, χ^1_{13}, χ^1_{23}, b^b_{12} and b^b_{13}. The optimal sets of values of these parameters were determined in a manner similar to that used for the ternary systems. However, in order to improve the sensitivity of the objective function to differences in salt concentrations, the values of which are much smaller than the polymer concentrations, the weight percent differences in equation (6.8) were converted to relative values by dividing the differences by the experimentally determined values.

The results of liquid-liquid equilibrium calculations for the three systems are presented in Tables 6.8–10 and Figures 6.11–13. For all three systems the model accurately correlates the equilibrium data, even for the salt which is present at a low concentration. The figures show the binodal curve for the polymers, in weight fractions which account for the salts. The curves for the three systems are similar since the salts are present in low concentrations. Optimal sets of values of the parameters are presented in Table 6.11.

Table 6.8: Experimental (wt%E) and calculated (wt%C) liquid-liquid equilibrium for the Dextran-70/PEG 6000/NaSCN/water system at 296 K

Phase I						
	Dextran-70		PEG 6000		NaSCN	
T-Line	wt%E*	wt%C	wt%E	wt%C	wt%E	wt%C
1	0.4	0.2	16.5	17.9	0.92	0.72
2	0.6	0.3	14.8	16.0	0.91	0.72
3	1.1	0.6	12.1	12.9	0.89	0.74
4	1.7	1.1	10.5	11.0	0.87	0.76
5	3.0	2.1	8.5	9.0	0.86	0.77
Phase II						
	Dextran-70		PEG 6000		NaSCN	
T-Line	wt%E	wt%C	wt%E	wt%C	wt%E	wt%C
1	29.1	25.9	0.2	1.0	0.69	0.87
2	26.6	23.5	0.3	1.2	0.70	0.86
3	21.9	19.3	0.6	1.7	0.72	0.85
4	19.0	16.8	0.8	1.9	0.74	0.84
5	16.1	14.6	1.3	2.1	0.75	0.83

* experimentally determined value (Zaslavsky, 1988).

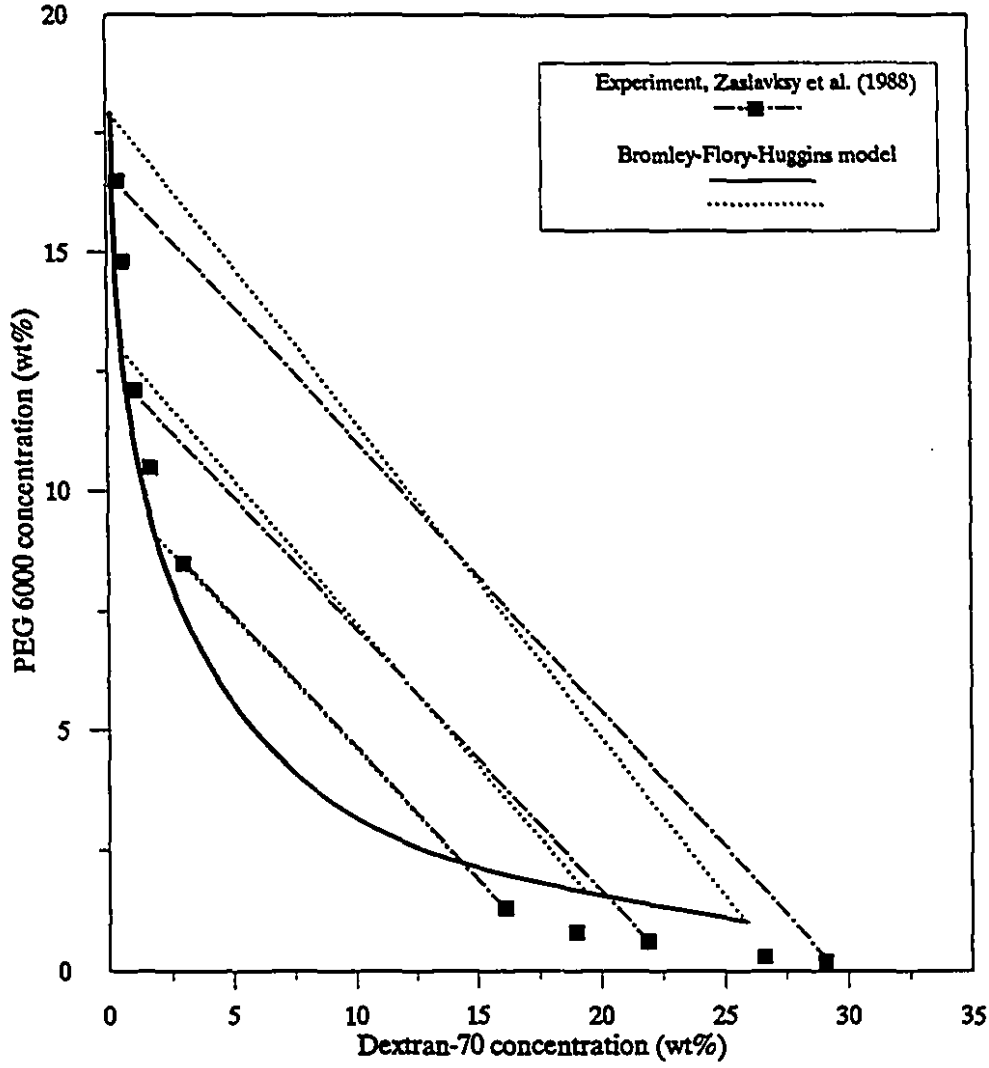

Figure 6.11: Experimental and calculated binodal curves for Dextran-70 and PEG 6000 in the presence of NaSCN at 296 K

Table 6.9: Experimental (wt%E) and calculated (wt%C) liquid-liquid equilibrium for the Dextran-70/PEG 6000/Cs_2SO_4/water system at 296 K

Phase I						
	Dextran-70		PEG 6000		Cs_2SO_4	
T-Line	wt%E	wt%C	wt%E	wt%C	wt%E	wt%C
1	0.2	0.02	17.6	17.3	2.39	2.69
2	0.3	0.03	16.1	15.5	2.49	2.78
3	0.6	0.03	13.3	12.8	2.73	2.84
4	1.7	0.05	9.8	9.8	2.95	3.01
Phase II						
	Dextran-70		PEG 6000		Cs_2SO_4	
T-Line	wt%E	wt%C	wt%E	wt%C	wt%E	wt%C
1	27.4	28.1	0.2	0.2	4.80	4.54
2	24.8	26.2	0.3	0.3	4.71	4.50
3	20.6	21.7	0.5	0.7	4.48	4.40
4	15.3	16.3	1.0	1.3	4.26	4.15

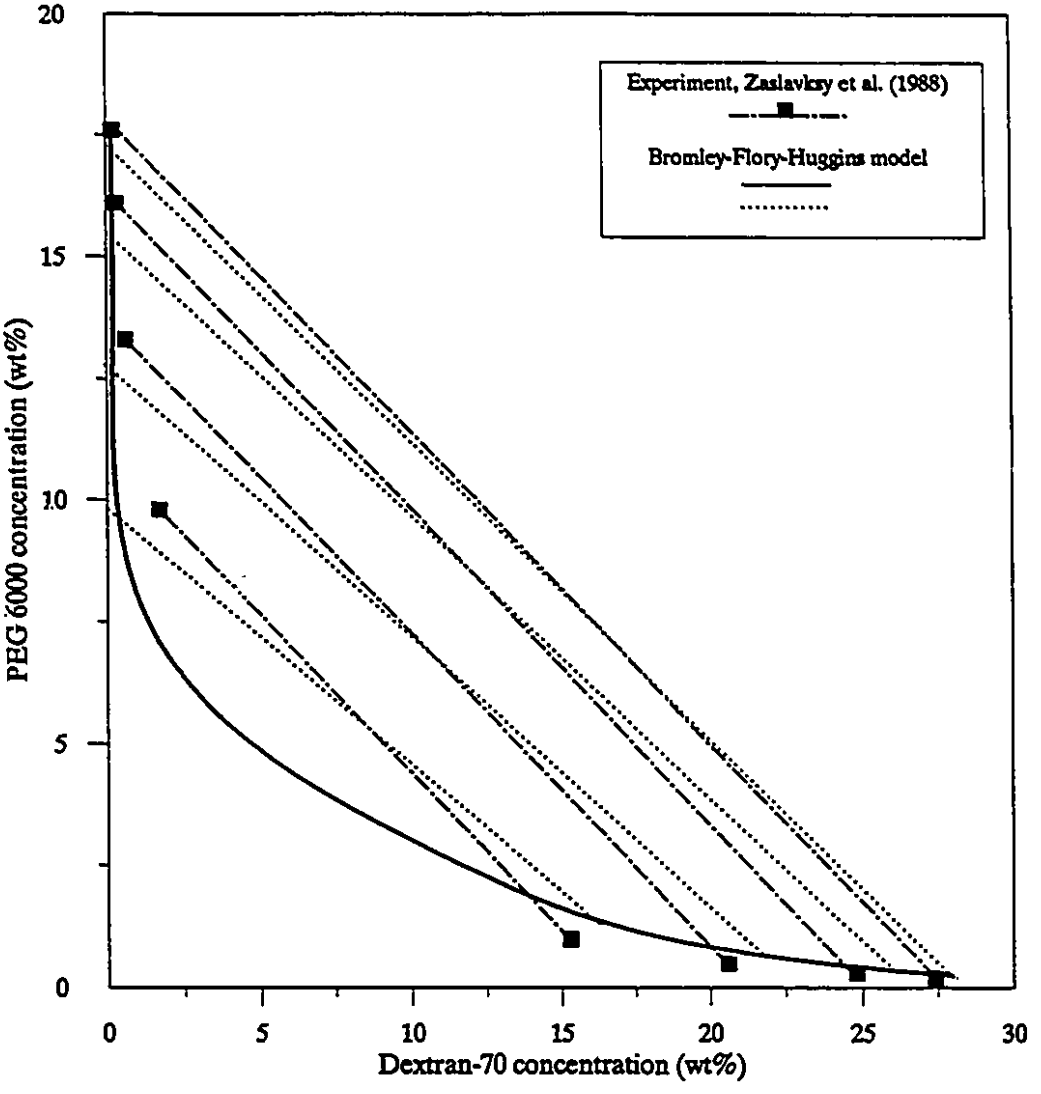

Figure 6.12: Experimental (wt%E) and calculated (wt%C) binodal curves for Dextran-70 and PEG 6000 in the presence of Cs_2SO_4 at 296 K

Table 6.10: Experimental (wt%E) and calculated (wt%C) liquid-liquid equilibrium for the Dextran-70/PEG 6000/Na_2SO_4/water system at 296 K

Phase I						
	Dextran-70		PEG 6000		Na_2SO_4	
T-Line	wt%E	wt%C	wt%E	wt%C	wt%E	wt%C
1	0.2	0.1	18.2	17.7	1.08	1.17
2	0.3	0.2	16.5	15.9	1.11	1.20
3	0.7	0.4	13.7	13.0	1.17	1.24
4	1.8	1.1	9.9	9.4	1.24	1.29
5	3.0	1.7	8.0	7.9	1.31	1.32
Phase II						
	Dextran-70		PEG 6000		Na_2SO_4	
T-Line	wt%E	wt%C	wt%E	wt%C	wt%E	wt%C
1	26.5	26.2	0.2	1.0	1.730	1.630
2	24.3	23.9	0.3	1.1	1.700	1.606
3	20.2	19.6	0.4	1.6	1.650	1.568
4	14.8	14.3	1.0	2.2	1.580	1.508
5	11.8	12.0	2.0	2.5	1.520	1.489

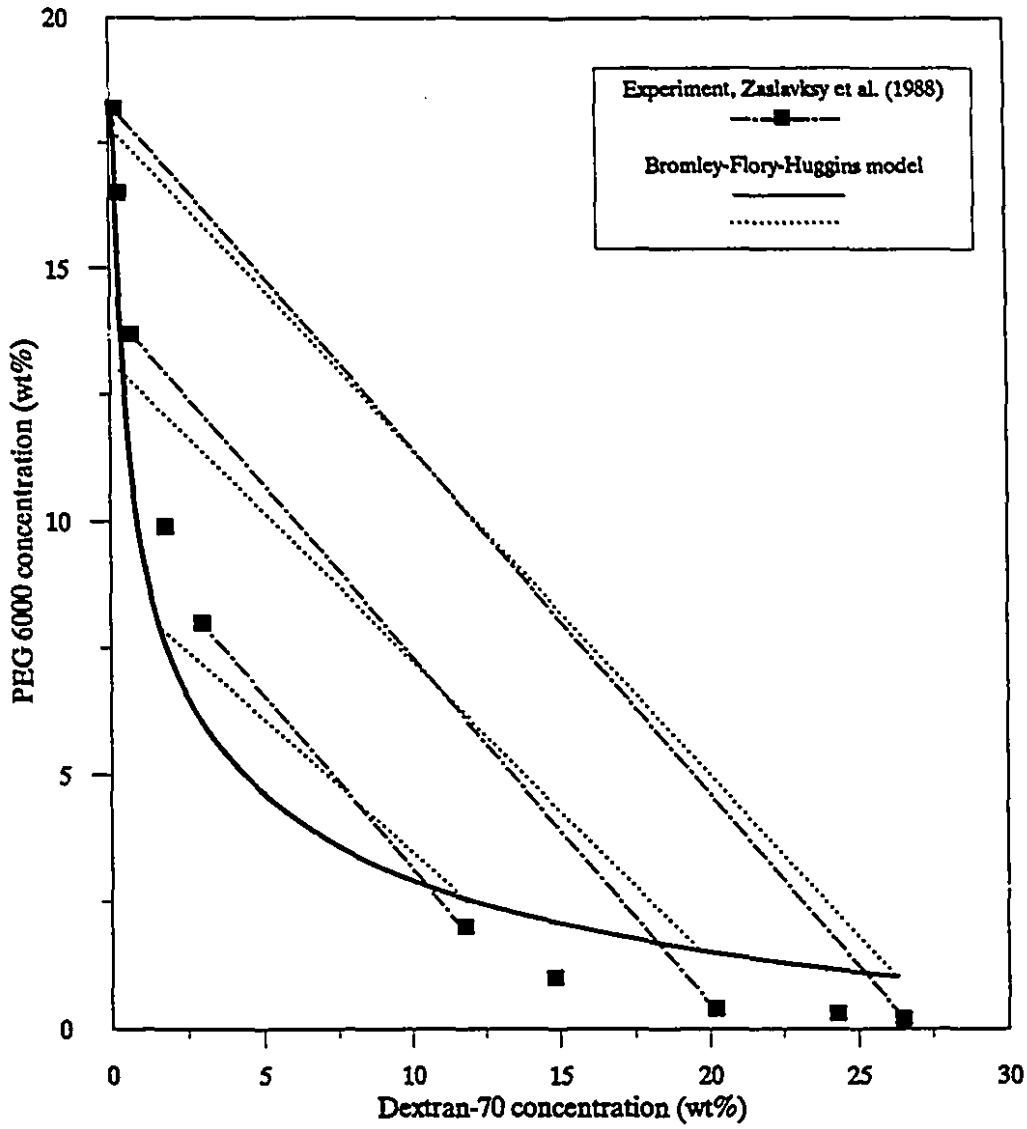

Figure 6.13: Experimental and calculated binodal curves for Dextran-70 and PEG 6000 in the presence of Na_2SO_4 at 296 K

Table 6.11: Optimal parameters for quaternary systems

salt	χ^1_{12}	χ^1_{13}	χ^1_{23}	b^b_{12}	b^b_{13}
NaSCN	0.349	2.880	-0.056	119.3	21.48
Cs_2SO_4	-4.48	1.115	-1.746	23.82	34.82
Na_2SO_4	-1.078	2.76	-2.807	-25.92	20.82

Chapter 7

Conclusions, Contributions and Recommendations

7.1 Conclusions

Liquid-liquid equilibrium experiments for locating the binodal curve and tie-lines of ternary systems were performed for alcohol–, surfactant– and polymer–NaCl–water mixtures. The systems investigated are listed in Table 7.1. For the 1-propanol and poly(propylene glycol) mixtures complete phase diagrams were determined, including regions of solid-liquid coexistence. For the poly(ethylene glycol) system, the complete two-liquid region of the phase diagram was determined. For the *n*-dodecylammonium chloride system only that part of the phase diagram corresponding to two isotropic liquids was characterized.

The binodal curves of the 1-propanol, poly(ethylene glycol), and poly(propylene glycol) systems have a similar shape. For these systems, the top phases are rich in alcohol or polymer while the bottom phases contain most of the NaCl and water. The shape of the binodal curve of the *n*-dodecylammonium chloride system is different from those of the other systems. Most of the surfactant is in the top phase while the NaCl is nearly evenly distributed between the phases. For a particular temperature, the effect of increasing the weight average molecular weight

Table 7.1: Systems studied experimentally

System	Temperature (K)
1-Propanol—NaCl—H_2O	298
n-Dodecylammonium chloride—NaCl—H_2O	303
Poly(ethylene glycol) 8000—NaCl—H_2O	333
Poly(propylene glycol) 425—NaCl—H_2O	278, 298, 333
Poly(propylene glycol) 725—NaCl—H_2O	278, 298

of the poly(propylene glycol) fraction is to increase the size of the biphasic region. Similarly, for a given fraction of poly(propylene glycol), the effect of increasing the temperature is to increase the size of the two phase region.

A modified form of the Flory-Huggins theory was used to calculate liquid-liquid equilibrium for binary aqueous liquid mixtures with closed–loop phase diagrams. A new method for determining the value of r in the Flory-Huggins theory using experimental liquid-liquid equilibrium data was tested. Two expressions for $\chi_{12}(T)$ were proposed. One of the expressions involves expanding the interchange free energy as a three-level partition function while the second is a polynomial function. The liquid-liquid equilibrium data of 15 aqueous binary systems, in the form of closed-loops and a UCT curve, were accurately correlated by the two expressions for $\chi_{12}(T)$.

A model for calculating liquid-liquid equilibrium in multicomponent biphasic systems containing a single salt was developed. The model is based on a combination of the Mean Spherical Approximation and modified forms of the Bromley

and Flory-Huggins expressions for the excess Gibbs energy. This model was used to calculate liquid-liquid equilibrium for ternary and quaternary systems.

For ternary systems, the Bromley–Flory-Huggins model contains 5 adjustable parameters. One of these, the Bromley constant B_1, was obtained from mean ionic activity coefficient data for salts in water. The Flory-Huggins binary interaction parameter χ^o_{ik} was determined from binary alcohol– and polymer–water vapor-liquid equilibrium data. Three parameters were obtained from correlating liquid-liquid equilibrium data. For quaternary systems, five parameters were obtained from liquid-liquid equilibrium data. The model was used to calculate liquid-liquid equilibrium data for 8 ternary and 3 quaternary systems. Depending on the system, the results are more accurate or less accurate than comparable models from the literature.

7.2 Original Contributions to Knowledge

Liquid-liquid equilibrium data for *n*-dodecylammonium–, poly(ethylene glycol)– and poly(propylene glycol)–NaCl–water systems, including the determination of the effects of temperature and molecular weight fraction on the binodal curves of the poly(propylene glycol)–NaCl-water system.

Modification of the Flory-Huggins binary polymer solution model to allow the accurate calculation of liquid-liquid equilibrium for binary aqueous systems which have closed-loop phase diagrams.

Development of a model for the excess Gibbs energy of multicomponent aqueous biphasic salt systems which combines modified forms of the Bromley and Flory-Huggins expressions with the Mean Spherical Approximation. The model predicts the binodal curve and tie lines of aqueous biphasic salt systems.

7.3 Recommendations for Future Work

Collection of vapor-liquid equilibrium data for alcohol/salt/water and polymer/salt/water systems of the aqueous biphasic type to provide information on the values of parameters in the excess Gibbs energy model.

Extension of the model to weak electrolyte buffer systems by substituting a modified form of the Pitzer (1973) equation for the Bromley term in the excess Gibbs energy function.

References

Abe, A., Imae, T., Shibuya, A., and S. Ikeda, 1988. The Effect of Protonation on the Phase Diagrams of Alkyldimethylamine Oxides. *J. Surface Sci. Technol.*, 4:67–80.

Akhadov, Y.Y., 1981. " Dielectric Properties of Binary Solutions," Pergamon Press, New York.

Albertsson, P.-Å., 1986. " Partition of Cell Particles and Macromolecules," 3rd Ed., John Wiley & Sons, New York.

Ananthapadmanabhan, K.P., and E.D. Goddard, 1987. Aqueous Biphase Formation in Polyethylene Oxide—Inorganic Salt Systems. *Langmuir*, 3:25–31.

Andersen, G.R., and J.C. Wheeler, 1978. Theory of Lower Critical Solution Points in Aqueous Mixtures. *J. Chem. Phys.*, 69:3403–3413.

Bailey, F.E., Jr., and R.W. Callard, 1959. Some Properties of Poly(ethylene oxide) in Aqueous Solution. *J. Appl. Polym. Sci.*, 1:56-62.

Baksir, J.N., Hatton, T.A., and U.W. Sutter, 1989. Protein Partitioning in Two-Phase Aqueous Polymer Systems. *Biotech. Bioeng.*, 34:541–558.

Ball, F.X., Fürst, W., and H. Renon, 1985. An NRTL Model for Representation and Prediction of Deviation from Ideality in Electrolyte Solutions Compared to the Models of Chen (1982) and Pitzer (1973). *AIChE J.*, 31:392–399.

Barker, J. and W. Fock, 1953. Theory of Upper and Lower Critical Solution Temperatures. *Discuss. Faraday Soc.*, 15:188–195.

Beutier, D., and H. Renon, 1978. Representation of NH_3–H_2S–H_2O, NH_3–CO_2–H_2O and NH_3–SO_2–H_2O Vapor–Liquid Equilibria. *Ind. Eng. Chem. Process Des. Dev.*, 17:220–230.

Blankschtein, D., Thurston, G.M., and G.B. Benedek, 1985. Theory of Phase Separation in Micellar Solutions. *Phys. Rev. Letts.*, 54:955–958.

Blum, L., and D.Q. Wei, 1987. Analytical Solution of the Mean Spherical Approximation for an Arbitrary Mixture of Ions in a Dipolar Solvent. *J. Chem. Phys.*, 87:555–565.

Blum, L., and W.R. Fawcett 1992. Application of the Mean Spherical Approximation to Describe the Gibbs Solvation Energy of Monovalent Monoatomic Ions in Polar Solvents. *J. Phys. Chem.*, 96:408–414.

Bodegom, E., and H.E. Meijer, 1984. Coexistence and Spinodal Curves in Directionally Bonded Liquids Using Four-Cluster Approximation. *J. Chem. Phys.*, 80:1617–1624.

Bromley. L.A., 1973. Thermodynamic Properties of Strong Electrolytes. *AIChE J.*, 19:313–320.

Broome, F.K., Hoerr, C.W., and H.J. Harwood, 1950. The Binary System of Water with Dodecylammonium Chloride and its N-Methyl Derivatives. *J. Amer. Chem. Soc.*, 73:3350–3352.

Brown, G.H., and E.M. Sallee, 1963. "Quantitative Chemistry," Prentice-Hall Inc., Englewood Cliffs, New Jersey.

Cabezas, H., Jr, Evans, J.D., and D.C. Szlag, 1990a. Statistical Thermodynamics of Aqueous Two-Phase Systems. Chapter 2 in "Downstream Processing and Bioseparation," Hamel, J.-F. P., Hunter, J.B., and S.K. Sidar, (eds), ACS Symposium Series 419, American Chemical Society, Washington, DC., 38–52.

Cabezas, H., Jr, Kabiri-Badr, M., and D.C. Szlag, 1990b. Statistical Thermodynamics of Phase Separation and Ion Partitioning in Aqueous Two-Phase Systems. *Bioseparations*, 1:227–233.

Cairns, B.P., and I.A. Furzer, 1990. Multicomponent Three-Phase Azeotropic Distillation. 2. Phase-Stability and Phase-Splitting Algorithms. *Ind. Eng. Chem. Res.*, 29:1364–1382.

Carnahan, B., Luther, H.A., and J.O. Wilkes, 1969. "Applied Numerical Methods," John Wiley & Sons, New York.

Chan, D.Y.C., Mitchell, D.J., and B.W. Ninham, 1979. A Model of Solvent Structure Around Ions. *J. Chem. Phys.*, 70:2946–2957.

Chen, F.P., Ames, A.E., and L.D. Taylor, 1990. Aqueous Solutions of Poly(ethyloxazoline)

and Its Lower Consolute Phase Transition. *Macromolecules*, **23**:4688-4695.

Corrin, M.L., and W.D. Harkins, 1947. The Effect of Salts on the Critical Concentration for the Formation of Micelles in Colloidal Electrolytes. *J. Am. Chem. Soc.*, **69**:683–688.

CRC, 1986, "Handbook of Chemistry and Physics," 66th Ed., CRC Press, Boca Raton, Florida.

Dahl, S., and E.A. Macedo, 1992. The MHV2 Model: A UNIFAC-Based Equation of State Model for Vapor-Liquid and Liquid-Liquid Equilibria of Mixtures with Strong Electrolytes. *Ind. Eng. Chem. Res.*, **31**:1195–1201.

Denbigh, K., 1955. "The Principles of Chemical Equilibrium," Cambridge University Press, Cambridge.

De Santis, R., Marrelli, L., and P.N. Muscetta, 1976. Liquid-Liquid Equilibria in Water-Aliphatic Alcohols in the Presence of Sodium Chloride. *Chem. Eng. J.*, **11**:207–214.

Diamond, A.D., and J.T. Hsu, 1990. Protein Partitioning in PEG/Dextran Aqueous Two-Phase Systems. *AIChE J.*, **36**:1017–1024.

Do, K.S., and W.K. Park, 1974. The Liquid-Liquid Equilibria for n-Propyl Alcohol–Water–Salt Systems. *J. KIChE*, **12**:57–64.

Edmond, E., and A.G. Ogston, 1968. An Approach to the Study of Phase Separation in Ternary Aqueous Systems. *Biochem. J.*, **109**:569–576.

Eisenberg, H., and G.R. Mohan, 1959. Aqueous Solutions of Polyvinylsulfonic Acid: Phase Separation and Specific Interaction with Ions, Viscosity, Conductance and Potentiometry. *J. Phys. Chem.*, **63**:671-680.

Eiteman, M.A., and J.L. Gainer, 1989. The Effect of Free-Volume Changes on Partitioning in Magnesium Sulfate–Poly(ethylene glycol) Aqueous Two-Phase Systems. *Biochim. Biophys. Acta*, **992**:125–127.

Firman, P., Haase, D., Jen, J., Kahlweit, M., and R. Strey, 1985. On the Effect of Electrolytes on the Mutual Solubility Between H_2O and Nonionic Amphiphiles. *Langmuir*, **1**:718–724.

Florin, E., Kjellander, R., and J.C. Eriksson, 1984. Salt Effects on the Cloud Point of the Poly(ethylene oxide) + Water System. *Chem. Soc., Faraday Trans. 1*, **80**:2889–2910.

Flory, P.J., 1953. " Principles of Polymer Chemistry," Cornell University, Ithaca, New

York.

Flory, P.J., 1965. Statistical Thermodynamics of Liquid Mixtures. *J. Amer. Chem. Soc.*, 87:1833–1838.

Franks, F., 1984. "Water," Royal Society of Chemistry, London.

Freed, K.F., 1985. New Lattice Model for Interacting, Avoiding Polymers with Controlled Length Distribution. *J. Phys. A:Math. Gen.* 18:871–887.

Gao, Y.-L., Peng, Q.H., Li, Z.-C., and Y.-G. Li, 1991a. Thermodynamics of Ammonium Sulfate–Polyethylene Glycol Aqueous Two-Phase Systems. Part 1. Experiment and Correlation Using Extended UNIFAC Equation. *Fluid Phase Equilib.*, 63:157–171.

Gao, Y.-L., Peng, Q.H., Li, Z.-C., and Y.-G. Li, 1991b. Thermodynamics of Ammonium Sulfate–Polyethylene Glycol Aqueous Two-Phase Systems. Part II. Correlation and Prediction Using Extended UNIFAC Equation. *Fluid Phase Equilib.*, 63:173–182.

Gault, J.D., Leite, M.A., Rizzatti, M.R., and H. Gallardo, 1988. The Effect of Chain Length and Salt on Phase Diagrams of the n-Alkyl Ammonium Halide–Water System. *J. Colloid Interface Sci.*, 122:587–590.

Gering, K.L., Lee, L.L., and L.H. Landis, 1989. A Molecular Approach to Electrolyte Solutions: Phase Behavior and Activity Coefficients for Mixed-Salt and Multisolvent Systems. *Fluid Phase Equilib.*, 48:111–139.

Gmehling, J., Onken, V., and W. Arlt, 1977. "Vapor-Liquid Equilibria Data Collection," DECHEMA, Franfurt/Main.

Goldstein, R.E., and J.S. Walker, 1983. Theory of Multiple Phase Separations in Binary Mixtures: Phase Diagrams, Thermodynamic Properties, and Comparisons With Experiments. *J. Chem. Phys.*, 78:1492–1512.

Goldstein, R.E., 1984. On the Theory of Lower Critical Solution Points in Hydrogen-Bonded Mixtures. *J. Chem. Phys.*, 80:5340–5341.

Goldstein, R.E., 1985. Phenomenological Theory of Multiply Reentrant Solubility. *J. Chem. Phys.*, 83:1246–1254.

Greve, A., and M.-R. Kula, 1991a. Recycling of Salts in Partition Protein Extraction Processes. *J. Chem. Technol. Biotechnol.*, 50:27–42.

Greve, A., and M.-R. Kula, 1991b. Phase Diagrams of New Aqueous Phase Systems Composed of Aliphatic Alcohols, Salt and Water. *Fluid Phase Equilib.*, 62:53–63.

Gustafsson, Å., Wennerstöm, H., and F. Tjerneld, 1986. The Nature of Phase Separation in Aqueous Two-Polymer Systems. *Polymer*, 27:1768–1770.

Hansen, J.-P., and I.R. McDonald, 1986. "Theory of Simple Liquids," 2nd Edition, Academic Press, New York.

Harned, H.S., and B.B. Owen, 1958. "The Physical Chemistry of Electrolytic Solutions," 3rd Edition, Rheinhold, New York.

Harned, H.S., and R.A. Robinson, 1968. "Multicomponent Electrolyte Solutions," Pergamon Press, New York.

Harvey, A., and J.M. Prausnitz, 1987. "Dielectric Constants of Fluid Mixtures Over a Wide Range of Temperature and Density," *J. Soln. Chem.*, *16*:857–869.

Haynes, C.A. Beynon, R.A., King, R.S., Blanch, H.W., and J.M. Prausnitz, 1989. Thermodynamic Properties of Aqueous Polymer Solutions: Poly(ethylene glycol)/Dextran. *J. Phys. Chem.*, 93:5612–5617.

Heidemann, R.A. 1983. Computation of High Pressure Equilibria. *Fluid Phase Equilib.*, 14:55–65.

Herrmann, K.W., 1964. Micellar Properties and Phase Separation in Dimethyldodecylamine Oxide–Sodium Halide–Water Systems. *J. Phys. Chem.*, 68:1540–1546.

Hildebrand, J.H., Prausnitz, J.M., and R.L. Scott, 1970. "Regular and Related Solutions," Van Nostrand Reinhold, New York.

Hill, T.L., 1957. Theory of Solutions. I. *J. Amer. Chem. Soc.*, 79:4885–4890.

Hill, T.L., 1960. "Introduction to Statistical Thermodynamics," Addison-Wesley, Reading, MA.

Hino, T., Lambert, S.M., Soane, D.S., and J.M. Prausnitz, 1992. Molecular Thermodynamics for Closed-Loop Liquid-Liquid Equilibria of Binary Systems Including Polymer Solutions. *Personal Communication.*

Hirschfelder, J., Stevenson, D., and H. Eyring, 1937. A Theory of Liquid Structure. *J. Chem. Phys.*, 5:896–912.

Horvath, A.L., 1985. "Handbook of Aqueous Electrolyte Solutions," Halsted Press, John Wiley & Sons, New York.

Ho Gutiérrez, I.V., 1992. "Equilibrium Compositions in Two–Phase Partition," M.Eng.

Thesis, Department of Chemical Engineering, McGill University, Montreal, Quebec

Hu, Y., Lambert, S.M., Soane, D.S., and J.M. Prausnitz, 1991. Double-Lattice Model for Binary Polymer Solutions. *Macromolecules*, 24:4356–4363.

Huot, J.-Y., and C. Jolicoeur, 1985. Hydrophobic Effects in Ionic Hydration and Interactions. Chapter 11 in "The Chemical Physics of Solvation," Part A: Theory of Solvation. Dogonadze, R.R., Kālmān, E., Kornyshev, A.A., and J. Ulstrup, (eds), Elsevier, Amsterdam.

Imae, T., and S. Ikeda, 1986. The pH Dependence of Upper and Lower Consolute Phase Boundaries for Aqueous NaCl Solutions of Dimethylamine Oxide. *J. Colloid Interface Sci.*, 113:449–455.

Imae, T., Konishi, H., and S. Ikeda, 1986. Lower and Upper Critical Consolute Boundaries of Dilute Aqueous Solutions of Dimethyloleylamine Oxide in the Presence of NaCl and HCl. A "Closed-Loop" Phase Diagram. *J. Phys. Chem.*, 90:1417–1422.

Imae, T., Sasaki, M., Abe, A., and S. Ikeda, 1988. Liquid-Liquid Phase Separation in Dilute Aqueous Solutions of Surfactants: The Effect of Added Salt. *Langmuir*, 4:414-418.

Jansson, L.-J., and I.A. Furzer, 1989. A Comparison of Thermodynamic Models for VLE data in Electrolyte Systems. *AIChE J.*, 35:1044–1048.

Joesten, M., and L. Schaad, 1974. "Hydrogen Bonding," Dekker, New York.

Johnson, A.I., and W.F. Furter, 1960. Salt Effect in Vapor-Liquid Equilibrium, Part II. *Can. J. Chem. Eng.*, 38:78–87.

Johnston, G., Meadows, M.R., Mockler, R.C., and W.J. O'Sullivan, 1983. The Choice of Composition Variable for the Walker and Vause Model for Binary Liquid Mixtures Having Closed-Loop Coexistence Curves. *Chem. Phys. Lett.*, 96:575–578.

Kabiri-Badr, M., 1990. "Thermodynamics of Salt-Polymer Aqueous Two-Phase Systems: Theory and Experiment." Ph.D Thesis, The University of Arizona.

Karlström, G., 1985. A New Model for Upper and Lower Critical Solution Temperatures in Poly(Ethylene Oxide) Solutions. *J. Phys. Chem.*, 89:4962–4964.

Kikic, I., Fermeglia, M., and P. Rasmussen, 1991. UNIFAC Prediction of Vapor-Liquid Equilibria in Mixed Solvent-Salt Systems. *Chem. Eng. Sci.*, 46:2775–2780.

Kim, Y.-C. and J.-D. Kim, 1988. New Calculation Method for Asymmetric Closed-Loop

Liquid-Liquid Equilibria by Lattice Decoration. *Fluid Phase Equilib.*, 41:229–244.

King, R.S., Blanch, H.W., and J.M. Prausnitz, 1988. Molecular Thermodynamics of Aqueous Two-Phase Systems for Bioseparations. *AIChE J.*, 34:1585–1594.

Kjellander, R., and E. Florin, 1981. Water Structure and Changes in Thermal Stability of the System Poly(ethylene oxide)–Water. *J. Chem. Soc., Faraday Trans. 1*, 77:2053–2077.

Koningsveld, R., and A.J. Staverman, 1967. Liquid-Liquid Phase Separation in Multicomponent Polymer Solutions. IV. Coexistence Curves. *Kolloid Z. & Z. Polymere*, 218:114–124.

Kusalik, P.G., and G.N. Patey, 1988. On the Molecular Theory of Aqueous Electrolyte Solutions. III. A Comparison Between Born-Oppenheimer and McMillan-Mayer Levels of Description. *J. Chem. Phys.*, 89:7478–7484.

Laughlin, R.G., 1978a. Solvation and Structural Requirements of Surfactant Hydrophilic Groups. Chapter 2 in "Advances in Liquid Crystals," Volume 3, G.H. Brown (ed.), Academic Press, New York.

Laughlin, R.G., 1978b. Relative Hydrophilicities Among Surfactant Head Groups. Chapter 3 in "Advances in Liquid Crystals," Volume 3, G.H. Brown (ed.), Academic Press, New York.

Macedo E.A., Skovborg, P., and P. Rasmussen, 1990. Calculation of Phase Equilibria for Solutions of Strong Electrolytes in Solvent–Water Mixtures. *Chem. Eng. Sci.*, 45:875–882.

Malcolm, G.N., and J.S. Rowlinson, 1957. The Thermodynamic Properties of Aqueous Solutions of Polyethylene Glycol, Polypropylene Glycol and Dioxane. *Trans. Faraday Soc.*, 53:921–931.

Marcus, Y., 1983. Ionic Radii in Aqueous Solutions. *J. Soln. Chem.*, 12:271–275.

Marcus, Y., Kamlet, M.J., and R.W. Taft, 1988. Linear Solvation Energy Relationships. Standard Molar Gibbs Free Energies and Enthalpies of Transfer of Ions from Water into Nonaqueous Solvents. *J. Phys. Chem.*, 92:3613–3622.

Michelsen, M.L., 1982. The Isothermal Flash Problem. Part I: Stability. *Fluid Phase Equilib.*, 9:1–19.

Modell, M., and R.C. Reid, 1974. "Thermodynamics and Its Applications," Prentice-Hall,

Englewood Cliffs, New Jersey.

Molyneux, P., 1975. Chapter 7 in "Water: A Comprehensive Treatise," Franks, F., (ed.), Volume 4, Plenum Press, New York.

Molyneux, P., 1983. "Water Soluble Synthetic Polymers: Properties and Behavior," Volume 1, CRC Press, Boca Raton, Florida.

Nord, F.F., Bier, M., and S.N. Timasheff, 1951. Investigations on Proteins and Polymers. IV. Critical Phenomena in Polyvinyl Alcohol–Acetate Copolymer Solutions. *J. Amer. Chem. Soc.*, **73**:289–292.

Orofino, T.A. and P.J. Flory, 1957. Relationship of the Second Virial Coefficient to Polymer Chain Dimensions and Interaction Parameters. *J. Chem. Phys.*, **26**:1067–1076.

Orwoll, R. A., 1977. The Polymer-Solvent Interaction Parameter χ. *Rubber Chem. Technol.*, **50**:451–479.

Oster, G., 1946. Some Dielectric Properties of Liquid Mixtures. *J. Amer. Chem. Soc.*, **68**:2036–2041.

Panayiotou, C., and J.H. Vera, 1984. Thermodynamics of Polymer-Polymer Solvent and Block Copolymer-Solvent Systems. II. Theoretical Treatment of Data with the Nonrandom New Flory Theory. *Polymer J.*, **16**:103–112.

Panayiotou, C., and I.C. Sanchez, 1992. Hydrogen Bonding in Fluids: An Equation-of-State Approach. *Personal Communication.*

Pathak, S.P., Sudha, S., Sawant, S.B., and J.B. Joshi, 1991. New Salt–Polyethylene-glycol Systems for Two-Phase Aqueous Extraction. *Chem. Eng. J.*, **46**:B31–B34.

Patterson, D., Delmas, G. and T. Somcynsky, 1967. A Comparison of Lower Critical Solution Temperatures of Some Polymer Solutions. *Polymer*, **8**:503–516.

Patterson, D., and G. Delmas, 1969. Critical State in Chain-Molecule Mixtures. *Trans. Faraday Soc.*, **65**:708–724.

Pitzer, K.S., and L. Brewer, 1961. "Thermodynamics," G.N. Lewis, and M. Randall, Revised, 2nd Edition, McGraw-Hill, New York.

Pitzer, K.S., 1973. Thermodynamics of Electrolytes. I. Theoretical Basis and General Equations. *J. Phys. Chem.*, **77**:268–277.

Prange, M.M., Hooper, H.H., and J.M. Prausnitz, 1989. Thermodynamics of Aqueous Systems Containing Hydrophilic Polymers or Gels. *AIChE J.*, **35**:803–813.

Prausnitz, J.M., 1969. "Molecular Thermodynamics of Fluid-Phase Equilibria," Prentice-Hall, Englewood Cliffs, New Jersey.

Prausnitz, J.M., Anderson, T.F., Grens, E.A., Eckert, C.A., Hsieh, R., and J.P. O'Connell, 1980. "Computer Calculations for Multicomponent Vapor-Liquid and Liquid-Liquid Equilibria," Prentice-Hall, Englewood Cliffs, New Jersey.

Press, W.H., Flannery, B.P., Teukolsky, S.A., and W.T. Vetterling, 1989. "Numerical Recipes in Pascal," Cambridge University Press, New York.

Qian, C., Mumby, S.J. and B.E. Eichinger, 1991a. Phase Diagram of Binary Polymer Solutions and Blends. *Macromolecules*, **24**:1655–1661.

Qian, C., Mumby, S.J. and B.E. Eichinger, 1991b. Existence of Two Critical Concentrations in Binary Phase Diagrams. *J. Polym. Sci: Part B: Polym. Phys.*, **29**:635–637.

Raastchen, W., Harvey, A.H., and J.M. Prausnitz, 1987. Equation of State for Solutions of Electrolytes in Mixed Solvents. *Fluid Phase Equilib.*, **39**:19–38.

Ralston, A.W., Hoffman, E.J., Hoerr, C.W., and W.M. Selby, 1941. Studies on High Molecular Weight Aliphatic Amines and Their Salts. I. Behavior of the Hydrochlorides of Dodecylamine and Octadecylamine in Water. *J. Amer. Chem. Soc.*, **63**:1598–1600.

Rastogi, A., and D. Tassios, 1987. Thermodynamics of a Single Electrolyte in a Mixture of Two Solvents. *Ind. Eng. Chem. Res.*, **26**:1344–1351.

Reid, R.C., Prausnitz, J.M., and T.K. Sherwood, 1977. "The Properties of Gases and Liquids," McGraw-Hill, New York.

Renard J.A. and A.G. Oberg, 1965. Ternary Systems: Water-Acetonitrile-Salts. *J. Chem. Eng. Data*, **10**:152–155.

Rizzatti, M.R., and J.D. Gault, 1986. Phase Diagrams of the Decylammonium Chloride/Ammonium Chloride/Water System in the Nematic Micellar Region. *J. Colloid Interface Sci.*, **110**:258–262.

Robard, A., 1978. "Phase Separation in Systems Containing Polymers," Ph.D. Thesis, Department of Chemistry, McGill University, Montreal.

Robinson, R.A., and Stokes, R.H., 1959. "Electrolyte Solutions," Butterworths Scientific Publications, London.

Saeki, S., Kuwahara, N., Nakata, M., and M. Kaneko, 1976. Upper and Lower Critical Solution Temperatures in Poly(ethylene glycol) Solutions. *Polymer*, 17:685–689.

Saint-Victor, M.E., 1988. "Heat Capacity and Structure in Small Molecule and Polymer Systems," Ph.D. Thesis, McGill University.

Sanchez, I.C., and R.H. Lacombe, 1978. Statistical Thermodynamics of Polymer Solutions. *Macromolecules*, 11:1145–1156.

Sanchez, I.C., and A.C. Balazs, 1989. Generalization of the Lattice-Fluid Model for Specific Interactions. *Macromolecules*, 22:2325–2331.

Sasaki, K.J., Christian S.D., and E.E. Tucker, 1989. Study of the Stability of 1:1 Complexes Between Aliphatic Alcohols and β-Cyclodextrins in Aqueous Solution. *Fluid Phase Equilib.*, 49:281–289.

Sasaki, K.J., Christian S.D., and E.E. Tucker, 1990. Use of a Visible Spectral Displacement Method to Determine the Concentration of Surfactants in Aqueous Solution. *J. Colloid Interface Sci.*, 134:412–416.

Schott, H., 1973. Salting In of Nonionic Surfactants by Complexation with Inorganic Salts. *J. Colloid Interface Sci.*, 43:150-155.

Schott, H., Royce, A.E., and S.K. Han, 1984. Effect of Inorganic Additives on Solutions of Nonionic Surfactants. .VII. Cloud Point Shift Values of Individual Ions. *J. Colloid Interface Sci.*, 98:196–201.

Schneider, G., and C. Russo, 1966. DruckeinfluB auf die Entimischung Flüssiger Systeme. V. Salzeffekte auf die Entimischung bei 1-Propanol–H_2O, 2-Butanol–H_2O und Pyridin-H_2O bis 6000 bar. *Berichte der Bunsengesellschaft*, 70:1008–1014.

Scott, R.L., 1949. The Thermodynamics of High Polymer Solutions. V. Phase Equilibria in the Ternary System: Polymer 1–Polymer 2–Solvent. *J. Chem. Phys.*, 17:279–284.

Sjöberg, Å., and G. Karlström, 1989. Temperature Dependence of the Phase Equilibria for the System Poly(ethylene glycol)/Dextran/Water. A theoretical and Experimental Study. *Macromolecules*, 22:1325–1330.

Smith, J.M., and H.C. Van Ness, 1987. "Introduction to Chemical Engineering Thermodynamics," 4th Edition, McGraw-Hill, New York.

Snyder, S.M., Cole, K.D., and D.C. Szlag, 1992. Phase Compositions, Viscosities, Densities for Aqueous Two-Phase Systems Composed of Polyethylene Glycol and Various

Salts at 25°C. *J. Chem. Eng. Data*, 37:268–274.

Sørensen, J.M. and W. Arlt, 1980a, "Liquid-Liquid Equilibrium Data Collection, 1" DECHEMA, Franfurt.

Sørensen, J.M. and W. Arlt, 1980b, "Liquid-Liquid Equilibrium Data Collection, 2" DECHEMA, Franfurt.

Tanford, C., 1973. "The Hydrophobic Effect," John Wiley & Sons, New York.

Thalberg, K., Lindman, B., and G. Karlström, 1990. Phase Diagram of a System of Cationic Surfactant and Anionic Polyelectrolyte: Tetradecyltrimethylammonium Bromide–Hyaluronan–Water. *J. Phys. Chem.*, 94:4289–4295.

Thalberg, K., Lindman, B., and K. Bergfeldt, 1991a. Phase Behavior of Systems of Polyacrylate and Cationic Surfactants. *Langmuir*, 7:2893–2898.

Thalberg, K., Lindman, B., and G. Karlström, 1991b. Phase Diagram of a System of Cationic Surfactant and Anionic Polyelectrolyte: The Effect of Salt. *J. Phys. Chem.*, 95:6004–6011.

Tiddy, G.J.T., 1980. Surfactant–Water Liquid Crystal Phases. *Phys. Rep.*, 57:1–46.

Tokiwa, F., and T. Matsumoto, 1975. Effect of Inorganic Electrolytes on the Cloud Point of Polyoxyethylene Dodecyl Ether. *Bull. Chem. Soc. Japan*, 48:1645–1646.

Tompa, H., 1956. "Polymer Solutions," Butterworths Scientific Publications, London.

Van Krevelen, D.W., and P.J. Hoftyzer, 1976. "Properties of Polymers," Elsevier Scientific, Amsterdam.

Van Ness, H.C., and M.M. Abbott, 1979. Vapor-Liquid Equilibrium. *AIChE J.*, 25:645–653.

Van Ness, H.C., and M.M. Abbott, 1982. "Classical Thermodynamics of Nonelectrolyte Solutions," McGraw-Hill, NY.

Vera, J.H., Sayegh, S.G., and G.A. Ratcliff, 1977. A Quasi Lattice-Local Composition Model for the Excess Gibbs Energy of Liquid Mixtures. *Fluid Phase Equilib.*, 1:113–135.

Vernau, J., and M.-R. Kula, 1990. Extraction of Proteins from Biological Raw Material Using Polyethylene Glycol–Citrate Phase Systems. *Biotechn. Biochem.*, 12:397–404.

Voet, A., 1937. Quantitative Lyotropy. *Chem. Rev.*, **20**:169–179.

Walker, J.S. and C.A. Vause, 1983. Lattice Theory of Binary Fluid Mixtures: Phase Diagrams with Upper and Lower Critical Solution Points From a Renormalization-Group Calculation. *J. Chem. Phys.*, **79**:2660–2676.

Walter, H., Brooks, D.E., and D. Fisher, 1985. " Partitioning in Aqueous Two-Phase Systems," (eds), Academic Press, New York.

Wei, D.Q., and L. Blum, 1987. The Mean Spherical Approximation for an Arbitrary Mixture of Ions in a Dipolar Solvent: Approximate Solution, Pair Correlation Functions, and Thermodynamics *J. Chem. Phys.*, **87**:2999–3007.

Wheeler, J.C., 1975. "Exactly Soluble" Two Component Lattice Solution With Upper and Lower Critical Solution Temperatures. *J. Chem. Phys.* **62**:433–439.

Wood, S.E., and R. Battino, 1990. "Thermodynamics of Chemical Systems," Cambridge University Press, New York.

Zaslavsky, B.Y., Miheeva, L.M., Aleschko-Ozhevskii, Y.P., Mahmudov, A.U., Bagirov, T.O., and E.S. Garaev, 1988. Distribution of Inorganic Salts Between the Coexisting Phases of Aqueous Polymer Two-Phase Systems *J. Chromatogr.*, **439**:267–281.

Zaslavsky, B.Y., Bagirov, T.O., Borovskaya, A.A., Gulaeva, N.D., Miheeva, L.H., Mahmudov, A.V., and M.N. Rodnikova, 1989. Structure of Water as a Key Factor of Phase Separation in Aqueous Mixtures of Two Nonionic Polymers. *Polymer*, **30**:2104–2111.

Zemaitis, Jr., J.F., Clark, D.M., Rafal, M., and N.C. Scrivner, 1986. "Handbook of Aqueous Electrolyte Thermodynamics," DIPPR, AIChE Publications, New York.

Zhou, Y., Stell, G., and H.L. Friedman, 1988. Note on Standard Free Energy of Transfer and Partitioning of Ionic Species Between Two Fluid Phases. *J. Chem. Phys.*, **89**:3836–3839.

Appendix A

Evaluation of $\chi_{12}(T)$ parameters

Once a value for r for a system is determined, it is possible to evaluate the values of temperature independent parameters of the function $\chi_{12}(T)$. Two of these parameters are determined from the critical consolute temperatures. The other parameters are chosen to best represent experimental data. The four models described in Chapter 2 will be examined in order of increasing complexity.

In the simplest case, that of the Goldstein model of equation (2.46), there are three parameters, β, γ and σ. For a given system γ and σ are determined from the critical consolute temperatures. First, the value of χ_{12} at the critical points, χ_{12}^c, is calculated using r. This is possible since the criticality conditions of equations (2.16-17) yield the following equation, which is valid at the upper and lower critical consolute temperatures (Hill, 1960)

$$\chi_{12}^c = \frac{(1+\sqrt{r})^2}{2r} \tag{A.1}$$

The equation above gives the numerical value of χ_{12} at T_{cu} and T_{cl}. At these critical

temperatures equation (2.46) also holds, i.e.

$$\frac{\chi_{12}^c}{z} = \frac{\beta}{T_{cu}} - \ln\left[1 + \exp(\frac{\gamma}{T_{cu}} + \sigma)\right] \tag{A.2}$$

and

$$\frac{\chi_{12}^c}{z} = \frac{\beta}{T_{cl}} - \ln\left[1 + \exp(\frac{\gamma}{T_{cl}} + \sigma)\right] \tag{A.3}$$

Equating the latter two expressions, eliminating σ, and solving for γ yields

$$\gamma = \frac{T_{cu}T_{cl}}{T_{cl} - T_{cu}} \ln\left[\frac{\exp(\beta/T_{cu} - \chi_{12}^c/z) - 1}{\exp(\beta/T_{cl} - \chi_{12}^c/z) - 1}\right] \tag{A.4}$$

Hence if the value of β is known, γ can be calculated from the critical temperatures. Once γ is determined, equation (A.2) or (A.3) can be used to calculate σ.

The procedure followed for the one-bond model is similar to that above, except that the value of two parameters, α and β, must be known before γ can be calculated from

$$\gamma = \frac{T_{cu}T_{cl}}{T_{cl} - T_{cu}} \ln\left[\frac{\exp(\alpha + \beta/T_{cu} - \chi_{12}^c/z) - 1}{\exp(\alpha + \beta/T_{cl} - \chi_{12}^c/z) - 1}\right] \tag{A.5}$$

Equation (2.45) is applied at either of the critical temperatures, in a manner similar to (A.2) or (A.3), and used to calculate σ. For the two-bond model, the most convenient approach is to estimate the values of γ, σ, ζ and λ and then to calculate α and β from the following relations:

$$\beta = \frac{T_{cu} - T_{cl}}{T_{cu} - T_{cl}} \ln\left[\frac{1.0 + \exp(\sigma + \gamma/T_{cl}) + \exp(\lambda + \zeta/T_{cl})}{1.0 + \exp(\sigma + \gamma/T_{cu}) + \exp(\lambda + \zeta/T_{cu})}\right] \tag{A.6}$$

and

$$\alpha = \frac{\chi_{12}^c}{z} - \frac{\beta}{T_{cu}} + \ln\left[1 + \exp(\frac{\gamma}{T_{cu}} + \sigma) + \exp(\frac{\zeta}{T_{cu}} + \lambda)\right] \tag{A.7}$$

The parameters in the above models are chosen to reproduce experimental liquid-liquid equilibria data from co-existing weight or mole fractions at a series of temperatures. The concentrations are converted to volume fractions using r determined in the manner described in Chapter 2. Trial and error is used to select values best representing observed compositions. For example, with the one bond model, for each guess of α and β, the above procedure is used to calculate γ and σ. These parameters are used in equations (2.38) and (2.45–46) to determine the value of $\chi_{12}(T)$ for each temperature between the upper and lower critical consolute temperatures for which there are experimental data on co-existing concentrations. At each temperature, the value of $\chi_{12}(T)$ is substituted into equations (2.14) and (2.15) and these two equations are solved simultaneously to give the compositions of the two coexisting phases.

This procedure is repeated for all temperatures for which experimental data are available. The calculated and experimental compositions are compared and another trial, using different values of α and β, is made. Suitable values of α and β should minimize the following objective function (2.54)

The coefficients in the polynomial expression for $\chi_{12}(T)$, equation (2.47), are determined as follows: For each temperature, the concentrations, converted to volume fractions, are used in equations (2.26) and (2.27) to calculate $\chi_{12}^1(T)$ and $\chi_{12}^2(T)$; The mean of these two values, $\overline{\chi_{12}}(T)$, is correlated to T using a polynomial. The two critical temperatures are used to determine the parameters a_0 and a_1 while the other four are chosen to best fit experimental data. For a given guess of a_2, a_3, a_4

and a_5, the parameter a_1 is calculated from the equation:

$$a_1 = \sum_{i=2}^{5} a_i \left(\frac{T_{cu}^i - T_{cl}^i}{T_{cl} - T_{cu}} \right) \tag{A.8}$$

following which a_0 is obtained as

$$a_0 = \chi_{12}^c - \sum_{i=1}^{5} a_i T_{cu}^i \tag{A.9}$$

For a fifth order polynomial, values of a_2, a_3, a_4 and a_5 are chosen to minimize an objective function over N_E experimental points

$$F_o = \sum_{j=1}^{N_E} | y_j^e - y_j^c | \tag{A.10}$$

with

$$y_j^e = (\overline{\chi_{12}}(T) - a_0 - a_1 T)/T^2 \tag{A.11}$$

and

$$y_j^c = a_2 + a_3 T + a_4 T^2 + a_5 T^3 \tag{A.12}$$

For lower order polynomials the procedure is identical except there are fewer adjustable parameters.

Finally, for systems with only a LCT or UCT curve, each of the models has one additional parameter. In these cases, one of the critical point relations, (A.2) or (A.3), depending on the type of system, is used to calculate one of the parameters in $\chi_{12}(T)$. An example is the use of the one-bond model for a system with an UCT curve. For each estimate of the parameters β, γ, and σ, equation (2.45), applied at

T_{cu}, is used to calculate α. The optimal values of β, γ and σ minimize the objective function of equation (2.54).

Appendix B

Values of $\chi_{12}(T)$ parameters

The following tables present parameters of $\chi_{12}(T)$ determined by minimizing objective function (2.54). The contents are:

- Table B.1: Temperature independent parameters for the one-bond model.
- Table B.2: Temperature independent parameters for the two-bond model.
- Table B.3: Temperature independent parameters for the polynomial $\chi_{12}(T)$.
- Table B.4: Performance of different models — comparison of values of F_o as given by equation (2.54).

Table B.1: Temperature independent parameters for the one-bond model

System	α	β x 10^{-3}
PEG 2 290	-3.129	3.278
PEG 2 270	-3.127	3.323
PEG 2 180	-3.130	3.211
1-Aza Cycloheptane	-3.700	3.207
i-Butoxyethanol	-3.119	2.397
n-Butoxyethanol	-3.753	2.566
2,6-Dimethyl pyridine	-3.708	2.882
2-Methylpiperidine	-3.075	2.819
3-Methylpiperidine	-3.083	2.878
4-Methylpiperidine	-3.522	2.914
Nicotine	-3.924	3.248
1-Propoxy-2-propanol	-3.736	2.832
2-Propoxy-1-propanol	-3.720	2.806
Tetrahydrofuran	-3.675	2.781

Table B.2: Temperature independent parameters for the two-bond model

System	σ	γ x 10^{-3}	λ	ζ x 10^{-3}
PEG 2 290	-3.412	0.37762	1.187	-1.24655
PEG 2 270	-5.036	-1.36946	0.956	-1.36877
PEG 2 180	-0.371	-1.35690	1.191	-1.38009
1-Aza Cycloheptane	-0.156	-1.28942	1.061	-1.34567
i-Butoxyethanol	1.388	-1.77860	1.366	-1.41553
n-Butoxyethanol	1.804	-1.49597	1.356	-1.27110
2,6-Dimethyl pyridine	5.466	-3.70099	3.454	-4.07752
2-Methylpiperidine	2.844	-3.08769	2.102	-2.46870
3-Methylpiperidine	2.809	-3.08758	2.102	-2.46870
4-Methylpiperidine	3.634	-2.97380	3.615	-4.07740
Nicotine	-0.899	0.56417	1.709	-1.18945
1-Propoxy-2-propanol	-4.075	0.43001	3.377	-0.92951
2-Propoxy-1-propanol	-2.621	0.32599	2.805	-0.92999
Tetrahydrofuran	-0.965	0.42539	3.377	-0.92949

Table B.3: Temperature independent parameters for polynomial $\chi_{12}(T)$

System	$a_2 \times 10^{-5}$	$a_3 \times 10^{-5}$	$a_4 \times 10^{-5}$	$a_5 \times 10^{-4}$
PEG 2 290	1.52729383	-0.457866914	0.626955160	-3.25685740
PEG 2 270	1.52749170	-0.457870000	0.626956346	-3.25690164
PEG 2 180	1.52617208	-0.457902926	0.626956998	-3.25690000
1-Aza Cycloheptane	-6.43900923	1.513416185	-1.769839190	8.23481916
i-Butoxyethanol	-9.51396341	2.534245117	-3.357510152	17.69031060
n-Butoxyethanol	-17.72386878	4.689669998	-6.187410000	32.55010000
2,6-Dimethyl pyridine	-3.63399094	0.932321130	-0.119208520	6.06984654
2-Methylpiperidine	-12.67431485	2.914178905	-3.334140824	15.18249918
3-Methylpiperidine	-4.29366426	1.015312291	-1.193972407	5.58248060
4-Methylpiperidine	-5.99608798	1.322663359	-1.439946648	6.16779337
Nicotine	-0.99042771	0.218957072	-0.241611757	1.06064679
1-Propoxy-2-propanol	-3.69875618	0.933515331	-1.171622886	5.84374912
2-Propoxy-1-propanol	10.15741990	2.616534150	-3.355899350	17.13874183
Tetrahydrofuran	-9.62016800	2.537343688	-3.353599557	17.75143759

Table B.4: Performance of different models — comparison of values of F_o as given by equation (2.54)

Aqueous solutions of	Goldstein	One-bond	Two-bond	Polynomial
PEG 2 290	0.0417	0.0158	0.0161	0.0088
PEG 2 270	0.0264	0.0205	0.0143	0.0129
PEG 2 180	0.0361	0.0135	0.0135	0.0121
1-Aza Cycloheptane	0.1309	0.0564	0.0752	0.0603
i-Butoxyethanol	0.1402	0.0407	0.0394	0.0428
n-Butoxyethanol	0.1510	0.0311	0.0263	0.0154
2,6-Dimethyl pyridine	0.0993	0.0284	0.0279	0.0314
2-Methylpiperidine	0.1898	0.1161	0.1206	0.1197
3-Methylpiperidine	0.1354	0.0749	0.0760	0.0843
4-Methylpiperidine	0.1365	0.0800	0.0783	0.0779
Nicotine	0.1518	0.0407	0.0400	0.0361
1-Propoxy-2-propanol	0.1247	0.0527	0.0416	0.0249
2-Propoxy-1-propanol	0.1335	0.0428	0.0377	0.0167
Tetrahydrofuran	0.1347	0.0427	0.0313	0.0359
C_8-Lecithin	0.0499	0.0219	0.0242	0.0156

Appendix C

Materials and calibration

This appendix presents information on materials and calibration methods used in some of the experiments. The contents are:

- Table C.1: suppliers of compounds used in experiments.
- Table C.2: refractive index calibration data for 1-propanol–NaCl–water.
- Figure C.1: refractive index calibration plot for PEG 8000–NaCl–water.
- Table C.3: refractive index data for PEG 8000–NaCl–water.
- Figure C.2: refractive index calibration plot for PPG 425–NaCl–water.
- Figure C.3: refractive index calibration plot for PPG 725–NaCl–water.

Table C.1: Suppliers of materials used in experiments

Compound	**Supplier**
n-Dodecylammonium chloride (> 99% wt)	Aldrich Chemical Company Milwaukee, Wisconsin
Poly(ethylene glycol) (molecular weight 8000)	Sigma Chemical Company St Louis, Missouri
Poly(ethylene glycol) (molecular weight 425, 725)	Aldrich Chemical Company Milwaukee, Wisconsin
1-propanol	American Chemicals Ltd Montreal, Quebec
sodium chloride	Anachemia Montreal, Quebec

Table C.2: Refractive index data for 1-propanol–NaCl–water at 298 K

No salt		2.5% NaCl		5% NaCl		7.5% NaCl		10% NaCl	
C_p*	RI	C_p	RI	C_p	RI	C_p	RI	C_p	RI
0.0	1.3325	0.0	1.3361	0.0	1.3404	0.0	1.3451	0.0	1.3490
10.0	1.3410	10.0	1.3447	8.0	1.3475	5.0	1.3497	3.0	1.3520
20.0	1.3493	20.0	1.3531	16.0	1.3549	10.0	1.3540	6.0	1.3545
30.0	1.3555	30.0	1.3591	24.0	1.3600	15.0	1.3579	9.0	1.3574
40.0	1.3610	40.0	1.3647	32.0	1.3642	20.0	1.3611	12.0	1.3599
50.0	1.3679	50.0	1.3698	36.0	1.3668	22.0	1.3624	15.0	1.3620
12.5% NaCl		15% NaCl		17.5% NaCl		20% NaCl		22.5% NaCl	
C_p	RI	C_p	RI	C_p	RI	C_p	RI	C_p	RI
0.0	1.3536	0.0	1.3580	0.0	1.3628	0	1.3673	0.0	1.3720
2.0	1.3557	2.0	1.3600	1.5	1.3641	1.0	1.3683	1.0	1.3730
4.0	1.3572	4.0	1.3618	3.0	1.3655	2.0	1.3692	2.0	1.3740
6.0	1.3595	6.0	1.3635	4.5	1.3670	3.0	1.3702	3.0	1.3749
8.0	1.3611	8.0	1.3654	6.0	1.3682	4.0	1.3712	4.0	1.3758
10.0	1.3628			6.5	1.3688	5.0	1.3720		

* C_p is the concentration of 1-propanol in percent weight

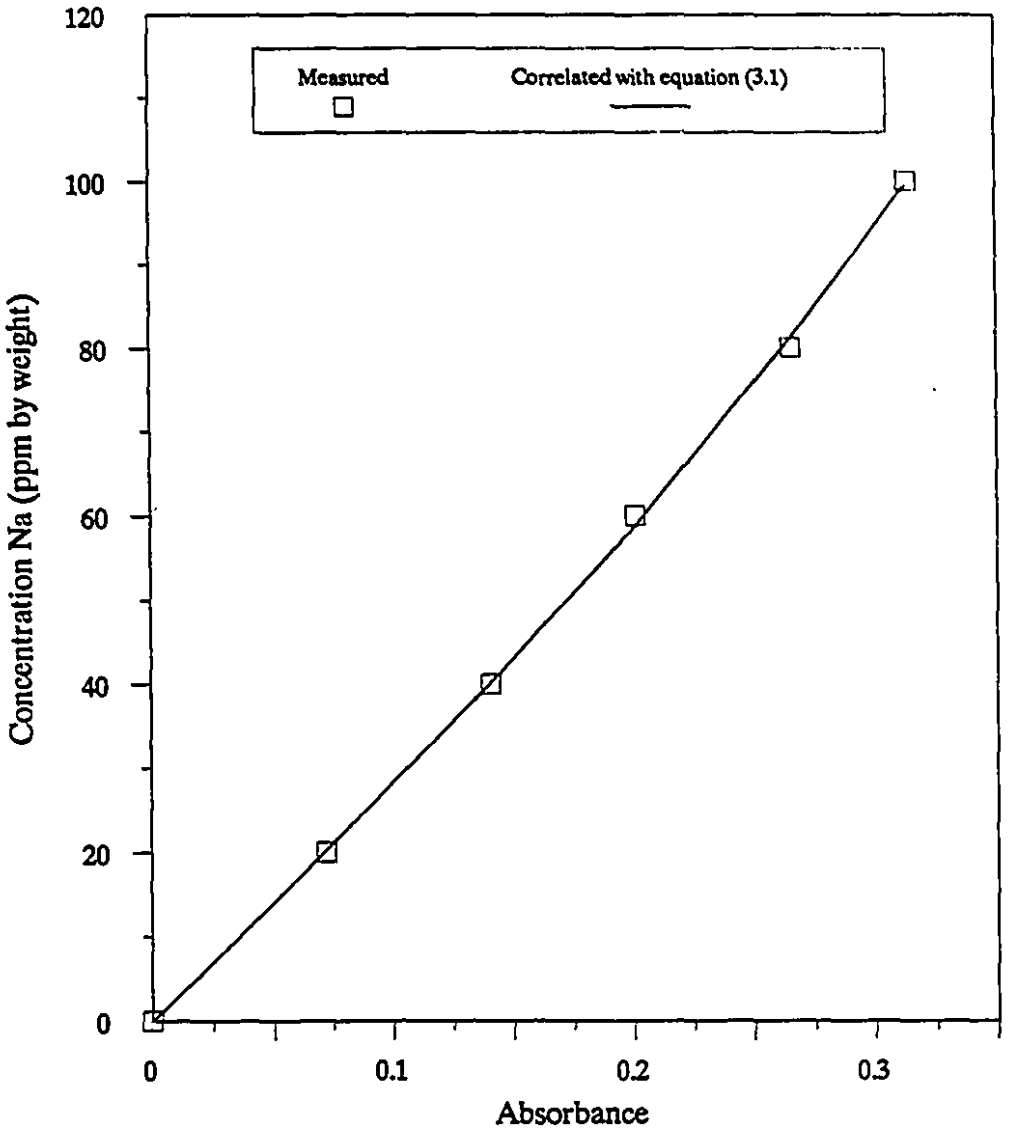

Figure C.1: Representative calibration plot for atomic absorption spectroscopy analysis of sodium

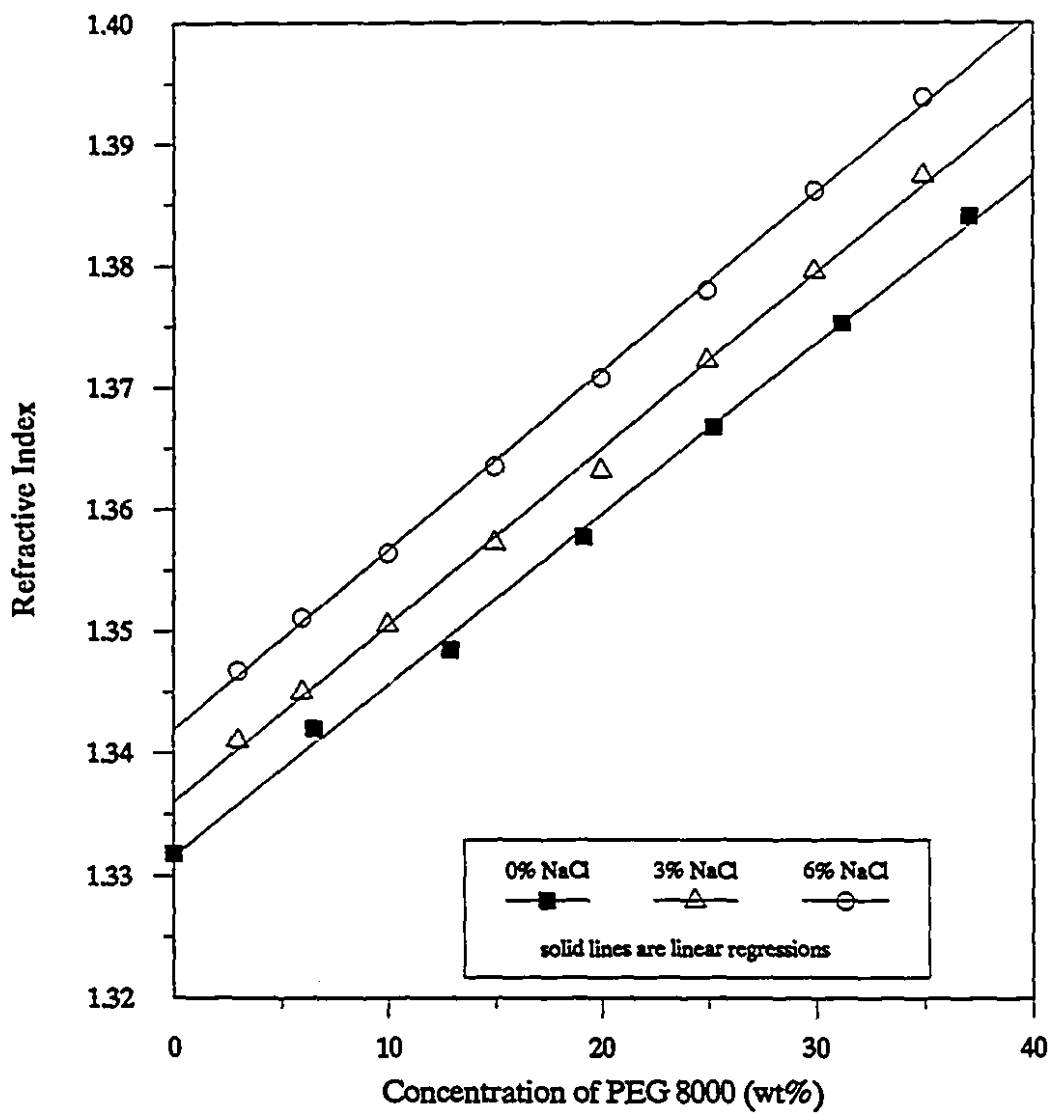

Figure C.2: Refractive index calibration plot for PEG 8000–NaCl–water at 298 K

Table C.3: Refractive index data for PEG 8000–NaCl–water at 298 K

No salt		3% NaCl		6% NaCl	
C_p*	RI	C_p	RI	C_p	RI
0.0	1.3318	3	1.3410	3	1.3468
6.5	1.3420	6	1.3450	6	1.3511
12.9	1.3485	10	1.3505	10	1.3564
19.2	1.3577	15	1.3572	15	1.3635
25.3	1.3667	20	1.3632	20	1.3708
31.3	1.3753	25	1.3722	25	1.3780
37.1	1.3841	30	1.3796	30	1.3862
42.9	1.3954	35	1.3874	35	1.3939
48.4	1.4033				
53.9	1.4135				
59.3	1.4212				

* C_p is the concentration of PEG in percent weight

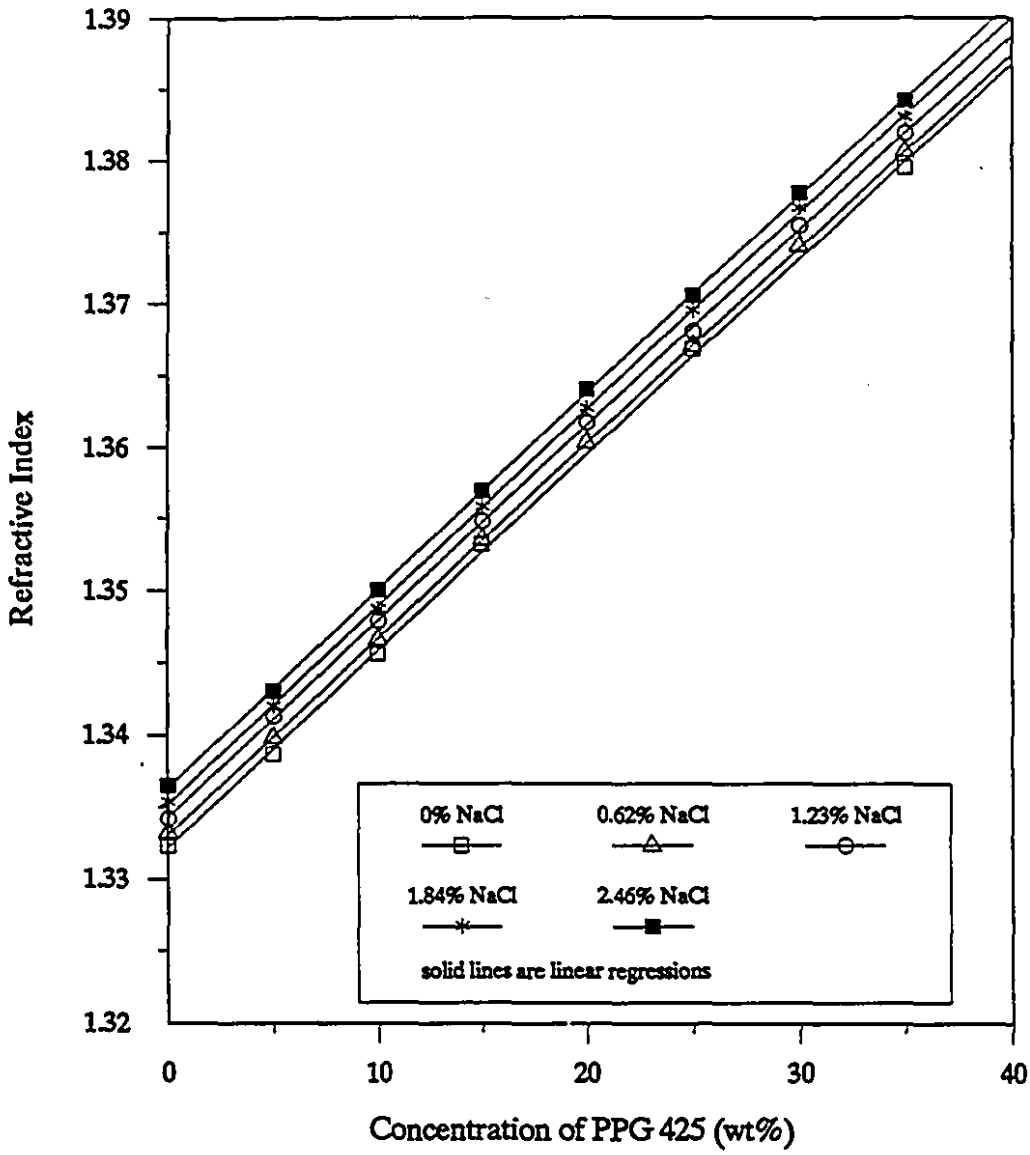

Figure C.3: Refractive index calibration plot for PPG 425–NaCl–water

Table C.4: Refractive index data for PPG 425–NaCl–water at 298 K

No salt		0.62% NaCl		1.23% NaCl		1.84% NaCl		2.46% NaCl	
C_p*	RI	C_p	RI	C_p	RI	C_p	RI	C_p	RI
0	1.3323	0	1.3332	0	1.3342	0	1.3354	0	1.3365
5	1.3387	5	1.3398	5	1.3413	5	1.3420	5	1.3430
10	1.3456	10	1.3466	10	1.3479	10	1.3487	10	1.3500
15	1.3532	15	1.3535	15	1.3548	15	1.3558	15	1.3569
25	1.3668	20	1.3603	20	1.3617	20	1.3627	20	1.3640
35	1.3795	25	1.3670	25	1.3680	25	1.3695	25	1.3705
40	1.3868	30	1.3740	30	1.3754	30	1.3767	30	1.3777
45	1.3930	35	1.3806	35	1.3819	35	1.3830	35	1.3842
50	1.3995								
55	1.4057								
60	1.4111								
65	1.4163								
70	1.4216								
75	1.4275								
80	1.4322								
85	1.4353								
90	1.4405								
95	1.4436								
100	1.4456								

* C_p is the concentration of PPG 425 in percent weight

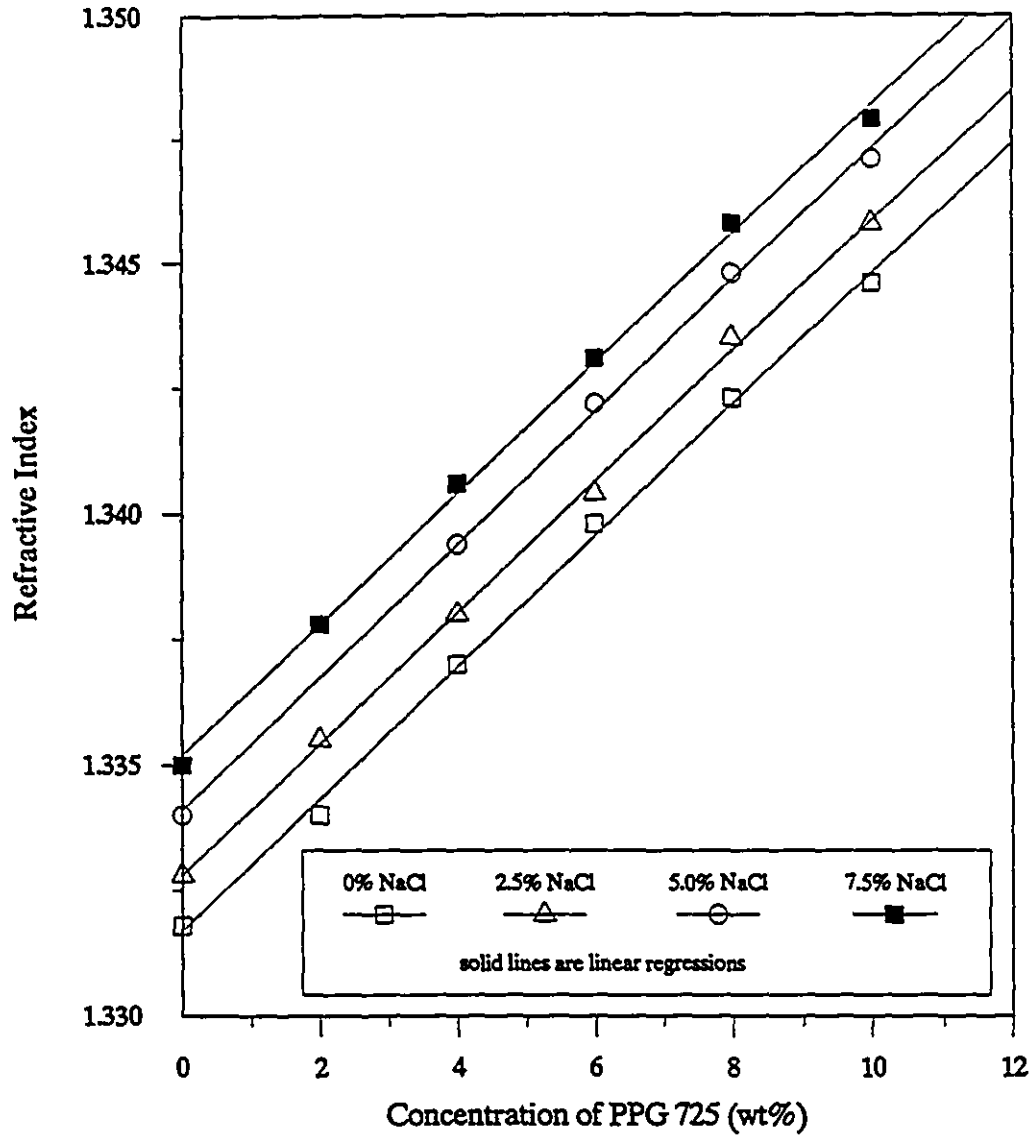

Figure C.4: Refractive index calibration plot for PPG 725–NaCl–water at 298 K

Table C.5: Refractive index data for PPG 725–NaCl–water at 298 K

No salt		2.5% NaCl		5.0% NaCl		7.5%NaCl	
C_p*	RI	C_p	RI	C_p	RI	C_p	RI
0	1.3318	0	1.3328	0	1.3350	0	1.3340
2	1.3340	2	1.3355	2	1.3378	4	1.3394
4	1.3370	4	1.3380	4	1.3406	6	1.3422
6	1.3398	6	1.3404	6	1.3431	8	1.3448
8	1.3423	8	1.3435	8	1.3458	10	1.3471
10	1.3446	10	1.3458	10	1.3479		

* C_p is the concentration of PPG 725 in percent weight

Appendix D

Experimental results

This appendix contains tabulations of experimentally determined compositions for the binodal curves and tie-lines. The contents are:

- Table D.1: Results of turbidity titrations for the binodal curve of 1-propanol–NaCl–water at 298 K.
- Table D.2: Results of tie-line experiments for 1-propanol–NaCl–water at 298 K.
- Table D.3: Results of turbidity titrations for the plait point of 1-propanol–NaCl–water at 298 K.
- Table D.4: Results of tie-line experiments for *n*-dodecylammonium chloride–NaCl–water at 303 K.
- Table D.5: Results of tie-line experiments for poly(ethylene glycol) 8000–NaCl–water at 333 K.
- Table D.6: Results of tie-line experiments for poly(propylene glycol) 425–NaCl–water at 278 K.

- Table D.7: Results of tie-line experiments for poly(propylene glycol) 425-NaCl–water at 298 K.
- Table D.8: Results of tie-line experiments for poly(propylene glycol) 425-NaCl–water at 333 K.
- Table D.9: Results of tie-line experiments for poly(propylene glycol) 725-NaCl–water at 278 K.
- Table D.10: Results of tie-line experiments for poly(propylene glycol) 725-NaCl–water at 298 K.

Table D.1: Results of turbidity titration for 1-propanol–NaCl–water at 298 K

Two–liquid phase region					
wt% propanol	wt% NaCl	wt% propanol	wt% NaCl	wt% propanol	wt% NaCl
6.2	18.3	23.2	7.4	43.7	4.4
6.7	17.7	26.1	6.8	49.7	3.5
8.0	15.6	26.9	6.9	59.4	2.6
10.1	13.0	28.4	6.3	63.8	2.2
12.2	11.7	31.7	6.1	69.6	1.7
18.3	8.7	35.7	5.4	81.0	1.2
18.3	8.8	39.7	4.8		
Two–liquid and solid boundary					
wt% propanol	wt% NaCl	wt% propanol	wt% NaCl	wt% propanol	wt% NaCl
11.3	21.6	40.4	13.5	55.3	9.4
24.8	18.0	45.0	12.3	58.1	8.4
29.5	16.6	48.9	11.2	69.3	5.5
35.1	15.0	52.3	10.2		
Single–liquid and solid boundary					
wt% propanol	wt% NaCl	wt% propanol	wt% NaCl	wt% propanol	wt% NaCl
0.0	26.5*	90.0	0.7	96.8	0.2
84.7	1.2	91.8	0.5	98.0	0.2
86.4	1.0	93.7	0.4	99.3	0.2†
88.2	0.9	95.6	0.2		

* solubility of NaCl in water

† solubility of NaCl in reagent propanol

Table D.2: Tie-line data for 1-propanol–NaCl–water at 298 K

Feed		Top phase		Bottom Phase	
wt% propanol	wt% NaCl	wt% propanol	wt% NaCl	wt% propanol	wt% NaCl
30.0	7.0	60.6	2.60	17.3	9.1
30.0	8.0	70.5	2.10	13.1	11.2
30.0	10.0	75.6	1.55	10.3	14.6
30.0	12.0	80.9	1.28	5.2	18.1
30.0	14.0	83.7	1.10	2.4	21.6
30.0	16.0	85.4	0.93	2.3	23.8

Table D.3: Results of turbidity titration for the plait point of 1-propanol–NaCl–water at 298 K

Single phase region		Two-phase region		Volumes		
wt% propanol	wt% NaCl	wt% propanol	wt% NaCl	V_{top} (ml)	V_{bot} (ml)	$100*V_{bot}/V_{top}$
32.28	5.88	32.25	5.90	108.0	54.3	66.5
32.87	5.78	32.85	5.80	106.0	53.7	66.4
33.46	5.69	33.43	5.70	135.0	22.2	85.9
34.04	5.61	33.99	5.64	103.0	51.9	66.5
34.55	5.58	34.53	5.59	87.0	65.7	57.0
35.08	5.46	35.03	5.49	82.5	68.3	54.7
35.81	5.24	35.66	5.32	75.0	73.5	50.5
36.22	5.19	36.07	5.28	69.0	78.0	46.9
36.52	5.22	36.48	5.23	63.0	82.5	43.3
37.41	5.02	37.24	5.10	54.5	88.4	38.1
37.88	4.97	37.72	5.06	54.0	87.3	38.2
38.21	4.99	38.17	5.01	41.0	98.8	29.3
39.04	4.85	38.97	4.89	20.5	116.8	14.9
39.72	4.80	39.68	4.82	14.0	121.1	10.4
40.31	4.70	40.27	4.72	0.1	133.3	0.1
40.91	4.61	40.83	4.65	6.0	125.8	4.6
41.40	4.57	41.36	4.59	5.0	125.3	3.8
42.04	4.47	41.95	4.51	12.0	116.7	9.3
42.60	4.40	42.52	4.44	14.0	113.2	11.0
43.41	4.23	43.19	4.34	1.0	124.5	0.8
44.21	4.18	43.98	4.29	13.5	110.0	10.9
44.84	4.11	44.60	4.22	10.0	112.0	8.2
45.48	4.04	45.24	4.15	11.5	109.0	9.5
46.15	3.97	45.90	4.08	12.0	107.0	10.1
46.83	3.89	46.58	4.00	12.0	105.5	10.2
48.50	3.74	47.50	3.94	8.0	107.5	6.9
50.23	3.00					

Table D.4: Tie-line data for *n*-dodecylammonium chloride–NaCl–water at 303 K

Feed		Top phase		Bottom Phase	
surfactant [M]	NaCl [M]	surfactant [M]	NaCl [M]	surfactant [M]	NaCl [M]
0.15	0.405	0.242	0.255	0.01	0.309
0.15	0.335	0.302	0.277	0.009	0.340
0.15	0.315	0.331	0.284	0.004	0.445
0.15	0.275	0.460	0.323	0.003	0.371

Table D.5: Tie-line data for poly(ethylene glycol) 8000–NaCl–water at 333 K

Feed		Top phase		Bottom Phase	
wt% PEG	wt% NaCl	wt% PEG	wt% NaCl	wt% PEG	wt% NaCl
13.5	15.0	19.4	13.4	1.1	19.0
13.5	15.0	20.0	13.1	1.9	18.4
12.5	17.0	26.3	12.5	0.5	20.5
9.0	22	36.2	11.7	0.1	24.9
7.5	23.0	39.9	11.4	0.05	25.8
—	—	43.4	11.8	0.01	26.9

Table D.6: Tie-line data for poly(propylene glycol) 425 at 278 K

Feed		**Bottom phase**		**Top Phase**	
wt% NaCl	wt% PPG 425	wt% NaCl	wt% PPG 425	wt% NaCl	wt% PPG 425
7.1	42.2	8.6	16.4	1.5	75.3
8.4	42.3	10.9	12.7	1.5	79.5
9.4	41.3	12.3	10.4	0.8	82.6
10.5	40.9	15.9	7.0	0.8	83.8
11.5	39.6	18.5	4.9	0.9	83.9
10.8	34.2	21.6	2.9	0.8	84.6
13.6	39.7	24.0	1.2	0.9	84.7
14.6	38.9	24.7	1.4	0.9	86.2
—	—	24.7*	1.4	0.9	86.3
—	—	24.7*	1.4	1.0	86.3
—	—	24.8*	1.3	0.9	86.7

* solid NaCl present

Table D.7: Tie-line data for poly(propylene glycol) 425 at 298 K

Feed		**Bottom Phase**		**Top Phase**	
wt% PPG 425	wt% NaCl	wt% PPG 425	wt% NaCl	wt% PPG 425	wt% NaCl
55.1	2.1	41.2	2.7	65.1	0.9
54.4	2.3	34.0	3.8	68.7	0.7
54.0	2.5	29.1	4.8	70.9	0.5
40.5	4.7	23.4	6.4	74.3	0.5
38.6	5.6	21.5	6.8	76.1	0.4
37.0	6.5	16.8	8.4	78.8	0.4
35.4	7.2	13.7	9.8	80.5	0.4
34.0	7.9	10.2	11.5	81.6	0.3
32.7	8.6	8.5	12.5	82.8	0.3
47.0	7.6	4.8	16.1	83.6	0.3
45.9	8.0	4.0	17.2	84.5	0.3
44.4	9.6	3.0	18.9	85.0	0.3
43.9	10.5	2.8	19.7	86.1	0.3
40.1	13.0	1.9	23.2	87.3	0.3
—	—	1.5	25.6*	89.3	0.4

* solid NaCl present

Table D.8: Tie-line data for poly(propylene glycol) 425 at 333 K

Feed		**Top phase**		**Bottom Phase**	
wt% PPG 425	wt% NaCl	wt% PPG 425	wt% NaCl	wt% PPG 425	wt% NaCl
40.4	3.1	81.07	0.06	6.53	5.26
40.6	2.4	81.90	0.05	6.61	4.75
40.4	5.1	82.70	0.07	4.16	8.62
39.9	7.0	83.55	0.08	3.30	11.32
39.5	4.0	84.30	0.07	4.30	6.87
39.9	6.0	84.55	0.08	2.36	10.30
39.9	8.0	86.01	0.09	1.81	13.89
39.9	8.9	86.48	0.11	0.28	16.20
40.1	11.1	86.55	0.11	0.44	19.70
40.2	13.0	88.18	0.12	0.79	22.60
39.9	14.0	89.41	0.13	0.63	23.91
39.3	14.9	91.79	0.14	0.01	26.08
—	—	88.25	0.18	0.21	26.99*
—	—	89.45	0.17	0.07	26.89*

* solid NaCl present

Table D.9: Tie-line data for poly(propylene glycol) 725 at 278 K

Feed		**Top phase**		**Bottom Phase**	
wt% PPG 725	wt% NaCl	wt% PPG 725	wt% NaCl	wt% PPG 725	wt% NaCl
50.0	1.0	87.29	0.91	21.55	1.98
50.0	1.0	89.10	1.31	11.32	5.29
48.0	2.0	90.33	1.04	3.41	9.26
47.0	2.5	91.66	0.84	1.59	12.83
46.0	4.5	93.14	0.82	1.22	15.82
45.0	6.5	93.93	0.72	1.16	22.30
—	—	93.99	0.64	1.36	25.18

Table D.10: Tie-line data for poly(propylene glycol) 725 at 298 K

Feed		Top phase		Bottom Phase	
wt% PPG 725	wt% NaCl	wt% PPG 725	wt% NaCl	wt% PPG 725	wt% NaCl
52.0	2.0	87.53	0.13	19.31	0.75
50.0	3.0	87.57	0.18	17.75	1.08
47.0	5.0	88.28	0.23	11.31	2.92
44.0	7.5	88.37	0.13	13.04	2.39
41.0	9.0	91.27	0.44	4.43	6.19
36.0	14.0	92.04	0.58	2.84	9.11
-	-	93.44	0.81	0.24	24.73

Appendix E

Reference and standard states in multisolvent systems

This appendix describes composition-dependent reference and standard states for salts in multi-solvent systems. The description involves the use of fugacities since these variables better illustrate the dependence of the standard state properties of the salt on the solvent in the infinitely dilute limit. In a system of the type illustrated in Figure 4.1, the chemical potential of a component i is related to its activity through

$$\mu_i = \mu_i^\theta + RT \ln a_i^\theta \tag{E.1}$$

where the superscript θ indicates the standard state. The fugacity, f_i, is related to the chemical potential through the following relation, valid for a fixed temperature:

$$d\mu_i = RT d \ln f_i \tag{E.2}$$

Integration of the expression above, at a fixed temperature, yields

$$\mu_i - \mu_i^\theta = RT \ln f_i - RT \ln f_i^\theta \tag{E.3}$$

where f_i^θ is the fugacity of i when the system is in the standard state for i. Comparison of equations (E.1) and (E.3) shows that the activity of i under given conditions is the ratio of the fugacity of i under those conditions to that in its standard state

$$a_i^\theta = \frac{f_i}{f_i^\theta} \tag{E.4}$$

Binary solutions

For a binary solution of water(1) and a strong electrolyte(2), the activity of the salt is given by equation (4.38):

$$a_2 = m_\pm^\nu \gamma_\pm^\nu \tag{E.5}$$

where $m_\pm$ and $\gamma_\pm$ are the mean ionic molality and activity coefficient, respectively. The fugacity of a salt in an ideal solution ($\gamma_\pm = 1$) is

$$f_2^{id} = m_\pm^\nu f_i^\theta \tag{E.6}$$

Hence on a plot of f_2 versus $m_\pm^\nu$, the fugacity of the salt in an ideal mixture is a straight line which passes through the origin and through the value of the fugacity of the salt at its reference state. If the unsymmetric convention for the normalization of activity coefficients is utilized then the reference state for the salt, at any temperature, is its state at infinite dilution in the solvent. Denoting this reference state by the superscript ∞, the fugacity of the salt in the system in the standard state, from equation (E.6), is given by

$$f_2^\theta = \left(\frac{f_2}{m_\pm^\nu}\right)^\infty \tag{E.7}$$

Thus, in order to evaluate the standard state fugacity of the salt, one has to determine the ratio of the fugacity to the mean ionic molality at infinite dilution. Since both properties tend to zero, the limit, using l'Hôpital's Rule, is the derivative of the f_2 versus $m_{\pm}^{\nu}$ curve at infinite dilution.

$$f_2^{\theta} = \lim_{m_{\pm} \to 0} \left(\frac{f_2}{m_{\pm}^{\nu}} \right) = \left[\frac{df_2}{dm_{\pm}^{\nu}} \right]_{m_{\pm}=0} = k_{2,1}(T,P) \tag{E.8}$$

where $k_{2,1}$ is independent of composition. Hence the standard state fugacity of the salt is the slope of the f_2 versus $m_{\pm}^{\nu}$ curve at $m_{\pm} = 0$. This corresponds to the use of a hypothetical standard state at $m_{\pm} = 1$, as described in Chapter 4. The relationships described above are illustrated in Figure E.1 which shows the fugacity of an electrolyte in real and ideal binary mixtures. From equations (E.4) and (E.5) the fugacity of the salt can be expressed as

$$f_2 = m_{\pm}^{\nu} \gamma_{\pm}^{\nu} k_{2,1}(T,P) \tag{E.9}$$

In order to illustrate the complications arising from the use of a composition-dependent standard state fugacity for a salt in a multi-solvent system, it is simpler to express the composition of the salt in mole fraction. In this situation, the activity of the salt is

$$a_2 = x_2 \gamma_2 \tag{E.10}$$

where x_2 is the mole fraction of the neutral electrolyte and γ_2 is the corresponding mole fraction-based activity coefficient. Use of the unsymmetric convention means

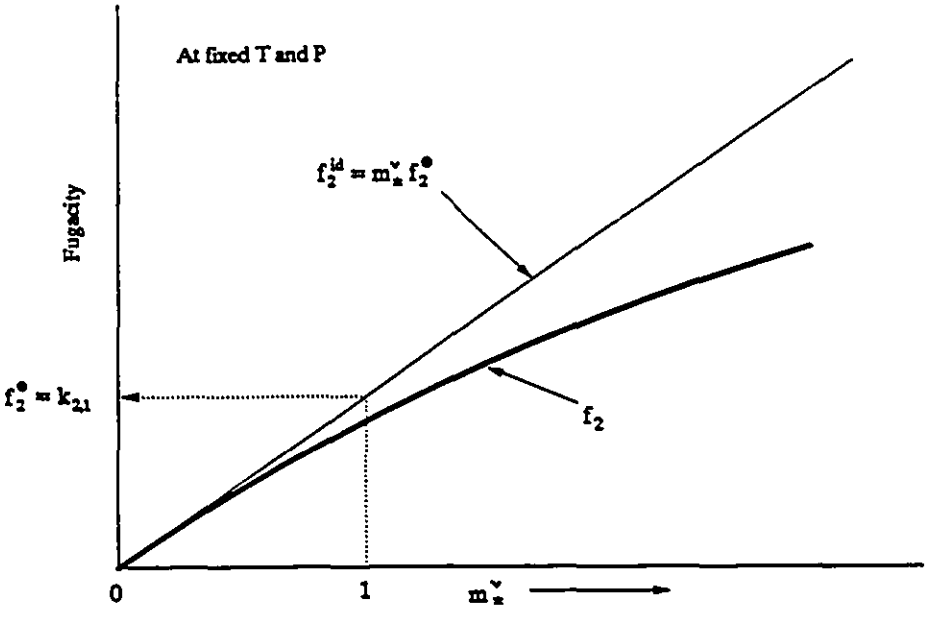

Figure E.1: Fugacity of salt in a binary system using the mean-ionic molality

that the standard state fugacity of the salt, following equation (E.8), is

$$f_2^\theta = \lim_{x_2 \to 0} \left(\frac{f_2}{x_2} \right) = \left[\frac{df_2}{dx_2} \right]_{x_2=0} = H_{2,1}(T, P) \tag{E.11}$$

Hence the standard state of the salt is the slope of the f_2 versus x_2 plot, as illustrated in Figure E.2. This value of f_2^θ corresponds to the fugacity of a hypothetical pure liquid salt at the temperature of the solution and is known as Henry's constant. In a binary system it is independent of the composition of the system. Although the pressure can be fixed arbitrarily, here we use the pressure of the system, P, for simplicity.

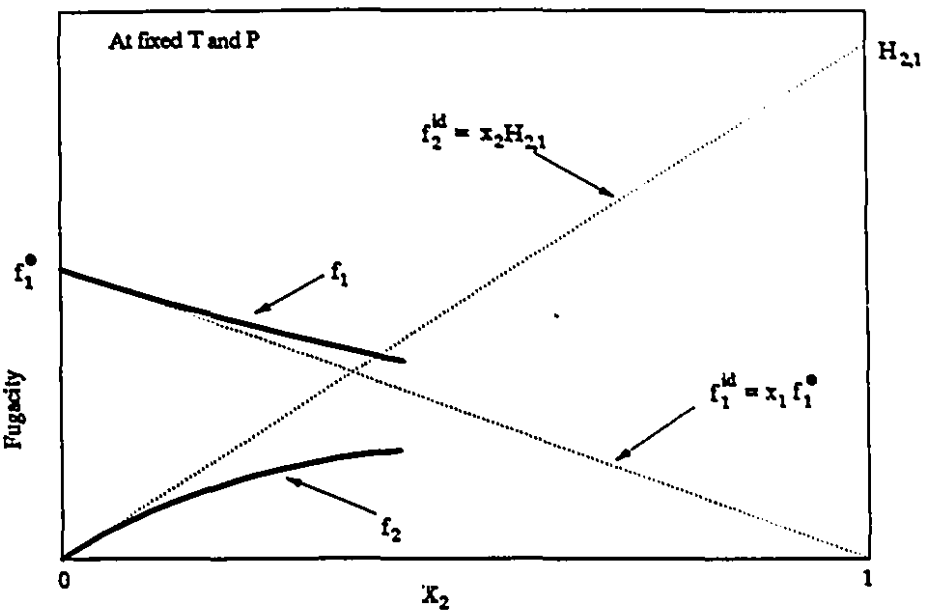

Figure E.2: Fugacities of components in a binary system using mole fractions

Ternary solutions

For a ternary system composed of two solvents(1,2) and a salt(3), the situation is different. Using mole fractions, the activities of all the components are given by the product of their mole fractions and activity coefficients, as in equation (E.10). Here, using the unsymmetric convention, the reference states for the solvents are the pure compounds at the temperature of the system. For the salt, the reference state is the state of the system when infinitely dilute in the salt, at an arbitrarily chosen ratio of the solvents 1 and 2. If only the binary solvent(1)–salt(3) pair is present, $x_2 = 0$ and $x_2/x_1 = 0$, and the standard state fugacity, $H_{3,1}$, following

(E.10), is

$$H_{3,1}(T,P) = \lim_{x_3 \to 0} \left(\frac{f_3}{x_3}\right)_{x_2/x_1=0} = \left[\frac{\partial f_2}{\partial x_2}\right]_{x_3=0,x_2/x_1=0} \tag{E.12}$$

Similarly, if only solvent 2 and the salt are present

$$H_{3,2}(T,P) = \lim_{x_3 \to 0} \left(\frac{f_3}{x_3}\right)_{x_1/x_2=0} = \left[\frac{\partial f_2}{\partial x_2}\right]_{x_3=0,x_1/x_2=0} \tag{E.13}$$

However, if the two solvents are present simultaneously the situation is more complicated.

Following Van Ness and Abbott (1982), a thermodynamic molar property (z) of a ternary system consisting of n_t moles is related to the appropriate partial molar property of one of the components, e.g. component 3, by

$$\overline{z}_3 = z + (1 - x_3)\left(\frac{\partial z}{\partial x_3}\right)_{T,P,r} \tag{E.14}$$

where $\overline{z}_3$ is the partial molar property

$$\overline{z}_3 = \left[\frac{\partial (n_t z)}{\partial n_3}\right]_{T,P,n_1,n_2} \tag{E.15}$$

and the subscript r indicates that the ratio of solvents (1) and (2) is held constant. Hence the partial molar property of the salt, $\overline{z}_3$, may be obtained from a knowledge of the molar property, z, and its partial derivative with respect to mole fraction when the ratio of solvents is held constant.

The logarithm of the fugacity of a solution taken as a whole, $\ln f$, is a thermodynamic property similar to z (Van Ness and Abbot, 1979). For $\ln f$ the appropriate partial molar properties are the logarithms of the ratios of the fugacities of the

individual components to their mole fractions $\ln(f_i/x_i)$, and

$$\ln f = x_1 \ln \frac{f_1}{x_1} + x_2 \ln \frac{f_2}{x_2} + x_3 \ln \frac{f_3}{x_3} \tag{E.16}$$

and from equation (E.4)

$$f_i = x_i \gamma_i f_i^\theta \tag{E.17}$$

Equation (E.16) can be written as

$$\ln f = x_1 \ln \gamma_1 f_1^\theta + x_2 \ln \gamma_2 f_2^\theta + x_3 \ln \gamma_3 f_3^\theta \tag{E.18}$$

The definition of a fugacity deviation function, $\Delta \ln f$, by subtraction of mole fraction-scaled logarithms of the standard state fugacities, and comparison with equation (4.48), shows that

$$\Delta \ln f \equiv \ln f - x_1 \ln f_1^\theta - x_2 \ln f_2^\theta - x_3 \ln f_3^\theta \tag{E.19}$$

$$= x_1 \ln \gamma_1 + x_2 \ln \gamma_2 + x_3 \ln \gamma_3 \tag{E.20}$$

$$= \frac{g^E}{RT} \tag{E.21}$$

where g^E/RT is the dimensionless molar excess Gibbs energy of the solution.

From equations (E.16) and (E.18) it is evident that when the system only contains one of the solvents then

$$\ln f = \ln f_i = \ln f_i^\theta \tag{E.22}$$

where f_i^θ is the pure component standard state fugacity which is a function of T and P only. For the salt, substitution of $\ln f$ for z in equation (E.14) gives

$$\ln \frac{f_3}{x_3} = \ln f + (1 - x_3) \left(\frac{\partial \ln f}{\partial x_3} \right)_{T,P,x_1/x_2} \tag{E.23}$$

which in the limit of $x_3 \to 0$ is

$$\ln H_3(T, P, x_1) = \lim_{x_3 \to 0} \frac{f_3}{x_3} = \ln f_{12} + \left(\frac{\partial \ln f}{\partial x_3} \right)^{\infty}_{T,P,x_1/x_2} \tag{E.24}$$

where f_{12} is the fugacity of the binary solvent system of composition r. The partial derivative term involves the slope of the logarithm of the solution fugacity, $\ln f$, for the system as it becomes infinitely dilute in the salt. Both of the terms on the right hand side of equation (E.24) depend on solvent composition.

The situation is illustrated in Figure (E.3), in which $\ln f$ is plotted as a function of the composition for a ternary two-solvent(1,2), one-salt(3) system. The base of the prism represents the composition of the ternary system in triangular coordinates, in a manner similar to Figure 3.12 for water(1)-propanol(2)-NaCl(3). The vertical axis represents $\ln f$, given by equation (E.16), and the function is plotted using bold curves. Since the salt is of limited solubility in both solvents the fugacities do not extend all the way to the pure-salt vertex of the diagram. The logarithm of the standard state fugacity of the salt in the binary 1-3 mixture, $H_{3,1}$, given through equations (E.16) and (E.12), is shown on the diagram. Similarly, if only solvent (2) is present the logarithm of the standard state fugacity for the salt is $H_{3,2}$. When both solvents are present, a line extending from the pure-salt vertex and intersecting the 1-2 axis of the triangular base indicates the composition of ternary mixtures in which the ratio x_1/x_2 is fixed. The components of the standard state fugacity for the salt, described in equation (E.24), are shown. The $\Delta \ln f$

function for binary solvent pair, and its relation to g^E/RT in the absence of salt is shown. The value of the standard state fugacity for the salt is dependent on the composition of the two solvents and, thus, on the system composition.

It is difficult to determine experimentally and model correctly the variation of Henry's constant, H_3, with solvent composition, hence it is preferable to use a standard state fugacity for the salt which is independent of composition. One approach is to use a particular (fixed) value of H_3^*, corresponding to a fixed solvent composition indicated by the superscript $*$, as the standard state fugacity. If this is done then, for a given T and P, the fugacity of the salt, from equation (E.17), is

$$f_3 = x_3 \gamma_3^* H_3^*(T,P) \tag{E.25}$$

where $\gamma_3^* \rightarrow 1$ only when the concentrations of the solvents tends to some fixed value corresponding to state (x_2^*/x_1^*). The fugacity of the salt can also can be expressed in terms of the activity coefficient γ_3 based on the composition-dependent standard state discussed previously.

$$f_3 = x_3 \gamma_3 H_3(T,P,x_1) \tag{E.26}$$

with $\gamma_3 \rightarrow 1$ as $x_3 \rightarrow 0$, at the concentrations of the solvents in the system. The limit of γ_3^* at infinite dilution in a mixture with solvent concentrations different from those of state $(*)$ can be obtained from equation (E.25):

$$\lim_{x_3 \rightarrow 0} \gamma_3^* = \lim_{x_3 \rightarrow 0} \frac{f_3}{x_3 H_3^*(T,P)} = \lim_{x_3 \rightarrow 0} \left(\frac{f_3}{x_3}\right) \frac{1}{H_3^*(T,P)} \tag{E.27}$$

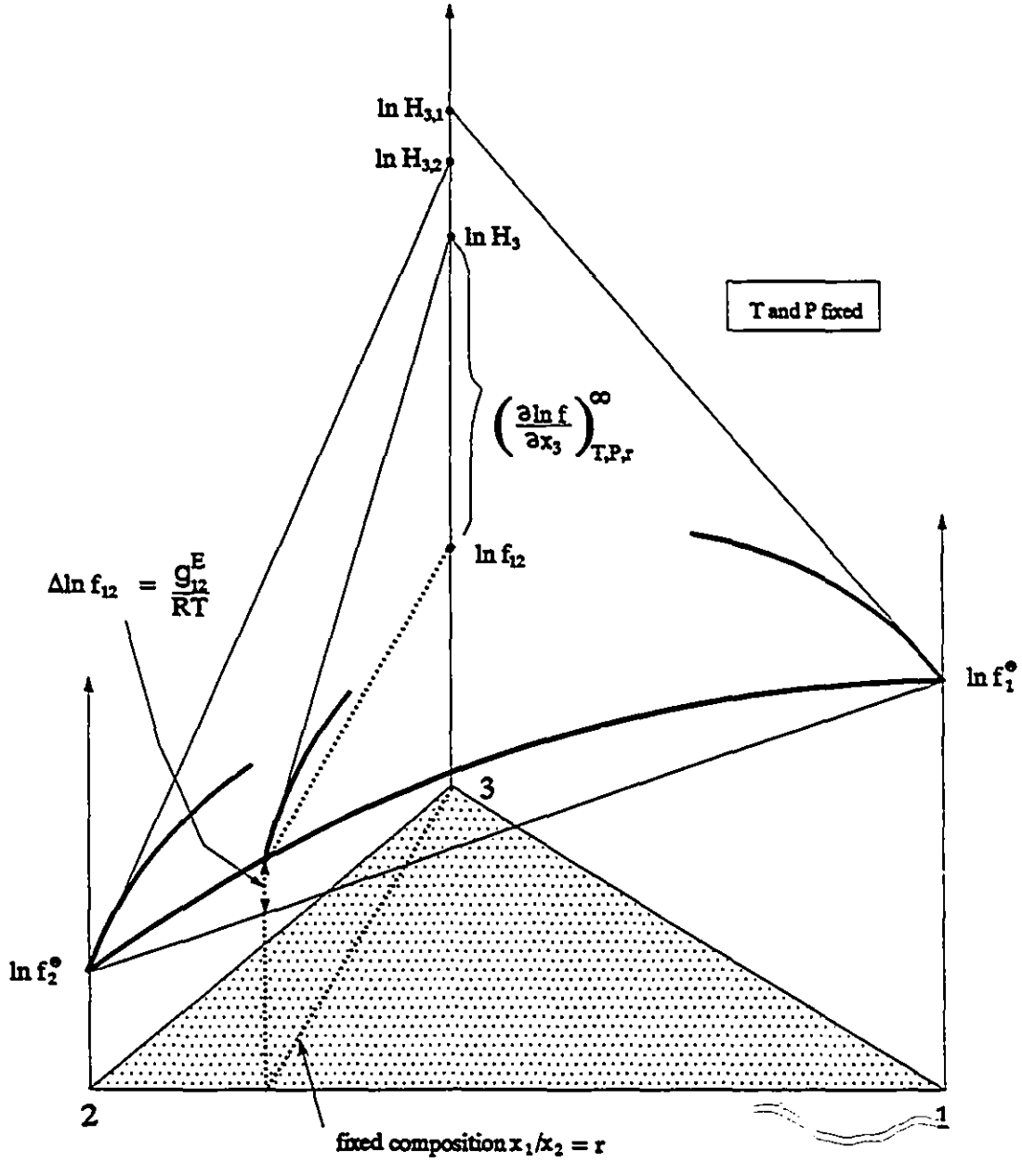

Figure E.3: A plot of $\ln f$ in a ternary two-solvent system (Van Ness and Abbott, 1982)

From equation (E.26), and the normalization of γ_3,

$$\lim_{x_3 \to 0} \left(\frac{f_3}{x_3} \right) = H_3(T, P, x_1) \tag{E.28}$$

and hence

$$\lim_{x_3 \to 0} \gamma_3^* = \frac{H_3(T, P, x_1)}{H_3^*(T, P)} \tag{E.29}$$

The latter equation shows that the limit of the activity coefficient γ_3^* at infinite dilution is unity only if the concentrations of the solvents correspond to those of state (*).

In this study, for multi-solvent systems, an activity coefficient of the type γ_3^*, but based on molalities, is adopted. For this case, the fugacity of salt j in terms of a solvent composition-dependent standard state is

$$f_j = m_{j,\pm}^{\nu} \gamma_{j,\pm}^{\nu} k_j(T, P, \underline{x}) \tag{E.30}$$

while that for the standard state (*) of infinite dilution in solvent 1, water, is

$$f_j = \left[m_{j,\pm} \gamma_{j,\pm}^* \right]^{\nu} k_{j,1}^*(T, P) \tag{E.31}$$

An analysis similar to that for the mole fraction-based activity coefficients shows that for a salt j in the multicomponent system of Figure 4.1

$$\lim_{m_j \to 0} \left[\gamma_{j,\pm}^* \right]^{\nu} = \frac{k_j(T, P, \underline{x})}{k_{j,1}^*(T, P)} \tag{E.32}$$

where $\underline{x}$ are the mole fractions of N_S-1 solvents and k's are the standard state fugacities corresponding to the molality-based activities of equation (E.8). The

solvation energy, or Born energy, term in the activity coefficient models the change in $k_j(T, P, \underline{x})/k^*_{j,1}(T, P)$ with solvent composition $\underline{x}$.

Appendix F

The Born equation

The electrical work, u, required to establish an electric field is calculated from the following expression (Pitzer and Brewer, 1961):

$$u = \int\int \underline{E} \cdot d\underline{\mathcal{D}}\, dV \tag{F.1}$$

where the variable $\underline{E}$ is the 3-dimensional field vector while $\underline{\mathcal{D}}$ is the 3-dimensional electric displacement vector. The volume integration dV is carried out over all space while the field integral $d\underline{\mathcal{D}}$ is performed from zero field to the final state. In a vacuum $\underline{\mathcal{D}}$ is proportional to $\underline{E}$ with the scalar proportionality constant ε_o, the permittivity of free space.

$$\underline{\mathcal{D}} = \varepsilon_o \underline{E} \tag{F.2}$$

In an isotropic medium of dielectric constant ε (equal to Pitzer and Brewer's ϵ/ϵ_o) the vector $\underline{\mathcal{D}}$ is proportional to $\underline{E}$ as follows

$$\underline{\mathcal{D}} = \varepsilon\varepsilon_o \underline{E} \tag{F.3}$$

The introduction of polarizable material of dielectric constant ϵ to free space containing fixed charges which generate an electric field leads to changes in the field of magnitude

$$\Delta \underline{E} = \frac{\underline{D}}{\epsilon \epsilon_o} - \frac{\underline{D}}{\epsilon_o} \tag{F.4}$$

and from equation (F.1), the work associated with the change in field in going from vacuum to a medium of dielectric constant ϵ is

$$\Delta u = -\frac{1}{\epsilon_o} \iint \left(1 - \frac{1}{\epsilon}\right) \underline{\mathcal{D}} \cdot d\underline{\mathcal{D}} \, dV \tag{F.5}$$

If the charges generating the electric field are produced by an ion i which is a charged sphere of radius r_i and charge q, then the field around the sphere is described by a displacement vector $\underline{\mathcal{D}}$ of radial orientation and magnitude equal to:

$$| \underline{\mathcal{D}} | = \frac{q_i}{4\pi r^2} \tag{F.6}$$

where $q_i = z_i e$ and z_i is the valence of ion i and e is the elementary charge. The free energy associated with the transfer of the ion from vacuum to a solvent of dielectric constant ϵ is obtained from equation (F.5)

$$\mu^E_{Born,i} = -\frac{1}{\epsilon_o} \int_{r_i}^{\infty} 4\pi r^2 dr \int_0^{z_i e/4\pi r_i^2} \left(1 - \frac{1}{\epsilon}\right) \underline{\mathcal{D}} \cdot d\underline{\mathcal{D}} \tag{F.7}$$

Integration of the above equation yields

$$\mu^E_{Born,i} = -\frac{z_i^2 e^2}{8\pi \epsilon_o r_i} \left(1 - \frac{1}{\epsilon}\right) \tag{F.8}$$

The equation above is the Born equation, which is the electrostatic free energy of a single ion, modelled as a sphere, in a medium of dielectric constant ϵ, relative

to its self energy. The Born equation solvation energy of an ion is a function of its charge, radius and the solvent's dielectric constant. The Born equation ignores the dependence of the dielectric constant on the electric field, the molecular nature of the solvent, and does not include the energy expended by solvents in forming cavities for accommodating ions in solution. Based on equation (F.8) the change in energy in transferring one mole of ions at infinite dilution from a solvent of dielectric constant ε_1 to one of dielectric constant ε_m is

$$g^E_{Born,i} = \frac{e^2 N_A}{8\pi\epsilon_o} \frac{z_i^2}{r_i} \left[\frac{1}{\varepsilon_m} - \frac{1}{\varepsilon_1}\right] \tag{F.9}$$

where N_A is Avogadro's number.

Hence the change in free energy in moving an ion from a medium of low dielectric constant to one of high dielectric constant is energetically favorable since $g^E_{Born,i} < 0$. One mole of strong electrolyte will dissociate in solution to give ν_+ moles of cations of charge z_+ and ν_- moles of anions of charge z_-. The Born equation prediction for the free energy change in transferring n_e moles of electrolyte e from solvent 1 to solvent m is:

$$G^E_{Born,e} = \frac{K_o}{2} \left(\frac{\nu_+ z_+^2}{r_+} + \frac{\nu_- z_-^2}{r_-}\right) n_e \left[\frac{1}{\varepsilon_m} - \frac{1}{\varepsilon_1}\right] \tag{F.10}$$

where K_o is given by equation (5.6). Although the number of moles of electrolyte appears in the equation above, it merely scales the free energy change per mole of solute; the free energy per a mole of solute is not a function of salt concentration since the solvation process occurs at infinite dilution.

Appendix G

The two-parameter Extended-Bromley equation

The Extended-Bromley equation is a modification of the Bromley equation (5.19) which increases the range of validity of the model to higher salt concentrations. It contains an additional term with a second adjustable parameter and has two different forms, depending on the type of electrolyte. The expression for the mean ionic activity coefficient of a salt in binary solution using this model is given by (Bromley, 1973)

$$\log \gamma_{\pm}^{\mathrm{ebr}} = \log \gamma_{\pm}^{\mathrm{br}} - \delta_{\nu_+\nu_-}\mathcal{E}\vartheta\sqrt{I}\left[1-\exp(-\vartheta\sqrt{I})\right] - (1-\delta_{\nu_+\nu_-})\mathcal{E}\ln\left(1+\vartheta^2 I\right) \quad \text{(G.1)}$$

where δ_{ij} is the Kronecker Delta, equal to one if $i = j$ or zero if otherwise. The expression for $\gamma_{\pm}^{\mathrm{br}}$ is given by equation (5.19). For symmetric electrolytes ($\nu_+ = \nu_-$) the third term on the right hand side of equation (G.1) is absent and, conversely, for unsymmetric electrolytes ($\nu_+ \neq \nu_-$) the second term is absent. For 1:1 electrolytes, the value of the constant ϑ is set to 1, while for 2:2 electrolytes it is equal to 70. The parameter $\mathcal{E}$ is an adjustable parameter, similar to $\mathcal{B}$ in $\gamma_{\pm}^{\mathrm{br}}$, and has a characteristic value for each electrolyte–solvent pair.

When the model above is applied to a system containing a mixed-solvent, the Extended-Bromley parameters $\mathcal{B}_m$ and $\mathcal{E}_m$ for the electrolyte–mixed solvent system must be calculated from the values characterizing individual binary electrolyte-solvent pairs. Here, equation (5.21) is used to calculate $\mathcal{B}_m$ and the following similar expression is used for $\mathcal{E}_m$:

$$\mathcal{E}_m = \sum_{\ell=1}^{N_S} (x_\ell^\circ)^2 \mathcal{E}_\ell + \sum_{\ell=1}^{N_S-1} \sum_{k=\ell+1}^{N_S} x_\ell^\circ x_k^\circ b_{\ell k}^{\mathcal{E}} \tag{G.2}$$

and $b_{\ell k}^{\mathcal{E}}$ is a binary interaction parameter.

For the case of a mixed-solvent, equation (G.1) can be expressed as

$$\ln \gamma_\pm^{\text{ebr}} = \ln \gamma_\pm^{\text{br}} + \delta_{\nu_+\nu_-} \sigma_m \vartheta \sqrt{I} \left[1 - \exp(-\vartheta\sqrt{I})\right] + \left(1 - \delta_{\nu_+\nu_-}\right) \sigma_m \ln\left(1 + \vartheta^2 I\right) \tag{G.3}$$

where $\gamma_\pm^{\text{br}}$ is given by equation (5.29) and

$$\sigma_m = -\ln(10)\mathcal{E}_m \tag{G.4}$$

If the Extended-Bromley equation is used for the mean ionic activity coefficient of a salt in a mixed-solvent solution, the activity coefficient of the mixed-solvent can be obtained by integrating the Gibbs-Duhem equation, as described in Appendix H, with the result

$$\ln \gamma_s^{\text{ebr}} = \ln \gamma_s^{\text{br}} - \frac{\nu n_c}{n_s} \left[\delta_{\nu_+\nu_-} \sigma_m h(\vartheta\sqrt{I}) + (1 - \delta_{\nu_+\nu_-}) \sigma_m \psi(\vartheta^2 I)\right] \tag{G.5}$$

where γ_s^{br} is given by equation (5.36) and the function h, with $\xi = \vartheta\sqrt{I}$, is

$$h(\xi) = \frac{1}{\xi^2}\left[4 + \frac{\xi^3}{3} + \left(\xi^3 - 2\xi^2 - 4\xi - 4\right)\exp(-\xi)\right] \tag{G.6}$$

while ψ, with $\xi = \vartheta^2 I$, is

$$\psi(\xi) = 1 - \frac{1}{\xi}\ln(1+\xi) \tag{G.7}$$

The excess Gibbs energy for the Extended-Bromley model is obtained by substituting equations (G.4) and (G.6) into equation (5.34).

Appendix H

Integration of the Gibbs-Duhem equation to obtain γ_s from $\gamma_\pm$

At a fixed temperature, and ignoring the effects of pressure, the Gibbs-Duhem equation can be applied to the pseudo-binary system of a mixed-solvent(s) and electrolyte(e)

$$n_s d\mu_s + n_e d\mu_e = 0 \tag{H.1}$$

The equation above can be expressed in terms of the activities of the components:

$$n_s d\ln a_s + n_e d\ln a_e = 0 \tag{H.2}$$

The activity of the mixed-solvent is equal to

$$a_s = x_s \gamma_s \tag{H.3}$$

where x_s is the mole fraction of mixed-solvent:

$$x_s = \frac{\sum_{\ell=1}^{N_S} n_\ell}{\sum_{i=1}^{N_C} n_i} \tag{H.4}$$

The activity of the electrolyte is given by the expression

$$a_e = m^\nu \gamma_\pm{}^\nu K \tag{H.5}$$

where $K = [\nu_+^{\nu_+} \nu_-^{\nu_-}]$. Using a basis of 1000 grams of mixed-solvent, $n_e = m$, where m is the molality of the salt in the mixed-solvent, equal to

$$m = \frac{n_e 1000}{\sum_{\ell=1}^{N_S} n_\ell M_\ell} \tag{H.6}$$

where M_ℓ is the molecular weight of solvent ℓ. Equation (H.2) can be expressed as

$$\frac{1000}{M_s} d\ln(x_s\gamma_s) + m\nu d\ln m + m\nu d\ln\gamma_\pm = 0 \tag{H.7}$$

where M_s is a mole fraction–averaged molecular weight for the mixed-solvent

$$M_s = \frac{\sum_{\ell=1}^{N_S} n_\ell M_\ell}{\sum_{\ell=1}^{N_S} n_\ell} \tag{H.8}$$

Equation (H.7) can be rearranged as

$$d\ln(x_s\gamma_s) = -\frac{\nu M_s}{1000}[m d\ln\gamma_\pm + dm] \tag{H.9}$$

and, since $m = I/\Phi$, equation (H.9) can be expressed as

$$d\ln(x_s\gamma_s) = -\frac{\nu M_s}{1000}\left[\frac{I}{\Phi}\left(\frac{d\ln\gamma_\pm}{dI}\right)dI + \frac{1}{\Phi}dI\right] \tag{H.10}$$

and rearranged to give

$$d\ln(x_s\gamma_s) = -\frac{\nu M_s}{1000\Phi}\left[1 + I\left(\frac{d\ln\gamma_\pm}{dI}\right)\right]dI \tag{H.11}$$

which can be integrated over the limits

$$\int_{\ln x_s\gamma_s=0}^{\ln x_s\gamma_s} d\ln x_s\gamma_s = -\frac{\nu M_s}{1000\Phi}\int_0^I \left[1 + I'\left(\frac{d\ln\gamma_\pm}{dI'}\right)\right] dI' \tag{H.12}$$

to yield the activity coefficient of the mixed-solvent

$$\ln\gamma_s = -\frac{\nu M_s I}{1000\Phi} - \frac{\nu M_s}{1000\Phi}\int_0^I I'\left(\frac{d\ln\gamma_\pm}{dI'}\right) dI' - \ln x_s \tag{H.13}$$

Hence if an expression for $\gamma_\pm$ is available, γ_s can be determined.

Appendix I

Activity coefficient term from the MSA

Unless otherwise indicated, the partial derivatives in this appendix are taken at constant T, P and all n_j where j is different from i.

The contribution to the activity coefficient of a solvent i from the Mean Spherical Approximation term in G^E is

$$\ln \gamma_i^{mea\infty} = \left(\frac{\partial G^E_{mea\infty}/RT}{\partial n_i} \right)_{T,P,n_{j\neq i}} \qquad i = 1, \ldots, N_S \tag{I.1}$$

while that for the salt is

$$\ln \gamma_{\pm}^{mea\infty} = \frac{1}{\nu} \left(\frac{\partial G^E_{mea\infty}/RT}{\partial n_c} \right)_{T,P,n_{j\neq c}} \tag{I.2}$$

The activity coefficient contribution for a solvent i from equation (5.5), is

$$\ln \gamma_i^{mea\infty} = -\frac{n_c K_o}{RT} \left[\frac{\Omega_m}{\varepsilon_m^2} \left(\frac{\partial \varepsilon_m}{\partial n_i} \right) + \left(1 - \frac{1}{\varepsilon_m} \right) \left(\frac{\partial \Omega_m}{\partial n_i} \right) \right] \qquad i = 1, \ldots, N_S \tag{I.3}$$

while that for the electrolyte is

$$\ln \gamma_{\pm}^{mea\infty} = \frac{K_o}{\nu RT} \left[\Omega_1 \left(1 - \frac{1}{\varepsilon_1} \right) - \Omega_m \left(1 - \frac{1}{\varepsilon_m} \right) \right] \tag{I.4}$$

From equation (5.8):

$$\left[\frac{\partial \Omega_m}{\partial n_i}\right] = -2\left[\frac{\nu_+ z_+^2}{(D_+ + 2D_{Sm})^2} + \frac{\nu_- z_-^2}{(D_- + 2D_{Sm})^2}\right]\left(\frac{\partial D_{Sm}}{\partial n_i}\right) \tag{I.5}$$

The derivative in equation (I.5) can be expanded as

$$\left(\frac{\partial D_{Sm}}{\partial n_i}\right) = \left(\frac{\partial D_{Sm}}{\partial \xi_m}\right)\left(\frac{\partial \xi_m}{\partial \varepsilon_m}\right)\left(\frac{\partial \varepsilon_m}{\partial n_i}\right) \qquad i = 1, \ldots, N_S \tag{I.6}$$

where, from equation (5.9),

$$\left(\frac{\partial D_{Sm}}{\partial \xi_m}\right) = -\frac{3D_m}{(1+4\xi_m)^2} \tag{I.7}$$

and, from equation (5.10),

$$\left(\frac{\partial \xi_m}{\partial \varepsilon_m}\right) = -\frac{(2\xi_m - 1)^7}{12(1+\xi_m)^3(1+4\xi_m)(2+5\xi_m)} \tag{I.8}$$

The dielectric constant for the mixed-solvent is given by the linear mixing rule of equation (5.27). From this equation the expression for the derivative of ε_m for solvent i is

$$\left(\frac{\partial \varepsilon_m}{\partial n_i}\right) = \sum_{\ell=1}^{N_S} \varepsilon_\ell \left(\frac{\partial x_\ell^\circ}{\partial n_i}\right) = \frac{(x_\ell^\circ)}{n_\ell}\left[\left(\frac{\partial n_\ell}{\partial n_i}\right) - x_\ell^\circ\right] = \frac{1}{n_s}(\varepsilon_i - \varepsilon_m) \tag{I.9}$$

Appendix J

Activity coefficient terms from the Bromley equation

The expression for G^{E}_{br}/RT of equation (5.34) can be expressed as

$$\frac{G^{E}_{br}}{RT} = \Psi + \Theta\,\Gamma \tag{J.1}$$

where

$$\Psi = -n_s \ln x_s \tag{J.2}$$

and

$$\Theta = \nu n_c \tag{J.3}$$

The function Γ is equal to

$$\Gamma = -1 + \frac{B_m I}{2} + \alpha_m F(\varrho\sqrt{I}) + \beta_m G(\kappa I) \tag{J.4}$$

where the parameters α_m, B_m, and β_m are functions of the mixed-solvent composition and, with $\xi = \varrho\sqrt{I}$,

$$F(\xi) = \frac{1}{\varrho}\left[\frac{2}{\xi^2}\ln(1+\xi) + \frac{\xi^2 - \xi - 2}{\xi(1+\xi)}\right] \tag{J.5}$$

The expression for $G(w)$, with $w = \kappa I$, is

$$G(w) = \frac{1}{\kappa}\left[\frac{\ln(1+w)}{w} - \frac{1}{1+w}\right] \tag{J.6}$$

The activity coefficient term derived from the Bromley equation term in G^E for solvent i is given by

$$\ln \gamma_i^{\text{br}} = \left(\frac{\partial G_{\text{br}}^{\text{E}}/RT}{\partial n_i}\right)_{T,P,n_{j\neq i}} \qquad i = 1,\ldots,N_S \tag{J.7}$$

while that for the electrolyte is

$$\ln \gamma_{\pm}^{\text{br}} = \frac{1}{\nu}\left(\frac{\partial G_{\text{br}}^{\text{E}}/RT}{\partial n_e}\right)_{T,P,n_{j\neq e}} \tag{J.8}$$

From equation (J.1), taking all partial derivatives at constant T, P, and n_j where j is different from i:

$$\left(\frac{\partial G_{\text{br}}^{\text{E}}/RT}{\partial n_i}\right) = \left(\frac{\partial \Psi}{\partial n_i}\right) + \left(\frac{\partial \Theta}{\partial n_i}\right)\Gamma + \Theta\left(\frac{\partial \Gamma}{\partial n_i}\right) \qquad i = 1,\ldots,N_S \tag{J.9}$$

The derivative of the Ψ function, from equation (J.2), is equal to

$$\left(\frac{\partial \Psi}{\partial n_i}\right) = -\frac{n_s}{x_s}\left(\frac{\partial x_s}{\partial n_i}\right) - \ln x_s\left(\frac{\partial n_s}{\partial n_i}\right) \qquad i = 1,\ldots,N_S \tag{J.10}$$

For solvent i the equation above is equal to

$$\left(\frac{\partial \Psi}{\partial n_i}\right) = -x_e - \ln x_s \qquad i = 1, \ldots, N_S \tag{J.11}$$

while the expression for the salt is

$$\left(\frac{\partial \Psi}{\partial n_c}\right) = x_s \tag{J.12}$$

For the second term in equation (J.1) the derivative of Θ for solvent i, from equation (J.3), is

$$\left(\frac{\partial \Theta}{\partial n_i}\right) = 0 \qquad i = 1, \ldots, N_S \tag{J.13}$$

while that for the salt is

$$\left(\frac{\partial \Theta}{\partial n_c}\right) = \nu \tag{J.14}$$

From equation (J.4) the derivative of the function Γ has the following form for all components

$$\begin{aligned}\left(\frac{\partial \Gamma}{\partial n_i}\right) = {} & \frac{I}{2}\left(\frac{\partial B_m}{\partial n_i}\right) + \frac{B_m}{2}\left(\frac{\partial I}{\partial n_i}\right) + F(\xi)\left(\frac{\partial \alpha_m}{\partial n_i}\right) \\ & + \alpha_m\left[\frac{\partial F(\xi)}{\partial n_i}\right] + G(w)\left(\frac{\partial \beta_m}{\partial n_i}\right) + \beta_m\left[\frac{\partial G(w)}{\partial n_i}\right] \\ & \qquad i = 1, \ldots, N_C \end{aligned} \tag{J.15}$$

which can be expanded as

$$\left(\frac{\partial \Gamma}{\partial n_i}\right) = \frac{I}{2}\left(\frac{\partial B_m}{\partial n_i}\right) + F(\xi)\left(\frac{\partial \alpha_m}{\partial n_i}\right) + G(w)\left(\frac{\partial \beta_m}{\partial n_i}\right) + \left\{\frac{B_m}{2} + \alpha_m\left[\frac{\partial F(\xi)}{\partial \xi}\right]\left(\frac{\partial \xi}{\partial I}\right) + \beta_m\left[\frac{\partial G(w)}{\partial w}\right]\left(\frac{\partial w}{\partial I}\right)\right\}\left(\frac{\partial I}{\partial n_i}\right) \qquad i = 1, \ldots, N_C \qquad \text{(J.16)}$$

The derivatives of the mixed solvent parameters B_m, α_m and $\mathcal{B}_m$ are equal to zero for the salt

$$\left(\frac{\partial B_m}{\partial n_e}\right) = \left(\frac{\partial \beta_m}{\partial n_e}\right) = \left(\frac{\partial \alpha_m}{\partial n_e}\right) = 0 \qquad \text{(J.17)}$$

The derivative of B_m for solvent i, from equation (5.32), is

$$\left(\frac{\partial B_m}{\partial n_i}\right) = \ln(10)\left(\frac{\partial \mathcal{B}_m}{\partial n_i}\right) \qquad i = 1, \ldots, N_S \qquad \text{(J.18)}$$

while that for β_m, from equation (5.31), is

$$\left(\frac{\partial \beta_m}{\partial n_i}\right) = 0.6\ln(10) \mid z_+ z_- \mid \left(\frac{\partial \mathcal{B}_m}{\partial n_i}\right) \qquad i = 1, \ldots, N_S \qquad \text{(J.19)}$$

Using the mixing rule of equation (5.21), the derivative of $\mathcal{B}_m$ for the solvents is

$$\left(\frac{\partial \mathcal{B}_m}{\partial n_i}\right) = \frac{2}{n_s}[x_i^o \mathcal{B}_i - \mathcal{B}_m] + \sum_{\ell=1, \ell \neq i}^{N_S} \frac{x_\ell^o b_{i\ell}^b}{n_s} \qquad i = 1, \ldots, N_S \qquad \text{(J.20)}$$

The derivative of α_m for solvents i, from equation (5.24) and (5.30), is equal to

$$\left(\frac{\partial \alpha_m}{\partial n_i}\right) = \frac{3 \mid z_+ z_- \mid \mathcal{A}_m}{2\varepsilon_m}\left(\frac{\partial \varepsilon_m}{\partial n_i}\right) - \frac{\mid z_+ z_- \mid \mathcal{A}_m}{2\rho_m}\left(\frac{\partial \rho_m}{\partial n_i}\right) \qquad i = 1, \ldots, N_S \qquad \text{(J.21)}$$

The derivative of the mixed-solvent density for solvent i is

$$\left(\frac{\partial \rho_m}{\partial n_i}\right) = \sum_{\ell=1}^{N_S} \rho_\ell \left(\frac{\partial w_\ell^\circ}{\partial n_i}\right) = \frac{w_i^\circ}{n_i}(\rho_i - \rho_m) \qquad i = 1, \ldots, N_S \tag{J.22}$$

similarly that for the dielectric constant is

$$\left(\frac{\partial \varepsilon_m}{\partial n_i}\right) = \sum_{\ell=1}^{N_S} \varepsilon_\ell \left(\frac{\partial x_\ell^\circ}{\partial n_i}\right) = \frac{x_i^\circ}{n_i}(\varepsilon_i - \varepsilon_m) \qquad i = 1, \ldots, N_S \tag{J.23}$$

The derivative of the function $F(\xi)$, from equation (J.5), is

$$\left[\frac{\partial F(\xi)}{\partial \xi}\right] = \frac{2}{\varrho \xi^2}\left[\frac{(2+\xi)}{(1+\xi)} - \frac{2}{\xi}\ln(1+\xi)\right] \tag{J.24}$$

The derivative of the function $G(w)$, from equation (J.6), is

$$\left[\frac{\partial G(w)}{\partial w}\right] = \frac{1}{\kappa w}\left[\frac{1+2w}{(1+w)^2} - \frac{\ln(1+w)}{w}\right] \tag{J.25}$$

with

$$\left(\frac{\partial \xi}{\partial I}\right) = \frac{\varrho}{2\sqrt{I}} \qquad \text{and} \qquad \left(\frac{\partial w}{\partial I}\right) = \kappa \tag{J.26}$$

The derivative of the ionic strength using the mixed solvent can be obtained from equation (5.15) and (5.20). For solvent i the expression is

$$\left(\frac{\partial I}{\partial n_i}\right) = -\frac{w_i^\circ I}{n_i} \qquad i = 1, \ldots, N_S \tag{J.27}$$

while that for the salt is

$$\left(\frac{\partial I}{\partial n_c}\right) = \frac{I}{n_c} \tag{J.28}$$

If the Extended-Bromley equation is used, then the excess free energy of equation (J.1) has an additional term

$$\frac{G^{E}_{ebr}}{RT} = \frac{G^{E}_{br}}{RT} + \Theta\,\Xi \tag{J.29}$$

where the function Θ is given by equation (J.3) and Ξ is given by the following expression

$$\Xi = \sigma_m \left[\delta_{\nu_+\nu_-} H(\vartheta\sqrt{I}) + (1 - \delta_{\nu_+\nu_-})\, U(\vartheta^2 I)\right] \tag{J.30}$$

and, with $y = \vartheta\sqrt{I}$,

$$H(y) = \frac{2y^3 - 12}{3y^2} + \exp(-y)\left(\frac{4}{y^2} + \frac{4}{y} + 2 - 2y\right) \tag{J.31}$$

and, with $t = \vartheta^2 I$,

$$U(t) = \frac{(t-1)}{t}\ln(1+t) - 1 \tag{J.32}$$

The activity coefficient term for solvent i for Extended-Bromley model is given by

$$\ln\gamma_i^{ebr} = \ln\gamma_i^{br} + \left(\frac{\partial\Theta}{\partial n_i}\right)\Xi + \Theta\left(\frac{\partial\Xi}{\partial n_i}\right) \qquad i = 1,\ldots,N_S \tag{J.33}$$

while that for the electrolyte is equal to

$$\ln\gamma_\pm^{ebr} = \ln\gamma_\pm^{br} + \left(\frac{\partial\Theta}{\partial n_e}\right)\Xi + \Theta\left(\frac{\partial\Xi}{\partial n_e}\right) \tag{J.34}$$

where

$$\left(\frac{\partial\Xi}{\partial n_i}\right) = \left[\delta_{\nu_+\nu_-} H(y) + (1 - \delta_{\nu_+\nu_-})U(t)\right]\left(\frac{\partial\sigma_m}{\partial n_i}\right)$$

$$+\sigma_m \left[\delta_{\nu_+\nu_-} \left[\frac{\partial H(y)}{\partial y}\right]\left(\frac{\partial y}{\partial I}\right) + \left[\frac{\partial U(t)}{\partial t}\right]\left(\frac{\partial t}{\partial I}\right)\right]\left(\frac{\partial I}{\partial n_i}\right)$$

$$i = 1, \ldots, N_C \tag{J.35}$$

The derivative of σ_m is

$$\left(\frac{\partial \sigma_m}{\partial n_i}\right) = -\ln(10)\left(\frac{\partial \mathcal{E}_m}{\partial n_i}\right) \qquad i = 1, \ldots, N_S \tag{J.36}$$

with

$$\left(\frac{\partial \mathcal{E}_m}{\partial n_i}\right) = \frac{2}{n_s}\left[x_i^o \mathcal{E}_i - \mathcal{E}_m\right] + \sum_{\ell=1, \ell \neq i}^{N_S} \frac{x_\ell^o b_{i\ell}^e}{n_s} \qquad i = 1, \ldots, N_S \tag{J.37}$$

The derivative of the function H is

$$\left[\frac{\partial H(y)}{\partial y}\right] = \frac{2}{3} + \frac{8}{y^3} + \exp(-y)\left(2y - 4 - \frac{4}{y} - \frac{8}{y^2} - \frac{8}{y^3}\right) \tag{J.38}$$

and while the derivative of U is

$$\left[\frac{\partial U(t)}{\partial t}\right] = \frac{t-1}{t(t+1)} + \frac{1}{t^2}\ln(1+t) \tag{J.39}$$

with

$$\left(\frac{\partial y}{\partial I}\right) = \frac{\vartheta}{2\sqrt{I}} \qquad \text{and} \qquad \left(\frac{\partial t}{\partial I}\right) = \vartheta^2 \tag{J.40}$$

and $(\partial I / \partial n_i)$ is given by equations (J.27) and (J.28).

Appendix K

Activity coefficient terms from the modified Flory-Huggins theory

The excess Gibbs energy function of equation (5.41) can be expressed as

$$\frac{G^{E}_{mfl}}{RT} = (\mathcal{F}_1 + \mathcal{F}_2)\,\mathcal{F}_3 \tag{K.1}$$

where

$$\mathcal{F}_1 = \sum_{\ell=1}^{N_S} \frac{\phi^{\circ}_{\ell}}{r_{\ell}} \ln \frac{\phi^{\circ}_{\ell}}{x^{\circ}_{\ell}} \tag{K.2}$$

and

$$\mathcal{F}_2 = \sum_{\ell=1}^{N_S-1} \sum_{k=\ell+1}^{N_S} \bar{\chi}_{\ell k} \phi^{\circ}_{\ell} \phi^{\circ}_{k} \tag{K.3}$$

and

$$\mathcal{F}_3 = \left(\sum_{\ell=1}^{N_S} r_{\ell} n_{\ell} \right) \tag{K.4}$$

The contribution from this term of G^E to the activity coefficient of solvent i is

$$\ln \gamma_i^{\text{mfl}} = \left(\frac{\partial G^{\text{E}}_{\text{mfl}}/RT}{\partial n_i}\right)_{T,P,n_{j\neq i}} \qquad i = 1,\ldots,N_S \tag{K.5}$$

while that for the salt is

$$\ln \gamma_{\pm}^{\text{mfl}} = \frac{1}{\nu}\left(\frac{\partial G^{\text{E}}_{\text{mfl}}/RT}{\partial n_e}\right)_{T,P,n_{j\neq e}} \tag{K.6}$$

From equation (K.1), taking all partial derivatives at constant T, P, and n_j where j is different from i:

$$\left(\frac{\partial G^{\text{E}}_{\text{mfl}}/RT}{\partial n_i}\right)_{T,P,n_{j\neq i}} = (\mathcal{F}_1+\mathcal{F}_2)\left(\frac{\partial \mathcal{F}_3}{\partial n_i}\right) + \mathcal{F}_3\left(\frac{\partial \mathcal{F}_1}{\partial n_i}\right) + \mathcal{F}_3\left(\frac{\partial \mathcal{F}_2}{\partial n_i}\right)$$

$$i = 1,\ldots,N_C \tag{K.7}$$

where

$$\left(\frac{\partial \mathcal{F}_1}{\partial n_i}\right) = \sum_{\ell=1}^{N_S}\left(\frac{1}{r_\ell}\right)\left[\ln\frac{\phi_\ell^\circ}{x_\ell^\circ}+1\right]\left(\frac{\partial \phi_\ell^\circ}{\partial n_i}\right) - \left(\frac{1}{r_\ell}\right)\left(\frac{\phi_\ell^\circ}{x_\ell^\circ}\right)\left(\frac{\partial x_\ell^\circ}{\partial n_i}\right)$$

$$i = 1,\ldots,N_S \tag{K.8}$$

and $(\partial \mathcal{F}_1/\partial n_e) = 0$. Similarly,

$$\left(\frac{\partial \mathcal{F}_2}{\partial n_i}\right) = \sum_{\ell=1}^{N_S-1}\sum_{k=\ell+1}^{N_S}\bar{\chi}_{\ell k}\left[\left(\frac{\partial \phi_\ell^\circ}{\partial n_i}\right)\phi_k^\circ + \phi_\ell^\circ\left(\frac{\partial \phi_k^\circ}{\partial n_i}\right)\right] + \phi_\ell^\circ\phi_k^\circ\left(\frac{\partial \bar{\chi}_{\ell k}}{\partial n_i}\right)$$

$$i = 1,\ldots,N_C \tag{K.9}$$

and

$$\left(\frac{\partial \mathcal{F}_3}{\partial n_i}\right) = r_i \qquad i = 1, \ldots, N_S \tag{K.10}$$

with $(\partial \mathcal{F}_3/\partial n_e) = 0$. The derivative of the salt-free mole fraction for solvent i, where $\ell \neq i$ is

$$\left(\frac{\partial x_\ell^\circ}{\partial n_i}\right) = -\frac{(x_\ell^\circ)^2}{n_\ell} \tag{K.11}$$

and for $\ell = i$

$$\left(\frac{\partial x_\ell^\circ}{\partial n_i}\right) = \frac{x_i^\circ}{n_\ell}(1 - x_\ell^\circ) \tag{K.12}$$

For the salt $(\partial x_\ell^\circ/\partial n_e) = 0$. Similarly, for the salt-free volume fraction

$$\left(\frac{\partial \phi_\ell^\circ}{\partial n_i}\right) = -\frac{(\phi_\ell^\circ)^2}{n_\ell} \tag{K.13}$$

and for $\ell = i$

$$\left(\frac{\partial \phi_\ell^\circ}{\partial n_i}\right) = \frac{\phi_\ell^\circ}{n_\ell}(1 - \phi_\ell^\circ) \tag{K.14}$$

and $(\partial \phi_\ell^\circ/\partial n_e) = 0$.

The derivative of $\bar{\chi}_{\ell k}$, from equation (5.43), is

$$\left(\frac{\partial \bar{\chi}_{\ell k}}{\partial n_i}\right) = \chi_{\ell k}^1 \left(\frac{\partial x_e}{\partial n_i}\right) \tag{K.15}$$

where for solvent i $(i \neq e)$

$$\left(\frac{\partial x_e}{\partial n_i}\right) = -\frac{x_e^2}{n_e} \tag{K.16}$$

and for the salt ($i = e$)

$$\left(\frac{\partial x_e}{\partial n_e}\right) = \frac{x_e}{n_e}(1 - x_e) \tag{K.17}$$